Over-expression and characterisation of Brassica napus and Escherichia coli 3-oxoacyl-[acyl carrier protein] reductase

Neil Ciaron Thomas

Over-expression and Characterisation of *Brassica napus* and *Escherichia coli* 3-Oxoacyl-[Acyl Carrier Protein] Reductase

Neil Ciaron Thomas B.Sc. (*Hons*)

A thesis submitted to the Department of Biological Sciences, University of Durham in accordance with the requirements for the degree of Doctor of Philosophy

Department of Biological Sciences, University of Durham

July 1999

Neil Ciaron Thomas

PhD. Thesis

1999

Over-expression and Characterisation of *Brassica napus* and *Escherichia coli* 3-Oxoacyl-[Acyl Carrier Protein] Reductase

Abstract

A full length cDNA clone of *Brassica napus* 3-oxoacyl-ACP reductase (β-ketoacyl-ACP reductase; E.C. 1.1.1.100; βKR) and the *Escherichia coli* gene for the same enzyme, have been over-expressed in *E. coli*. Both the *Brassica napus* seed and *Escherichia coli* βKR proteins have been purified by a rapid two-step, single chromatography matrix method. Glutaraldehyde cross-linking studies show the plant βKR is expressed as a tetramer and the *E. coli* enzyme is expressed as a dimer. The secondary structure of the two proteins was predicted via analysis of circular dichroism spectra, which also show dilution dependent unfolding of α-helical structure in the plant enzyme, a possible explanation for the dilution inactivation of βKRs. Ultrafiltration substrate binding studies and a bireactant initial velocity study show that *Brassica napus* βKR employs a fixed order ternary complex mechanism with NADPH binding to the enzyme first. One-dimensional western blot analysis indicates two isoforms of βKR (28 kDa and 31 kDa) in crude *B. napus* seed extracts. Further analysis using two-dimensional western blots demonstrates the presence of four major isoforms. Comparison with 2D blots from *B. campestris* suggests that one of the major isoforms has originated from that source. The crystal structure of the *E. coli* βKR enzyme is also discussed.

Table of Contents

List of Figures

List of Tables

Declaration

No part of this thesis has been previously submitted for a degree at this or any other university. All the material is my own original work except where otherwise stated. Data on the crystal structure of β-ketoacyl-ACP reductase was provided by Professor David Rice and Dr John Rafferty at the University of Sheffield.

Neil Thomas

July 1999

Acknowledgements.

Firstly, I would like to thank my supervisor, Professor Toni Slabas, for the assistance and guidance I have received during this project. I would also like to express my gratitude to Professor Ken Bowler for the provision of facilities in the Department of Biological Sciences and to S.E.R.C. for the studentship which enabled me to carry out this work.

Thanks must also go to Tony Fawcett and Kieran Elborough for their patient advice during the project and during the writing of this thesis. Thanks also to Bill Simon, Russell Swinhoe, John Gilroy and Julia Bartley for their excellent technical assistance.

My gratitude is also expressed to those outside Durham who contributed to this work. In particular, Professor David Rice, Dr John Rafferty and their co-workers at the University of Sheffield for their provision of data on the crystal structure of the subject enzyme of the study, without which this thesis would not have been properly concluded. Thanks go to Professor Nicholas Price and Dr Sharon Kelly of the University of Stirling for their kind assistance in performing the circular dichroism experiments and advice on protein concentration estimation. Thanks also go to Professor Paul Engel of University College Dublin for his helpful input regarding enzyme kinetics.

I should also make known my gratitude to the following who made the Durham Lab a more enjoyable place to work, Matt, Jonathan, Lee, Duncan, Johan, Bob, Caroline, Marta, Clare, Andy, Adrian, Colin, Simon, Hayley, Helen, Sipo, Judy, Mark, Bethan, José, Siân, Ikuo Nishida, and of course my close colleague and fellow student Dr Anne Fowler whose optimism in the face of adversity set me a fine example.

I would like also to thank my non-biological friends for their support and encouragement during the times when I have struggled through the writing of this thesis. Thanks in this regard must also go to my colleagues at Stevens Hewlett and Perkins, especially my patient patent preceptor, Pyers Pennant.

Ultimately I must thank and dedicate this thesis to my parents for their love, unconditional support, and seemingly endless patience. The beginning and eventual conclusion of this work would not have been possible without you.

Neil.

Abbreviations

1D	One dimensional
2D	Two dimensional
Å	Angstrom unit
ACP	Acyl carrier protein
ADP	Adenosine diphosphate
ATP	Adenosine triphosphate
AU	Absorbance unit
bp	Nucleotide base pair
βKR	β-ketoacyl-ACP reductase (3-oxoacyl-ACP reductase)
BSA	Bovine serum albumin
CD	Circular Dichroism
cDNA	complementary DNA
CoA	Coenzyme A
cv	Cultivar
DNA	Deoxyribonucleic acid
Dnase	Deoxyribonuclease
DTT	Dithiothreitol
EDTA	Ethylenediaminetetra-acetic acid
ER	Enoyl reductase
FAS	Fatty acid synthase
g	Acceleration due to gravity
Hb	Haemoglobin
HEAR	High erucic acid rape
IPTG	Isopropyl β-D-thiogalactopyranoside
kDa	Kilodalton
K_m	Michaelis constant
mRNA	messenger Ribonucleic acid
Mw	Relative molecular mass
NADH	β-nicotinamide adenine dinucleotide, reduced form
NADPH	β-nicotinamide adenine dinucleotide phosphate, reduced form
PAGE	Polyacrylamide gel electrophoresis
PBS	Phosphate Buffered Saline
PEG	Polyethylene glycol
pfu	Plaque forming units
RNAse	Ribonuclease
SDS	Sodium dodecyl sulphate
Tris	Tris (hydroxymethyl) aminoethane
U	Unit of enzyme activity
U. V. light	Ultra-violet light
var	Variety
VLCFA's	Very long chain fatty acids
V_{max}	Maximum velocity
v/v	Volume for volume
v/w	Volume for weight
w/v	Weight for volume
w/w	Weight for weight

"The life of a writer is absolute hell compared to the life of a businessman. The writer has to force himself to work. He has to make his own hours and if he doesn't go to his desk at all there is nobody to scold him."

ROALD DAHL - *Boy*, 1984

Chapter 1: Introduction

1.1. Plant Lipids

Plant lipids are an important heterogeneous group of biomolecules and are found in all cell types. As phospholipids, galactolipids and sterol esters they are the predominant components of biomembranes. The level of desaturation of these components dictates the fluidity of the membrane, an important determining factor in frost tolerance [Wada *et al.*, 1990]. The lipid nature of these membranes provides the correct environment for the function of several enzymes such as UDP-galactose:diacylglycerol galactosyltransferase [Coves *et al.*, 1988].

Cutins and wax esters coat the aerial surfaces of plants protecting it from water loss and other environmental stress as well as protecting against biological stress such as fungal attack. Another lipid, suberin, is utilised by root tissues as a waterproof barrier and can be produced as a response to wounding.

Lipids in the form of vegetable oils are an important raw material for both the chemical and food industries. Oilseeds such as soybean, sunflower, oil palm, safflower, maize and rape can contain up to 40% of the seed dry weight in the form of lipid. Storage triacylglycerols in plants can occur in an enormous variety of combinations utilising up to 300 different types of fatty acid. This tolerance of diversity holds promise for potential genetic engineering of plant storage oils, and contrasts with the uniform nature of membrane fatty acid composition.

Lipids can also play a variety of roles in plants that are less well characterised. Such functional roles include hormones, insect attractants and phytoalexins [Andrews and Ohlrogge 1991]. Lipid entities play an important role in cell signalling in animals for example, the inositol phosphate pathway, where the initial signal results in the cleavage of phosphatidylinositol 4,5-bisphosphate to form inositol 1,4,5-tris-phosphate

and diacylglycerol second messengers. A similar function is predicted in plants but is as yet to be fully delineated. A more well defined role for a lipid entity is seen in the interaction of the nodulating bacterium *Rhizobium meliloti* with its host. A sulphated lipo-oligosaccharide is released by the bacteria and induces nodule forming organogenesis in the root hairs of the host, alfalfa. It is the lipid entity, the akyl side chain, that determines the host specificity of the signal molecule [Truchet *et al.*, 1991].

The genetic and biochemical manipulation of the content of oil seeds will be of great commercial importance to a wide range of industries and medicine. Such manipulations are possible and effective as the storage products are synthesised under the control of enzymes present at relatively low levels in comparison to seed storage proteins. Changes made to the enzymes of a biochemical pathway can have a considerable effect on the end product. The problems encountered with previously ineffective manipulations of seed protein content, such as the introduction of high-lysine mutant proteins into barley [Shewry *et al.*, 1987], should not therefore be encountered. The variety of fatty acids utilised for triacylglycerols in plants suggests that altering the fatty acid profile of storage lipid in a plant should be permissible. This has been demonstrated by Knutzon *et al.* [1992] who showed, via antisense techniques, that the reduction of a single enzyme, stearoyl-ACP Δ9 desaturase, results in a shift in the fatty acid profile from oleic acid to stearic acid in *Brassica napus*.

If, as it appears, plants can tolerate seed triacylglycerols containing one type of fatty acid, then fractionation costs could be reduced by manipulating seed fatty acid synthesis to produce one predominant product. Another important commercial aspect of lipid research is that the enzymes of plant fatty acid biosynthesis are susceptible to herbicide action.

Whilst plants may tolerate artificial alteration of seed storage lipids, even minor alterations to membrane lipids could prove fatal to the plant. Successful genetic

engineering of plant lipids can only be achieved if this is taken into account. Certain features of storage triacylglycerol synthesis should allow effective manipulation to take place. Storage triacylglycerol biosynthesis has temporal and spatial restrictions i.e., within a certain *time* period of *seed* development. Specific enzymes and subcellular compartments are involved, distinct from those of membrane lipid biosynthesis, for example the spatial separation of the two different diacylglycerol pools contributing to storage and membrane lipids . Thus, there is a need for the researcher to furnish the engineer with information concerning the precise biochemical nature of plant fatty acid synthesis, the genetic control of its differential regulation (temporal and spatial), and the peptide targeting mechanisms which pinpoint proteins to the correct subcellular compartment [Slabas and Fawcett, 1992].

1.2. Fatty Acid Synthesis

1.2.1. Location

Isolated chloroplasts have been shown to synthesise fatty acids. No cytoplasmic *de novo* biosynthesis takes place in plants, unlike animals and other eukaryotic organisms. This places a burden on the plastid to import or produce its own precursors and to export its product for external membrane synthesis and storage. In seeds the biosynthesis of fatty acids up to carbon length C18 takes place in both chloroplasts and non-photosynthetic plastids. Evidence for the *de novo* synthesis of fatty acids taking place in the plastid was provided by Weaire and Kekwick [1975] and Yamada *et al.* [1990] by plastid isolation and enzyme activity measurements. This evidence has since been reinforced with the use of immunogold labelling of the plastid with antibodies raised against fatty acid synthase (FAS) enzymes e.g. β-ketoacyl-ACP reductase [Sheldon *et al.*, 1990]. Further proof comes from cDNA clones of acyl carrier protein, β-ketoacyl-ACP synthase I, β-ketoacyl-ACP reductase and enoyl reductase. These FAS

enzymes are nuclear encoded but all possess N-terminal transit peptides, for targeting to the plastid, in the deduced amino acid sequence [Slabas *et al.*, 1992a; Loader *et al.*, 1993]. Desaturation at the Δ9 carbon-carbon bond through the action of soluble stearoyl ACP desaturase, also takes place in the plastid. Fatty acid elongation above C18, hydroxylation, and desaturation of Δ12 and Δ15 carbon-carbon bonds, all take place outside the plastid, in the endoplasmic reticulum (see figure 1.1).

The chloroplast is not the only plant organelle in which *de novo* fatty acid synthesis takes place. Acyl carrier protein (ACP) was first reported in the mitochondria of *S. cerevisiae* and plants in 1989 [Chuman and Brody, 1989]. Wada *et al.* [1997] investigated the function of mitochondrial acyl carrier protein in pea leaf. Labelled [2-^{14}C]-malonic acid was found to be incorporated into fatty acids, and, simultaneously, ACP was acylated. This incorporation was inhibited by cerulenin and required ATP and magnesium cations, indicating that plant mitochondria contain all of the enzymes required for *de novo* fatty acid synthesis. More than 30% of the radioactive products from pea mitochondria were recovered in 'H protein', a subunit of glycine decarboxylase which contains lipoic acid. This indicates that *de novo* fatty acid synthesis in mitochondria primarily serves for the production of lipoic acid precursors.

1.2.2. The Precursor of Fatty Acids

Early experiments with radiolabelled acetate showed it to be incorporated into fatty acids [Stumpf and Barber, 1957]. Similar experiments showed the same for acetyl-CoA and malonyl-CoA, acetyl-CoA contributing the C_1 and C_2 carbon atoms, malonyl-CoA contributing the rest of the chain. There is some controversy over the origin of the acetyl-CoA used to synthesise fatty acids. Andrews and Ohlrogge state in their review [1991] that acetyl-CoA can be derived from either pyruvate dehydrogenase activity

within the plastid, or from extraplastidal production of acetate followed by its activation inside the plastid by acetyl-CoA synthase, located in the stroma.

Another suggestion is that acetyl groups enter the plastid as acetylcarnitine in a similar manner to the system in mitochondria where a specific carnitine translocator is active. Results from feeding experiments in the laboratory of Thomas [Masterson *et al.*, 1990], have shown that radiolabelled L-[1-^{14}C acetyl] carnitine gives a five-fold better incorporation of radioactivity into fatty acids compared to [1-^{14}C] acetate in pea leaf chloroplasts. A possible scheme for the transport of acetyl-CoA from the mitochondria is:

- 1. Conversion from acetyl-CoA to acetyl-carnitine in the mitochondria by the action of carnitine acyltransferase.
- 2. Transport of the acetyl carnitine to the plastid.
- 3. Entry via a permease into the plastid
- 4. Conversion back to acetyl-CoA by carnitine acyltransferase.

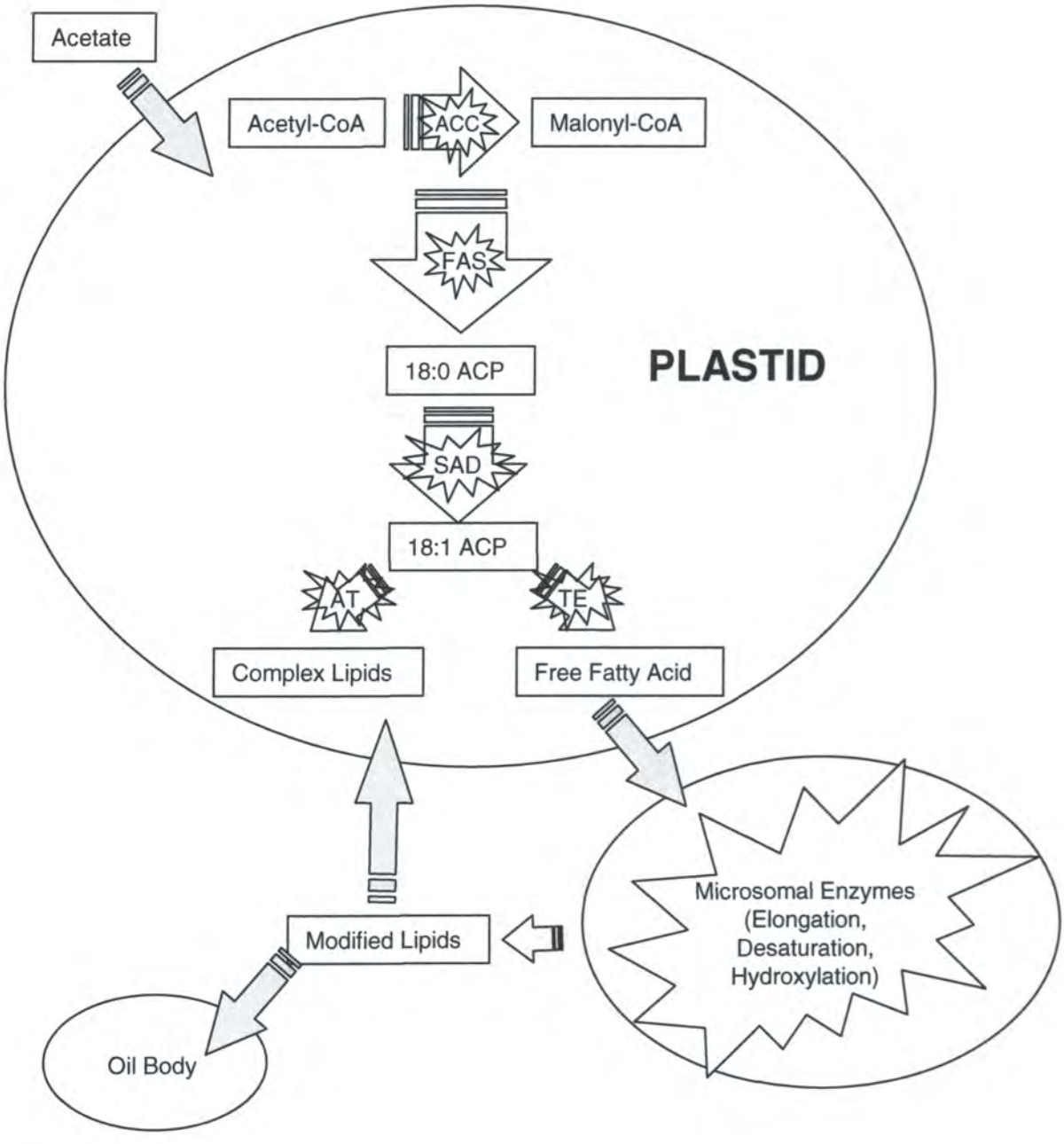

Figure 1.1 Localisation of fatty acid synthesis within the plant cell

Fatty acid synthesis from acetate to C18 and Δ9 desaturation via soluble stearoyl ACP desaturase (SAD) take place in the plastid. Fatty acid elongation above C18, hydroxylation, and desaturation of Δ12 and Δ15 carbon-carbon bonds, all take place in the endoplasmic reticulum. Modified lipids may be re-imported into the plastid for assembly into complex membrane lipids. Key: 'ACC' acetyl-CoA carboxylase; 'AT' acyltransferase, 'TE' thioesterase.

This particular proposed acetyl group import mechanism was placed under some scrutiny with the demonstration by Roughan *et al.* [1993] that in amaranthus, maize, pea and spinach chloroplasts, acetylcarnitine was not involved in fatty acid synthesis. This suggests that the above hypothesis is wrong or that there may be differences in the mechanism between plant species.

Differences in precursors have been demonstrated within species. Lichtenthaler and Golz [1995] have shown that acetate is the precursor used in oat seedling chloroplasts, but that pyruvate is used in etioplasts. Confusion remains about the source, nature, intracellular origin and transport of precursors of fatty acid synthesis.

Kang and Rawsthorne [1996], have demonstrated in developing rape embryo plastids that pyruvate and glucose-6-phosphate (via the oxidative pentose phosphate pathway) can both be utilised as a source of acetyl-CoA for fatty acid synthesis. The supply of glucose-6-phosphate in the presence of either pyruvate or pyruvate and acetate, was found to result in a threefold increase in the total flux from these metabolites to fatty acids compared to when either glucose-6-phosphate or pyruvate were supplied singly. They suggest that metabolism of exogenous Glc6P via the oxidative pentose phosphate pathway can partially contribute to the NADPH requirements of fatty acid synthesis.

1.2.3. Acetyl-CoA Carboxylase

Before the acetyl-CoA group can be utilised as a two carbon condensation unit for fatty acid synthesis, it must be carboxylated to give malonyl-CoA. Acetyl-CoA carboxylase (ACC) is the enzyme that carries this out. ACC is a biotin containing enzyme which represents the branch point of metabolism towards fatty acid synthesis. The biotin group is attached covalently to one of three functional domains, biotin carboxyl carrier protein (BCCP). Another domain, biotin carboxylase attaches CO_2 to

the biotin group. Subsequently, the CO_2 is transferred, via BCCP, to the acetyl-CoA by a further domain of the enzyme, the acetyl-CoA malonyl-CoA transcarboxylase domain.

ACC was considered to be the rate limiting step in lipid synthesis in the seeds of *Brassica napus*. ACC activity rapidly decreases after maximum lipid accumulation has occurred [Turnham and Northcote, 1983]. Therefore it was proposed that loss of ACC activity limits the level of lipid synthesis. However, Kang *et al.* [1994] devised an improved method of determining ACCase activity which allowed them to observe that ACCase activity declines relative to the rate of lipid synthesis throughout embryo development. As ACCase activity was not found to be correlated with the rate of lipid-synthesis, it seems unlikely that this enzyme constitutes a rate limiting step.

ACC is susceptible to the action of herbicides. It seems that the difference in herbicide tolerance between monocots and dicots is due to differing ACC species, the dicot ACC being resistant to herbicides effective on monocot ACC [Parker *et al.*, 1990]. Monocot acetyl CoA carboxylase is the target site for the monocotyledon-specific aryloxy-phenoxypropionate and cyclohexanedione groups of herbicides. Thus the twin issues of a regulatory role and an involvement with herbicide tolerance have sparked interest in cloning and characterising the ACC gene.

Prior to their discovery in plants, cDNAs for ACC were cloned from rat, chicken, yeast and *E. coli* [Dai *et al.*, 1986; Al-Feel *et al.*, 1992]. Like fatty acid synthetase, the component activities of ACCase are found in two organisational forms; as freely dissociable protein subunits (as in *E. coli*), or as a multifunctional polypeptide (as found in the cytosol of yeast and animals). Both types of association have been found in plants. Early reports suggested that the prokaryotic dissociable system was predominant in plants. Other early reports reported multifunctional forms of the enzyme in parsley [Egin-Buhler and Ebel, 1983] and *B. napus* [Slabas and Hellyer, 1985]. Subsequently, the multifunctional form was reported as a 220 kDa protein in wheat leaf

and germ [Elborough *et al.*, 1994a], a 230 kDa dimer in maize [Ashton *et al.*, 1994] and a 250 kDa protein in alfalfa [Shorrosh *et al.*, 1994]. All of these proteins had amino acid sequence similarity to yeast and animal ACCases.

Dicotyledonous plants such as pea and *Brassica napus,* and monocotyledonous plants such as *Hemerocallis fulva* L. (day lily), *Iris* L., and *Allium cepa* L. (onion), have been shown to possess both forms of acetyl-CoA carboxylase [Konishi and Sasaki, 1994; Elborough *et al.*, 1996; Roesler *et al.*, 1996]. A type I ACCase, the single polypeptide 220 kDa form, resides in the cytosol and may produce malonyl-CoA for use in secondary metabolic pathways. A type II multi-subunit complex analogous to that of *Escherichia coli* and *Anabaena* resides in the chloroplast and contributes to *de novo* fatty acid synthesis. The type II complex consists of 4 subunits, biotin carboxylase, biotin carboxyl carrier protein, and the α and β carboxyltransferases. The type II multi-subunit system has not been detected in the Gramineae, which lack the *accD* gene, encoding the β carboxyltransferase subunit of the prokaryotic form of ACCase, in their chloroplast genomes. These species do not have the prokaryotic form of the enzyme but have the eukaryotic form. The origin of the herbicide susceptibility of the Gramineae plants appears to be due to the sensitivity of the eukaryotic ACCase and the absence of the insensitive prokaryotic form in the chloroplast.

Elborough *et al.* [1994b] isolated cDNA clones from a rape embryo library and showed that the mRNA for ACCase has a higher level of expression in rape seed than in rape leaf. Expression levels during rape embryogenesis were compared with both oil deposition and expression of enoyl-(acyl-carrier-protein) reductase and β-ketoacyl-(acyl-carrier-protein) reductase. Levels of mRNA encoding all three FAS enzymes were shown to peak at 29 days after anthesis during embryonic development.

1.2.4. The Reactions of Plant Fatty Acid Synthase

Plant fatty acid synthase (FAS) is a type II enzyme that consists of a set of six freely dissociable enzymes in conjunction with acyl carrier protein (ACP). This arrangement, and the type II FAS of prokaryotes, is in contrast to the type I FAS seen in animals which is a single polypeptide carrying all of the FAS enzyme activities in an α_2 arrangement. Yeast utilises two interacting multifunctional type I polypeptides in an $\alpha_6\beta_6$ arrangement.

After the conversion of acetyl-CoA to malonyl-CoA the processes of condensation and elongation of the fatty acid chain can proceed. These steps require ACP.

Firstly malonyl-CoA produced by ACCase is transferred to ACP by the action of malonyl transacylase:

1. Malonyl-CoA + ACP-SH $\Leftrightarrow$ Malonyl-ACP + CoA-SH

Then acetyl-CoA (C2) and malonyl-ACP (C3) are condensed via the action of β-ketoacyl-ACP synthase III (KAS III) to produce acetoacetyl-ACP. CO_2 is given off in this reaction, which drives the reaction forwards, and renders it essentially irreversible:

2. Acetyl-CoA + Malonyl-ACP $\Leftrightarrow$ Acetoacetyl-ACP + $CO_2\uparrow$ + CoA-SH

The acetoacetyl-ACP is then reduced to form β-Hydroxyacyl-ACP by the enzyme β-ketoacyl-ACP reductase, the subject of this thesis. NADPH is used as the electron donor:

Acetoacetyl-ACP + NADPH + H^+ ⇔ β-Hydroxyacyl-ACP + $NADP^+$

A molecule of water is removed from the β-Hydroxyacyl-ACP by the enzyme β-Hydroxyacyl-ACP dehydrase to yield *trans*-2-acyl ACP.

5. β-Hydroxyacyl-ACP ⇔ Trans 2-butenoyl-ACP + H_2O

This enoyl-ACP molecule is then reduced to form a saturated fatty acid (linked to ACP as a thioester) by the enzyme enoyl-ACP reductase. This completes one cycle of fatty acid synthesis as the acyl chain has been extended by two units *i.e.* acetic acid (C2) has been converted to butyric acid (C4)

6. Trans 2-butenoyl-ACP + $NADH + H^+$ ⇔ Butyryl-ACP + NAD^+

The reactions of the latter enzymes are repeated with the addition of malonyl-ACP followed again by ketoreduction, dehydration, and enoyl reduction to further increase the acyl chain length by two carbon units.

Subsequent condensations are carried out by β-ketoacyl-ACP synthase I (KASI) to C16 carbons chains, and β-ketoacyl-ACP synthase II (KASII) for the C16 to C18

condensation, by the following reaction:

Acyl-ACP + Malonyl-ACP $\Leftrightarrow$ β-Ketoacyl-ACP + $CO_2\uparrow$ + ACP-SH

Acyl carrier protein and the enzymes of fatty acid synthesis are discussed in detail in the following sections. β-ketoacyl-ACP reductase, the subject of this thesis, is discussed separately in §1.5.

1.2.5. Acyl Carrier Protein

The most well studied component of fatty acid synthesis is the acyl carrier protein (ACP). ACP has a central role in fatty acid biosynthesis (see figure 1.2). It was the first protein of fatty acid biosynthesis to be purified to homogeneity. It has a molecular weight of 10 kDa and resembles Co-enzyme A. It possesses a 4'-phosphopantetheine moiety which is covalently attached to a highly conserved serine residue. This attachment is carried out by holo-acyl carrier protein synthase (ACPS), which transfers the 4'-phosphopantetheine (4'-PP) moiety from coenzyme A (CoA) to the serine residue of ACP. The ACPS enzyme from *Escherichia coli* has been over-produced and characterised [Lambalot and Walsh, 1995]. In plants, the attachment of a phosphopantetheine group, transferred from coenzyme A, occurs during the import of the precursor for acyl carrier protein (apoACP) into chloroplasts; ApoACP is converted to holoACP by a chloroplast holoACP synthase [Fernandez and Lamppa, 1990]. This reaction normally takes place in the stroma after the transit peptide has been cleaved. A partially purified spinach chloroplast holoACP synthase has been used to attach a 4'-PP group to *E. coli* synthesised spinach 'pre-ACP' (still possessing the transit peptide), to convert it to 'pre-holoACP' [Yang *et al.*, 1994]. When this protein was incubated with chloroplasts, it was seen to be able to take part in the import process with the prosthetic group already attached.

ACP levels rise prior to the onset of triacylglycerol biosynthesis. Spatial and temporal regulation must therefore be taking place, making ACP a good subject for the study of such mechanisms.

A strong conservation of amino acid sequence has been found between ACP from leaf and seed from different species, this is not reflected at the nucleotide level. The over-expression of plant ACP genes in *E. coli* allows the protein produced to be used for NMR studies to determine its three dimensional structure [Kim *et al.*, 1990; Oswood *et al.*, 1997].

Genomic clones of ACP have been isolated from *Arabidopsis* [Lamppa, 1991; Post-Beittenmiller, 1989] and *Brassica napus* [deSilva *et al.*, 1990]. They have a similar intron-exon structure as determined by protein sequence alignment studies. *Brassica napus* has approximately 35 copies of seed expressed ACP genes per haploid genome. The degree of sequence diversity of ACP from different tissue types suggests a multigene family.

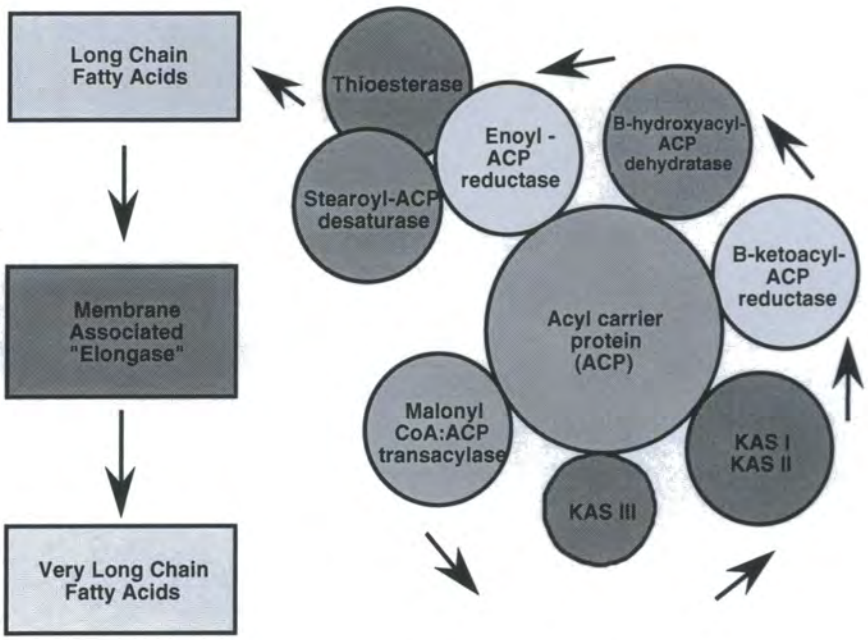

Figure 1.2 The central role of acyl carrier protein in fatty acid synthesis.

Acyl carrier protein is depicted centrally. After it is loaded with the an acetyl group by KASIII, it presents the growing acyl chain to each of the reactions of fatty acid synthesis, until it is severed from it by ACP thioesterase.

1.2.6. Malonyl-CoA:ACP Transacylase

This protein was purified to homogeneity from avocado [Hilt, 1984], and was partially purified in barley [Hoj and Mikkelsen, 1982], leek [Lessire and Stumpf, 1983], spinach [Stapelton and Jaworski, 1984] and soybean [Guerra and Ohlrogge 1986]. Soybean and leek preparations have appeared to contain isoforms, for which no function has been ascribed.

Bruck *et al.*, [1994], reported the first N-terminal sequence for Malonyl-CoA-acyl carrier protein transacylase in a higher plant, with the purification of the enzyme from developing seeds of *Cuphea lanceolata*. The N-terminal sequence of the enzyme showed a 25 % homology to the enzyme from *Escherichia coli*. The *E. coli* malonyl-CoA:ACP transacylase gene had been previously cloned by complementation of the *fab D* mutant, and has since used to produce transgenic rape and tobacco [Verwoert *et al.*, 1994]. With the expression of heterologous FAS genes for the purpose of modifying plant lipid profiles in mind, the effects of over-producing a bacterial FAS component were investigated using *E. coli fabD* as a model gene.

The *fabD* gene, under the control of a napin seed-specific and developmental-specific promoter, was introduced into tobacco and rapeseed via *Agrobacterium tumefaciens* transformation. The use of the rapeseed enoyl-ACP reductase transit peptide succeeded in targeting the bacterial protein to the plastid. The activity of the bacterial enzyme at the end of seed development was up to 55 times the maximum endogenous MCAT activity. No significant changes in fatty acid profiles of storage lipids or total seed lipid content of the transgenic plants were found, suggesting that MCAT does not catalyse a rate-limiting step in plant fatty acid biosynthesis.

1.2.7. β-Ketoacyl-ACP Synthases

The enzyme β-ketoacyl-ACP synthase (KAS) performs the initial condensation and subsequent elongation of the acyl-ACP by C_2 unit additions up to an acyl chain length of C18. Two KAS isoforms have been clearly resolved in spinach leaf extracts [Shimakata and Stumpf, 1982a]. Reconstitution experiments with purified spinach leaf FAS components using hexanoyl-ACP or palmitoyl-ACP as primers and [^{14}C]-malonyl-CoA were carried out. "KAS I" was shown to be involved in chain elongation of C2 to C16, and "KAS II" elongated C16 to C18 acyl chains. The other enzymes of FAS, β-ketoacyl-ACP reductase, β-hydroxyacyl-ACP dehydrase and enoyl-ACP reductase were all active for elongation from C2 to C18. In the reconstitution experiments neither KAS I or II could extend stearoyl-ACP, demonstrating that alternative condensation enzymes must be required for very long chain fatty acid synthesis.

KAS I and II from spinach leaf are both sensitive to inactivation and covalent modification by cerulenin. Cerulenin will inhibit condensing enzymes by binding irreversibly to the any cysteine residues present in the active site. KAS I has greater sensitivity to cerulenin than KAS II. A rapid *in vitro* complementation assay was used to isolate KAS I from rape seed [MacKintosh and Slabas, 1989]. Fractions were tested for restoration of fatty acid synthesis to a cerulenin-inhibited *E. coli* extract. Cerulenin labelling has also been used to purify the KAS I enzyme from barley chloroplasts, this time using tritiated cerulenin [Siggaard-Andersen *et al.*, 1991].

Cerulenin was employed to help identify KAS III, a short chain condensing enzyme, shown to be responsible for the initial reaction of fatty acid synthesis in both bacteria and plants [Jackowski and Rock, 1987; Jaworski *et al.*, 1989]. It is cerulenin-insensitive, but inhibited by an oxidative breakdown product of thiolactomycin (as are KAS I and KAS II).

Both KAS I and II use acyl-ACPs as substrate; KAS III uses acetyl-CoA and

malonyl-ACP as substrates and thus is distinct from them in its activity (figure 1.3 illustrates the respective activities of the KAS enzymes). The reaction it catalyses is:

Acetyl-CoA +Malonyl-ACP ⇔ Acetoacetyl-ACP + CO_2↑+ CoA-SH

The existence of KAS III in plants and bacteria poses an important question. Previous opinion held that acetyl-CoA:ACP transacylase (ACAT) was a rate limiting enzyme in fatty acid synthesis. ACAT catalyses the following reaction:

Acetyl-CoA + ACP-SH ⇔ Acetyl-ACP + CoA-SH

With the discovery of KAS III, there does not seem to be an absolute requirement for a separate ACAT enzyme in the plant. Cooper *et al* [1989] proposed that *E. coli* KAS III possesses ACAT activity, as a partial reaction of its catalysis, to explain the presence of ACAT activity.

KAS III has now been purified from avocado [Gulliver and Slabas, 1994], and from spinach [Clough *et al.*, 1992]. Gulliver separated the activities of KAS III and ACAT via purification by gel filtration and differing extraction methods. The two activities differ in their pH optima. This reinforces the notion that there is indeed a separate ACAT protein even though KAS III has been shown to bypass its function.
KAS III from a monocot (leek) has been cloned [Chen and PostBeittenmiller, 1996]. The deduced amino acid sequence of the cloned cDNA showed significant similarities to other KAS III sequences although the leek sequence had some notable differences in regions otherwise completely conserved in dicots. Leek KAS III is expressed in a manner comparable to leek oleoyl-ACP thioesterase, in both epidermal and parenchymal leaf tissues.

1.2.8 β-Hydroxyacyl-ACP Dehydratase

The dehydratase has been purified to homogeneity from spinach leaves [Shimakata and Stumpf, 1982b] and partially purified from developing safflower seeds [Shimakata and Stumpf, 1982]. No protein or gene sequence has yet been reported for this enzyme in higher plants. *Escherichia coli* possesses two β-hydroxyacyl-ACP dehydratases, encoded by the genes *fabA* and *fabZ*. The enzyme encoded by *fabZ* enzyme has activity on short chain β-hydroxyacyl-ACPs and long chain saturated and unsaturated β-hydroxyacyl-ACPs, whereas the *fabA* gene product has most activity on intermediate chain length β-hydroxyacyl-ACPs. *FabA* acts as a pivotal enzyme in the synthesis of the unsaturated fatty acid cis-vaccinate in *E. coli* [Heath and Rock, 1996a]. The *fabA* gene from *E. coli*, under the control of a cauliflower mosaic virus 35S RNA promoter and fused to the DNA sequence coding for the chloroplast targeting transit peptide of pea ribulose 1,5 bisphosphate, has been used to transform tobacco via *Agrobacterium* transformation. The enzyme was detected in the chloroplasts of transformed plants but no significant changes were observed in the fatty acid profile of the chloroplasts or selfed seeds [Saito *et al.*, 1995].

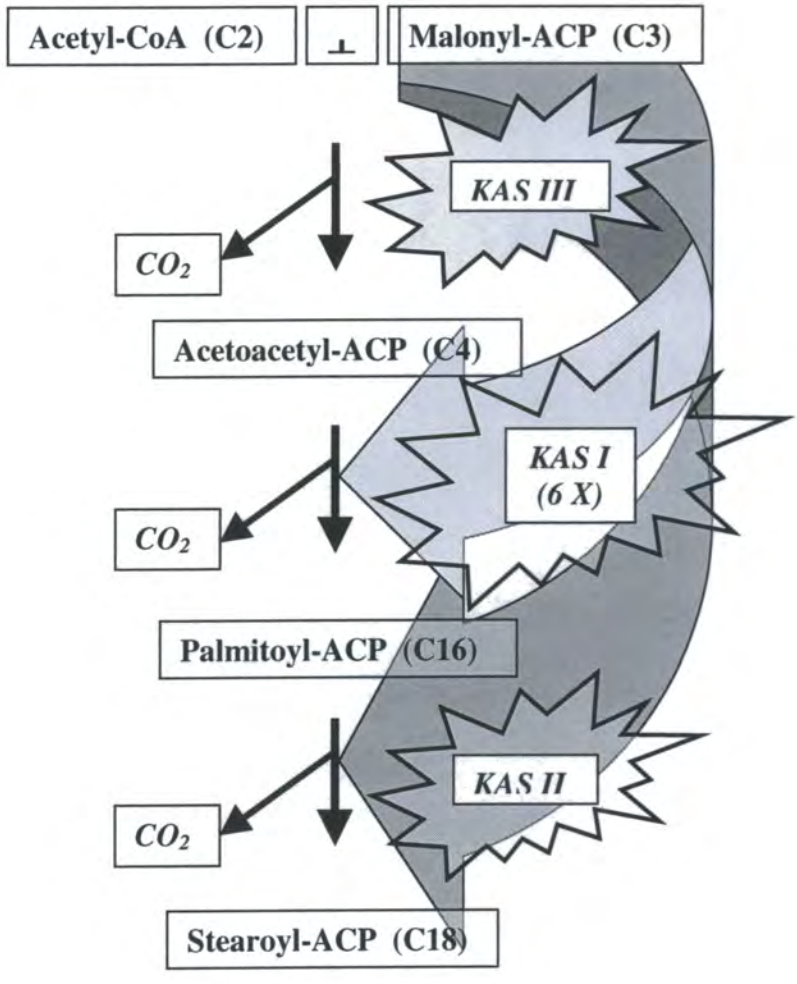

Figure 1.3 Respective activities of the KAS enzymes

The condensation of Acetyl-CoA and Malonyl-ACP is carried out by KAS III. Elongation via condensation of 2-carbon units (Malonyl-ACP) to the growing acyl chain up to C16 is carried out by KAS I. KASII carries out the final condensation within the plastid to produce C18. Each of these reactions liberates CO_2 and is therefore essentially irreversible.

1.2.9. Enoyl-ACP-reductase

In *Brassica napus* this enzyme appears prior to lipid accumulation, it is thus a suitable candidate for the study of possible seed and time specific regulatory controls. The activity of enoyl reductase remains high even after fatty acid synthesis has ceased. This phenomenon is distinct from the acetyl-CoA carboxylase in rape and castor bean, where the activity is rapidly dissipated after maximum lipid accumulation. A difference in stability of either the protein or the mRNA between the two enzymes might be the cause [Slabas *et al.*, 1986]. This enzyme has been detected in two forms, type I utilising NADH and type II utilising NADPH in preference to NADH [Harwood *et al.*, 1990]. Both types of enzyme have been found in seed material but only the type I enzyme has been found in leaf tissue. The NADH specific enzyme has been purified from avocado [Caughey and Kekwick, 1982], spinach [Shimakata and Stumpf, 1982b] and *Brassica napus* [Slabas *et al.*, 1986]. The enoyl reductase purified from spinach has a unit molecular mass of 32kDa from SDS/PAGE data. Gel filtration gave the mass to be 115 kDa, suggesting the enzyme to be a tetramer.

The enoyl-ACP reductase from developing seeds of rape was isolated and purified using a combination of affinity chromatography techniques consisting of conventional blue Sepharose chromatography combined with HPLC ion-exchange chromatography and hydrophobic chromatography. Two non-identical subunits of 33.6 and 34.8 kDa were revealed by SDS/PAGE. Attempts were made to separate the two subunits without success and it was concluded that the enzyme might incorporate both polypeptides. Further work by Cottingham *et al.* [1988] incorporated an improved method for the purification of rapeseed enoyl-ACP reductase. Using this they were able to separate the larger of the two proteins and sequence it. Armed with this sequence they were able to differentiate the mixed sequences from the un-separated preparation. The

two proteins were shown to differ by a six amino acid N-terminal extension. The remainder of the proteins did not differ markedly in amino acid composition. A 1989 paper from the same group [Cottingham *et al.*, 1989] suggested that the two polypeptides might differ due to processing differences or the presence of a purification artefact. Immunological studies showed that the smaller peptide of 33.6 kDa was not a component of the seed in rape and is therefore a proteolysed artefact of the purification procedure. This suggested that the enzyme is a homotetramer and not a heterotetramer as previously postulated. Also, localisation, via the use of labelled antibodies, demonstrated that the plastid is the subcellular position of enoyl-ACP reductase. The enzyme was therefore thought to possess a transit peptide leader sequence for such targeting [Slabas *et al.*, 1990].

Inhibition studies have identified the possible active residues of enoyl-ACP reductase. Shimakata and Stumpf [Shimakata and Stumpf, 1982b] used p-chloromercuribenzoate (p-CMB) and N-ethylmaleimide (NEM) to test for inhibition of the three enzymes they purified from spinach leaves, β-ketoacyl-ACP reductase, β-hydroxyacyl-ACP dehydrase and enoyl-ACP reductase. The p-CMB treatment was successful with all three enzymes, whilst NEM failed to inhibit them. It was proposed that the more hydrophobic reagent p-CMB was able to penetrate the enzyme to reach an active sulphydryl group. The more hydrophilic reagent NEM was proposed to be unable to penetrate a hydrophobic region of the enzyme to inactivate such residue. The same results were seen by Slabas *et al.* [1986] for the enoyl-ACP reductase in *B. napus* seeds. This also suggested that cysteine residues play an important role in enzymatic activity.

Cottingham *et al.* [1989] used phenylglyoxal to inhibit and covalently modify enoyl-ACP reductase to identify the residues involved in catalysis. Phenylglyoxal (2 mM) specifically modifies arginine residues when used in conjunction with a sodium bicarbonate (85 mM, pH 8.3) buffer. Loss of activity is seen when the enzyme is

incubated with phenylglyoxal, and this is shown to be due to the modification of two arginine residues. These two arginine residues are proposed to be located at either the active site of the enzyme or in an environment that is protected from phenylglyoxal when CoA is bound to the enzyme.

The lack of available protein hindered the study of essential residues and the general structure of enoyl-ACP reductase. The cloning and subsequent over-expression of the *B. napus* cDNA has been reported [Kater *et al.*, 1991]. As previously predicted, the clone encoded a 73 amino acid leader sequence for targeting the enzyme to the plastid. Over-expression of the protein encoded by this clone has allowed the crystal structure of enoyl reductase to be elucidated [Rafferty *et al.*, 1994; 1995]. The recombinant enzyme was purified from an *E. coli* crude extract and crystallised. The crystals were subjected to X-ray irradiation and diffract at a resolution of 1.9 Å. The subunits of the tetramer possess a dinucleotide binding fold. The crystal structure shows a striking similarity to the short-chain alcohol dehydrogenases, of which β-ketoacyl ACP reductase is a member. The conservation of a catalytically important lysine that stabilises the transition state, and the use of a tyrosine as a base is common to enoyl reductase and this family of enzymes.

The enoyl acyl carrier protein reductase from *Escherichia coli* is the target for diazaborine, an antibacterial agent. The bacterial enzyme has been crystallised complexed with NAD(+) and in the presence and absence of a thienodiazaborine [Baldock *et al.*, 1996]. This structural determination, in the presence of diazaborine, provides information on the nature of the drug binding site which will assist in rational drug design.

Evidence exists for multiple isoforms of enoyl reductase in *B. napus*. The *B. napus* cDNA used to over-produce enoyl reductase in *E. coli*, when used as a Southern blot probe, showed that four genes for the enzyme are present in *B. napus*, of which each ancestor plant species (*B. oleracea* and *B. campestris*) provide two [Kater *et al.*,

1991]. Earlier evidence from Slabas *et al.* [1991], based upon sequence anomalies in tryptic protein fragments, has been built upon at the whole protein level by the work of Fawcett *et al.* [1994], who has shown that four isoforms exist in seed and leaf. All four isoforms are present at the same ratio in seed and leaf, though at a lower level in leaf. All four seed isoforms show increasing abundance during seed development rather than a single isoform.

1.2.10. Fatty Acid Synthesis Termination

When the fatty acid chain length reaches C16, the palmitoyl-ACP may be acted upon in three ways. It might be elongated to C18 by KAS II, used in glycerolipid synthesis in the plastid or might be hydrolysed to the free fatty acid for export and use outside the plastid. Such incorporation into plastid lipids is carried out by acyltransferases. C16 and C18 acyl-ACPs are hydrolysed to free fatty acids, by acyl-ACP thioesterase, and are exported. If the ratio between the acyltransferases and thioesterases is high, the C16 fatty acids will be incorporated into glycerolipids; the "prokaryotic pathway". If the ratio is in favour of thioesterase then fatty acids will enter an extra-plastidal "eukaryotic" pathway in the endoplasmic reticulum [Roughan, 1987]. The thioesterases in general have a substrate specificity of 18:1 » 18:0 » 16:0, though others exist with short-chain specificities e.g. C12:0 – see below.

In plants, acyl-ACP thioesterase has been purified to homogeneity from rape seed. The enzyme has a subunit molecular mass of 38 kDa and has a high specificity for oleoyl-ACP, C18:1. This substrate specificity is consistent with a thioesterase that would fit into the termination step after the soluble Δ9-desaturase has acted [Hellyer and Slabas, 1990]. Protein sequence data from this enzyme facilitated the isolation of two cDNA clones encoding acyl-ACP thioesterase from *B. napus*. The two clones shared 96% identity at the DNA level and 98% identity at the amino acid level. Southern blot data showed the enzyme to be encoded by a small multi-gene family [Loader *et al.*,

1993]

A medium-chain specific acyl-ACP thioesterase has been isolated from California bay laurel. Introduction of this gene into the *fad D* mutant of *E. coli*, resulted in the production of medium-chain fatty acids in high quantities. The gene encoding this enzyme has been shown to be capable of altering the lipid profile towards that of medium chain fatty acids (C12:0) in transgenic plants [Voelker *et al.*, 1992; Eccleston *et al.*, 1996]. Thioesterase enzymes from members of the *Cuphea* spp. have also been widely studied as they also uncouple medium chain fatty acids from fatty acid synthesis. High levels of C8:0 and C10:0 are produced in the seeds of *B. napus* transformed with the *Ch FatB2* gene from *Cuphea hookeriana* at the expense of linoleate (C18:2) and linolenate (C18:3). In *Cuphea hookeriana* this thioesterase is accompanied by another, specific for 16:0-ACP which is expressed throughout the plant as opposed to the seed alone, having a housekeeping function [Dehesh *et al.*, 1996]. The use of such heterologous thioesterase genes will enable the production of plants synthesising 'designer oils' unobtainable by plant breeding alone [Topfer *et al.*, 1995].

1.3. Fatty Acid Synthesis in *E. coli*

Both plant and *E. coli* fatty acid synthesis systems utilise a dissociable set of type II FAS enzymes. In spite of this similarity, the two systems are not identical and care should be take not to confuse the respective nomenclature of each system. The C10 chain length stage is a branch point at which a double bond may be retained in the chain. The resulting saturated C16:0, and unsaturated C16:1, C18:1 carbon chains are the major fatty acyl moieties of membrane phospholipids. Two genes were identified from the condensation reaction mutants *fab B* and *fab F*. The *fab B* gene encodes β-ketoacyl-ACP synthase I, required for the elongation step to the branch point leading to C16:1

and C18:1. The *fab F* gene encodes β-ketoacyl synthase II, necessary for the elongation of C16:1 to C18:1. With use of complementation experiments, the *fab B* gene has been isolated and sequenced. A third condensing enzyme has been identified, acetoacetyl-ACP synthase, which is required for the primary condensation reaction which yields a four carbon chain [Kauppinen *et al.*, 1988].

Cerulin inhibition has been used on *E. coli* to test for components that might reconstitute unsaturated fatty acid synthesis. A β-ketoacyl-ACP synthase I activity was found to be missing in a mutant which exhibits a temperature dependant requirement for unsaturated fatty acids [Siggaard-Andersen, 1988]. A putative fourth fatty acid condensing enzyme was isolated from *Escherichia coli* by the above method [Siggaard-Andersen *et al.*, 1994]. This 'KAS IV' was purified and a 30 amino acid sequence was used to clone the encoding *fabJ* gene. The protein was ascribed a specialised putative function in the supply of octanoic substrates for lipoic acid biosynthesis. The prediction was made that an analogue of KAS IV with the same function would be found in plant mitochondria. The discovery of the new gene encoding a KAS IV was refuted by Magnuson, Carey and Cronan [Magnuson *et al.*, 1995], who pointed out that the *fabJ* gene is the previously reported *fabF* gene that encodes the known beta-ketoacyl-acyl carrier protein synthase II.

Kater *et al.* have demonstrated the use of a hybrid genetic system to study the functional relationship between prokaryotic and plant multienzyme FAS complexes involving enoyl reductase [Kater *et al.*, 1994]. The putative *envM* gene from *E. coli* and *Salmonella* was revealed to encode enoyl-ACP reductase on the basis of amino acid sequence similarities with *B. napus* enoyl-ACP reductase. Over-expression studies confirmed that the *envM* gene encodes enoyl-ACP reductase. An anti-bacterial agent called diazaborine was shown to be a specific inhibitor of the bacterial enoyl-ACP reductase, whilst the antibiotic had no effect on the plant enzyme. Genetic

complementation of an *Escherichia coli envM* mutant was observed with the plant gene. The plant enoyl reductase, though somewhat unstable at high temperature, was also shown to functionally replace its counterpart within the bacterial multienzyme complex. Lipid analysis of recombinant hybrid *E. coli* strains also revealed that enoyl-ACP reductase is rate-limiting in the conversion of C16:1 to C18:1 in *E. coli.*

The regulatory role of enoyl reductase has since been studied further [Heath and Rock, 1996b]. Acyl-ACP degradation by thioesterase over-expression leads to constitutive, unregulated fatty acid production. Hence, long chain acyl-ACP has been implicated as a feedback inhibitor of fatty acid biosynthesis. Two biosynthetic enzymes were found to be sensitive to acyl-ACP feedback inhibition with palmitoyl-ACP in cell-free extracts of *Escherichia coli*, β-ketoacyl-ACP synthase III (fabH) and more stringently, enoyl-ACP reductase (fabI). The equilibrium of the dehydratase reaction lies in favour of β-hydroxyacyl-ACP, therefore enoyl reductase is required to complete each cycle of elongation; acyl-ACP inhibition, possibly via product inhibition, will effect each of the cycles.

The reporting of linoleic acid (C18:2) in stationary phase *E. coli* would have caused a revision of theories of *E. coli* fatty acid synthesis, had it not been refuted by work in the lab of Cronan, where no evidence of accumulation of the fatty acid was found [Cronan and Rock, 1994].

Several *E. coli* FAS enzymes have been structurally examined via crystallographic studies, enoyl reductase [Rafferty, 1994; Wagner, 1994; Baldock *et al.*, 1996], biotin carboxylase subunit from ACCase; (the first X-ray model of a biotin-dependent carboxylase) [Waldrop *et al.*, 1994], malonyl-CoA-acyl carrier protein transacylase [Serre *et al.*, 1995], and KAS I; (reported as the first X-ray diffraction study of a condensing enzyme) [Olsen *et al.*, 1995]. The over-production of plant FAS components will allow structural comparisons with the bacterial enzymes to be made.

1.4. Over-Expression of FAS Components in *E. coli*

1.4.1. Heterologous Expression of Foreign Genes in *E. coli*

Factors to be considered when the expression of a heterologous gene in *E. coli* is to be attempted include promoter strength, transcriptional termination, translational initiation sequences, codon choice, stability and secondary structure of mRNA, plasmid copy number, plasmid stability and the physiology of *E. coli* itself. Sawers and Jarsch [1996] provide a review describing a range of promoters and expression systems currently used in for the expression of heterologous genes in *E. coli.*

Various studies have been carried out in the past to assess promoter strength, for example by placing the promoter to be tested in front of a galactokinase (galK) gene carried on a plasmid and measuring the level of galactokinase synthesised in a galK$^-$ host [de Boer *et al.*, 1983]. Using this system it was shown that promoter strength is directly proportional to the degree of similarity with a consensus sequence. -35 region (5'-TTGACA-) and the -10 region or Pribnow box (5'-TATAAT), the transcription start point being assigned position +1. Maximal transcription of a foreign gene may require more features than a promoter with -35 and -10 regions that are close to the consensus sequence. With some promoters DNA sequences 10-100 base pairs upstream from the -35 site can act as 'upstream activators'. The deletion and/or insertion of DNA sequences can distort these activators and decrease transcription [Gourse *et al.*, 1986]. Promoters found in modern expression vectors will match or exceed the transcriptional activity of the 'consensus sequence'. An alternative to providing an efficient promoter for *E. coli* transcription, it is possible to use a phage promoter together with a source of phage polymerase as for example, the pET expression system used in this study - see below.

The presence of transcription terminators at the ends of cloned genes prevents the synthesis of unnecessarily long transcripts, the formation of undesirable secondary structures and read-through from the strong promoter into other plasmid sequences

which may disrupt plasmid replication or cell function.

Factors which can affect translational initiation include the sequence and the accessibility, within the secondary structure of the mRNA, of the ribosome binding site. In naturally occurring prokaryotic mRNAs, sequences that are positioned 5' to the initiation codon have little self-pairing and do not pair extensively with the proximal coding region. The composition of the triplet immediately preceding the AUG start codon can also affect the translation efficiency, as can the length between the gene and its promoter. When the distance between the 5' end of the message and the ribosome binding site falls below 15 bases it can result in a marked decrease in translational efficiency.

Provided that an mRNA encoding a foreign gene can be efficiently translated, the rate of synthesis of a particular protein will depend on the steady-state level of mRNA present in the cell. This level is maintained in commercial expression systems by the use of strong promoters to maximise the rate of synthesis. The reduction of degradation of messenger by endonucleases or 3'-exonuclease attack can also be used to maintain mRNA levels. Susceptibility to such degradation depends upon mRNA sequence and structure. In *E. coli* the average half-life of an mRNA molecule is only 1-2 minutes. By contrast, the mRNA from gene 32 of bacteriophage T4 has a half-life of 20 minutes or longer due to the presence of specific sequences upstream of the initiation codon which confer stability. These sequences can be used to extend the life of transcripts.

The degeneracy of the genetic code provides more than one codon for most of the amino acids. A bias in codon usage exists in all organisms. This bias correlates with tRNA availability in the cell and non-random choices between pyrimidine ending codons. Ikemura [1981] noted that the most highly expressed genes in *E. coli* contain mostly those codons corresponding to major tRNA species, but few codons of minor

tRNA species. By contrast, genes that are expressed less well use more sub-optimal codons. A shortage of a charged tRNA during protein synthesis can lead to the misincorporation of amino acids and frame-shifting. Thus the arrangement of the successive codons in the coding region of a natural mRNA as well as its corresponding overlapping triplets may have evolved in order to minimise such frame-shifts *in vivo*. Replacing rare *E .coli* codons in foreign gene coding sequences with more common ones can improve expression.

In addition to using a strong promoter, another method of maintaining high levels of foreign gene transcripts in the cell is to increase the gene dosage by use of a high copy-number plasmid in which replication repressors have been removed. The use of high antibiotic concentrations can be used to maintain suitably high population levels of plasmids harbouring the relevant resistance gene.

The high-level expression of a particular gene can have several effects on the host bacterium such as a reduction in cell growth rates or morphological changes. If a mutant arises which through rearrangement of the plasmid no longer expresses the foreign gene, or which has a reduced plasmid copy number, then this will have a faster growth rate and may become predominant in the culture. The use of antibiotic resistance markers on the plasmid together with growth in the presence of the antibiotic can be used to overcome this possibility. The establishment of protein production cultures from fresh seed stocks rather than continual sub-culturing of the production strain can also be employed in this regard. Selection pressure upon cells producing large amounts of foreign protein can also be reduced by delaying the onset of expression until the later stages of the cell culture when a high cell number has been attained. This can be achieved by the use of a promoter which is only activated upon the addition of a substance to the culture medium, for example, the addition of IPTG to initiate expression from plasmids containing functional *lac* operator and repressor sequences.

The physiology of the host cell can also affect levels of foreign gene expression. The effects on the cell of nutrient content in the growth medium used, temperature and oxygen availability require consideration. For example, the overproduction of proteins in *E. coli* can result in the formation 'inclusion bodies' of aggregated foreign protein, a phenomenon which can be dependent on growth temperature (growth at 37 °C can lead to formation of inclusion bodies whilst growth at 30 °C can lead to yields of soluble active protein).

Even if the desired protein has been successfully expressed within the host cell only favourable conditions with regard to protein stability will ensure a suitable yield Foreign proteins can be rapidly degraded in the new host if their configuration or amino acid sequence do not protect them from intracellular proteases or protein degradation pathways. Factors which may modulate the *in vivo* half-life of a foreign protein include, the flexibility, accessibility and sequence of the N- and C-termini, the presence of chemically blocking amino-terminal groups such as the acetyl group, and the exposure of the folded protein surface to protease cleavage sites. For example Tobias *et al.* [1991] discovered that when Arg, Lys, Phe, Leu, Trp or Tyr were present at the N-terminus, proteins had a half life of only 2 minutes, compared to > 10 hours when other amino acids were present at the same position.

Various strategies have been developed to cope with the instability of foreign proteins in *E. coli*. One such strategy is to clone the desired gene in frame with an *E. coli* gene such as β-galactosidase so that a fusion protein is produced. This strategy was used to slow the degradation of somatostatin, the first human polypeptide to be expressed in *E. coli* [Itakura *et al.*, 1977]. In such methods the native protein is only obtained when the fused *E. coli* protein has been removed by cleavage. Some modern expression vectors contain a cloning site capable of giving rise to a fusion protein, perhaps encoding a purification tag or a periplasmic export tag, which also incorporates

a cleavage sequence recognised by a specific protease for the release of the native protein. Alternatively mutants of *E.* coli which have a reduced complement of intracellular proteases may be used as expression hosts, for example strains lacking the *lon or ompT* proteases.

The solubility of proteins expressed at a high level can be affected by the lysis buffer used during extraction. Proteins which are hydrophobic or which normally associate with membranes may reside in the insoluble fraction upon cell lysis unless a suitable detergent is used. Highly charged proteins may bind to cellular debris e.g. DNA. This can be prevented by adjustment of the salt content of the lysis buffer.

The presence of foreign proteins in the form of inclusion bodies can be an advantage as inclusion bodies are easily isolated, relatively pure and protect the protein from proteolytic attack. Toxic proteins which may affect cell growth are usually inactive when sequestered in inclusion bodies. There are now several efficient re-folding procedures available to allow soluble active protein to be isolated from inclusion bodies. Re-folding is not always necessary as most inclusion bodies are accompanied by a proportion of soluble active protein, which is available for purification upon cell lysis.

Certain post translational modifications to an over-expressed foreign protein cannot be carried out in a bacterial expression host, for example the glycosylation of a eukaryotic protein. If heterologous expression of such a protein is required, systems exist for the transformation and culture of yeast, plant and animal cells in order to produce such modified proteins. For a review of the heterologous expression of plant genes in such systems see Frommer and Ninnemann [1995].

1.4.2. The pET Expression System

The above considerations have given rise to the expression system used in this study, the pET expression system (Novagen Inc., Madison Wisconsin, USA). Comprising the vectors pET11-a and pET11-d (**pET** - **p**lasmid for **e**xpression by **T**7

RNA polymerase), the system is derived from the novel expression system developed by Tabor and Richardson [1985] and Studier and Moffat [1986] which employs the bacteriophage T7 polymerase and promoter. Bacteriophage T7 RNA polymerase will only recognise T7 promoters, the recognition being such that it will often transcribe around a plasmid several times, sometimes transcribing sequences not efficiently transcribed by *E. coli* polymerase. As this is the case, several transcription terminators are found in the pET series plasmids, downstream of the cloning site. T7 RNA polymerase is able to elongate chains five times faster than *E. coli* RNA polymerase, and in some cases can become the sole source of transcription in a cell. The system is capable of expressing a wide variety of prokaryotic and eukaryotic genes. Under favourable conditions the resources of the cell are allocated entirely to the production of target RNA and protein. Within one to three hours, target RNA can accumulate to amounts comparable to rRNA, and target proteins can make up the bulk of total cell protein [Studier *et al.*, 1990].

Two components are required in a T7 expression system:

- T7 RNA polymerase

This is a product of bacteriophage T7 *gene 1* and can be provided on an infecting bacteriophage vector or from a gene copy inserted into the *E. coli* chromosome. If the expression of the cloned product is toxic to the cell, then the level of phage T7 polymerase must be kept low during cell growth. This is accomplished by using *E. coli* lysogen strain BL21 (DE3), in which T7 *gene 1* is expressed from a *lacUV5* promoter. If it is necessary to use cells in which no T7 RNA polymerase is present until expression is desired then cells containing the expression plasmid (without the T7 RNA polymerase gene) can be infected with phage containing the T7 *gene1*.

- T7 RNA polymerase promoter

This promoter should be placed upstream of the gene to be expressed. The pET

series of plasmids have a cloning site, a T7 transcription terminator, an RNase III cleavage site, and a T7 *gene 10* translation start site (ribosome binding site).

The *E. coli* strain usually used for cloning into pET vectors and maintaining them is K12 strain HMS174. The most favourable strain to use as the expression strain is BL21. This is an advantage as the BL21 strains lack the *lon* protease and the *ompT* outer membrane protease that can degrade proteins during purification [Grodberg and Dunn, 1988]. HMS174 has the disadvantage that rifampicin cannot be used to inhibit transcription by the host RNA polymerase when background synthesis of host RNA and proteins may be a problem due to their toxicity to the cell.

Bacteriophage DE3 which is found as a lysogen in strain BL21(DE3), used in this study, is a derivative phage containing a DNA fragment encoding the *lacI* gene, the *lacUV5* promoter, the beginning of the *lacZ* gene and the gene for T7 RNA polymerase. The fragment is inserted into the *int* gene and as a consequence DE3 requires a helper phage for integration or excision from the *E. coli* chromosome. In a DE3 lysogen strain such as BL21(DE3) the only promoter able to direct transcription of the T7 RNA polymerase gene is the *lac UV5* promoter which is inducible by IPTG. The T7 RNA polymerase messenger produced is translated from its own translation start and does not form part of a *lacZ* fusion protein.

If the target gene is found or known to be toxic to the host then precautions must be taken to prevent basal level T7 RNA polymerase activity, which could result in uninduced transcription, until cell numbers are high enough to initiate T7 polymerase expression via IPTG addition. Basal T7 polymerase activity, and hence unwanted toxic expression products, can be countered by expressing T7 lysozyme from an additional plasmid, an inhibitor of T7 RNA polymerase. The T7 lysozyme protein plays two natural roles, cutting a specific bond in the peptidoglycan layer of the *E. coli* cell wall and binding to T7 RNA polymerase, inhibiting transcription [Moffatt and Studier, 1987]. If the protein is expressed within the cell then the protein remains within the cell

(as opposed to outside the cell where the T7 phage would normally present it to gain entry) and is thus tolerated - it does not pass through the inner membrane to attack the peptidoglycan layer. It must be noted that inner membrane treatments such as the addition of chloroform or mild detergents will induce rapid lysis due to the presence of the T7 lysozyme. T7 lysozyme can be provided on a plasmid pACYC184 under control of a *tet* promoter. The construct pLysE will result in high levels of T7 lysozyme if present and is used for more intolerance-causing target genes. pLysS has T7 polymerase inserted in the opposite orientation, cells with this plasmid produce much lower levels of T7 lysozyme. This has the advantage of not affecting growth rate, whilst transformation with pLysE does have a negative effect upon the growth rate. The presence of either of these two plasmids can enable toxic protein encoding plasmids to be maintained and expressed, although some gene products are too toxic to be maintained even with use of pLysE.

Target plasmids that are too toxic despite the use of pLysE can be expressed in cells where the T7 RNA polymerase is provided by an infecting bacteriophage when cell numbers are sufficiently high enough in the culture. A suitable bacteriophage for this task is CE6 which is a derivative that carries T7 RNA polymerase under control of the phage pL and pI promoters and also has a thermolabile repressor and *Sam 7* lysis mutations [Studier and Moffat, 1986]. When this phage is used to infect HMS174 cells carrying the target gene the transcription of that gene proceeds so rapidly that phage development is retarded. Comparable levels of target gene mRNA and protein are seen with both induction or infection methods of providing T7 RNA polymerase.

1.5. β-Ketoacyl-ACP Reductase

1.5.1. Plant β-ketoacyl-ACP reductase

Plant β-ketoacyl-ACP reductase (βKR) (also known as 3-oxoacyl-ACP reductase; EC 1.1.1.100) has been purified to homogeneity from spinach [Shimakata and Stumpf, 1982b], avocado [Sheldon *et al.*, 1990], and rape [Sheldon, 1988]. The enzyme catalyses the second of a sequence of four reactions that elongate the growing fatty acid chain via the addition of two-carbon units. This second reaction involves the reduction of the beta-ketone to a secondary alcohol, employing NADPH as electron donor. An NADH-linked βKR has also been reported in plants [Caughey and Kekwick, 1982], the function of which is unknown. The plant fatty acid biosynthesis system utilises the NADPH-linked species, the function of the other form requires further research for its elucidation.

The spinach leaf β-ketoacyl-ACP reductase was purified with use of polyethylene glycol fractionation, blue agarose chromatography, gel filtration with Sephadex G-200, hydroxyapatite chromatography and further gel filtration with Sephacryl S-300. Gel electrophoresis by SDS/PAGE gave the molecular mass of the enzyme monomer to be 24.2 kDa. Gel filtration revealed a tetramer of molecular mass 97 kDa. The purified spinach enzyme was able to utilise NADH or NADPH as the reductant, but NADPH was found to be more effective [Shimakata and Stumpf, 1982b]. Partially purified βKR activity from safflower (*Carthamus tinctorius*) seeds was found to have 100 fold higher activity with NADPH as compared to NADH [Shimakata and Stumpf, 1982], though this may have been due to the activities of more than one enzyme in the preparation.

In avocado, an NADPH-linked β-ketoacyl-ACP reductase was isolated from a plastid preparation from the mature fruit mesocarp by Sheldon *et al* [1988; 1990]. The

enzyme was found to be unstable at low temperature and low ionic strength, so some purification procedures were carried out at room temperature, using strong ionic strength buffers. This instability is echoed in β-ketoacyl-ACP reductase activities in other organisms such as *E. coli* [Toomey and Wakil, 1966], *Euglena* [Hendren and Bloch, 1980] and even in the multifunctional enzyme of chicken liver, perhaps suggesting structural similarity [Sheldon, 1988].

The flesh of the avocado fruit was extruded through muslin and centrifuged to produce a plastid-enriched layer which, after homogenisation and further treatment, was fractionated with $(NH_4)_2SO_4$ and subjected to three successive chromatographic separations to yield the pure enzyme. The protein preparation was shown on SDS-PAGE to migrate as a single polypeptide with a molecular mass of 28 kDa. The apparent molecular mass of 130 kDa shown by gel filtration chromatography is ascribed to the enzyme existing as a tetramer. The enzyme has a broad pH optimum around pH 7.0. It was inactivated by phenylglyoxal, inferring that there is an arginine residue in the active site. The localisation of the enzyme in the plastid was demonstrated using immunoelectron microscopy [Sheldon *et al.*, 1992]. Amino acid sequencing showed similarities between the N-terminus and cytochrome *f*, and also between internal trypsin digests and the *Nod G* product of *Rhizobium meliloti*, and the *graIII* and *actIII* genes from *Streptomyces spp.* No inactivation of the avocado enzyme was seen with thiol reagents, as had been observed with the enzyme from spinach leaf by Shimakata and Stumpf.

The researchers who purified the avocado enzyme used a similar procedure of ammonium sulphate fractionation and chromatography to purify β-ketoacyl-ACP reductase from the seeds of *Brassica napus* [Sheldon, 1988; Sheldon *et al.*, 1992]. The purified enzyme appeared as several components of between 20 -30 kDa frequently present in dimeric form, particularly in the absence of dithiothreitol.

Several similarities were seen between the rape β-ketoacyl-ACP reductase and the previously purified avocado enzyme. The enzyme was found to be inactivated by low ionic strength and temperature. The chromatographic procedures were therefore carried out at room temperature with high ionic strength buffers. Antibodies raised to the avocado enzyme cross-reacted with the rape enzyme suggesting similarities in the amino acid sequence. The antibodies used for immuno-electron microscopy in avocado were also able to visualise the reductase inside the plastids of embryo and leaf tissues from *B. napus*. From the molecular mass of 120 kDa determined by gel filtration, the rape enzyme also appeared to be tetrameric. Amino acid sequencing of two trypsin digest peptides showed marked conformity between the enzymes from the two species and similarities with the *Nod G* gene product from *Rhizobium meliloti.*

A communication from Slabas *et al* [1992a] reported the molecular cloning of β-ketoacyl-ACP reductase from *Brassica napus* and *Arabidopsis thaliana.* The purified proteins from avocado and rape were digested with trypsin and subjected to HPLC with the fractions collected manually to maximise the separation and purification of the peptides. All fractions corresponding to absorbance peaks were sequenced in a gas-phase amino acid sequencer. A sequence derived from *Brassica napus* β-ketoacyl-ACP reductase, EDMEKK, was used to design a degenerate complementary oligonucleotide. This sequence was chosen for its lack of degeneracy and thus the predictability of possible DNA sequences encoding it. A λgt10 cDNA library was constructed from mRNA extracts from developing seeds of rape. This cDNA library was screened with the [-^{32}P]ATP labelled degenerate oligonucleotide. The positive clones were plaque-purified and the phage purified by a CsCl density gradient. One clone containing three *Eco*R1 fragments was purified and the fragments sub-cloned into a pBluescript vector. The plasmid was then purified and sequenced. One of the fragments was chosen to re-screen the library but this failed to yield clones of greater length. This clone was found

to code for a truncated open reading frame for β-ketoacyl-ACP reductase. It was subsequently used to screen an *Arabidopsis thaliana* leaf λZAP II cDNA library, yielding a 1.2 kb clone. Upon sequencing this clone revealed a complete open reading frame for β-ketoacyl-ACP reductase.

Peptide sequences from avocado and rape allowed the two clones to be confirmed as encoding β-ketoacyl-ACP reductase, and the derived sequence from the *B. napus* clones were highly similar to the amino acid sequence of the isolated *B. napus* protein. The *Arabidopsis* clone derived sequence was aligned to the N-terminal sequences of the rape and avocado sequences, revealing a sequence of high identity. This suggested that the protein might first be produced as a pre-cursor with an N-terminal extension. This extension contains two methionine residues that might be the point of translation initiation. The methionine that gives the longer leader peptide, 59 amino acids, is deemed more likely to be the initiator as this peptide resembles a generic stromal targeting transit peptide.

The *Arabidopsis* βKR full length clone encodes a protein of theoretical molecular mass 27 208 Da - not including the proposed leader sequence - this matches the mass data obtained from SDS/PAGE for the *Brassica* and avocado enzymes, 30 kDa and 28kDa respectively. As with those two purified enzymes there was a strong identity between the *Arabidopsis* clone deduced amino acid sequence and the *NodG* gene product of *Rhizobium meliloti*. The sequences of the mammalian and yeast fatty acid synthase multifunctional polypeptides show no similarity to the plant β-ketoacyl-ACP reductase, and no bacterial β-ketoacyl-ACP reductase sequences were available for comparison at the time of writing the 1992 paper.

Comparison of the N-termini of βKR purified from rape [Sheldon *et al.*, 1992] and Avocado [Sheldon, 1988] with the deduced amino acid sequence of cDNA clones

from *Arabidopsis* and rape, suggests that the protein is produced as a pre-cursor with an N-terminal extension required for targeting the nuclear encoded protein to the chloroplast; for reviews see [Soll and Alefsen, 1993; Theg and Scott, 1993]. The deduced N-terminal sequence for this extension resembles a generic stromal targeting transit peptide [von Heijne *et al.*, 1989], in that it possesses three characteristics of such peptides, namely an N-terminal domain that is uncharged (MAAAVAA), a central domain with few or no acidic residues and a C-terminal domain (residues 34-57) able to form an amphiphillic β-strand. Figure 1.4 shows an alignment of published plant βKRs with the putative sequence from a full length *B. napus* βKR clone. The sequences encoding the transit peptide as predicted in Slabas *et al.* [1992] are shown.

Figure 1.4 Alignment of published plant βKRs with the putative sequence from a full length *B. napus* βKR clone.

A multiple sequence alignment (*CLUSTAL W (1.7)* [Thompson *et al.*, 1994]) of β-ketoacyl-ACP reductases from *Arabidopsis thaliana* 'ATBKR' [Slabas *et al.* 1992a], *Cuphea lanceolata* 'CLBKR' [Klein *et al.*, 1992] and *Brassica napus* 'BNBKRJRS' and 'BNBKR' [Slabas *et al.*, 1992a].

Key: '' = identical residue; ':' = very similar residue; '.' = similar residue; 'N' = transit peptide sequence; ' ' = N-terminus of mature protein.*

Amino acid data for BNBKRJRS is deduced from the sequence of the cDNA clone for B. napus βKR (pJRS10.1) used in this study.

The isolation and characterisation of a cDNA from *Cuphea lanceolata* which encodes β-ketoacyl-ACP reductase has been reported [Klein *et al.*, 1992]. This 1276 bp cDNA encodes a polypeptide of 320 amino acids. The first 63 residues are presumed to be a transit peptide, leaving 257 residues in the mature protein. The deduced sequence gives a mature protein of molecular mass 27 kDa. A glutathione-S-transferase – *Cuphea* β-ketoacyl-ACP reductase fusion protein was successfully expressed in *E. coli.* Assays showed that it had β-ketoacyl-ACP reductase activity and that it was dependant on NADPH as the electron donor. The enzyme activity was reduced significantly upon inhibition with phenylglyoxal. Substantial homology was seen between the deduced protein sequence and the sequences of the previously mentioned β-ketoacyl-ACP reductases from other plants. Strong homology was seen with polyketide synthesis enzymes from *Streptomyces spp.* which are thought to carry out similar chain elongation reaction to those of plant FAS. Homology was also observed between this enzyme and the *nod G* gene product from *Rhizobium meliloti* and the short chain alcohol dehydrogenase protein family [Krook *et al.*, 1990].

Southern hybridisation data suggested that the *C. lanceolata* βKR is encoded by a small gene family of at least two members. This finding was in agreement with observations of other plant FAS components investigated thus far, which are also encoded by gene families such as ACP [Lamppa and Jacks, 1991]. *C. lanceolata* βKR expression was found in roots, leaves, flowers and seeds, which suggested that it is not encoded by a seed-specific set of genes, though tissue-specific expression of single members of this gene family was not ruled out.

A recent report outlines the use of recombinant plant βKR in the study of regulatory steps in fatty acid biosynthesis [Winter *et al.*, 1997]. It was demonstrated that accumulation of β-ketoacyl-ACPs can inhibit the KAS enzymes and also cause them to

carry out the abnormal decarboxylation of malonyl-ACP; which may act as a regulatory mechanism for its degradation. This finding might have relevance in storage product-engineering situations were it is desired to divert the precursors of 'luxury' fatty acid synthesis, in that βKR becomes a possible target for down-regulation of FAS. Such an approach is being pursued in this laboratory.

Hendren and Block [1980] studied the βKR of 'FAS-II' of the alga *Euglena gracilis*. This organism contains two fatty acid synthetases which are controlled by a photoregulatory mechanism (1-4). Dark-grown cells of *E. gracilis* contain a cytoplasmic ACP-independent fatty acid synthetase multienzyme complex (FAS-1). When grown in the light, the cells contain, in addition to FAS-I, a chloroplast-localised ACP-dependent fatty acid synthetase (FAS-II).

The NADH and NADPH requirements of FAS-II were tested after separation of FAS-II from FAS-I by ammonium sulphate fractionation. FAS-II was optimally active with NADPH alone, which indicated that both the βKR and enoyl-reductase of FAS-II are specific for NADPH. The substrate specificities of the Euglena FAS-II βKR was studied with respect to thioester as well as reductant. The fastest rate of reduction of N-acetyl-S-acetoacetyl-ACP was found with a combination of NADH and NADPH. The acetoacetyl-coenzyme A was much more rapidly reduced than acetoacetyl-ACP by a combination of NADH and NADPH. In contrast, when NADPH was used as the sole reductant, acetoacetyl-ACP was readily reduced, but acetoacetyl-CoA was completely inactive. A substantial portion of the acetoacetyl-reductase activity determined in the presence of both NADH and NADPH is likely due to the β-hydroxyacyl-CoA dehydrogenase activity of the fatty acid β-oxidation pathway. The specific reduction of acetoacetyl-ACP was, therefore, only validly measured in *Euglena* crude extracts when NADPH alone is used as the reductant.

1.5.2. Bacterial *E. coli* β-Ketoacyl-ACP Reductase

E. coli β-ketoacyl-ACP reductase was first purified by Vagelos *et al.* in 1964 - discussed in the 'Methods in Enzymology' publication by the same authors [Vagelos *et al.,* 1969]. The enzyme was found to accept a wide range of saturated and unsaturated substrates [Birge and Vagelos, 1972] and has equal activity towards β-ketoacyl-ACP derivatives of C_4 to C_{16} [Toomey and Wakil, 1966]. The enzyme is stereospecific for the β-D-hydroxyacyl-ACP product; the stereoisomer can not take part in the reverse reaction, in addition, the enzyme is totally inactive with NADH. In the study by Toomey and Wakil [1966] the enzyme was purified 250-fold, at which level of purity the preparation was free from various contaminating FAS enzymes. βKR showed a broad pH optimum (pH 6.0 to 7.0). The equilibrium of the reaction was found to be pH-dependent. The reduction of acetoacetyl-ACP was almost complete at pH 7.0 or below but only about 40% complete at pH 9.0. The enzyme, which was specific for NADPH, was found to catalyse the reduction of acetoacetyl-ACP and acetoacetyl-CoA, Under the conditions employed, the rate of reduction of the β-ketoacyl-CoA derivative was about 2% of the rate of reduction of β-ketoacyl-ACP derivatives, indicating that the enzyme is specific for ACP derivatives. This is in contrast to the specificity of the β-hydroxyacyl-CoA dehydrogenase, which is about 4 times as active upon the acetoacetyl-CoA derivative as on the acetoacetyl-ACP derivative. This results highlighted the fact that although phosphopantetheine is the group to which the β -ketoacyl derivatives were attached in both CoA and acyl carrier protein, the enzymes of the fatty acid oxidation sequence prefer the CoA derivatives, whereas the enzymes of fatty acid synthesis prefer the ACP derivatives. β-ketoacyl ACP reductase was found to have a wide specificity towards the β-ketoacyl group. It reduced not only acetoacetyl-ACP but also β-

ketohexanoyl-ACP, β-ketooctanoyl ACP and β-ketodecanoyl ACP. The product of the reduction of the acetoacetyl group was shown to be the D(-)β-hydroxybutyrl derivative as demonstrated by the ability of the mitochondrial enzyme, D(-)β-hydroxybutyric-CoA dehydrogenase, to oxidise the hydrolysed reaction product. This is in contrast with the (L) configuration of the β-hydoxyacyl-CoAs found in β-oxidation and illustrates that the pathway of fatty acid synthesis is not a simple reversal of the pathway of fatty acid degradation.

The isolation and sequence of a gene encoding *Escherichia coli* β-ketoacyl-ACP reductase was reported by Rawlings and Cronan [1992]. The gene was found to lie within a cluster of fatty acid biosynthetic genes including ACP (*acpP*), β-ketoacyl-ACP synthase (*fabF*) and malonyl CoA-ACP transacylase (*fabD*). An open reading frame was found between *acpP* and *fabD* that encoded a 26.5-kDa protein with significant sequence identity (>40%) with two acetoacetyl-CoA reductases. On this basis, the gene (*fabG*), which is cotranscribed with *acpP,* was ascribed to β-ketoacyl-ACP reductase.

Heath and Rock [1996b], reported the use of purified over-expressed *E. coli* β-ketoacyl-ACP reductase from the previously reported gene in a reconstituted FAS system comprising recombinant enzymes. The recombinant enzyme included a His-Tag® for purification purposes but remained suitably active for the purposes of the experiment, i.e. the confirmation that enoyl reductase is a rate limiting enzyme in *E. coli* fatty acid synthesis.

βKR sequences have also been reported for *Vibrio harveyi* [Shen and Byers, 1996], *Haemophilus influenzae* [Fleischmann *et al.*, 1995], *Bacillus subtilis* [Morbidoni *et al.*, 1996] and *Mycobacterium smegmatis* [SWISS-PROT accession number P71534]. Figure 1.5 shows a multiple sequence alignment of these and published bacterial β-ketoacyl-ACP reductases, namely from *Escherichia coli* [Rawlings and Cronan, 1992],

Vibrio harveyi [Shen and Byers, 1996], *Haemophilus influenzae* [Fleischmann *et al.*, 1995], *Bacillus subtilis* [Morbidoni *et al.*, 1996] and *Mycobacterium smegmatis* [SWISS-PROT accession number P71534].

The gene from *Vibrio harveyi* [Shen and Byers, 1996] was cloned from a 3,973 bp region containing several FAS genes including *fabG* encoding a 25.5 kDa βKR, *acpP* encoding ACP and *fabF* encoding KASIII.

```
ECOLI       ------------------MNFEGKIALVTGASRGIGRAIAETLAARGAKVIG-TATSENG 41
VIBHA       ------------------MNLEGKIALVTGASRGIGRAIAELLVERGATVIG-TATSEGG 41
HAEIN       --------------------MQGKIALVTGSTRGIGRAIAEELSSKGAFVIG-TATSEKG 39
BACSU       -------------------MLNDKTAIVTGASRGIGRSIALDLAKSGANVVVNYSGNEAK 41
MYCSM       MTVTDNPADTAGEATAGRPAFVSRSVLVTGGNRGIGLAIARRLAADGHKVAV----THRG 56
                              : .: .:***..**** :**  *   *  *      ..

ECOLI       AQAISDYLGANGK---GLMLNVTDPASIESVLEKIRAEFGEVDILVNNAGITRDNLLMRM 98
VIBHA       AAAISEYLGENGK---GLALNVTDVESIEATLKTINDECGAIDILVNNAGITRDNLLMRM 98
HAEIN       AEAISAYLGDKGK---GLVLNVTDKESIETLLEQIKNDFGDIDILVNNAGITRDNLLMRM 96
BACSU       ANEVVDEIKSMGRKAIAVKADVSNPEDVQNMIKETLSVFSTIDILVNNAGITRDNLIMRM 101
MYCSM       SGAPDDLFG--------VQCDVTDSAGVDRAFKEVEEHQGPVEVLVANAGISKDAFLMRM 108
            :      :         :  :*::  .::  ::      . :::** ****::* ::***

ECOLI       KDEEWNDIIETNLSSVFRLSKAVMRAMMKKRHGRIITIGSVVGTMGNGGQANYAAAKAGL 158
VIBHA       KDDEWNDIINTNLTPIYRMSKAVLRGMMKKRAGRIINVGSVVGTMGNAGQTNYAAAKAGV 158
HAEIN       KDEEWFDIMQTNLTSVYHLSKAMLRSMMKKRFGRIINIGSVVGSTGNPGQTNYCAAKAGV 156
BACSU       KEDEWDDVININLKGVFNCTKAVTRQMMKQRSGRIINVSSIVGVSGNPGQANYVAAKAGV 161
MYCSM       TEERFEEVINTNLTGAFRCAQRASRTMQRKRFGRIIFIGSVSGMWGIGNQANYAAAKAGL 168
            .::.: :::: **.  :. ::   * * ::* **** :.*: *  *  .*:** *****:

ECOLI       IGFSKSLAREVASRGITVNVVAPGFIETDMTRALSDDQRAGILAQVPAGRLGGAQEIANA 218
VIBHA       IGFTKSMAREVASRGVTVNTVAPGFIETDMTKALNDDQRAATLSNVPAGRLGDPREIASA 218
HAEIN       VGFSKSLAKEVAARGITVNVVAPGFIATDMTEVLTDEQKAGILSNVPAGRLGEAKDIAKA 216
BACSU       IGLTKSSAKELASRNITVNAIAPGFISTDMTDKLAKDVQDEMLKQIPLARFGEPSDVSSV 221
MYCSM       IGMARSISRELDKAGVTANVLPPGYIDTEMTRALDERIQGGAIDFIPDKRVGTVEEVAGA 228
            :*:::* ::*:   .:*.*.:.**:* *:**  * .  :   :  :*  *.*   ::: .

ECOLI       VAFLASDEAAYITGETLHVNGGMYMV- 244
VIBHA       VVFLASPEAAYITGETLHVNGGMYMV- 244
HAEIN       VAFLASDDAGYITGTTLHVNGGLYLS- 242
BACSU       VTFLASEGARYMTGQTLHIDGGMVM-- 246
MYCSM       VSFLASEDASYIAGAVIPVDGGMGMGH 255
            * ****  * *::* .: ::**: :
```

Figure 1.5 Alignment of several published bacterial βKRs

A multiple sequence alignment (*CLUSTAL W (1.7)* [Thompson *et al.*, 1994]) of β-ketoacyl-ACP reductases from *Escherichia coli* 'ECOLI', *Vibrio harveyi* 'VIBHA', *Haemophilus influenzae* 'HAEIN', *Bacillus subtilis* 'BACSU' and Mycobacterium smegmatis 'MYCSM'.

Key: ' * *' = identical residue; '* **:** *' = very similar residue; '* **.** *' = similar residue*

1.6. The short chain alcohol dehydrogenase super family.

Both *B. napus* and *E. coli* β-ketoacyl-ACP reductases (in addition to enoyl reductase and the rhizobial nodG protein) are members of the short chain alcohol dehydrogenase super family (SDR) [Jörnvall *et al.*, 1995] which is based upon amino acid sequence similarity. The SDR family is a widely varied selection of enzymes, spanning three EC classes (oxidoreductases, lyases and isomerases), that share 15-30% homology with the retention of certain amino acid residue motifs. Most SDR enzymes are dimers and tetramers

Only one residue is strictly conserved (Tyr 151 in the numbering system of human NAD^+-linked prostaglandin dehydrogenase). Chemical modifications, site-directed mutagenesis, and a conserved position in the active site of tertiary structures so far elucidated, confirm that this tyrosine residue has an essential role in catalysis. In addition, a lysine residue four residues downstream, found in *E. coli* and plant βKRs, is also largely conserved. A common GlyXXXGlyXGly pattern, characteristic of a dehydrogenase coenzyme binding fold [Wierenga *et al.*, 1985] also exists in the family. Binding of the coenzyme, NAD(H) or NADP(H), is in the N-terminal part of the enzymes, where the GlyXXXGlyXGly pattern occurs. The presence or absence of an aspartic acid residue has been proposed to confer NAD^+ or $NADP^+$ specificity on the enzyme through constraints on coenzyme binding. Figure 1.6 shows the conserved SDR residues marked on an alignment of the *B. napus* and *E. coli* βKR putative sequences of the subject proteins of this study.

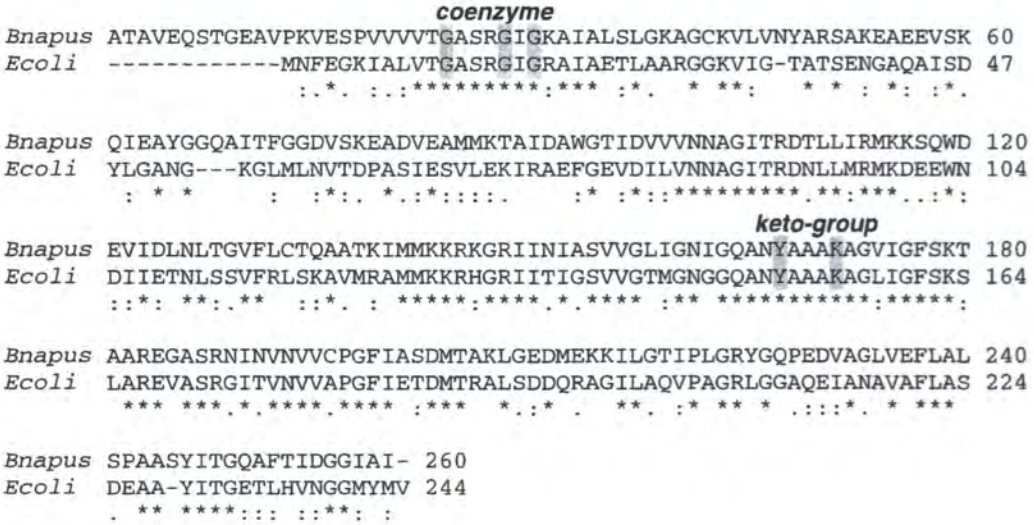

Figure 1.6 Conservation of short chain dehydrogenase/reductase superfamily residues in *B. napus* and *E. coli* βKRs.

The 'GlyXXXGlyXGly' and 'TyrXXXLys' motifs common to the SDR family of enzymes are marked on the above (*CLUSTAL W (1.7)* [Thompson *et al.*, 1994]) multiple sequence alignment of the two subject proteins of this study, *E. coli* and *B. napus* β-ketoacyl-ACP reductase. Proposed sites for the two substrates of the enzyme are marked above the conserved residues.

Key: '' = identical residue; ':' = very similar residue; '.' = similar residue*

Amino acid data is deduced from the published sequence of Rawlings and Cronan [1992] for E. coli βKR and from the sequence of the cDNA clone for B. napus βKR (pJRS10.1) used in this study.

Tanaka, *et al.* [1996] report the crystal-structure of the ternary complex of mouse lung carbonyl reductase at 1.8-Å resolution. Mouse lung carbonyl reductase (MLCR) is a member of the SDR family, it has a strong preference for NADPH, though it uses both NADPH and NADH. The three-dimensional structure of MLCR, the first SDR family protein structure to be solved in complex with NADPH (rather than NADH), reveals a pair of basic residues (Lys17 and Arg39) interacting with the 2'-phosphate group of NADPH. This pair of residues is well conserved among the NADPH-preferring enzymes of the SDR family, but not among the NADH-preferring enzymes. SDR family enzyme cofactor preferences are mainly determined by the electrostatic environment surrounding the 2'-hydroxyl (or phosphate) group of the adenosine ribose moiety of NADH (or NADPH). Thus, positively charged and negatively charged environments correlate with preferences for NADPH and NADH respectively. Basic residues (arginine and lysine) or a neutral residue (alanine) can be seen in *B. napus* and *E. coli* βKR deduced sequence data in positions corresponding to the positions of the functional basic residues of MLCR and the 'GlyXXXGlyXGly' coenzyme binding motif (see figure 1.6). Two other SDR ternary complex crystal structures, E. coli 7-α-hydroxysteroid dehydrogenase [Tanaka *et al.*, 1996b] and E. coli UDP-galactose 4-epimerase [Thoden *et al.*, 1996] both NADH utilising enzymes, have shown a serine residue to act with the 'TyrXXXLys' motif in ternary complex formation. This residue is also present in *B. napus* and *E. coli* βKR - see figure 1.7. Once the structure of the over-expressed βKR enzymes is known, it should be possible to use the protocols developed in this study in site directed mutagenesis experiments. The effect of residue changes could be examined on over-expressed mutant enzymes. In the light of knowledge provided by Tanaka *et al.* [1996a] it may be possible to convert a plant βKR to an NADH utilising form by swapping acidic for basic residues at the relevant positions.

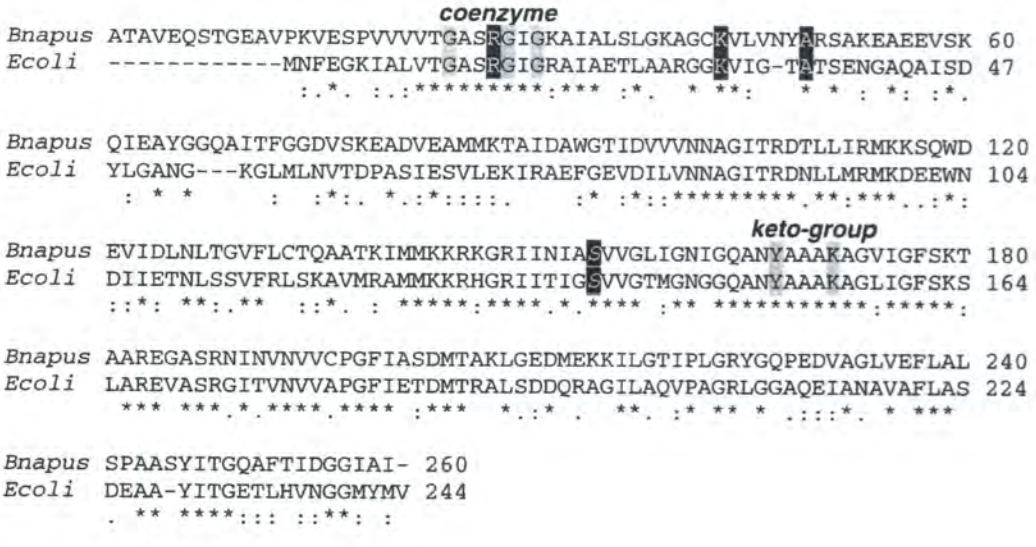

Figure 1.7 Possible residues in *B. napus* and *E. coli* βKR deduced sequences corresponding to ternary complex structure active site residues.

In the light of recent data from an SDR enzyme ternary complex structure [Tanaka *et al.*, 1996a] further residues have been proposed as being important in NADPH utilising SDR enzymes. The possible corresponding positions of such conserved basic/neutral sites in βKR are indicated within and adjacent to the coenzyme binding site in inverted characters (R + K/A).

Two further recent SDR crystal structures [Tanaka *et al.*, 1996b; Thoden *et al.*, 1996] propose that it a serine residue is also involved with the previously noted tyrosine and lysine residue C-terminal to the serine, in the formation of a ternary complex. This serine is also present in *B. napus* and *E. coli* βKR, and is marked above in inverted characters.

Key: '' = identical residue; ':' = very similar residue; '.' = similar residue*

Amino acid data is deduced from the published sequence of Rawlings and Cronan [1992] for E. coli βKR and from the sequence of the cDNA clone for B. napus βKR (pJRS10.1) used in this study.

Catalytic models based on the conserved tyrosine and lysine residues have been proposed [McKinley-McKee *et al.*, 1991] and supported by observations of tertiary structure [Ghosh *et al.*, 1994]. Figure 1.8 shows a possible reaction mechanism with the Tyr in ionised form, stabilised via the side chain of Lys, partaking in nucleophillic attack on the keto group of the substrate. Jörnvall *et al.* point out that though the Tyr/Lys mechanism gives a good explanation of the conservation of these residues, others may be involved, or indeed others may carry out catalysis within the SDR family. They state that the hypothesis of a uniform mechanism for SDR enzymes requires further scrutiny.

Information gleaned from amino acid sequences has, at present, limited use in three-dimensional structure prediction. In the case of the SDR family, such primary sequence similarities have been borne out in the form of structural similarities between member enzymes. Except for variations in the C-termini, the conformational patterns of the SDR enzymes established by X-ray crystallography are highly similar.

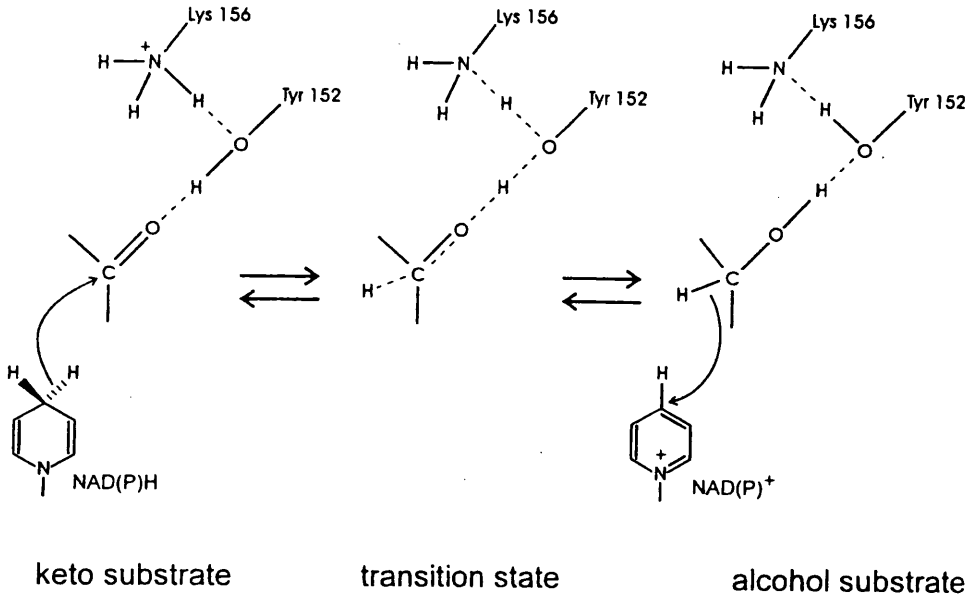

Figure 1.8 Proposed reaction mechanism for enzymes of the short chain dehydrogenase/reductase superfamily.

The above mechanism has the conserved tyrosine residue in ionised form, stabilised via the side-chain of the conserved lysine residue, partaking in nucleophillic attack on the keto group of the substrate. *(Taken from [Jörnvall et al., 1995])*

1.7 Aims of the Project

The primary aim of this project was to over-express and purify β-ketoacyl-ACP reductase using a *Brassica napus* developing seed cDNA clone. It was hoped that if this was achieved, it would facilitate immunological, kinetic and structural studies of the enzyme, that are difficult to perform with the amount of enzyme available from the plant.

The cDNA for *B. napus* βKR had been cloned by another worker in the laboratory prior to the outset of the project. Therefore an exercise to clone a plant βKR, from an avocado cDNA library, formed the first part of the study. This exercise had the dual role of extending the methodology of the project and providing a further βKR sequence for comparison with known sequences.

The construction of an over-expression vector, containing the *B. napus* βKR, would be followed by determining over-expression conditions and a suitable purification strategy. Once the protein was in a pure state, it would be partially sequenced to check the N-terminus. Further cell culture and purification would then be carried out to provide βKR for the planned studies of the project.

One such study was an attempt to determine the amount of the enzyme, and the number of its isoforms, present in crude developing seed extracts, through use of polyclonal antibodies raised against the over-produced βKR protein. One-dimensional western blots would be used on a developing seed series to observe induction of the enzyme, whilst two-dimensional western blots would be used to characterise the isoforms present in seed tissue.

Another avenue of study was the investigation of the kinetic mechanism of βKR. The derivation of pseudo Michaelis-Menten constants and the elucidation of the order of

addition of substrates, through steady-state initial velocity studies, were two tasks to be undertaken.

Bulk samples of over-expressed βKR in milligram quantities would be needed in order to facilitate crystallographic studies at a collaborating lab at the University of Sheffield. In addition, experiments at performed by the author at Durham and elsewhere were planned to obtain data on the secondary structure and subunit arrangement of the *B. napus* βKR.

In the course of the crystallisation and analysis of *B. napus* βKR, it became apparent that the complex structural data obtained might be better resolved with data from another βKR enzyme. To furnish the crystallographers with this data the *E. coli* enzyme was similarly over-expressed and purified. The *E. coli* enzyme was therefore included in the studies of secondary structure and subunit arrangement described herein.

Chapter 2: Materials and Methods

2.1. Materials

2.1.1. Reagents

Restriction endonucleases, T4 DNA ligase and oyster glycogen were from Boehringer Mannheim UK, Bell Lane, Lewes, East Sussex, BN7 1LG. Taq DNA polymerase and VENT polymerase was supplied by New England Biolabs.32 Tozer Road, Beverly MA USA. Megaprime labelling kit, [^{32}P] dCTP, ECL antibody detection kit and ^{125}I-labelled donkey anti-rabbit IgG antibody were purchased from Amersham International, Little Chalfont, Amersham, Buckinghamshire, HP7 9NA. Ampicillin and tetracycline were purchased from NBL Gene Sciences Ltd., South Nelson Industrial Estate, Cramlington, Northumberland, NE23 9HL. Agar and media nutrients were supplied by DIFCO laboratories, P.O. Box 14B, Central Avenue, West Molesey, Surrey, KT8 2SE. IPTG and DTT were obtained from Melford Laboratories Ltd., Ipswich, Suffolk, IP7 7LE.

Acrylamide mix for SDS-PAGE gels, SDS, ammonium persulphate, TEMED and Affigel cross-linking matrix were supplied by Bio-Rad Laboratories, Hemel Hempstead, Hertfordshire, HP2 7TD. Ultrafree-MC filters were purchased from Millipore UK, The Boulevard, Blackmoor Lane, Watford, Hertfordshire, WD1 8YW.

Chromatography media (Fast, HiLoad, FPLC and SMART) and two-dimensional gel electrophoresis reagents were obtained from Pharmacia Biotech Ltd 23 Grosvenor Road, St Albans, Herts AL1 3AW, and used on Pharmacia chromatography systems.

X-ray film was obtained from Fuji Photo Film (UK) Ltd., Fuji Film House, 125 Finchley Road, Swiss Cottage, London, NW3 6JH. Film developer and fixer were supplied by H.A. West (X-Ray) Ltd., 41 Watson Crescent, Edinburgh, EH11 1ES.

All other chemicals used were obtained from either BDH, Merck Ltd., Merck House, Poole, BH15 1TD or Sigma Chemical Co., Fancy Road, Poole, Dorset, BH17 7NH.

2.1.2. Biological material

R408 helper bacteriophage were obtained from Stratagene Cambridge Science Park, Cambridge CB4 4GF. pET vectors and *E. coli* strain BL21(DE3) were supplied by Novagen (Cambridge Bioscience) 24-25 Signet Court, Cambridge CB5 8LA . The plasmid pJRS10.1, encoding *B. napus* seed βKR, was cloned and provided by Dr. Jose M. Martinez-Rivas of this laboratory.

Seeds of known developmental stages were obtained from glass house grown *Brassica napus* cv. Miranda (High Erucic Acid Rape) and bulk seed of estimated developmental stages from field grown cv. Falcon and cv. Spock. Developing seeds were also obtained from growth room grown *Brassica campestris* var. Oleifera. The seeds were stored in liquid nitrogen immediately after removal from the pods.

Polyclonal rabbit antisera raised against over-expressed *B. napus* βKR were a gift from Zeneca Pharmaceuticals, Alderley Park, Macclesfield, Cheshire.

The avocado cDNA library was kindly provided by Dr Berta Dopico of the Department of Physiology and Environmental Science at the University of Nottingham

2.2. Molecular biology methods

Unless listed below or in the following chapters, genetic techniques and protocols followed were those set out in Sambrook *et al.*, [1989].

2.2.1. Antibiotics

Two antibiotics were used for plasmid, transposon and strain selection in this work:

Ampicillin

Affects bacterial cell wall synthesis. The resistance gene is *bla* - β-lactamase, an enzyme which cleaves the lactam ring.

Tetracycline

A bacteriostatic; binds to the 30S ribosome sub-unit and affects protein synthesis. The *tet* resistance gene modifies bacterial membranes and prevents uptake.

Antibiotic	Stock solution ($mg.ml^{-1}$)	Working conc. ($mg.ml^{-1}$)
Ampicillin (Amp)	**25** (in Milli Q water at -20 °C; filter sterilised (0.22 μm)	**50**
Tetracycline (Tc)	**12.5** (in 50% v/v ethanol at –20 °C; store in foil covered bottle)	**15**

2.2.2. Growth conditions and media

Luria Broth was used exclusively in this work: Luria broth (LB) (per litre in Milli Q grade water): 10 g Bacto-tryptone, 5 g Bacto-yeast, 10 g NaCl, (pH 7.5). Liquid medium was solidified where necessary through the addition of 1.5 % (w/v) agar or 0.7 % (w/v) agarose. Antibiotics were added to media after autoclaving. In the case of solid media, the antibiotic was added whilst the molten medium was just bearable to the touch.

Liquid cultures were incubated on a rotary shaker at 220 rpm at 37 °C. Cultures of 5 and 10 ml were grown in 15 ml test tubes, 50 and 100 ml cultures were grown in 250 ml conical flasks, and 250 and 500 ml cultures were grown in 2000 ml flasks. Solid agar plates were dried in a 37 °C oven prior to inoculation. After bacterial growth, plates were sealed with laboratory film and stored at 4 °C.

2.2.3. Plasmid preparation

An alkaline lysis method was employed for plasmid preparation:

Stocks	Volume(ml)	Final concentration
SOLUTION 1		
H_2O	**8.85**	
20% glucose	**0.5**	**1%**
250mM EDTA pH8.0	**0.4**	**10mM**
1M Tris/HCl pH 8.0	**0.25**	**25mM**
SOLUTION 2		
H_2O	**8.8**	
10M NaOH	**0.2**	**0.2M**
10% SDS	**1.0**	**1%**

An 1.5 ml overnight culture containing the plasmid of interest was centrifuged at 5000 x g. The supernatant was removed and the pellet was resuspended in 100µl of solution 1 then left at room temperature for 5 minutes. Then, 200µl of freshly prepared solution 2 was added, mixed by 3 quick inversions (not vortexed) and stored on ice 5 minutes. Addition of 150µl ice-cold potassium acetate pH 4.8 was followed by brief vortexing (2 seconds in an inverted position). The preparation was kept on ice for a further 5 minutes before centrifugation for 5 minutes (at top speed in an benchtop 1.5 ml tube microfuge) and removal of the supernatant to a fresh tube. An equal volume of phenol/chloroform solution was added, followed by vortexing for 15 seconds and centrifugation for 2

minutes. The supernatant was transferred to a fresh tube and 2 volumes of ethanol were added.

After standing at room temperature for 5 minutes, the DNA was recovered with a 5 minute centrifugation. The supernatant was discarded and the pellet rinsed in 1 ml of 70% (v/v) ethanol before re-centrifugation, removal of the supernatant and drying of the pellet under vacuum. The pellet was solubilised in 50µl T.E. containing 50mg ml^{-1} DNAase-free pancreatic RNAase (10mg ml^{-1} stock)* and vortexed briefly.

Larger scale preparations from 50ml cultures were carried out using 2 ml of solution one, 4 ml of solution two and 3 ml of potassium acetate, with centrifugation in 8x50ml rotor. Resuspension of DNA was in 500µl of T.E. with RNAase.

**DNAase free RNAase: Pancreatic RNAase (RNAaseA) was dissolved at a concentration of 10mg ml^{-1} in 10 mM Tris/HCl pH 7.5, 15 mM NaCl. The solution was heated to 100°C for 15 minutes and allowed to cool slowly to room temperature before storage at -20°C.*

2.2.4. DNA gel electrophoresis

DNA gel electrophoresis was carried out routinely in 0.7% (w/v) agarose gels made with TAE buffer (40 mM Tris/acetate, 1 mM EDTA; pH 8.0) and containing ethidium bromide at 0.5 mg ml^{-1}. Prior to electrophoresis, DNA loading buffer was added to the samples (10 x stock solution: 0.2 % (w/v) bromophenol blue, 50 % (w/v) sucrose, 100 mM EDTA, pH 8.0). Gels were run in TAE buffer containing 0.5 mg ml^{-1} ethidium bromide at 100 V. Electrophoresis was halted when the bromophenol blue dye front neared the end of the gel. Gels were trans-illuminated with UV light for visualisation and photography of the DNA fragments via fluorescence of the intercalated ethidium bromide.

2.2.5. Isolation of DNA from agarose gels

A freeze-elution (freeze-squeeze) method was used to isolate DNA fragments from agarose gels. The DNA fragment was cut out from the gel in the smallest possible piece of agarose, taking care not to expose the DNA to UV light for longer than absolutely necessary. The agarose piece(s) were placed in an Eppendorf tube containing 0.9 ml sterile distilled water, 0.1 ml 3M sodium acetate and 10mM EDTA for 15 min with occasional gentle shaking. Meanwhile, a small Eppendorf tube was holed in the bottom and plugged with siliconised glass wool, placed in a large Eppendorf tube and washed through with 0.5 ml sterile distilled water. The gel slice was removed from the sodium acetate solution, blotted off, placed in the small Eppendorf and placed at -80 °C for 20 min. The smaller tube was placed in the larger tube and centrifuged 15 minutes, starting the spin before the fragment(s) melted. The eluent was then subjected to oyster glycogen precipitation.

2.2.6. Oligonucleotide probe labelling

Oligonucleotides were radioactively labelled with [^{32}P]dCTP using a Megaprime kit (Amersham International Plc.), following the manufacturer's recommendations.

The reaction mixture contained 300 ng of the DNA to be labelled with 7.5 µl of primer solution (containing random hexanucleotide primers) in a total volume of 50 µl. The DNA was denatured by boiling for 5 minutes before 15 µl of labelling buffer (containing dNTPs), 100 µCi [^{32}P] dCTP and 2 µl of Klenow fragment (from DNA polymerase I) were added and the reaction mixture incubated at room temperature for 80 minutes. The reaction was stopped with 1 µl of stop mix (20 mM EDTA pH 8.0, 2 mg ml^{-1} blue dextran, 0.02 mg/ml xylene cyanol) - the chelation of Mg^{2+} ions by EDTA

preventing further DNA polymerase I activity. Blue dextran and xylene cyanol are added as dyes to allow visualisation of DNA on a spin column.

Unincorporated nucleotides were separated from the labelled probe by centrifuging the reaction through a Bio-Rad Bio-Spin column containing Bio-Gel P-6 polyacrylamide gel that had an exclusion limit of approximately 5 bp. The column storage buffer was removed by centrifuging at 1100 g for 2 min. The reaction volume was carefully loaded onto the top of the column and the column placed in a collection tube and centrifuged at 1100 g for 4 min. The labelled probe was recovered from the collection tube and the specific activity of the incorporated radioactivity (dpm μg^{-1} DNA) was calculated after counting 1 µl of the probe solution with 5 ml of scintillation fluid in a scintillation counter.

2.2.7. DNA sequencing

DNA samples were sequenced using an ABI 373 DNA sequencer, which uses a thermal cycling, fluorescent terminator version of the Sanger method of dideoxy-mediated chain termination. Samples were handled by Julia Bartley of the department. Bluescript plasmids were sequenced using -21M13 (forward) and M13 (reverse) primers. pET vectors were sequenced through the transcription start site using primers based on the T7 promoter sequence and an internal primer corresponding to the appropriate βKR sequence (*B. napus* or *E. coli*). Oligonucleotide primers were synthesised using an ABI 381A DNA Synthesiser by John Gilroy of the department. Primers were resuspended in TE buffer after synthesis and an absorbance reading at 280nm of 1 µl in 1ml of Milli Q water was taken to assess concentration.

2.2.8. Preparation of bacterial chromosomal DNA

An aliquot (1.5 ml) of an *E. coli* overnight culture was added to an Eppendorf tube, centrifuged for 1 minute and the supernatant removed. The pellet was resuspended

in 380 µl of protease buffer (see below) and add 20µl Protease XI (20 mg ml^{-1} stock solution in H_2O). The suspension was incubated for 60 min at 37 °C until it became a clear and viscous solution. The DNA in the solution was sheared by pipetting up and down with a Pasteur pipette. Then 400 µl of phenol/chloroform was added, the mixture was vortexed and then centrifuged for 2 min. The upper phase was removed to a fresh tube. This was repeated five times and then finally a chloroform only extraction was performed. A 1/10 volume of 3 M sodium acetate, pH 4.8 and 2 volumes of ethanol were then added. The solution was stored at –70 °C for 20 min (store for 2 h if the DNA is not immediately apparent). It was then centrifuged for 10 min, and the resulting pellet was rinsed in 70% ethanol and dried under vacuum. The pellet was resuspended in 100 µl T.E. containing 200 µg ml^{-1} RNAase.

Solution used:

Protease buffer: 250 µl 1M Tris/HC1 pH 8.0.

40 µl 10 % (w/v) SDS

40 µl 250 mM EDTA pH 8.0

4.67 ml H_2O

2.2.9. Production and transformation of competent cells

The method used for the production and transformation of competent cells was based on that of Mandel and Higa, [1970]. Competent cells were prepared from a 100 ml culture grown to an optical density (550 nm) of 0.2, corresponding to $\approx 5 \times 10^7$ cells. The culture was chilled on ice for 10 minutes before harvesting via centrifugation at 4000 x g for 5 min at 4 °C. The supernatant was discarded and the cell pellet re-suspended in half the original volume of ice-cold, sterile 100 mM $CaCl_2$, pH 8.0. After a 15 min incubation on ice, the cells pellet was reformed at 4 000 x g for 5 min at 4 °C. The pellet was then re-suspended in 1/15 of the original volume of ice-cold 100 mM

$CaCl_2$, pH 8.0. After chilling on ice for 1-2 h, the now competent cells were aliquoted into 200 µl aliquots with 20 % (v/v) glycerol, flash frozen and stored at –80 °C.

To carry out cell transformation, a 200 µl aliquot of competent cells was brought to 500 µl with 100 mM $CaCl_2$, pH 8.0 and 100 µl used for each transformation. Approximately 20 ng of the transforming plasmid DNA was added to the competent cells and the mixture chilled on ice for 30 min. The cells were heat shocked at 42 °C for 2 min and then chilled on ice for a further 2 min. Pre-warmed LB liquid medium (1 ml) was added and the cells were incubated at 37 °C for 1 hour to permit expression of the β-lactamase antibiotic resistance gene. The cells , 1/10 and 9/10 of the volume of the tube, were then plated on LB agar plates containing 50 µg ml^{-1} ampicillin. After an overnight incubation, colonies were picked from the plates with a sterile toothpick, taking care to avoid smaller 'satellite' colonies of untransformed cells, which can grow in proximity to β-lactamase producing transformants. The transformed colonies were stored at –80 °C in 100 µl LB medium containing 15 % (v/v) glycerol. One 100 µl aliquot was sufficient to inoculate a 5 ml culture.

2.3. Protein methods

Specific methods are detailed in the following chapters. More general methods are further described below.

2.3.1. SDS-PAGE electrophoresis of proteins

For one-dimensional analyses, protein samples were run on acrylamide gels using the BioRad PROTEAN II system and BioRad reagents following the method of Laemmli [Laemmli, 1970].

Routinely, gels of 0.75 mm thickness were cast between 7 x 10 cm glass plates, with a 10% (w/v) 37.5:1 acrylamide/bis-acrylamide resolving gel and a 5% (w/v) 37.5:1 acrylamide/bis-acrylamide. The resolving gel acrylamide solution contained 0.375 M Tris-HCl, pH 8.8, 0.1 % (w/v) SDS, 0.014 % (w/v) ammonium persulphate and 0.2 % (v/v) TEMED. The stacking gel acrylamide solution consisted of in 0.1 % w/v SDS,

0.125 M Tris-HCl pH 6.8, 0.014 % (w/v) ammonium persulphate and 0.4 % v/v TEMED. The gel was cast in two stages. The resolving gel was cast in 3/5 of the available space between the glass plates. Before solidification, water saturated butanol was gently layered on top to give an even and bubble free surface upon which to cast the stacking gel. After setting, the butanol was drained from the cast and the gel rinsed with distilled water. The stacking gel solution was added so as to almost fill the remaining space between the plates and the well comb was inserted whilst the stacking solution remained liquid.

Prior to SDS-PAGE, protein samples were brought to 2 % (w/v) SDS, 60 mM DTT, 62.5 mM Tris-HCl, pH 6.8, 10% glycerol, 0.01% (w/v) bromophenol blue, by the addition of a 0.2 volume of a 5X stock. Prior to being loaded into the wells of the gel, the samples were held at near boiling point for 2 minutes in a water bath, briefly placed on ice and centrifuged for 10 seconds in a microfuge to spin down any unsolubilised material.

To perform the electrophoresis, one or two gels were assembled in a clamp, set in an tank and submerged in running buffer (0.1 % (w/v) SDS, 192 mM glycine and 25 mM Tris-HCl, pH 8.3). The bromophenol dye front of the samples was run through the stacking gel at a voltage of 100 V for approximately 10 min and then through to the bottom of the resolving gel at 200 V (which took approximately 30 min).

2.3.2. Gel staining procedures

After SDS-PAGE electrophoresis had been performed, the proteins present in the samples on the gel were stained with a Coomassie blue solution. The gel was placed in a microwave heated (60-70 °C) aqueous solution of 0.025 % (w/v) Coomassie Brilliant Blue in 25 % (v/v) propan-2-ol and 10 % (v/v) glacial acetic acid. After a

period of 5 min, or overnight, the gel was drained of the staining solution and destained in a similarly heated solution of 10 % (v/v) acetic acid and 1 % (v/v) glycerol. Further heating of this solution and exchange with fresh solution was performed to remove non-protein staining from the gel. Gels were dried in a stream of hot air between water soaked cellulose sheets after soaking in distilled water to remove remaining acetic acid.

2.3.3. Methanol /chloroform precipitation of proteins

To concentrate, desalt and remove lipid and other contaminants from protein samples for electrophoresis, the precipitation method of Wessel and Flügge [1984] was used. For a 100 µl protein sample, 400 µl of methanol was added, the mixture was vortexed for 10 s, and spun in a microfuge for 10 s. An addition of 100 µl of chloroform, was then followed by vortexing for 10 s and a 10 s spin. After a further brief vortex, 300 µl of Milli Q grade water was added. A further spin for 5 min was carried out and the upper phase, about 75% of the total, was discarded - with care taken to leave the precipitated proteins at the interface. Methanol (300 µl) was added and the solution vortexed and then spun for 3 min. The resulting supernatant was then discarded and the pellet dried under nitrogen. The pellet was then resuspended in the appropriate electrophoresis buffer.

2.3.4. TCA-Lowry protein assay

Protein concentration was estimated via a modified Lowry method [Peterson, 1983]. The method requires three major steps, sample and standard preparation, deoxycholate - trichloroacetic protein precipitation, and the protein assay. A series of ovalbumin standards from a zero to 80µg is set up. Several samples of the protein of interest of varying volumes and dilution are provided such that at least one final reading lies on the standard curve. All samples are brought to 1 ml with Milli Q water in

Eppendorf tubes. Precipitation of the protein in the sample is then carried out, starting with the addition of 100 µl 0.15% (w/v) deoxycholic acid. The resulting mixture is vortexed and allowed to stand at room temperature for 10 min, whereupon 100µl 72% trichloroacetic acid is added. The sample is then vortexed and spun for 10 min in microcentrifuge, after which the supernatant is decanted carefully with a pipette.

To perform the assay, the pellet is re-dissolved in 1 ml of Solution C (see below), vortexed and left to stand at room temperature for 5-10 min. After this time 100µl of Solution D is added and the sample is vortexed. After 20-30 minutes the absorbance of the samples and standards is read at 750 nm. Data from the standards is plotted and a line of best fit found to allow protein concentration values to be assigned to the samples.

Solutions used:

'Solution A': For 100 ml: 0.5g $CuSO_4.5H_2O$; 1g $Na_3C_6H_5O_7$; Add Milli Q water to 100 ml. May be stored indefinitely at room temperature.

'Solution B': For 1000 ml: 20g Na_2CO_3, 4g NaOH; Add Milli Q water to 1000 ml. May be stored indefinitely at room temperature.

'Solution C': Solution A: Solution B, 1:50 ratio. Make required volume fresh.

'Solution D': Milli Q water : Folin-Ciocalteu phenol reagent in a 1:1 ratio.

2.3.5. Determination of protein concentration in purified samples of *B. napus* βKR

As the deduced sequence of recombinant *B. napus* βKR was known, the concentration of protein in purified solutions of *B. napus* βKR was calculated using an calculated extinction coefficient of 72560 M^{-1} cm^{-1}. This coefficient provides an absorbance value at 280 nm of 0.671AU for a 1 mg^{-1} ml^{-1} solution of βKR tetramer. The extinction coefficient was calculated from the deduced amino acid sequence data of the

expression construct, and a theoretical molecular weight for the βKR tetramer from the same data of 108204.2, using the following formula: Abs 280nm [1 mg^{-1} ml^{-1}] = (5690nW + 1280nY + 120nC) / Mw according to Gill and von Hippel [1989].

2.3.6. β-Ketoacyl-ACP reductase assay

Routine enzyme assays were followed spectrophotometrically at 340 nm using an extinction coefficient of 6.22 x 10^3 M^{-1} cm^{-1} for calculation of the oxidation of NADPH. Each assay contained, 100 mM potassium phosphate buffer pH 7.0, 100 μM NADPH, 1-10 μl of sample and Milli Q grade water to a final volume of 100 μl. The reaction was initiated via the addition of the substrate analogue Acetoacetyl Coenzyme A (AcAcCoA) to a final concentration of 800 μM. The addition of substrates and enzyme in this order was found to be critical for the plant enzyme. Initiation of the reaction via the addition of enzyme gave rise to non-reproducible initial velocities. Extracts of over-expressed protein gave negligible rates of loss of NADPH prior to addition of the AcAcCoA substrate and therefore, the initial velocity data did not require correction.

2.3.7. Protein sequencing

Samples of purified proteins were loaded onto ProSpin cartridges (Applied Biosystems) for concentration and binding to a 3 kDa-cut-off PVDF filter, and spun at 5000 g for 70 min. The filter was loaded into the cartridge of an ABI477A Sequencer for gas phase sequencing via Edman chemistry.

2.3.8. Two-dimensional protein electrophoresis

Two-dimensional protein electrophoresis carried out by use of a Multiphor II electrophoresis system with Immobiline DryStrips and ExcelGel SDS gels (all Pharmacia). The method followed, based on that of O'Farrell [1975], was as suggested

by the manufacturer. Crude extracts were treated as described in §5.3.4 by ultracentrifugation and methanol/chloroform precipitation. The precipitated protein pellets (corresponding to 50-100 mg of protein) were dissolved in 50 µl sample buffer (2 % v/v Pharmalyte 3-10 ampholines, 8 M urea, 268 mM 2-mercaptoethanol, 0.5 % v/v Triton X-100) for 1 hour at room temperature. The ampholines contained in the sample buffer are a mixture of aliphatic amino acids with a range of iso-electric points which are used to set up the pH gradient used in the first dimension iso-electric focusing (IEF) separation).

The first dimension separation was carried out on Immobiline DryStrips, pH 3.0-10.5. The strips were re-hydrated in the provided cassette for 6 h or overnight in a solution of 8 M urea, 10 mM DTT, 2 mM acetic acid, 0.5 % (v/v) Triton X-100, in which enough crystals of Orange G were dissolved to stain the strips, thus aiding their visibility. The strips were then aligned on the provided tray and immersed in silicon oil (Dow-Corning 200 – Merck). The protein samples were loaded into sample cups, positioned flush with the surfaces of the DryStrips, beneath the surface of the silicon oil. The proteins were subjected to currents of 300 V for 3 h, 300 V ramping to 2000 V for 5 h, and 2000 V for 8 h; to a total of 22650 kVh. The oil-containing tray in which the strips were aligned was cooled to 15 °C throughout the focusing step by means of a hollow ceramic plate connected to a circulating waterbath. Focused DryStrips were either used immediately in the second stage electrophoresis step, or sealed in glass tubes and stored at –20 °C.

To prepare the DryStrips for second dimension electrophoresis, they were placed in equilibrating solution 1 {1 % (w/v) SDS, 6 M urea, 30 % (v/v) glycerol and 50 mM Tris/HCl, pH 6.8, 16 mM DTT} for 10 min, followed by solution 2 {1 % (w/v) SDS, 6 M urea, 30 % (v/v) glycerol and 50 mM Tris/HCl, pH 6.8, 243 mM iodoacetamide and a few grains of bromophenol blue per 10 ml} for 10 minutes, both equilibration steps

being at room temperature. Iodoacetamide is included in the second solution to react with excess DTT, which can cause streaking on the gels.

Precast ExcelGel SDS 8-18 % gradient gels were used for the second dimension. The IEF strips were placed in pairs on each gel, which was in turn placed on the 15 °C cooling block. A current of 20 mA was applied to the gel via buffer gel strips for 20 min, followed by 50 mA for 10 min. The IEF DryStrips were then removed and the cathodic buffer strip placed in their place. A current of 50 mA was then applied to the gel for 70 min to resolve the proteins, the progress of which was indicated by the dye front provided by the bromophenol blue incorporated in the equilibration solution.

2.3.9. Electro-blotting of proteins on to nitrocellulose.

Gels from 1D and 2D procedures were subjected to semi-dry blotting using the MultiPhor/MultiDrive system (Pharmacia). Hybond C extra nitrocellulose (Amersham), and nine sheets of Whatman 3MM filter paper cut to the size of the gel were soaked in transfer buffer (49 mM Tris, 39 mM glycine, 0.037% (w/v) SDS, 20% methanol). Six sheets of soaked filter paper were layered on the anodic plate. The nitrocellulose was placed on top of the filter paper followed by the gel. The gel was also briefly soaked in transfer buffer to make it easier to manipulate on the filter and to aid air bubble removal. A final three sheets of filter paper were placed on top of the gel, before the cathodic plate was placed on top of the blot. Transfer was carried out at 0.8 mA cm^{-2} for 1 hour at room temperature. After transfer, the blot was air dried and stained with a solution of Ponceau S dye (0.1 % (w/v) Ponceau S; 1 % (v/v) glacial acetic acid) to visualise Mw standards, and de-stained with several 1 % (v/v) glacial acetic acid washes followed by a final rinse with Milli Q water.

2.3.10. Immunodetection of Proteins

To prepare blots for immunodetection, they were blocked with 1% haemoglobin in phosphate buffered saline (1%Hb-PBS) including 0.02% sodium azide (PBS; 137 mM NaCl, 3 mM KCl, 8 mM $Na_2HPO_4 \cdot 2H_2O$, 2 mM KH_2PO_4, pH 7.4). This was carried out for a minimum of two hours at room temperature in a rotary hybridisation oven or overnight at 4 °C. The blots were briefly rinsed in 50 ml of phosphate buffered saline containing 0.1 % v/v Tween-20 (PBS-T). The primary (1°) antibody (anti-βKR) was then added at a suitable dilution (e.g. 1:1000) in 10 ml of 1% haemoglobin-PBS and incubated for 2 h. The 1° antibody was drained off and the blot rinsed with 5 x 50 ml phosphate buffered saline (0.1% Tween-20) over 30 min. The 2° antibody (5 μCi of donkey anti-rabbit IgG ^{125}I (Amersham) in 10 ml of 1% Haemoglobin-PBS) was then applied for 1 h. The blot was rinsed as before, sealed in Saran wrap (DuPont) and exposed to x-ray film (Fuji) at -80°C overnight. Where mouse-derived polyclonal antibodies were used as the primary antibody, a rabbit anti-mouse IgG was used as a secondary antibody (Pierce) to facilitate detection by a, now tertiary, labelled anti-rabbit IgG antibody.

Chapter 3: Over-expression and purification of *B. napus* βKR

3.1 Introduction

Over-expression of a plant βKR is desirable as the enzyme is generally only present in plant materials in appreciable amounts during storage lipid deposition. The amount of enzyme that can be purified from storage lipid producing plant tissues is far lower than the milligram amounts potentially obtainable from the over-expression of a βKR gene in *E. coli*. Such increased availability would enhance and facilitate structural immunological and kinetics studies on the enzyme.

Previous to this study, a full length clone for βKR from *Arabidopsis thaliana* was obtained in our laboratory [Slabas *et al.*, 1992a]. A 0.4 kb probe corresponding to a 5' region of the mature protein coding sequence of this clone was used by Dr José Martinez-Rivas to screen a lambda-ZAP II cDNA library of *Brassica napus* developing seed. Several clones were isolated, the largest of which were sequenced.

One of the clones, pJRS10.1, containing the complete coding sequence for *B. napus* seed βKR in an open reading frame of 944 bp, was chosen for over-expression in *E. coli*. As this clone was not obtained by the author, the subject study of this thesis included the use, to gain experience in essential techniques, of the *B. napus* pJRS10.1 cDNA in the cloning of a βKR partial cDNA sequence from an avocado (*Persea americana*) cDNA library. Figure 3.1 shows the DNA sequence of the insert in clone pJRS10.1.

It was intended to modify the *B. napus* βKR cDNA clone via PCR to allow insertion of the mature protein coding into a pET over-expression vector for subsequent transformation of *E. coli* strain BL21(DE3). Once this had been achieved, expression trials would be carried out to confirm over-expression of the plant enzyme. Large quantities of the transformed cells would then be grown in liquid culture as a source of the plant enzyme.

Once in possession of crude extracts containing active *B. napus* βKR, a convenient method of chromatography would be sought to produce purified βKR samples suitable for raising antibodies, and for performing kinetic and structural studies.

```
pJRS10.1    cctctctctctctctccctctccacccgtctccacctcctcctccgtt
                    10         20         30         40         50
pJRS10.1    cgATGGCAACCACCGTCGCAGCAACAAAGCTCACCTCCTTGAAAGCCGTC
                   60         70         80         90        100
pJRS10.1    AAGAAGCTCGGTTTCCGTGAGATCCGTCAGGTCCGTCAATGGACTCCGCT
                  110        120        130        140        150
pJRS10.1    TCAGTCTTCGATGCCTCATTTCGGATCGCGGCAGTCATTCGCAACCTCCA
                  160        170        180        190        200
pJRS10.1    CTGTTGTGAAAGCTCAAGCGACAGCTGTTGAGCAATCGACAGGAGAAGCT
                  210        220        230        240        250
pJRS10.1    GTTCCGAAAGTGGAGTCTCCGGTGGTCGTTGTGACTGGTGCTTCGAGAGG
                  260        270        280        290        300
pJRS10.1    GATTGGTAAAGCTATTGCTCTTTCCTTGGGCAAAGCTGGCTGCAAGGTCT
                  310        320        330        340        350
pJRS10.1    TGGTGAACTATGCTAGGTCAGCAAAGGAGGCTGAGGAAGTTTCTAAACAG
                  360        370        380        390        400
pJRS10.1    ATTGAAGCATATGGAGGCCAGGCTATTACTTTTGGGGGTGATGTCTCCAA
                  410        420        430        440        450
pJRS10.1    AGAGGCTGATGTGGAAGCCATGATGAAAACCGCTATTGATGCATGGGGAA
                  460        470        480        490        500
pJRS10.1    CCATTGATGTCGTCGTCAACAATGCAGGAATCACTCGGGATACCTTGTTG
                  510        520        530        540        550
pJRS10.1    ATACGAATGAAGAAGTCCCAATGGGATGAAGTGATTGATTTGAATCTCAC
                  560        570        580        590        600
pJRS10.1    TGGAGTCTTTCTCTGTACCCAGGCAGCAACAAAGATCATGATGAAGAAGA
                  610        620        630        640        650
pJRS10.1    GAAAGGGAAGAATCATCAACATTGCGTCAGTTGTTGGTCTCATTGGTAAT
                  660        670        680        690        700
pJRS10.1    ATTGGCCAAGCAAACTACGCTGCTGCTAAAGCTGGTGTTATTGGGTTCTC
                  710        720        730        740        750
pJRS10.1    CAAGACTGCCGCCAGAGAGGGTGCGAGCAGGAATATAAATGTCAATGTGG
                  760        770        780        790        800
pJRS10.1    TTTGCCCTGGGTTCATTGCATCTGACATGACTGCCAAGCTTGGAGAAGAC
                  810        820        830        840        850
pJRS10.1    ATGGAAAAGAAAATCTTGGGAACAATCCCATTAGGACGATATGGACAACC
                  860        870        880        890        900
pJRS10.1    TGAAGATGTGGCTGGCTTGGTAGAATTCTTGGCTCTCAGTCCTGCAGCTA
                  910        920        930        940        950
pJRS10.1    GTTACATCACAGGACAGGCATTCACCATTGATGGAGGTATTGCCATCTAG
                  960        970        980        990       1000
pJRS10.1    gcatttgttaagagttgctttgtgtttaggcaaaaccgatttggtaaaac
                 1010       1020       1030       1040       1050
pJRS10.1    agacaaagttgagtttattccggcacttggtcggatttctgttctgtgga
                 1060       1070       1080       1090       1100
pJRS10.1    ttctgttcggagagaaatctaaaacgcattgcttaaactaagttacgtaa
                 1110       1120       1130       1140       1150
pJRS10.1    aaaaaaaaaaaaaaaaaa
                 1160
```

Figure 3.1 DNA sequence of clone pJRS10.1 encoding *B. napus* βKR.

The diagram shows the DNA sequence of the βKR encoding insert contained in clone pJRS10.1 (a bluescript plasmid). The open reading frame encoding βKR is shown in capital letters.

3.2 Cloning of a partial cDNA corresponding to βKR from Avocado

As previously stated the clone used in this study was not obtained by the author. For this reason, the same clone was used to clone a plant βKR sequence from an avocado cDNA library. Although 3-oxoacyl-ACP reductase was purified from avocado several years ago [Sheldon *et al.*, 1990; Sheldon, 1988], no DNA sequence, either genomic or cDNA, has been reported for this enzyme. The amino acid sequences that were obtained in the above work from tryptic peptides of purified βKR are not of low enough genetic redundancy to allow effective oligonucleotide probes to be synthesised from them.

A 700 bp fragment of the *B. napus* βKR cDNA pJRS10.1 was isolated, radioactively labelled and used to probe an avocado λZAPII cDNA library. Six positive plaques were observed in the first round of screening. These were reduced to two distinct clones after three further rounds of plaque purification (figure 3.2). Plasmids were excised from the two clones and were subjected to automated DNA sequencing. The data returned showed the two clones to be closely related and both truncated part-way through the encoded βKR sequence at a region rich in adenosine residues. The raw sequence data were compiled and corrected to give a partial deduced amino acid sequence for avocado βKR - see figure 3.3. This sequence was compared with peptide sequences previously obtained for the avocado enzyme and with deduced sequences from βKR cDNAs obtained from other plant species (§7.4). The results of this work provided sequence data that could be used to specifically identify and isolate a full length sequence encoding βKR from avocado at some future date.

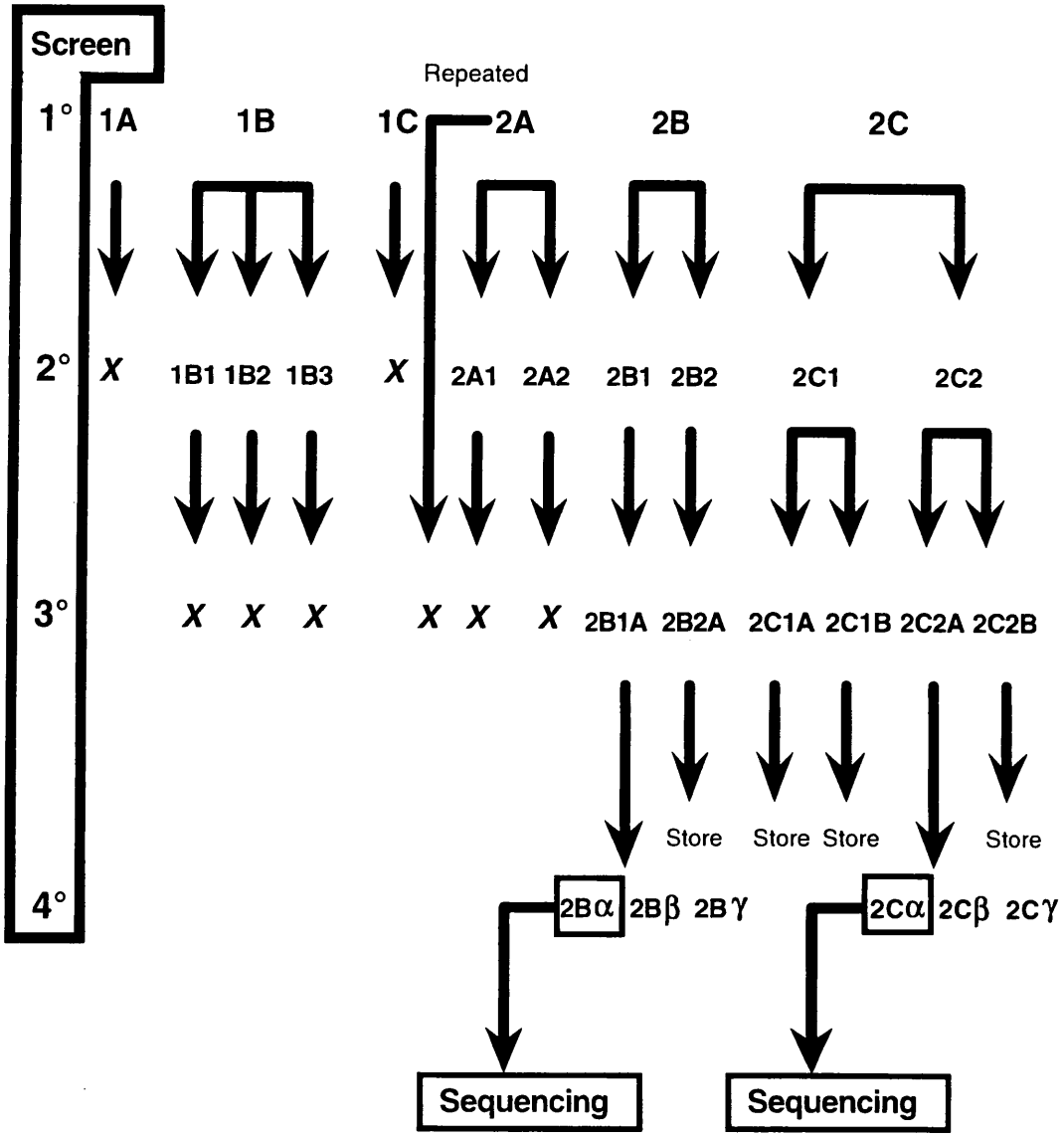

Figure 3.2 Results of screenings of an avocado cDNA library with a 700 bp fragment of *B. napus* βKR mature protein coding sequence.

The diagram shows the progress of the four screens carried out on the avocado cDNA library. The sequenced clones 2Bα and 2Cα are boxed.

```
GGA CCC CCG GGC TGC AGG GAA TTC GGC ACG      30
G   P   P   G   C   R   E   F   G   T

AGG GGG AAA GCT GGT TGT AAG GTA CTT GTA      60
R   G   K   A   G   C   K   V   L   V

AAT TAT GCA AGG TCC TCA AAA GAG GCT GAA      90
N   Y   A   R   S   S   K   E   A   E

GAA GTT TCC AAG GAG ATT GAA GCA TCT GGT     120
E   V   S   K   E   I   E   A   S   G

GGC CAA GCC CTT ACT TTT GGG GGA GAT GTT     150
G   Q   A   L   T   F   G   G   D   V

TCA AAA GAA GCT GAT GTG GAA GCT ATG ATA     180
S   K   E   A   D   V   E   A   M   I

AAA ACT GCA GTT GAT GCA TGG GGA ACA GTT     210
K   T   A   V   D   A   W   G   T   V

GAT GTA TTG ATA AAC AAT GCA GGA ATT ACT     240
D   V   L   I   N   N   A   G   I   T

CGG GAT ACA TTG TTG ATG AGA ATG AAG AAA     270
R   D   T   L   L   M   R   M   K   K

TCT CAA TGG CAA GAA GTT ATT GAT TTA AAT     300
S   Q   W   Q   E   V   I   D   L   N

CTT ACT GGT GTA TTT CTC TGC ACA CAG GCT     330
L   T   G   V   F   L   C   T   Q   A

GCA ACC AAA ATT ATG ATG                     348
A   T   K   I   M   M
```

Figure 3.3 The deduced partial amino acid sequence of the cloned βKR cDNA from avocado.

The cDNA sequence shown above was derived from non-degenerate sequence data from the consensus sequence of clones 2Bα (reverse primers) and 2Cα (forward and reverse primers) - see figure 3.2. A multi-frame translation of this data was compared with the *B. napus* βKR cDNA deduced amino acid sequence to refine the final sequence from the raw sequence data, which contained two erroneous frame shifts. These data were used in a comparison of published plant βKR sequences – see §7.4.

3.3 Construction of βKR over-expression plasmid pETJRS10.1

3.3.1 Characterisation of clone pJRS10.1

DNA from plasmid pJRS10.1 was prepared on a midi scale from cells from a glycerol stock held in the laboratory, designated 'TG-2 (K7)'. The identity of the plasmid was confirmed via comparison of restriction digest products with the restriction map obtained from previous sequencing of the plasmid. A pET-11d over-expression vector designated pEAR2 (containing an enoyl reductase clone) was also checked via restriction digest. A restriction map of the vector is given in figure 3.4. The reactions contained approximately 160 ng of DNA, with 1 unit of each restriction enzyme (*Nco*I and *Bam*HI) and the appropriate manufacturer's buffer in a reaction volume of 10 µl. After the addition of 1 µl of loading dye, the whole volume of each reaction was run out on a 0.7% agarose TAE gel. Figure 3.5 shows the restriction products of the two digests.

3.3.2 Primer design

The *B. napus* βKR clone, pJRS10.1, was used as a PCR template with primers designed to amplify the mature protein coding sequence and flank it with *Nco*I and *Bam*HI restriction sites. The primers were as follows: primer #590 (upstream *Nco*I site) 5'-GC GCC ATG GCG ACA GCT GTT GAG-3'; primer #593 (downstream *Bam*HI site) 5'-CAG GAT CCA CAG AAC AGA AAT CCG-3'. Figure 3.6 shows the alignment between the primers and the βKR sequence. The primers were also designed to incorporate additional bases adjacent to the inserted restriction sites, to allow recognition and restriction of the target sequences by the restriction enzymes used.

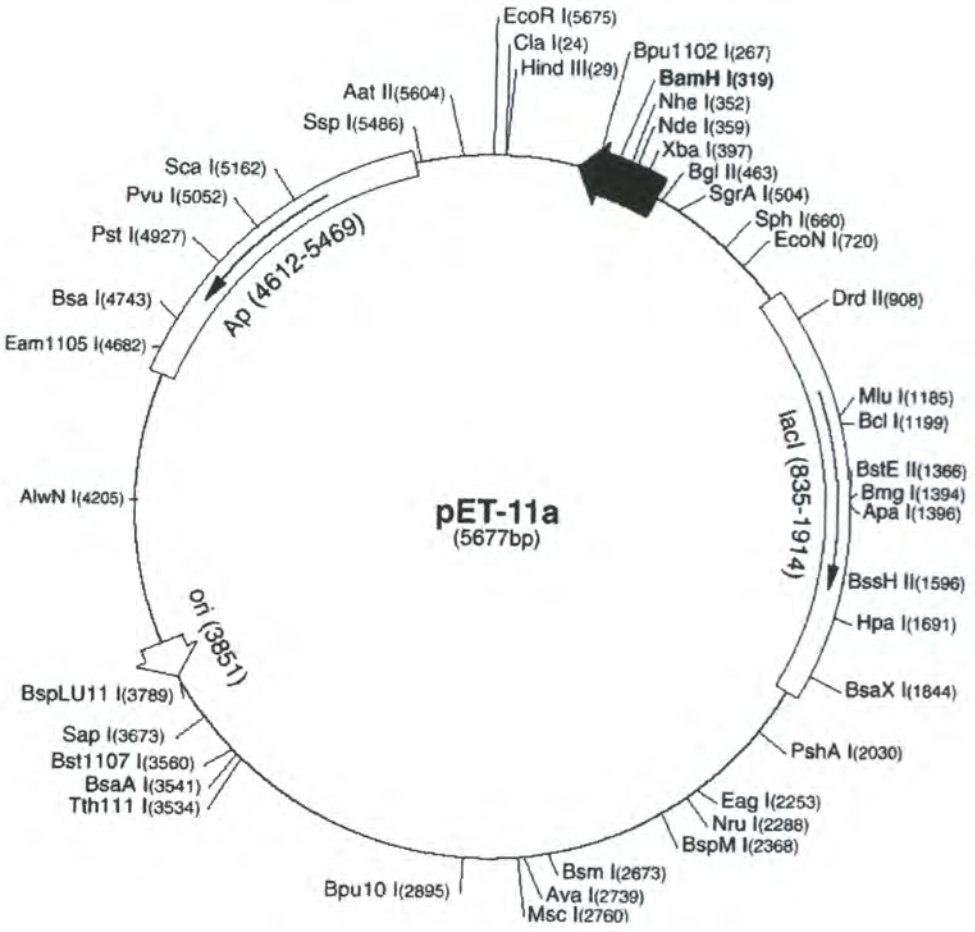

Figure 3.4 Restriction map of plasmid pET11a.

This plasmid, the use of which is described in §4, is equivalent to the plasmid pET11d which was used, in the guise of plasmid pEAR2, to create pETJRS10.1 a βKR over-expression plasmid. The only difference between the two vectors is that in pET11d the *Nde*I site at position 359 is replaced by an *Nco*I site. The features marked are 'Ap' = ampicillin resistance gene (β-lactamase), 'lacI' = *lac* repressor, 'ori' = ColE1 derived origin of replication, black arrow = multiple cloning site incorporating the T7*lac* promoter containing the T7 promoter sequence and lac operator sequence.

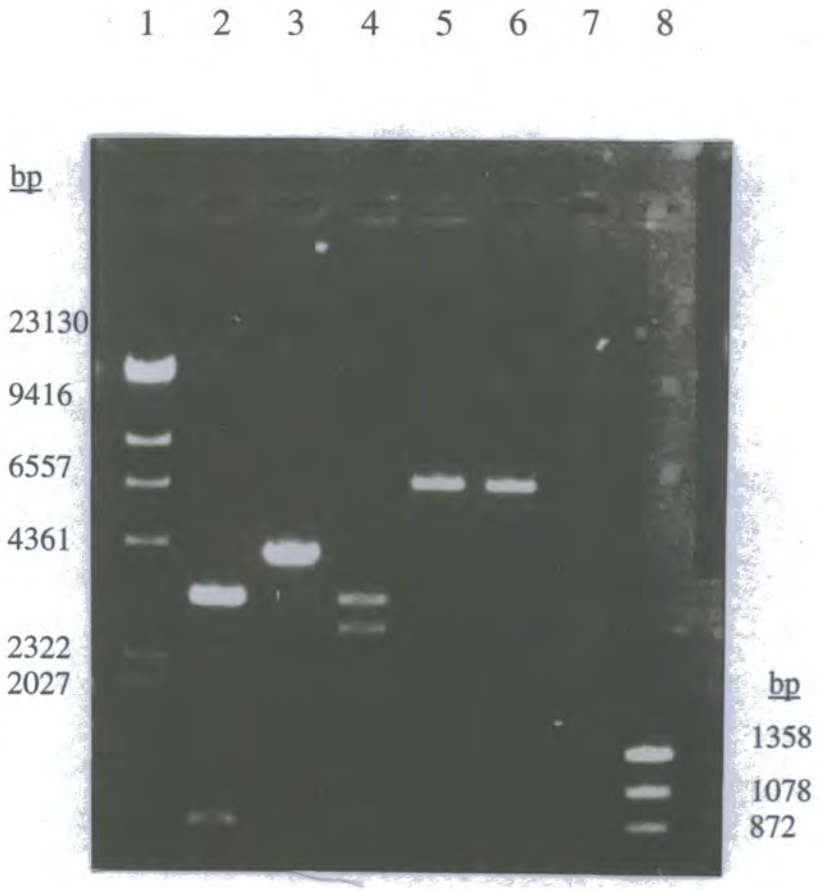

Figure 3.5 Agarose TAE gel (0.7%) showing restriction products of plasmids pJRS10.1 and pEAR2.

Lane 1, λ*Hind*III digest Mw markers; lane 2, pJRS10.1 restricted with *Eco*RI; lane 3, pJRS10.1 restricted with *Bam*HI; lane 4, pJRS10.1 restricted with *Eco*RI and *Bam*HI; lane 5, pEAR2 restricted with *Nco*I; lane 6, pEAR2 restricted with *Bam*HI; lane 7, pEAR2 restricted with *Nco*I and *Bam*HI; lane 8, ϕX-174 *Hae*III digest Mw markers.

Lanes 2, 3, 6 and 7 show the expected fragment sizes from restriction map data. The use of an inappropriate buffer caused the ambiguous double digest results in lanes 3 and 4. The double digest was facilitated in a repeat of these digests by swapping the buffer to that of another manufacturer's recommendation and the correct fragment sizes obtained.

3.3.3 PCR modification of pJRS10.1

Polymerase chain reactions, in a final volume of 100 µl, contained 50-100 ng of template DNA (pJRS10.1), each dNTP at 200 µM, the above primers at 20 µM, 1 unit of Taq polymerase (New England Biolabs) and the supplied buffer (final concentration 50 mM KCl, 10 mM Tris/HCl pH 8.8, 0.08% Nonidet P40, 1.5 mM $MgCl_2$). The reaction temperatures were cycled 26 times, 30 s at 91 °C, 30 s at 55 °C and 90 s at 72 °C (5 min at 72 °C for the final cycle). The reaction volume (100 µl) was removed with a pipette from beneath the oil layer, and 500 µl of chloroform was added. The phases were vortexed and subjected to a brief microcentrifuge pulse-spin to separate them. The aqueous phase was incubated in a 42 °C water bath to evaporate any remaining chloroform.

Four reactions were set up containing the aforementioned components plus template DNA. Reactions 1 and 2 contained one of each of the two primers, reaction 3 contained the complete reaction mixture and in reaction 4 the template DNA was omitted. To visualise the reaction products, 1 µl of each reaction was run out on a 0.7% agarose TAE gel, which is shown in figure 3.7. The expected 890 bp product is seen in lane 4. To provide sufficient amplified DNA for restriction and ligation three 100 µl reactions identical to reaction 3 above were carried out. To check the reaction products, 1 µl of each reaction was run out on a 0.7% agarose TAE gel. Again, the expected 890 bp product was obtained. The remainder of the three reactions was pooled and cleaned of primers, dNTPs and polymerase with the use of Promega 'Magiclean' columns according to the manufacturer's instructions. An aliquot (1 µl) of the cleaned PCR product was run on a gel to estimate its concentration, which was found to be 22.5 ng μl^{-1}.

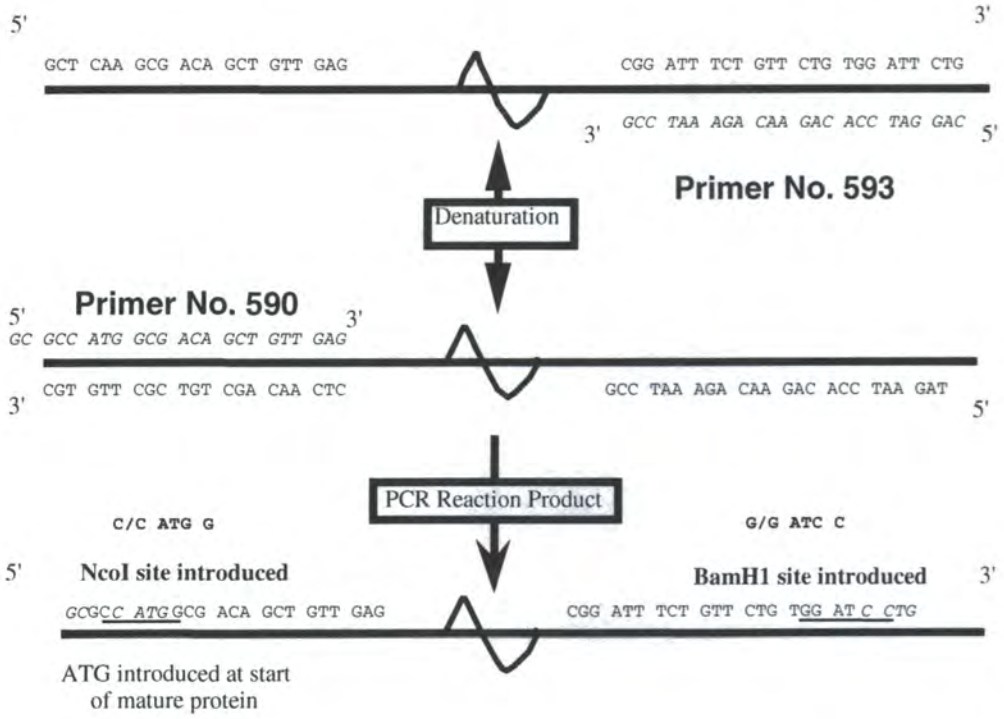

Figure 3.6 Diagram showing the alignment and reaction product of primers designed to amplify the *B. napus* mature protein coding sequence and flank it with *Nco*I and *Bam*HI restriction sites.

Primer DNA and altered bases are shown in italics, and inserted restriction sites are underlined.

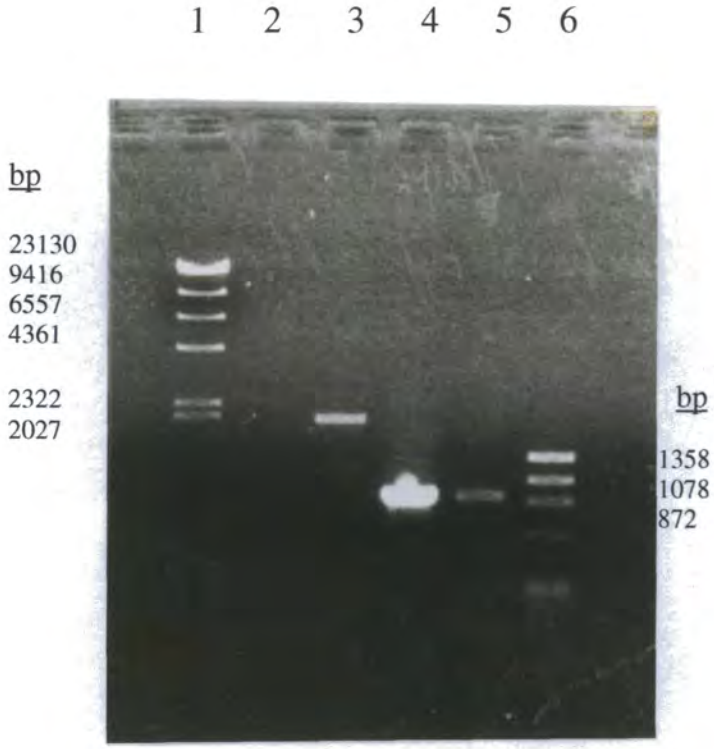

Figure 3.7 Agarose TAE gel (0.7%) showing products from a PCR reaction designed to amplify and modify the *B. napus* βKR mature protein coding sequence.

Lane 1, λ*Hind*III digest Mw markers; lane 2, reaction containing pJRS10.1 as template and primer #593; lane 3, reaction containing pJRS10.1 as template and primer #590; lane 4, reaction containing pJRS10.1 as template and primers #593 and #590; lane 5, reaction containing no template DNA and primers #593 and #590; lane 6, ϕX-174 *Hae*III digest Mw markers.

The expected 890 bp product is seen in lane 4. The product visible in lane 5 was either carried over during gel loading or during the setting up of the reactions. Subsequent reactions containing no template DNA showed no products.

3.3.4 Vector construction

Plasmid pEAR2, a pET-11d over-expression vector, was previously characterised by restriction digest (see figure 3.5). To remove the enoyl-ACP reductase sequence, DNA from a midi-scale preparation of the plasmid was restricted with *Nco*I and *Bam*HI, and the cut plasmid was subsequently gel purified. Figure 3.8 shows the 0.7% agarose TAE gel used to purify the cut vector. The bands containing the vector were excised from the gel and the DNA contained within them was electro-eluted from the agarose pieces in a Bio-Trap apparatus (Schleicher and Schuell, Dassel, Germany) for 1 hour at 100 V followed by 1 min of reverse polarity current to release the DNA from the trapping membrane. The eluent was phenol/chloroform extracted, ethanol precipitated and resuspended in 20 µl of TE. The resuspended eluent (1 µl) was run out on a 0.7% agarose TAE gel with λ*Hind*III markers. The concentration of the vector was estimated to be 22.5 ng μl^{-1} from this gel.

A simultaneous digest of the *B. napus* βKR mature coding sequence PCR product was carried out using *Nco*I and *Bam*HI restriction enzymes. After a 3.5 h incubation the 100 µl reaction was treated with phenol / chloroform to remove the restriction endonucleases before ligation was carried out. The vector and insert, now possessing complementary 'sticky ends' were capable of undergoing a ligation reaction. As both vector and insert had a concentration of 22.5 ng μl^{-1}, the ligation reaction contained 4 µl of each to give a final mass of 100 ng. One unit of T4 ligase and 1 µl of the manufacturers' supplied buffer concentrate were also included; the reaction was incubated at room temperature overnight. A range of ligation products was visible when 5 µl of the reaction was run out on a 0.7% agarose TAE gel, shown in figure 3.9

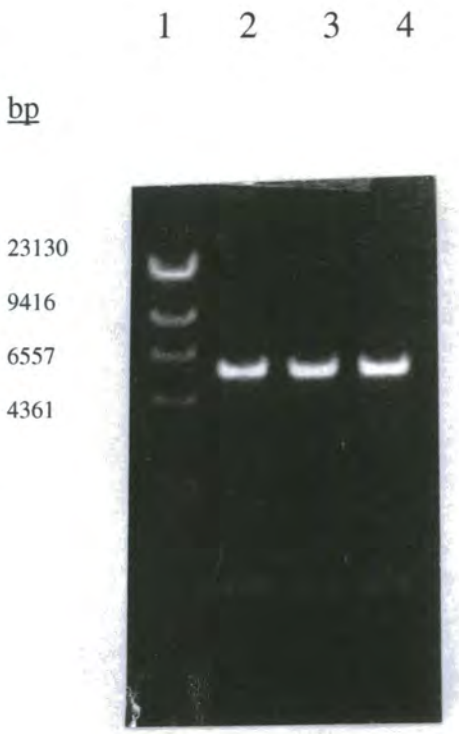

Figure 3.8 Purification of pET-11d from restricted pEAR2 using a 0.7% agarose TAE gel.

Lane 1, λ*Hind*III digest Mw markers; lanes 2-4, pEAR vector cut with *Nco*I and *Bam*HI to release pET-11d vector.

Bands containing the cut vector (minus insert) were excised from this gel and subjected to electro-elution. DNA fragments from a λ*Hind*III digest were used as size markers.

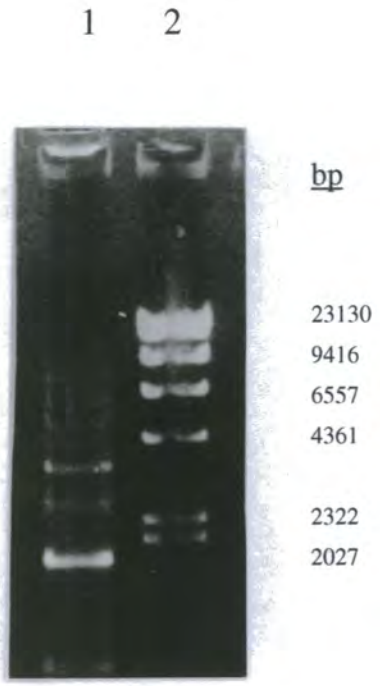

Figure 3.9 Agarose TAE gel (0.7%) showing products of the ligation between pET-11d and the *B. napus* βKR mature protein coding sequence.

Lane 1, ligation reaction products; lane 2, λ*Hind*III digest Mw markers.

An aliquot (5 µl) of the ligation reaction was run out on a 0.7% Agarose TAE gel. As expected, a range of multimeric products is seen.

3.3.5 Characterisation of over-expression plasmid pETJRS10.1

Competent XL1-Blue and BL21(DE3) cells were transformed with the remaining 5 µl of the ligation reaction. The transformed cells, 1/10 and 9/10 of the transformation volume, were then plated on LB agar plates containing 50 µg ml^{-1} ampicillin to select for the ampicillin resistance gene carried on the pET-11d vector. Both sets of plates were incubated overnight at 37 °C. After incubation colonies were found on the plate containing XL1-Blue cells from a 9/10 ligation volume inoculation. None was present on the other XL1-Blue or BL21(DE3) plates. Twelve randomly picked colonies from the plate were used to produce a stock plate and twelve corresponding 5 ml LB (plus ampicillin) liquid cultures. These cultures were incubated overnight at 37 °C. Mini-scale plasmid preparations were carried out on the cells from the twelve transformant cultures. The DNA produced was characterised by restriction digest with *Bam*HI, to linearise the plasmid. Figure 3.10 shows the restriction pattern of the twelve clones after running the digests out on a 0.7% agarose TAE gel. Transformants 1, 2, 6, 7, and 11 show the correct plasmid size of 6567 bp (5677 bp vector + 890 bp insert). These transformants were further characterised by a double restriction digest with *Nco*I and *Bam*HI. Figure 3.11 shows the products of these digests. All transformants show the expected products; 5677 bp vector fragment and a 890 bp insert fragment. The plasmids within these transformants were designated pETJRS10.1 (1, 2, 6, 7, and 11).

Two 50 ml LB (plus ampicillin) liquid cultures of transformants 1 and 2 were set up and incubated overnight. A midi-scale plasmid preparation was carried out and the DNA precipitated with polyethylene glycol and run on a gel to estimate concentration prior to DNA sequencing. A concentration estimation of 240 ng μl^{-1} was used to provide the required amount of DNA for sequencing (i.e. 1.5 µg in 6 µl). A primer, designated #358, previously designed to sequence an *A. thaliana* βKR cDNA clone was

used to read through the junction between insert and the T7 promoter present in the pET vector. The sequence data returned are shown in figure 3.12. The data from both transformants confirm that the insert is in frame with the ATG start codon contained within the *Nco*I site. The pETJRS10.1 plasmid is shown in figure 3.13.

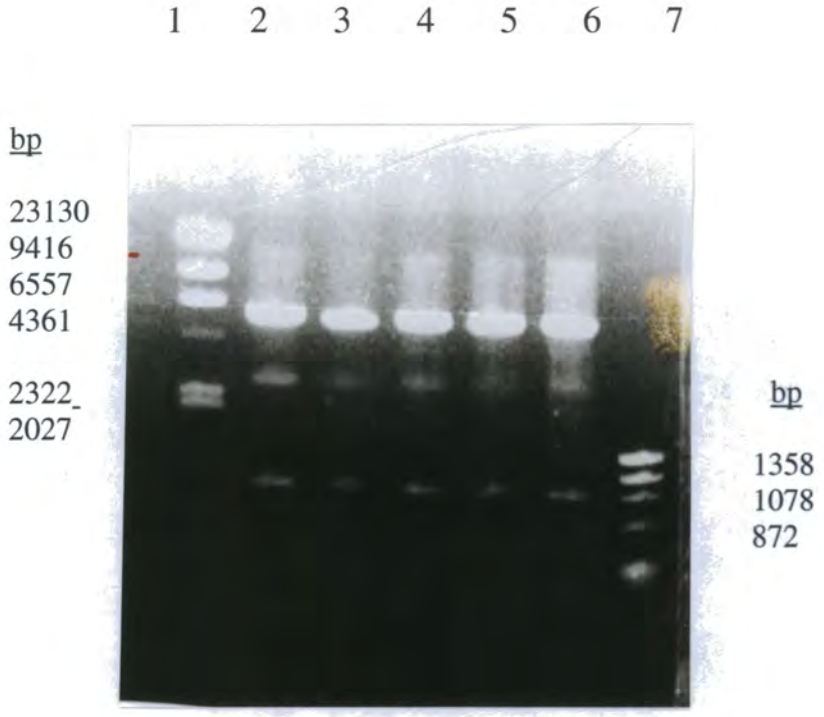

Figure 3.11 Further characterisation of pET-11d - (pETJRS10.1) transformants via double restriction digest.

Lane 1, λ*Hind*III digest Mw markers; lanes 2-6, transformants 1, 2, 6 ,7 and 11; lane 7, ϕX-174 *Hae*III digest Mw markers.

All transformants show the expected products, 5677 bp vector fragment and a 890 bp insert fragment, upon digestion with *Nco*I and *Bam*HI.

pET-11d sequence: TAT AC/C ATG GCT AGC ...

*Nco*I site

pETJRS10.1 sequence: TAT ACC ATG GCG ACA GCT GTT ...

Mature βKR sequence

Figure 3.12 Data from the sequencing of the transformants pETJRS10.1 (1 & 2).

The sequence data from both transformants confirmed that the positioning of the insert is correct and in frame.

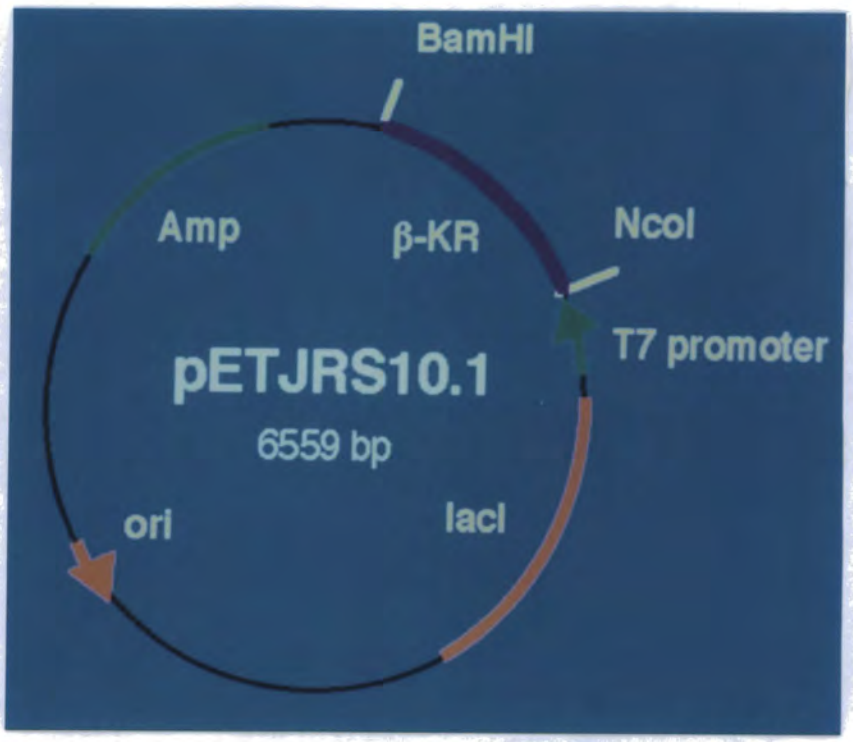

Figure 3.13 *B. napus* βKR over-expression plasmid, pETJRS10.1

This figure shows the 890 bp *Nco*I-*Bam*HI fragment corresponding to the βKR mature protein coding sequence under the control of a *lac* inducible T7 promoter, in a pET-11d vector selectable via ampicillin resistance.

3.4 Production of βKR in *E. coli*

3.4.1 Transformation of *E. coli* BL21(DE3)

As the previous transformations had only been successful with XL1-Blue cells and not with the BL21(DE3) over-expressing strain, a new preparation of competent *E. coli* BL21(DE3) cells was prepared and transformed with pETJRS10.1. Transformations were carried out with plasmid DNA from the previous transformants - which contained pETJRS10.1 and were numbered 1, 2, 6, 7 and 11. Colonies were picked from an LB agar (plus ampicillin) plate and used to make a stock plate containing each of the five plasmids in BL21(DE3).

3.4.2 Over-expression trials

Transformed *E. coli* strain BL21(DE3) pETJRS10.1 (transformants 1 and 6) was used in trial over-expression cultures. These were grown in 5 ml Luria Broth (LB) containing 100 μg ml^{-1} ampicillin, for selection of transformants, on a rotary shaker at 220 rpm for 16 h at 37°C. Aliquots of 50 μl were inoculated into 5 ml of LB plus 100 μg ml^{-1} ampicillin and cultured for three hours. The cultures were then divided into 2 x 2.5 ml cultures, one of which was brought to 100 μM IPTG, and both were grown for a further three hours. Uninduced cell cultures and cells transformed with the unmodified pET-11d vector were grown as controls. The centrifuge-harvested cells from each 2.5 ml culture were resuspended in 200 μl of Laemmli SDS-PAGE loading buffer [Laemmli, 1970], boiled for 3 min, centrifuged briefly, and 10 μl aliquots were loaded in each gel lane.

Over-expression of βKR in cells containing pETJRS10.1 was visualised via SDS-PAGE, this is shown in figure 3.14. Over-expression of the plant gene is clearly seen at 27 kDa in the IPTG induced cultures of transformed cells containing plasmid pETJRS10.1.

3.4.3 Assays for βKR activity

In addition to comparison via SDS-PAGE, lysozymal extracts (for method see §3.5.2.) from transformed strains were assayed for βKR activity. To facilitate detection of enzyme activity, a βKR assay (§2.3.6) was first set up using a protein extract from developing *B. napus* seeds. A sample of frozen *B. napus* seed (5 g) was ground in liquid

N_2 to a fine powder in a chilled pestle and mortar. The powder was added to 10 ml of homogenisation buffer: 100 mM KH_2PO_4 / K_2HPO_4 , 1 mM DTT, 4 mM EDTA, pH 7.0. The mixture was homogenised in a Polytron for 10 seconds at full speed, and then filtered through 4 layered muslin cloth into a cold beaker on ice. The filtrate was then centrifuged at 40 000g for 15-20 min at 4 °C. After centrifugation the supernatant was poured through glass fibre and the eluent collected. Assays (1 ml) were carried out with 1-50 µl of this extract in mixtures containing 100 mM KH_2PO_4 / K_2HPO_4 pH 7.0, 100µM NADPH, 100µM Acetoacetyl-CoA, with the components (minus the thioester substrate) pre-incubated at 30°C for 1 min prior to the assay. The decrease in absorbance at 340 nm was recorded to monitor substrate dependent oxidation of NADPH. The assay was checked for linearity through the measurement of βKR activity in several different volumes of extract.

The same assay conditions were used to assay lysozymal extracts from the BL21(DE3) (pETJRS10.1) strain for βKR activity. With the amount of extract used in each assay (approximately 5 µg of total extracted protein per 1 ml assay) and the assay conditions used, activity was only measurable in extracts from cells containing pETJRS10.1. Activity was not detectable in untransformed cells. Comparable levels of activity, 7.7 x 10^{-3} U μg^{-1} total protein, were observed between extracts that derived from IPTG induced and non-induced cultures, giving evidence of 'leaky expression' with this particular plasmid construct. This can be a major problem when the gene product is toxic to the over-expressing cell. However, in this case, cell growth and protein expression did not seem to be affected. IPTG was still used for induction in subsequent cultures to ensure maximal expression.

3.4.4 Immunological detection of over-expressed βKR

The identity of the over-produced protein was further confirmed as *B. napus* βKR, using an antibody raised against Avocado βKR [Sheldon, 1988; Sheldon *et al.*, 1990] on a western blot of an SDS-PAGE gel containing protein from the transformed cells. The exposed x-ray film is shown in figure 3.15. Only pETJRS10.1 transformed extracts gave a cross reaction in the 27 kDa region of the gel-blotted filter after

immunodetection procedures were carried out. No cross-reaction was seen in the extract from untransformed BL21(DE3). The enzyme was also detected in an extract of avocado, but not in a sample of *B. napus* developing seed, despite being loaded on the gel at 100 μg versus 18 μg for the avocado extract. As the rape βKR enzyme is immunodetected when over-produced in *E. coli*, it may possess differing antigenic determinants. Secondary determinants common to both enzymes may only be detectable when the level of *B. napus* βKR antigen is increased in an immunoassay

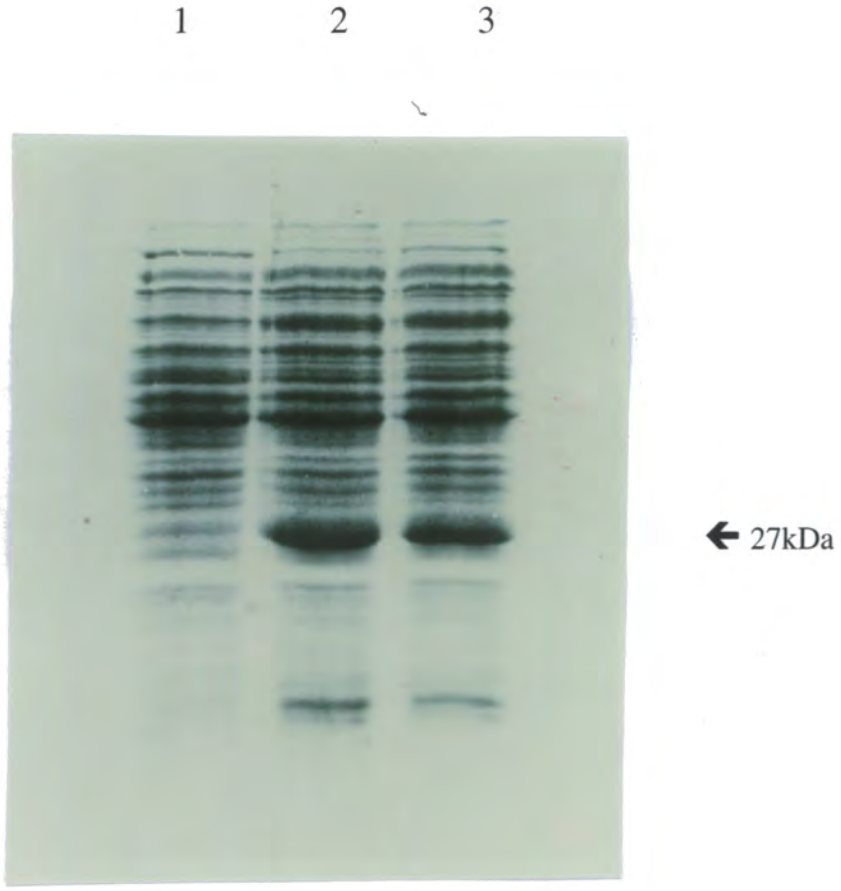

Figure 3.14 SDS-PAGE analysis of trial over-expression cultures of BL21(DE3) pETJRS10.1.

Lane 1, untransformed BL21(DE3); lane 2, pETJRS10.1 (transformant 1); lane 3, pETJRS10.1 (transformant 6).

The plant gene product is clearly seen at 27 kDa in the IPTG induced cultures of transformed cells containing plasmid pETJRS10.1.

1 2 3 4 5 6 7 8 9

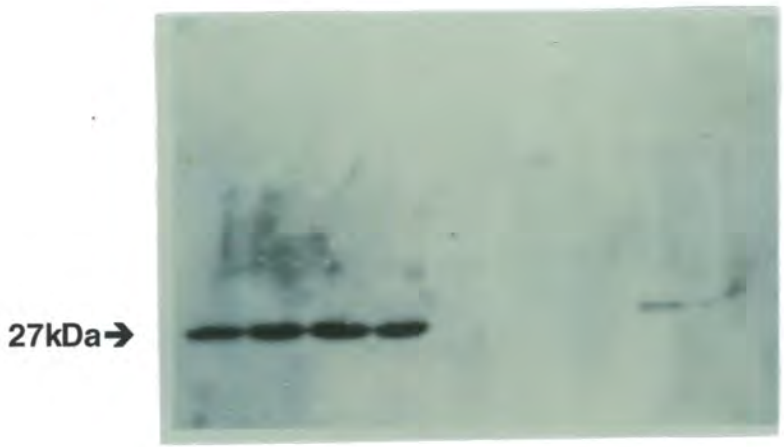

Figure 3.15 Confirmation of identity of over-produced protein in cell extracts as βKR by immunodetection with anti-avocado βKR antibodies.

Lane 1, pETJRS10.1 transformant 6 (uninduced); lane 2, pETJRS10.1 transformant 6 (IPTG induced); lane 3, pETJRS10.1 transformant 1 (uninduced); lane 4, pETJRS10.1 transformant 1 (IPTG induced) ; lane 5 untransformed BL21(DE3) - lanes 1-5 contained 90 μg of total protein; lane 6, *B. napus* developing seed extract (150 μg total protein); lane 7, *B. napus* developing seed extract (100 μg total protein); lane 8, avocado extract (18 μg total protein); lane 9, avocado extract (6 μg total protein).

Extracts from pETJRS10.1 transformed cells gave a cross-reaction with anti-avocado βKR antibodies in the 27 kDa region of the gel-blotted filter shown above. No cross-reaction was seen in the extract from untransformed BL21(DE3). The enzyme was also detected in an extract of avocado, but not in a sample of *B. napus* developing seed.

3.5 Purification Strategies for βKR

Analysis of the trial cultures had confirmed that *B. napus* βKR could be successfully over-expressed in an active form. This gave a good indication that the plant protein was properly encoded, translated and processed in *E. coli* - however, see §7.1. The task was to find a suitable purification strategy to produce large quantities of pure active protein.

3.5.1 Large scale culture of *E. coli* strain BL21(DE3) pETJRS10.1

Cells containing over-expressed βKR were produced using 500 ml liquid cultures. Transformed cells (transformant 6) were grown in a 5 ml LB starter cultures containing 100 μg ml^{-1} ampicillin on a rotary shaker at 37 °C overnight. These cultures were used at a dilution of 1:100 to inoculate 500 ml of LB plus ampicillin at 100 μg ml^{-1}, which was grown under the same conditions until an OD_{600} of 0.8 AU was reached. Over-production of βKR was facilitated by adding IPTG to 100 μM. The cultures were grown for a further three hours before cell harvesting via centrifugation at 5000 g.

To provide βKR protein for chromatographic studies bulk liquid cultures of *E. coli* strain BL21(DE3) pETJRS10.1 were grown (4 x 500 ml). After cell harvesting at 5000 x g, cell pellets were transferred to four 50 ml Falcon tubes and the tubes flash-frozen in liquid N_2. The cell pellets were stored at -80 °C until required.

3.5.2 Crude extract preparation

A lysozyme based method was used to release the over-expressed protein from cultured transformed cells. Cells from liquid culture were harvested by centrifugation at 4 000 x g for 15 min and the resulting pellet or a previously frozen pellet was resuspended in 50 mM Tris-HCl pH 8.0, 1 mM EDTA, 5 mM DTT; 0.5 ml for a 5 ml culture, 30 ml for a 500 ml culture. The cell suspension could be frozen at this stage if necessary. To lyse the cells 0.04 volumes of 20 mg ml^{-1} lysozyme, in 10 mM Tris-HCl pH 8.0, were added to the cell suspension. The mixture was placed in iced water for 1 h prior to addition of $MgSO_4$ to 5 mM and 0.01 volumes of 1 mg ml^{-1} DNase. Digestion

of the DNA was deemed complete when the extract lost its initial viscosity. This mixture was kept on ice for 5 min prior to spinning down the debris at top speed in a micro-centrifuge and retaining the protein containing supernatant.

3.5.3 Initial purification of βKR

3.5.3.1 Fast Flow Sepharose ion exchange chromatography

Fast Flow Sepharose ion exchange matrices (Pharmacia) were initially chosen for the purification of over-produced *B. napus* βKR. Fast Flow-Q anionic matrix was used first, with buffers at pH 8.0. Matrix (100 ml) was buffer-exchanged (into 25 mM sodium phosphate pH 8.0, 1 mM EDTA, 2 mM β-mercaptoethanol) by running 5 volumes of the buffer sequentially through the matrix in a sintered glass funnel.

The matrix was poured into a suitable container and mixed with the crude extract (approximately 30 ml), at pH 8.0, on a rocking stage at 4 °C for 1h overnight. The level of binding was assessed by taking 500 µl of the mixture, spinning down in a microcentrifuge tube and performing a βKR enzyme assay (see §2.3.6). An amount of the extract was kept separate from the matrix under the same conditions for a comparative assay. Unbound proteins were removed with 4 x 50 ml washes of starting buffer in a sintered glass funnel. The washes were retained and the volume and activity of each was checked.

When evaluating a new chromatography matrix, it is very important that the washes are retained as the protein of interest may be only loosely bound. Though 80% of the enzyme activity appeared to have bound during batching with the matrix, the bulk of the activity was actually found to be in the washes of the "Q" matrix at pH 8.0. As a result of this, the 150 ml of anionic column wash was batch treated with 100 ml of cationic matrix at pH 6.0 (Fast S-Sepharose equilibrated with 25 mM sodium phosphate pH 6.0, 1 mM EDTA, 2 mM β-mercaptoethanol). The enzyme exhibited 100% binding during batching. No activity was detected in the matrix washes (5 x 100 ml in a sintered glass funnel).

The matrix was packed into a 150 ml column with 5 volumes of equilibration buffer at a flow rate of 400 ml h^{-1}. A 150 ml (six column volumes) gradient of NaCl

from 0-1.0 M in the equilibration buffer was set up by placing 75 ml of buffer containing 0 M and 75 ml of buffer containing 1 M NaCl in to each chamber of a stirred two-chamber gradient maker. The gradient was run through the column over 2.5 h via a peristaltic pump and collected in eighty 5 ml fraction collector tubes.

Groups of five fractions were marked and 100 µl pooled from each. These mixtures were assayed for βKR activity and identified fractions individually assayed. No absorbance detector or chart recorder was used to monitor protein elution in this instance and so enzyme activity was the only indication of the presence of the purified protein. SDS-PAGE gels of the fractions in and around the activity peak were run to obtain a visual estimation of enzyme levels in the fractions. These gels are shown in figure 3.16. Aliquots from the crude extract and the Fast-Q chromatographic step were also run on the gel to observe the progress of purification. It can be seen that the fractions containing the highest levels of βKR are considerably more pure than the retained Fast Q matrix wash, which displays a similar level of βKR.

The use of the S matrix after subtractive chromatography on the Q matrix purified 2 mg of the over-produced protein to an estimated level of at least 70% purity and a specific activity of 40 U mg^{-1}, as calculated for fraction 30 corresponding to the elution peak of βKR. However, the sample was not electrophoretically pure. Higher molecular weight components were visible on the gels, and would be noticeably prominent if the gel sample loading was increased. However the part-pure protein was deemed sufficiently pure to attempt amino acid sequencing of its N-terminus.

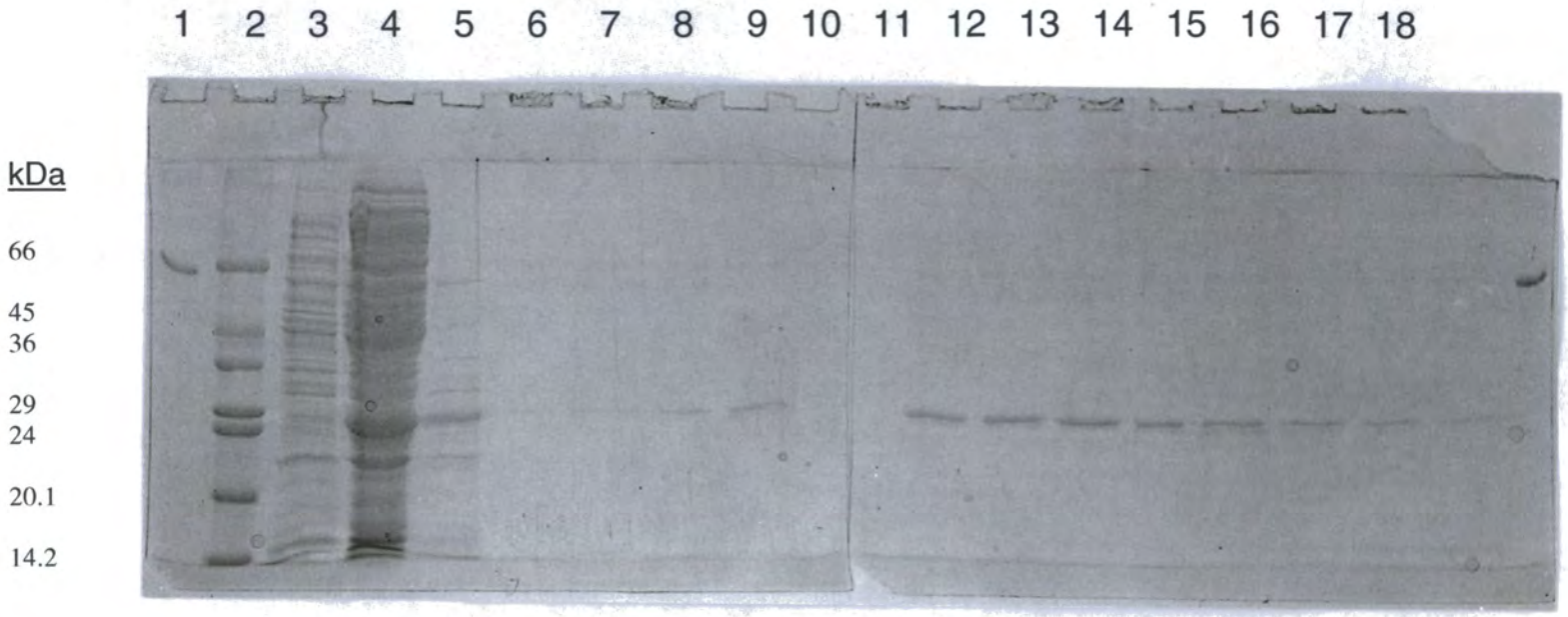

Figure 3.16 SDS-PAGE gels showing active fractions from the Fast-S purification of *B. napus* βKR.

Lane 1, Bovine serum albumin (1 µg); lane 2, SDS-VII markers; lane 3, untransformed BL21(DE3) protein extract (20 µl); lane 4, bulk crude extract BL21(DE3) (pETJRS10.1) protein extract (20 µl); lane 5, retained Fast Q pH 8.0 wash (20 µl); lanes 6-17, fractions 26-37 (20 µl); lane 18 bovine serum albumin (1 µg).

Purified βKR is seen in lanes 6-17. Fractions containing the highest levels of βKR (lanes 10-15) are considerably more pure than the retained Fast Q matrix wash (lane 5) which displays a similar loading of βKR protein.

3.5.3.2 *Immunodetection of partially-purified βKR*

To confirm the identity of the major purified band, an SDS-PAGE gel containing samples of crude extract and the part-pure protein was subjected to a western blot and immunodetection using antibodies raised against avocado βKR in rabbit as the primary antibody [Sheldon, 1988; Sheldon *et al.*, 1990]. An ECL antibody detection kit (Amersham), which employed a horseradish peroxidase linked secondary antibody, was used to detect the primary antibody. Detection was carried out following the manufacturers instructions. The resulting exposed x-ray film is shown in figure 3.17. Protein cross-reacting with the anti-βKR antibodies was observed in the 27 kDa region of the gel in both the crude extract and part-pure protein lanes. This cross-reaction backed up the βKR activity previously measured in confirming the major component of the preparation being βKR.

3.5.3.3 *Amino acid sequencing of part-purified βKR*

N-terminal sequencing of the first five residues of the purified βKR was attempted. The protein had a concentration of 100 μg ml^{-1} which corresponds to 3.57 nmole ml^{-1} for a 27 kDa protein. Consequently, 100 μl (357 pmole) of the protein was loaded onto a Prospin column (Applied Biosystems) for sequencing (see §2.3.7). The Problot filter from the spun column was loaded on to the sequencer disc of an ABI 477A Protein Sequencer and run for five cycles of Edman chemistry. Manual adjustment of the returned data by the operator, John Gilroy of the Department, gave the sequence ATAVE. The 'raw' and '*background and lag corrected*' yields of each residue in pmol from a 100 pmol sample were: A(209.5;*135.8*), T(79.9;*73.3*), A(175.3;*124.9*), V(98.8;*71.0*) and E(89.2;*66.7*) respectively. This sequence was predicted by the cDNA sequence, and the previously purified *B. napus* βKR (ATAV/QE) [Sheldon *et al.*, 1992]. This further confirmed the identity of the purified protein and established that the N-terminus was correctly formed in *E. coli*.

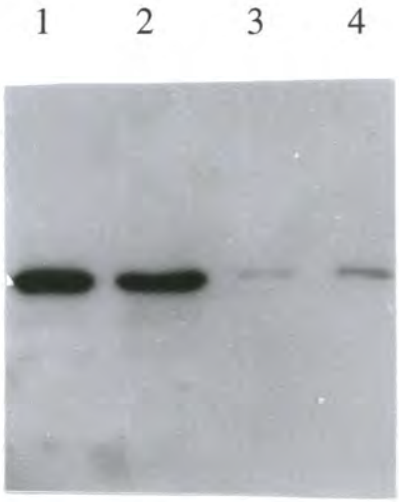

Figure 3.17 Immunodetection of near-pure βKR

Lane 1, Crude extract (5 µl); lane 2, crude extract (2.5 µl); lane 3, fraction 30 (from figure 3.16 – lane 10) (10µl); lane 4, fraction 30 (5 µl).

The cross-reaction observed in the 27 kDa region of the gel, in both the crude extract and part-pure protein lanes, confirmed that the major purified component was βKR.

3.5.4 Purification method development

The initial use of the ion-exchange matrices purified the over-produced protein to a level estimated to be greater than 70% pure. As the sample was not electrophoretically pure, an alternative method of chromatography was sought to provide pure protein. Chromatographic methods investigated included hydrophobic interaction, dye-ligand affinity and FPLC ion-exchange.

3.5.4.1 Production of part-pure βKR using Fast S matrix at pH 6.0

From the demonstration of binding between enzyme and matrix seen in §3.5.3.1, it was decided to perform the first step of chromatography at pH 6.0 using the Fast S ion-exchange matrix. A cell pellet corresponding to a 500 ml bulk liquid culture of *E. coli* strain BL21(DE3) pETJRS10.1 was used to provide over-expressed βKR for these experiments. Crude extract was produced as outlined in §3.5.2. and assayed. The extract from a 500 ml culture pellet had a total activity of 3180 U and a specific activity of 10.5 U mg^{-1}. After bringing the crude extract to pH 6.0 by dropwise addition of 1M HCl in a stirred beaker, its total activity was 2315 U - 72% of the previous activity (possibly due to brief exposure to pH 4.0 for several seconds during pH adjustment – corrected with dropwise addition of 1M NaOH).

The crude extract was loaded onto a 50 ml bed of Fast S matrix that had been previously equilibrated with six column volumes (300 ml) 25 mM sodium phosphate, 1 mM EDTA, 2 mM β-mercaptoethanol, pH 6.0. No βKR activity was detected in the pass or the subsequent 50 ml wash with the above buffer. A 150 ml gradient from 0 to 1 M NaCl in the same buffer was run through the matrix using a Pharmacia HiLoad chromatography workstation. Fractions corresponding to the major protein peak, as measured by 280 nm absorbance, at approximately 450-600 mM NaCl, were found to contain the eluted βKR activity upon assay. The total recovered activity of these active fractions was 1268 U, corresponding to a yield of 55% from the loaded activity. Samples of the active fractions (20 µl), the near-pure βKR from the previous purification, an untransformed cell extract and the crude extract were run on 5% acrylamide stacking/10% acrylamide resolving SDS-PAGE gels, shown in figure 3.18

to visually estimate the extent of purification to be 75% βKR.

A Lowry protein assay (§2.3.4) was used to determine the protein concentrations of the crude extract and the active fractions. The crude extract contained 303 mg of protein whilst the active fractions contained 41 mg of protein; estimated to be 75% pure via SDS-PAGE (giving 30 mg of βKR). From these data it was estimated that the proportion of protein corresponding to βKR in the extracted protein from the transformed cells was approximately 10%. The specific activity of the active fractions was calculated to be 31 U mg^{-1}, corresponding to a fourfold increase in purity over the crude extract loaded onto the column. The purification data for this first step of chromatography are tabulated in table 3.1.

The fractions containing active, part-pure βKR, were snap frozen in liquid nitrogen for later use.

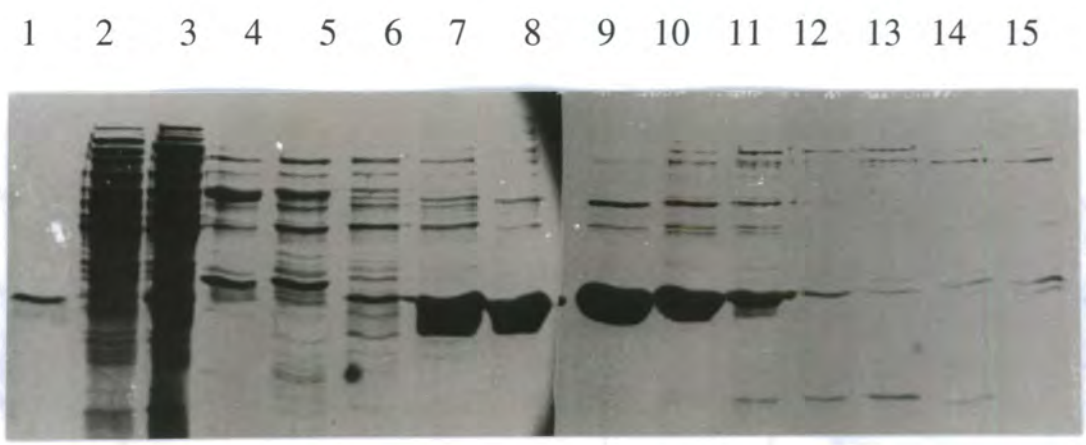

Figure 3.18 Partial purification of βKR on Fast S matrix at pH 6.0

Lane 1, Near pure βKR (fraction 30 from §3.5.3.1.) (20 µl); lane 2, untransformed BL21(DE3) extract (20 µl); lane 3, bulk crude extract from BL21(DE3) (pETJRS10.1) (7.5 µl); lanes 4-15, fractions 10-21 (20 µl).

Samples of the active fractions were run on 5% acrylamide stacking/10% acrylamide resolving SDS-PAGE gels, shown above, to visually estimate the proportion of βKR to be approximately 75%.

	Volume ml	Total Protein mg	Total Activity U	Specific Activity U/mg	Purification	Yield
Crude Extract	**30**	**303**	**3180**	**10.5**	**1**	**100%**
Post pH adjustment	**30**	**303**	**2315**	**7.6**	**0.72 (activity lost)**	**72%**
Fast S pH 6 fractions	**35**	**40**	**1268**	**31.7**	**3 (3.8 of load)**	**40% (55% of load)**

Table 3.1 Purification table for first step purification of βKR on Fast S matrix at pH 6.0

One third of the enzyme activity was lost during pH adjustment when the pH fell momentarily to pH 4.0

3.5.4.2 Attempted βKR purification on other matrices.

Various attempts were made to improve on the purification of βKR provided by the FastS matrix at pH 6.0, though the use of non-ion exchange chromatographic media. Matrices tested included MonoP, an FPLC phenyl-Superose hydrophobic interaction chromatography matrix (Pharmacia), and Amicon Matrex Gels (Blue A, Red A, Green A and Orange A) dye-ligand affinity matrices. None of the alternative media gave a significant increase in the purity obtained by the first chromatographic step.

3.6 Two-step cation exchange chromatography of βKR

The purification capability of two consecutive ion-exchange steps were observed previously during the evaluation of such matrices for βKR purification (§3.5.3.1). It was decided that a two-step purification strategy using the same ion-exchange ligand at two different pH values would be attempted.

3.6.1 Development of the two-step method; chromatography of part-pure βKR on a Mono S FPLC column at pH 6.0

The Fast S purification of §3.5.4.1 was repeated with similar results in terms of purity and activity, except the specific activity obtained was 40 U mg^{-1} as opposed to 31 U mg^{-1}. One of the βKR containing fractions from the aforementioned Fast S purification, containing 6.1 mg of approximately 75% pure βKR in 5 ml, was dialysed against 2 x 1000 ml of buffer A (25 mM sodium phosphate, 1 mM EDTA, 2 mM β-mercaptoethanol, pH 6.0) over 3 hours. A high capacity matrix, namely Mono S in a pre-packed 1 ml column, was fitted and equilibrated on an FPLC system in the same buffer as used for the Fast S purification. The containing dialysate containing βKR was filtered (0.2 μm filter), loaded on to the column and 10 ml of buffer A was run through the column to elute non-bound material. A 50 ml gradient to 100% buffer B (buffer A plus 1 M NaCl) was then run through the column at a flow rate of 2 ml min^{-1}. The absorbance, at 280 nm, of the eluent was recorded prior to collection in 1 ml fractions.

The resulting trace is shown in figure 3.19. Enzyme assays confirmed that βKR activity was located in the fractions corresponding to the absorbance peak. Fractions 19 - 25 (20 μl of each plus 5 μl of loading buffer) were run on a 5% acrylamide stacking/10% acrylamide resolving SDS-PAGE gel to assess purity; the stained gel is shown in figure 3.20.

A contaminating protein band of higher molecular weight is seen accompanying the eluted βKR protein. To observe the relative amounts of βKR and the contaminating proteins, a further gel was run with various loadings of fraction 22. This gel is shown in figure 3.21, where the presence of the contaminating bands is seen at a loading of 1 μl.

It was clear from this result that to achieve homogeneity of the βKR protein an alternative method of secondary chromatography was still required. In continuation of the line of inquiry employing the S matrices, it was decided to continue with the high-resolution Mono S column, but to shift the pH of the chromatography buffers to pH 7.0. The theoretical pI of βKR was calculated by amino acid sequence analysis software to be pH 8.33 (see figure 7.2), thus it was reasoned that βKR should still have the net positive charge required to bind the cationic S matrix at pH 7.0.

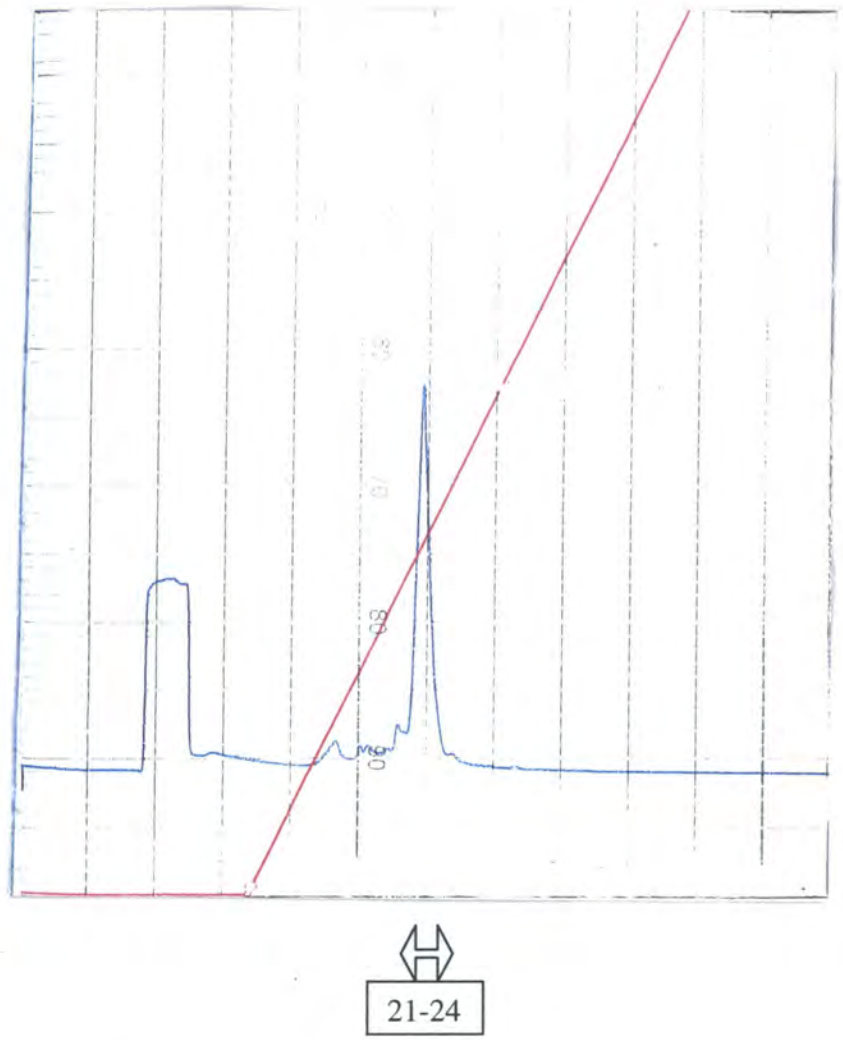

Figure 3.19 Absorbance trace (280 nm) of eluent from a Mono S FPLC column at pH 6.0 loaded with part-pure βKR

A second consecutive chromatography (S matrix at pH 6.0) was carried out on a part pure βKR sample using a Mono S column on an FPLC system. The above trace shows the increased separation possible with this chromatography method; contaminating proteins are eluted prior and during the gradient. The absorbance peak eluting at 25% in the 0-1M NaCl gradient corresponds to fractions 21-24 which are depicted on the gel in the following figure.

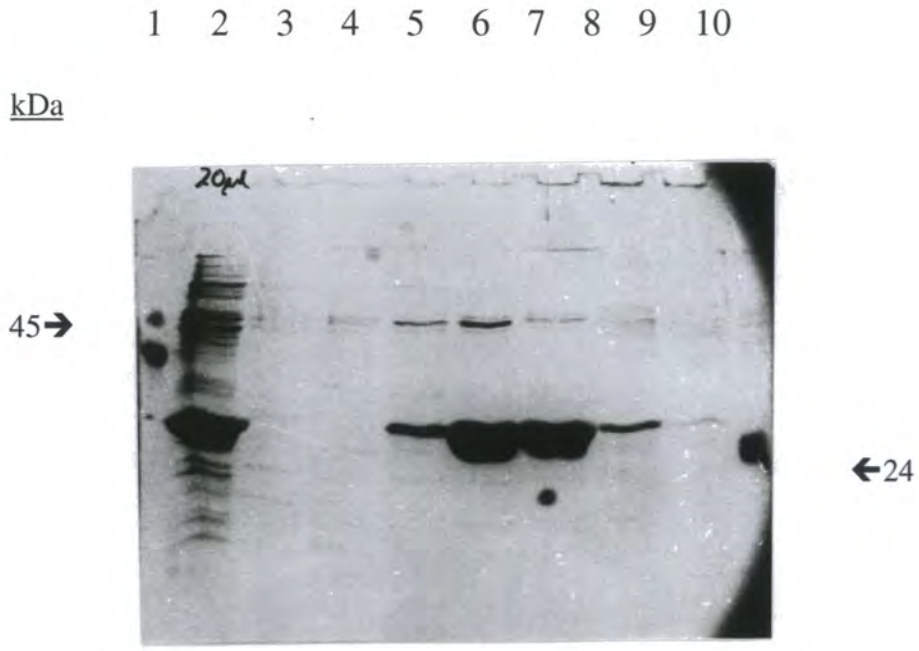

Figure 3.20 SDS-PAGE gels (5% acrylamide stacking/10% acrylamide resolving) showing active fractions eluted from a Mono S FPLC column at pH 6.0 loaded with part-pure βKR

Lane 1, Ovalbumin (45 kDa) (1 µg); lane 2, loaded βKR source (20 µl); lanes 3-9, eluted fractions 19-25 (20 µl); lane 10, trypsinogen (1 µg).

Visual comparison between the partially purified βKR sample loaded on to the column (lane 2) and the active fractions (lanes 5-8) shows that βKR is purified considerably.

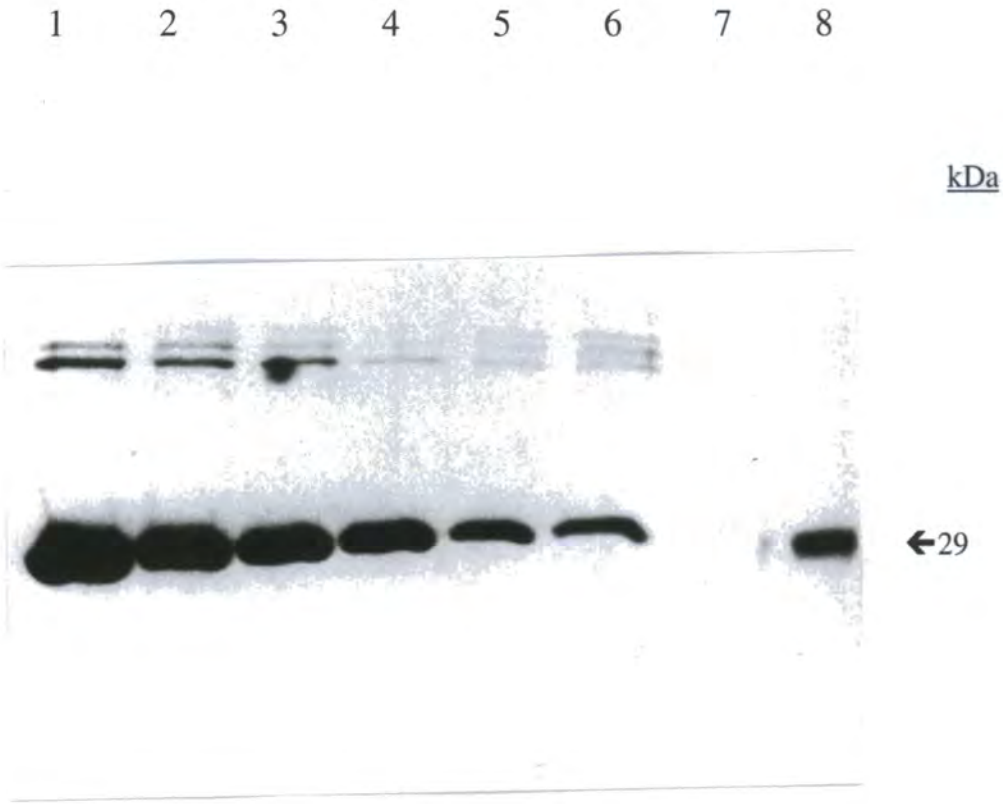

Figure 3.21 SDS-PAGE gel (5% acrylamide stacking/10% acrylamide resolving) showing various loadings of fraction #22 from figure 3.19

Lane 1, 20 µl; lane 2, 15 µl; lane 3, 10 µl; lane 4, 5 µl; lane 5, 2.5 µl; lane 6, 1 µl; lane 7, empty; lane 8, carbonic anhydrase (29 kDa) (1 µg).

Various loadings of fraction 22 eluted from the Mono S column at pH 6.0, were loaded on to the gel above to obtain a more accurate visual estimate of the extent of contamination by other proteins.

3.6.2 Chromatography of partially-pure βKR on a Mono S FPLC column at pH 7.0

Results from the above work suggested that the second step of chromatography should be attempted on the same cationic 'S' matrix, but with the pH of the buffers shifted to pH 7.0. Two fractions from the FastS purification of §3.6.1 (19 mg of approximately 75% pure βKR in 10 ml), were thawed and dialysed against 2 x 1000 ml of buffer A (25 mM sodium phosphate, 1 mM EDTA, 2 mM β-mercaptoethanol, pH 7.0) over 3 hours. Two separate runs were carried out with the two fractions of βKR. For each run, the dialysate was filtered (0.2 μm filter), loaded on to the column and 10 ml of buffer A was run through the 1ml MonoS column to elute non-bound material. βKR activity was not detected upon assay of the pass or wash from the column, indicating complete binding of βKR at this pH. For the first run, a 100 ml gradient to 100% buffer B (buffer A plus 0.5 M NaCl) was run through the column at a flow rate of 2 ml min^{-1}. For the second run, a 100 ml gradient to 25% buffer B (buffer A plus 1 M NaCl) was run through the column at a flow rate of 2 ml min^{-1}. The absorbance, at 280 nm, of the eluents was recorded prior to collection in 1 ml fractions. The resulting traces are shown in figure 3.22. Enzyme assays confirmed that βKR activity was located in the fractions corresponding to the absorbance peak. Active fractions (20 μl of each plus 5 μl of loading buffer) were run on 5% acrylamide stacking/10% acrylamide resolving SDS-PAGE gels to assess purity. The gels from both runs showed βKR to elute over 10 x 1 ml fractions with 5 ml being free of the principal contaminating band; this higher molecular weight component eluted slightly later at pH 7.0 than βKR, but there was an overlap of the two elution peaks (gel erroneously discarded - not shown).

This second step of purification, on a cationic matrix at pH 7.0, produced essentially pure βKR at a milligram scale for the first time in this study. This particular preparation produced 11.5 ml of βKR active pooled fractions with an estimated concentration (via absorbance at 280 nm) of 1 mg ml^{-1}.

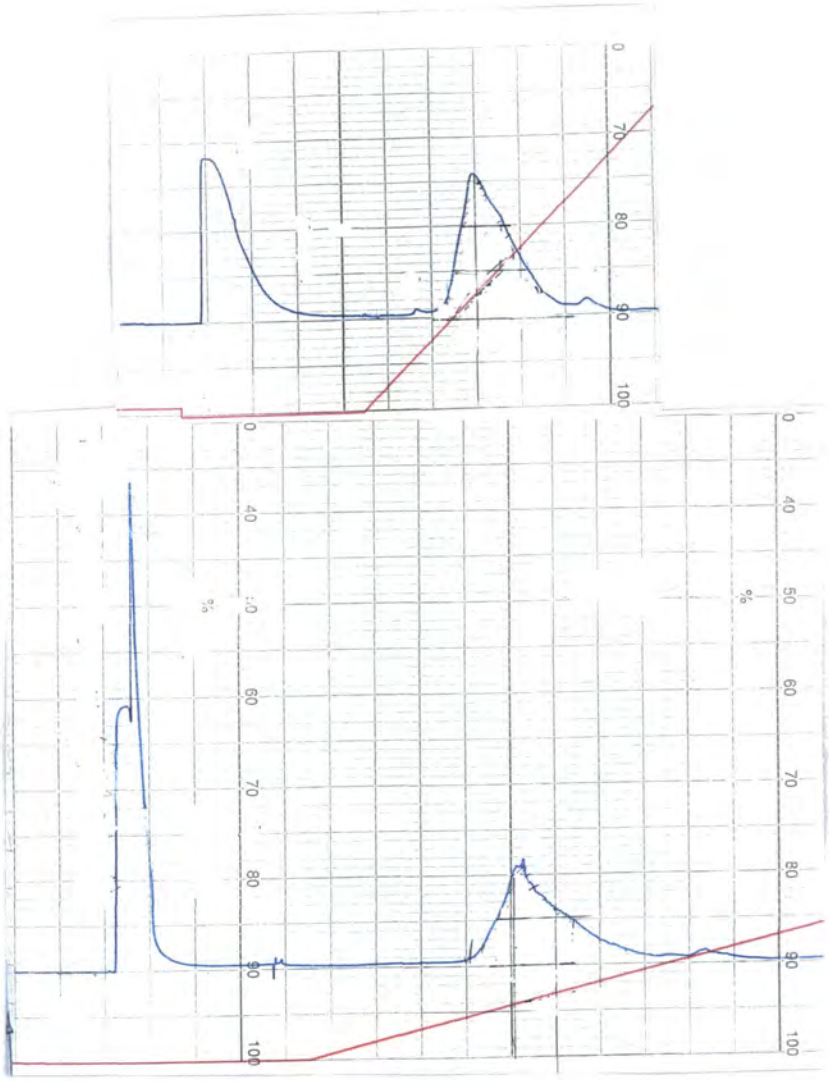

Figure 3.22 Absorbance traces (280 nm) from Mono S FPLC chromatography of partially pure βKR at pH 7.0

The above chart recorder traces show the absorbance at 280 nm of the eluents from two Mono S FPLC runs at pH 7.0. Some protein in the loaded sample, that co-eluted with the βKR activity at pH 6.0 on a similar matrix, is seen to be eluted in the pass and subsequent wash of the column in both runs. The main protein peak, eluting at around 60-65 mM NaCl, was essentially homogenous for βKR, though the later active fractions at the tail end of the βKR elution, contained a small amount of contaminating protein.

3.6.3 Preparative Chromatography of βKR

To circumvent the limitations of the one-litre-scale liquid culture facilities available in the laboratory, a stock of the *E. coli* strain BL21(DE3) pETJRS10.1 was sent to Zeneca Pharmaceuticals (Cheshire, UK) for large scale culture in a fermenter. The cells harvested from this culture were passed through a cell disrupter (French press) and were provided as a cell-free-extract in the form of frozen pellets. This source of βKR became available after the method of purification had been defined and was used for later purifications, predominately for crystallographic samples. An outline of the preparative chromatography method and relevant diagrams follow.

Preparative chromatography of βKR used the two-step, one-matrix method developed in §3.6.

3.6.3.1 Step one - Fast S and HiLoad SP matrices

Prior to the availability of the HiLoad SP 26/10 column, the method given in §3.5.4.1 was used to produce part-pure βKR from cell-free extract, using a Fast S column at pH 6.0.

When a pre-packed high volume, high capacity HiLoad SP column became available this was tested under the same conditions. Difficulties arose with the loading of the cell-free extract on this column at first as only poor binding of βKR could be achieved. This problem was solved by subjecting the crude extract to an 85% ammonium sulphate cut prior to this first chromatography step. The 50 ml bed volume, HiLoadSP column was subsequently used with the following method for large scale preparations.

For routine preparations, 60g (frozen weight) of cell-free-extract from BL21(DE3) containing pETJRS10.1 was diluted with buffer A (25 mM sodium phosphate pH 6.0, 1 mM DTT) to 100 ml resulting in a protein concentration of 25 mg ml^{-1}. Denatured protein and other debris were removed by centrifugation at 30,000 x g for 10 min. The supernatant was brought to 24% ammonium sulphate saturation (132 g l^{-1}) and stirred for 1 hour, at 4 °C prior to a further centrifugation at 10,000 x g for 15 min. The supernatant was brought to 85% ammonium sulphate(596 g l^{-1}), stirred for 30 min at 4 °C and spun at 10,000g for 10 min. The pellet was resuspended in 25 ml of

buffer A and dialysed against 2 x 2 l of buffer A over 4 hours at 4 °C. The dialysate was spun at 30.000g for 15 min and filtered through a 0.7 μM GF-F filter (Whatman), and diluted to 200 ml with filtered buffer A..

βKR dialysate (pH 6.0, conductivity < 2.5 mS) was loaded onto a 50 ml bed volume HiLoad SP 26/10 column (cationic exchange matrix - Pharmacia) previously equilibrated with buffer A at pH 6.0. The column was washed free of 280 nm absorbing material with 200 ml of buffer A. Elution of βKR activity was carried out using a 360 ml linear gradient leading to 100% buffer B (buffer A plus 1 M NaCl) at a flow rate of 5 ml min^{-1}. *B. napus* βKR activity was detected at approximately 250 mM NaCl in the gradient. This first step on the 50 ml high-capacity HiLoad column, purified βKR to 60-70%, a typical elution profile is shown in figure 3.23.

Figure 3.24 shows the pooled active fractions from a HiLoad SP chromatography run and two Fast S runs carried out before the arrival of the HiLoad SP column. These chromatographic steps resulted in a similar purification as observed previously in that active fractions had specific activities in the range of 31-40 U mg^{-1} and yielded ~40 mg of partially purified βKR from 25 g of pelleted cell-free extract. Table 3.2 gives a typical recovery and yield for this step.

	Volume ml	Total Protein mg	Total Activity U	Specific Activity U/mg	Purification	Yield
Crude Extract	30	285	2907	10.2	1	100%
Fast S pH 6.0 fractions	20	28.6	1191	41.5	4.1	41%

Table 3.2 Purification table for first step purification of βKR on Fast S matrix at pH 6.0

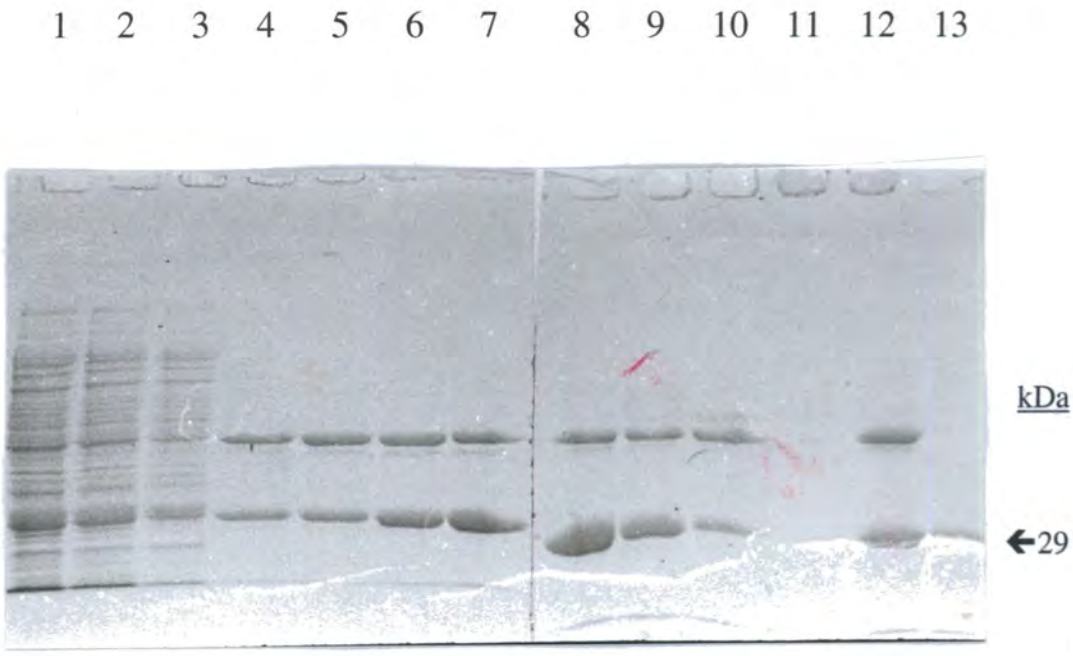

Figure 3.23 Elution profile from HiLoad SP chromatography of βKR at pH 6.0

Lanes 1-3, loaded protein (cell free extract) (1 μl); lanes 4-10, active fractions (23-29); lane 11, empty; lane 12, pooled fractions; lane 13, pure βKR Mw marker (all 20 μl).

SDS-PAGE (5% acrylamide stacking/10% acrylamide resolving) gels showing the elution profile of a typical HiLoad SP chromatography run using cell free extract containing βKR. The preparation is approximately 50% pure with the major protein contaminant running at a higher molecular weight on the gels. The cell free extract, produced from fermenter grown cells by Zeneca, shows a lower level of βKR over-expression than that observed in lab grown cultures (see figure 3.14).

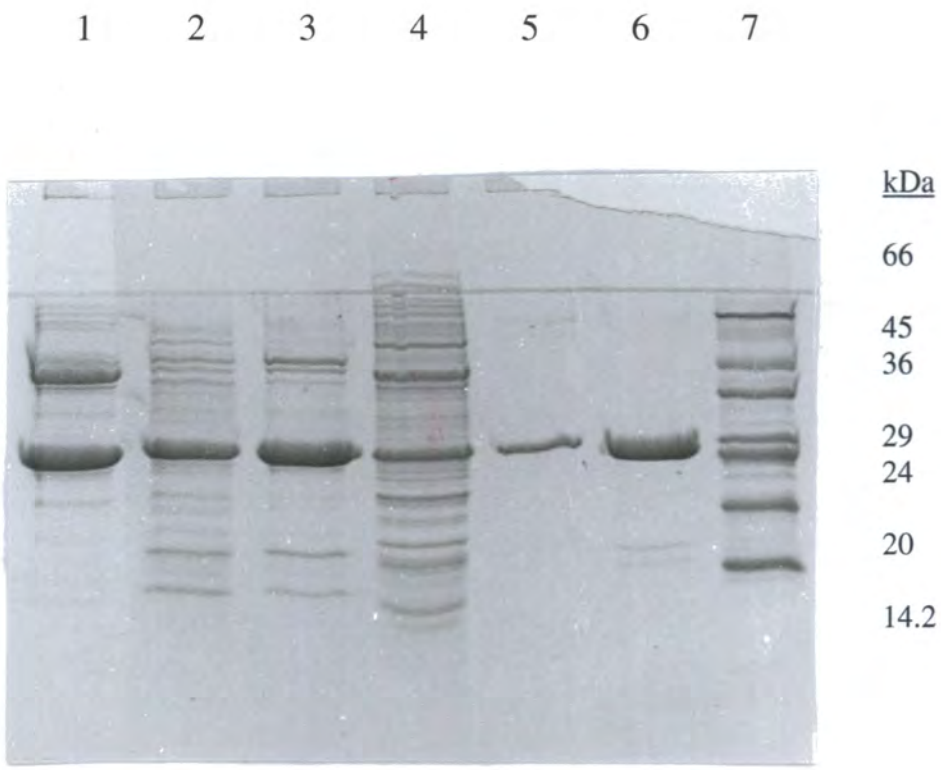

Figure 3.24 Pooled active fractions from chromatographic runs using HiLoad SP and Fast S matrices at pH 6.0

Lane 1, HiLoad SP; lanes 2-3, Fast S; lane 4, unbound material from a Fast S column; lane 5, βKR 1 μg; lane 6, βKR 5μg, lane 7, SDS-VII markers.

The results of first step chromatography runs are shown for comparison. Active fractions from the HiLoad SP column contain fewer contaminating proteins and one major contaminant, whereas the Fast S active fractions are equally pure but contain more protein species.

3.6.3.2 Step two - Fast S matrix

This second step preparative step of this method was developed using a 1 ml Mono S column (§3.6.2). To further increase the capacity of this method, the second step at pH 7.0 was carried out using a packed column (15 ml) of Fast S matrix. This column was mounted on an FPLC system, to make use of the precise gradients produced on the system. The eluted active fractions had a purity of >98% as assessed by SDS-PAGE analysis and exhibited specific activities of up to 65 U mg^{-1} as determined from assay data and the calculated extinction coefficient for purified βKR - see §2.3.5. The method was scaled up to a 50 ml HiLoad SP column when required, which gave adequate purity (>95 %) for crystallographic studies of the enzyme

The methodology was essentially identical for each matrix/column used. Active fractions from the first chromatographic step at pH 6.0 were pooled and dialysed into buffer A (25 mM sodium phosphate, 1 mM DTT, 1 mM EDTA, pH 7.0). The dialysate was centrifuged at 30,000 x g for 15 minutes, filtered through a 0.22 μm filter and loaded onto the appropriate sized column, on an FPLC or HiLoad system, equilibrated with buffer A (pH 7.0). Unbound protein was washed from the column and the βKR activity was eluted with a six-bed volume gradient leading to 100% buffer B (buffer A plus 1 M NaCl).

Figure 3.25 shows an absorbance trace of the eluted protein from a 15 ml Fast S column. As with the Mono S column traces in figure 3.22, material that co-eluted with βKR at pH 6.0 can be seen in the wash of the column at pH 7.0. Figure 3.26 shows fractions from the same chromatographic run on two SDS-PAGE gels, upon which βKR is seen to be electrophoretically pure. Enzyme purified via this method was used for kinetic studies and as an antigen for immunisation.

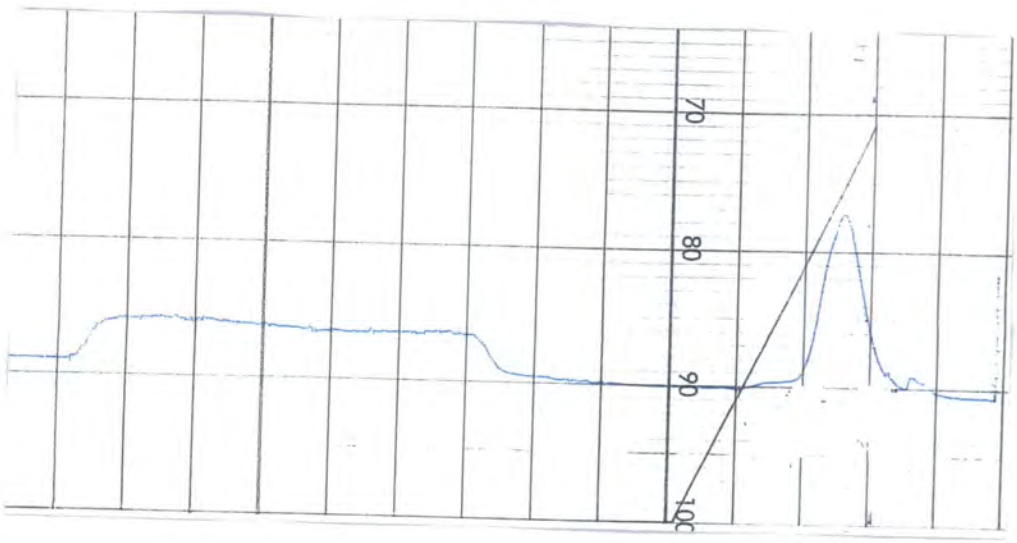

Figure 3.25 Absorbance trace of the eluent from a Fast S column at pH 7.0, loaded with part-pure βKR.

Material that co-eluted with βKR on a Fast S column at pH 6.0 can be seen in the wash of this Fast S column at pH 7.0 prior to the start of the 0-1M NaCl gradient. βKR elutes as the major protein peak and is essentially homogeneous.

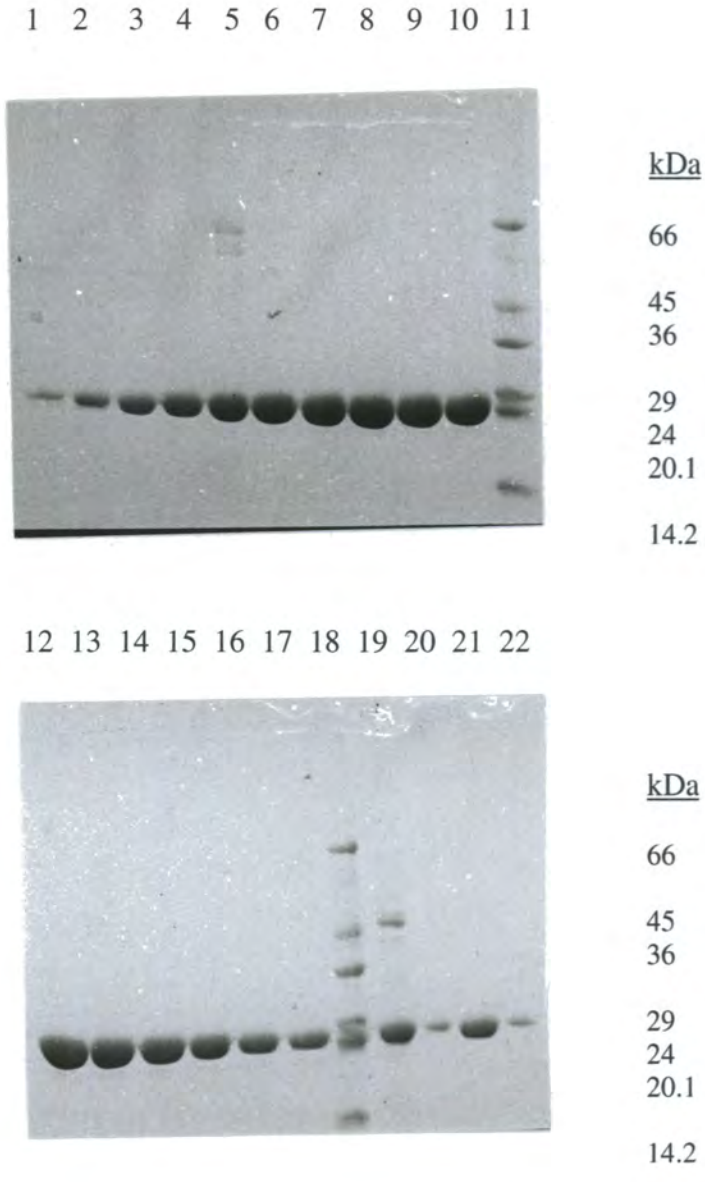

Figure 3.26 Active fractions eluted from a Fast S column at pH 7.0, loaded with part-pure βKR.

Lanes 1-10, fractions 27-36; lane 11, SDS-VII Mw markers; lanes 12-17, fractions 37-42; lane 18 SDS-VII Mw markers; lane 19, loaded part-pure βKR; lane 20, βKR Mw marker 1 μg; lane 21, βKR Mw marker 5 μg, lane 22, pooled active fractions from a previous Fast S 2nd chromatographic step.

The elution profile above shows all but one (lane 5) of the βKR active fractions to be electrophoretically pure, in comparison to the loaded protein (lane 20).

3.7 Summary

Over-expression of βKR was facilitated by modifying βKR clone pJRS10.1 by PCR and inserting it into a pET over-expression vector. PCR primers were used to insert an *Nco*I site (containing ATG start codon) immediately prior to the mature protein start, and *Bam*HI after the stop codon. After the necessary restriction digests, the vector and βKR insert were ligated (to give pETJRS10.1), checked and used to transform *E. coli* BL21(DE3). Clones were characterised by restriction digest and those giving the correct products were used for over-expression trial cultures. DNA sequencing from an internal βKR sequence primer into the pETJRS10.1 plasmid showed the coding sequence to be in frame with ATG of *Nco*I site. To test for over-expression, transformed clone extracts were compared to untransformed BL21(DE3) extracts via SDS-PAGE. A clearly visible 27 kDa band was present in transformant extracts. The identity of the over-expressed protein as βKR was confirmed by several methods. Firstly, transformed extracts gave a high levels of βKR activity upon assay whilst no appreciable activity was measured in untransformed cell extracts under the same assay conditions. Secondly, the protein band visible via SDS-PAGE was of the expected denatured (monomeric) size: 27 kDa. Finally, this major protein band cross-reacted with an Avocado βKR antibody. This cross-reaction had not been previously observed in *B. napus* seed extracts, probably due to the low abundance of the rape protein.

Bulk preparations of βKR over-expressing cells were set up, and the cell extracts prepared using a lysozymal method. The initial purification of βKR used a Fast Q anion exchange matrix at pH 8.0. The total βKR activity of the extract eluted from the column in the pass but was retained, resulting in a purification step arising from the subtraction of bound proteins. This sample was then loaded onto a Fast S cationic matrix at pH 6.0. The total βKR activity eluted from the column between 0.45-0.6M on a 0-1 M NaCl gradient to give an almost homogeneous band at 27 kDa on SDS-PAGE analysis. Amino acid sequencing of first five residues at the N-terminus of this preparation confirmed the N-terminus as ATAVE (as predicted by the cDNA).

The first purification step used a Fast S cationic exchange matrix at pH 6.0. This method gave approximately 54 mg of 70-80% pure βKR from the lysed cell pellet of a

500 ml over-expression culture. To attempt to purify βKR further, various matrices were used: Amicon Matrex Gels, Phenyl Superose FPLC column (Mono P), Mono Q FPLC at pH 6.0 and an Affigel-ACP matrix. None provided the additional purification sought. A suitable final purification step was found using a 1 ml Mono S column on an FPLC workstation, with the chromatography buffers at pH 7.0. The one-unit pH change used was sufficient to differentiate the mixture of proteins co-eluted from the first column (pH 6.0) to give a level of purity of >99% via a rapid and convenient purification procedure.

Purified samples of over-produced *B. napus* βKR had specific activities of up to 65 μmol (NADPH) min^{-1} mg^{-1}. This compares with 91 μmol (NADPH) min^{-1} mg^{-1} for βKR purified from *Brassica napus*. [Sheldon *et al.*, 1992]. Thus the recombinant enzyme appeared to have 71% of the reported activity of the plant enzyme. This figure may not be far outside the error limits of the assays carried out on the two enzymes, or may be due to differences between their execution (the same assay protocol was followed however). If the difference observed is real then it may be due to the recombinant nature of the enzyme, e.g. folding of the enzyme was not carried out correctly in the *E. coli* host, post-translational modification by the plant had not occurred, partial degradation had occurred due to the action of host proteases, or perhaps an error introduced during the PCR amplification of the expression construct had caused a mutant enzyme with reduced activity to be produced - see §7.

The originally reported figure of 136 μmol (NADPH) min^{-1} mg^{-1} by Sheldon *et al.* was based an estimation of protein concentration of [Abs 280nm] = 1.0AU for a 1 mg^{-1} ml^{-1} solution of protein. The previously reported specific activity equates to the figure given above when the calculated extinction coefficient - see §2.3.5, is used to permit comparison of the recombinant and native enzymes.

Previous attempts to purify *B. napus* βKR yielded 0.22 mg of enzyme from 100 g of developing seed [Sheldon, 1988]. The over-production of βKR in milligram quantities facilitated structural, kinetic and immunological studies normally impeded by the low yield of enzyme obtainable from the plant.

Chapter 4: Over-expression and purification of *E. coli* βKR

4.1 Introduction

Crystallographic studies of the *B. napus* βKR enzyme produced in the previous chapter showed it to have a very small unit cell dimension, making its three-dimensional structure difficult to solve. It was suggested that the structure of the *E. coli* βKR enzyme might prove to be more amenable to X-ray diffraction studies. Thus it was decided to attempt to over-express the *E. coli* enzyme, using the DNA sequence published previously [Rawlings and Cronan, 1992]. It was intended to isolate the bacterial gene sequence from genomic DNA using specially designed primers in a cycled primer extension reaction. These primers were to be designed to simultaneously flank the protein coding sequence with restriction sites, allowing its ligation into an over-expression vector. The vector would be used for expression trials with an over-expressing *E. coli* strain. If successful, the transformed over-expressing strain would be used for bulk liquid cultures to produce large amounts of the βKR protein. A convenient purification method for the enzyme would be sought, perhaps based on the one-matrix, two-pH value method developed for purifying the over-produced the plant enzyme in the previous chapter.

4.2 Construction of βKR over-expression plasmid pETNEβ1

4.2.1 Primer design

The Genbank sequence for *E. coli* βKR (M84991) [Rawlings and Cronan, 1992] was used to design primers to amplify the βKR coding sequence from genomic DNA and flank it with *Nde*I and *Bam*HI restriction sites. These restriction sites were chosen for their absence in the coding sequence of the *E. coli* βKR gene and their presence in a suitable over-expression vector, namely pET-11a (Novagen) - see figure 3.4. The primers were as follows: primer #1137 (upstream *Nde*I site) 5'-C GAA TTC CAT ATG AAT TTT GAA GGA AAA ATC GCA CTG G-3'; primer #1136 (downstream *Bam*HI site) 5'-GCG GAT CCA CTA ATT ATT ACT CAT AAC CAC GC-3'. The primers were made as 38 and 32 - mers so as to allow modification of the sequence and subsequent recognition of the restriction site via 5' overhangs, and at the same time, to

allow the primers to have sufficient specificity in their non-modifying regions for the βKR sequence in the chromosomal DNA. The alignment of the primers to the genomic sequence is shown in figure 4.1.

4.2.2 Isolation of *E. coli fab*G and PCR modification

To provide template DNA for the amplification of the *E. coli* βKR gene, *E. coli* chromosomal DNA was prepared from the K-12 strain, JM83 [Vieira and Messing, 1982] (see §2.2.8). Polymerase chain reactions, in a final volume of 100 µl, contained 2 µg of chromosomal DNA, dNTPs at 200 µM each, the supplied polymerase buffer (final concentration 10 mM KCl, 20 mM Tris/HCl pH8.8, 10 mM $(NH_4)_2SO_4$, 0.1% Triton X-100, 2 mM $MgSO_4$), and the above primers at 20 µM. The reactions were held at 94 °C for at least 30 seconds prior to initiation with 1 unit of $VENT_R$ polymerase (New England Biolabs), delivered through the oil layer. The temperature was cycled 35 times, 1 min at 94 °C, 1 min at 55 °C, and 1 min at 72 °C (5 min at 72°C for the final cycle).

To visualise the PCR products, 5 µl of each reaction was run out on a 0.7% agarose gel, shown in figure 4.2, the expected 817 bp product is seen in lane 3. The remainder of the reactions were run out on the preparative gel, shown in figure 4.3.

4.2.3 Vector construction and sequencing

The pET-11a over-expression vector was chosen for use in these experiments in preference to the pET-11d vector used in the over-expression of *B. napus* βKR, as it contained an *Nde*I cloning site as opposed to a *Nco*I cloning site; which could not be used as the *E. coli* βKR gene contained an internal *Nco*I site. A simultaneous digest using *Nde*I and *Bam*HI of the pET-11a plasmid (1000 ng) and the *E.coli* βKR PCR product (500 ng) was carried out, the products of which are shown in figure 4.4. A T4 DNA ligase ligation was set up using 100 ng each of vector and insert.

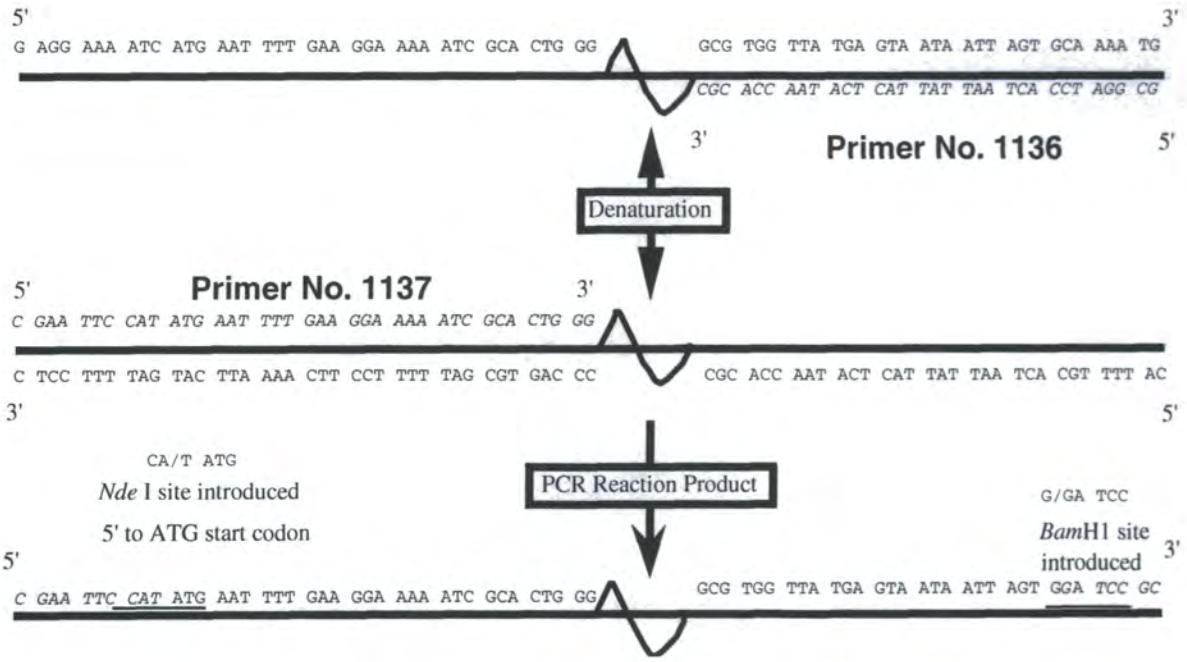

Figure 4.1 Diagram showing the alignment and reaction product of primers designed to amplify the *E. coli* βKR coding sequence and flank it with *Nde*I and *Bam*HI restriction sites.

Primer DNA and altered bases are shown in *italics*, and inserted restriction sites are underlined.

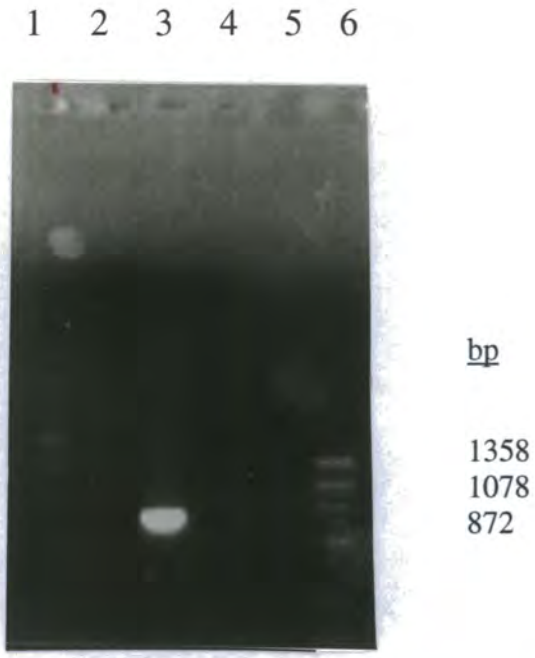

Figure 4.2 Agarose TAE gel (0.7%) showing products from a PCR reaction designed to amplify and modify the *E. coli* βKR coding sequence.

The expected 817 bp product is seen in lane 3.

Lane 1, reaction containing *E. coli* chromosomal DNA and primer #1137; lane 2, reaction containing *E. coli* chromosomal DNA and primer #1136; lane 3, reaction containing *E. coli* chromosomal DNA and primers #1136 and #1137; lane 4, reaction containing no template DNA and primers #593 and #590; lane 5, empty; lane 6, ϕX-174 *Hae*III digest size markers.

Lane 3 contained the expected product (817 bp) from the polymerase chain reaction designed to amplify and modify the *E. coli* βKR coding sequence from chromosomal DNA.

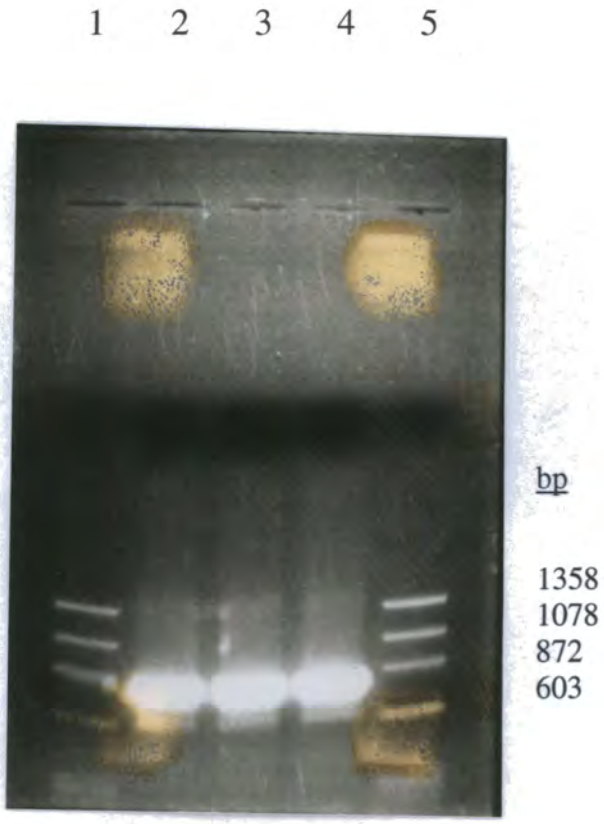

Figure 4.3 Agarose TAE gel (0.8%) showing gel purification of *E. coli* βKR PCR product

Lane 1, ϕX-174 *Hae*III digest size markers; lanes 2-4, remainder of PCR product from figure 4.2, (lane 3 [3 x 30 µl]); lane 5, ϕX-174 *Hae*III digest size markers.

The remainder of the PCR reaction was run out on a 0.8% agarose (Pharmacia GNA-100) TAE preparative gel. The gel was trans-illuminated and bands corresponding to the 817 bp PCR product were excised from the gel. An aliquot of the gel purified PCR product was run out on an agarose TAE gel (0.7%) to estimate its concentration against a known standard.

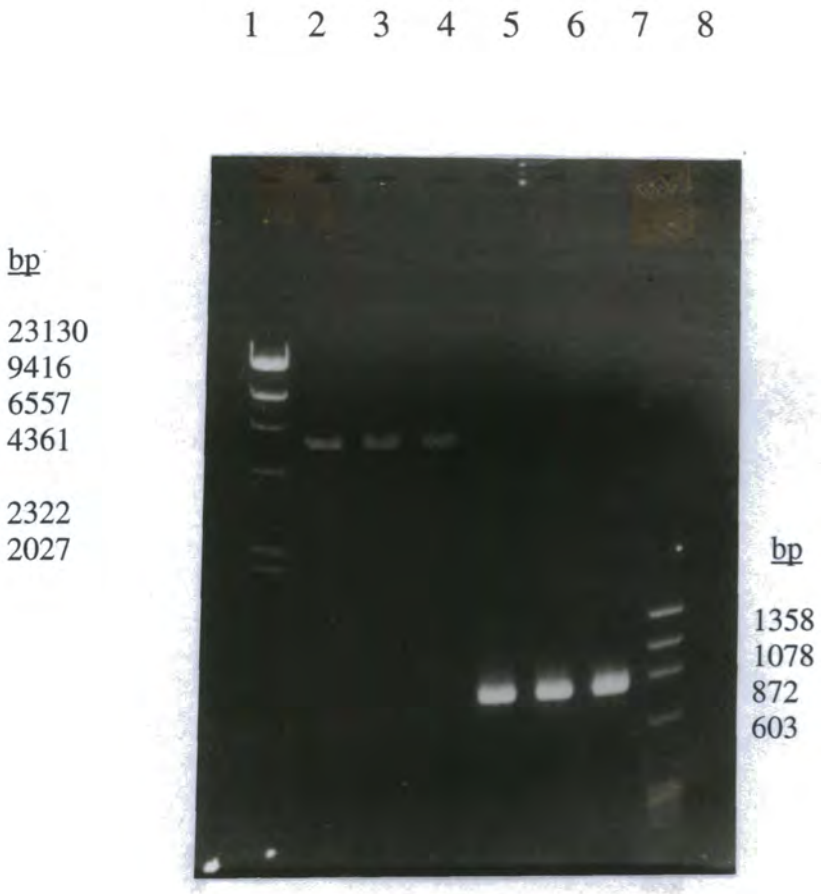

Figure 4.4 Agarose (0.8%) TAE gel showing gel purification of restriction products of the pET-11a vector and *E. coli* βKR PCR product double-digests.

Lane 1, DNA size markers from a λ*Hind*III digest; lanes 2-4 5367bp pET-11a *Bam*HI - *Nde*I digestion product; lanes 5-7, 802 bp *E. coli* βKR PCR product *Bam*HI - *Nde*I digestion product; lane 8, DNA size markers from a ϕX-174 *Hae*III digest.

The bands corresponding to the vector and insert were excised from this gel and cleaned of agarose using a QIAEX kit.

4.3 Over-production of βKR in *E. coli*

4.3.1 Transformation of *E. coli* BL21(DE3)

Prior to transforming the BL21(DE3) expression strain, it was decided to avoid potential transformation problems by first preparing a large amount of vector DNA in XL2-Blue ultracompetent cells (Stratagene). The ten resulting transformants cells were subjected to a mini plasmid. The resulting ten plasmids were checked for size by digesting 5 μl of the plasmid preparation with 1 unit of *Bam*HI at 37 °C for 3.5 h, and running the digest out on an agarose TAE (0.7%) gel with DNA size markers. This gel is shown in figure 4.5. The correctly sized plasmids were designated 'pETNEβ'.

Transformants designated 1, 2 and 3 were re-cultured and subjected to a further mini-Prep to produce plasmid DNA for transformation of the over-expression strain BL21 (DE3). Competent BL21 (DE3) cells were thawed on ice and incubated with aliquots of pETNEβ1 (from transformant 1) DNA. After the required treatment and incubation two colonies were streaked out on to an LB ampicillin plate for overnight incubation and storage as a stock plate.

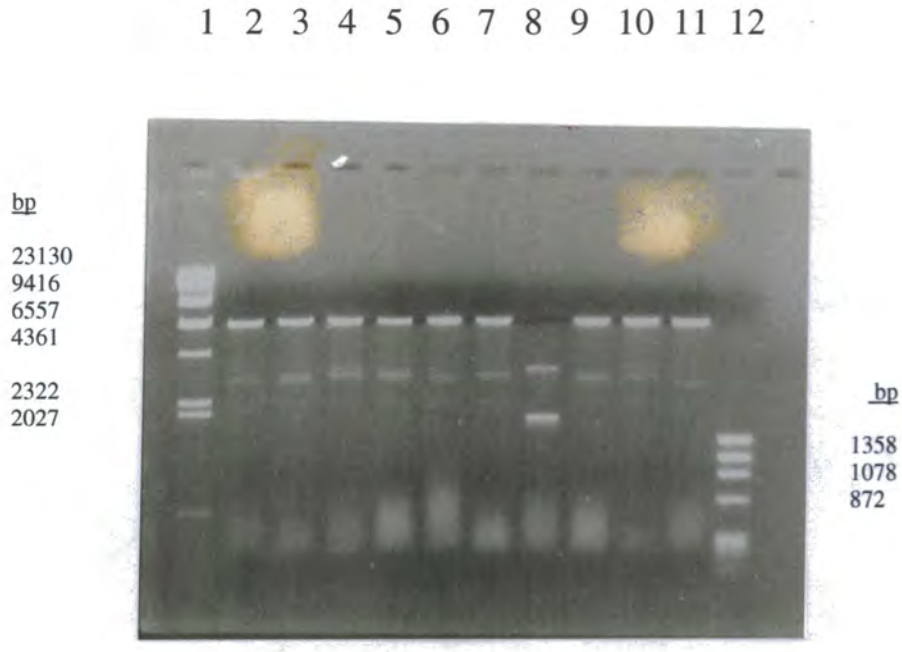

Figure 4.5 Agarose (0.7%) TAE gel showing sizes of plasmids formed from the ligation of pET-11a and the *E. coli* βKR PCR reaction product.

Lane 1, DNA size markers from a λ*Hind*III digest; lanes 2-11 pET-11a - *E. coli* βKR ligation products; lane 12, DNA size markers from a ϕX-174 *Hae*III digest.

Plasmids from ten randomly picked viable transformants were linearised with *Bam*HI and run on the above gel to check their size. All of the transformants except that shown in lane 8 had the correct plasmid size of 6169 bp (vector 5367 bp + insert 802 bp).

4.3.2 Over-expression studies

The plasmid pETNEβ1 was used to transform *E. coli* strain BL21(DE3). Trial over-expression cultures were grown in 5 ml Luria Broth (LB) containing 100 μg/ml ampicillin, for selection of transformants, on a rotary shaker at 220 rpm for 16 h at 37°C. An aliquot of 50 μl was inoculated into 50 ml of LB plus 100 μg ml^{-1} ampicillin and cultured for three hours. A 1 ml sample of cell suspension was taken at this point and incubated separately. The 49 ml culture was then brought to 100 μM IPTG, and grown for a further three hours. The centrifuge-harvested cells from the 50 ml culture. Two baths were set up, one containing ethanol and dry-ice, the other containing water and ice. The cell pellet was placed in a thin polythene bag and subjected to a modification of the freeze-thaw protein isolation method of Johnson and Hecht [1994] The cell pellet was frozen in the ethanol/dry ice bath for 2 min, followed by a thawing step lasting 8 min in the water/ice bath. These steps were repeated two further times, before 1.25 ml of buffer (25 mM sodium phosphate, 1 mM DTT pH 7.0) at 4 °C was added. The tube was tapped gently for 30 seconds to resuspend the cell pellet and then placed in a water/ice slurry for 30 min. The partially lysed cells were separated from the protein containing buffer via a centrifugation step at 10000 x g for 10 min at 4 °C.

4.3.3 SDS-PAGE detection of over-expression

Samples taken from growing cultures of BL21(DE3) pET-11d (empty over-expression vector), and BL21(DE3) pETNEβ1 (uninduced by IPTG) loaded on the SDS-PAGE gel shown in figure 4.6. A computer analysis of the predicted amino acid sequence of the *E. coli* βKR had given its predicted molecular weight to be 25.5 kDa. The over-expressed βKR protein was clearly observable at approximately 22-23 kDa in pETNEβ1 transformant protein extracts from IPTG induced, and uninduced cell cultures.

Figure 4.6 SDS-PAGE gel (5% acrylamide stacking/10% acrylamide resolving) showing over-expression of E.coli βKR in strain BL21(DE3) pETNEβ1.

Lane 1, SDS-VII Mw markers; lane 2, Laemmli buffer protein extract from cells containing pET-11d; lane 3, Met C mutant BL21(DE3) pETNEβ1 transformant uninduced - Laemmli buffer extract; lane 4, Met C mutant BL21(DE3) pETNEβ1 transformant IPTG induced - Laemmli buffer extract; lane 5, Met C mutant BL21(DE3) pETNEβ1 transformant IPTG induced - freeze-thaw extract; lane 6, BL21(DE3) pETNEβ1 transformant uninduced - Laemmli buffer extract; lane 7, BL21(DE3) pETNEβ1 transformant IPTG induced - Laemmli buffer extract; lane8, BL21(DE3) pETNEβ1 transformant IPTG induced - freeze-thaw extract.

The over-expressed βKR protein is clearly observable at 22-23 kDa in pETNEβ1 transformant protein extracts from IPTG uninduced, and induced cell cultures. See §6.4 for description of the Met C mutant.

4.4 Purification strategy for *E. coli* βKR

The freeze-thaw gentle lysis-method, employed as a replacement for the lysozymal extraction method used on the *B. napus* protein in the previous chapter, greatly simplified the purification and handling of the *E. coli* βKR over-produced protein as the previous experiments had shown the starting material to be a protein extract that was already approximately 50% pure. To obtain suitable amounts of *E.coli* βKR for structural studies, the pETNEβ1 transformed BL21(DE3) strain would require litre-scale culture. A convenient purification method, based on the single ion-exchange matrix - two pH buffer method devised in the last chapter would be sought to provide protein of sufficient purity for study of the enzyme. A computer analysis of the predicted amino acid sequence of the *E. coli* βKR had given its predicted isoelectric point to be 6.76. Thus the protein's behaviour on an ion-exchange matrix could be loosely predicted for the purification exercise.

The exercise of over producing the *E. coli* βKR was primarily to obtain material for structural studies. As such an excess of active βKR was present in the crude extracts produced, a convenient purification procedure with an emphasis on purity rather than recovery was sought. The crude preparations contained some 50% of the protein content as βKR at the outset of the purification procedure (see figure 4.6, lane 7). Therefore, precise monitoring of the purification via quantitative assays of enzyme activity and the compilation of purification tables was not undertaken. Qualitative assays were used to follow the location of βKR during purification.

4.4.1 Large scale culture of *E. coli* BL21(DE3) pETNEβ1

Cells transformed with pETNEβ1 were grown in a 5 ml LB starter cultures containing 100 μg ml^{-1} ampicillin on a rotary shaker at 37 °C overnight. These cultures were used at a dilution of 1:100 to inoculate 1 l of LB plus μg ml^{-1} ampicillin, which was grown under the same conditions until an OD_{600} of 0.8 AU was reached. Over-production of βKR was maximised by adding IPTG to 100 μM. The cultures were grown for a further three hours before cell harvesting via centrifugation at 5000 x g. The cell pellets were immediately used for protein extraction or flash frozen in liquid nitrogen and stored at -80 °C.

4.4.2 Crude extract preparation

As with the over-expression trial experiments, a freeze-thaw lysis method was routinely used to release the over-produced *E. coli* βKR protein. Cell pellets from the 1 l cultures were resuspended in 10 pellet volumes of chromatography starting buffer (buffer A; 25 mM sodium phosphate, 1 mM DTT, 1 mM EDTA, of the appropriate pH (i.e., 7.0, 8.0 or 7.6 – see below). The timing of the pellets' submersion in the freezing and thawing baths was adjusted to account for the increased pellet volume. The freezing stage in ethanol/dry-ice was extended to 4 min whilst the thawing step in water/ice was extended to 10 min. The suspension was kept on ice for 1 h and centrifuged to reform the cell pellet and give a supernatant of predominately βKR protein. Freeze-thaw supernatants were centrifuged at 30000 x g for 15 min to remove debris, flash frozen in liquid N_2 in droplet form, and stored at -80 °C.

The freeze-thaw extract was found to have a high level of βKR activity upon enzyme assay. The specific activity of the extract, approximately 60% pure by SDS-PAGE estimation, was found to be 35 U (μmol NADPH min^{-1}) mg^{-1} total protein concentration measured by a Lowry protein assay.

In preparation for chromatography, cell-free extract (50 ml) was diluted to 100 ml with buffer A and centrifuged at 30,000 g for 10 min at 4°C. The resulting supernatant was brought to 85% saturation $(NH_4)_2SO_4$, (596 g l^{-1}) stirred for 1 hour, and centrifuged at 10,000 g for 15 min. The pellet was resuspended in 25 ml of buffer A and dialysed against 2 x 2 l of buffer A over 4 hours. All steps were carried out at 4°C. After filtration, Milli Q grade water was added to reduce the conductivity to below 3 mS.

Upon experimentation, a second freeze-thaw treatment on the reformed cell pellets was found to release an additional amount of βKR (65% extra). As the second freeze-thaw step and the continued storage of the pellets may have increased the permeability of the cells, a 24% saturation ammonium sulphate cut was carried out on the supernatant to remove any non-protein contaminants, e.g. DNA, that may have accompanied the over-produced protein.

4.4.3 Development of a two step ion exchange chromatography method for the purification of over-expressed *E. coli* βKR

The purification of *B. napus* βKR in the previous chapter was achieved using a convenient two step chromatographic procedure on the same ion-exchange matrix. It was decided, in the first instance, that a similar method of purification would be sought for the over-expressed *E. coli* βKR protein.

4.4.3.1 Step 1: Anionic exchange (HiLoad Q matrix) pH 7.0

Using the computer predicted isoelectric point of the *E. coli* βKR (6.76), it was believed that the protein would bind to a Q anionic exchange matrix at pH levels above pH 6.76. This approach was first tested on a 'HiLoad Q 26/10' anionic exchange column with buffers at pH 7.0. A freeze-thawed cell pellet corresponding to 4 litres of culture was resuspended in 150 ml of 100 mM sodium phosphate pH 7.0, 1mM DTT, 1mM EDTA, and centrifuged and filtered through a Whatman GF-A (0.7 μm) glass fibre filter to remove debris. The protein extract was loaded on to the previously equilibrated column. The pass from the column was assayed optically and found to have the same level of activity as the loaded sample, so loading was aborted.

Binding had not occurred because of one or more possible reasons, the pH of the buffer (pH 7.0) may have been too close to the actual isoelectric point of the protein. Thus the protein would have carried insufficient charge to bind to the matrix. Also, there may have been other substances in the extract which competed for binding sites on the matrix.

4.4.3.2 Step 1: HiLoad Q matrix pH 7.6

To enable the enzyme to bind to the HiLoad Q column, it was buffer exchanged into a buffer of pH 7.6, via an ammonium sulphate precipitation to concentrate the protein and to attempt to remove interfering non-protein contaminants. Ammonium sulphate, 567 g/l was added to the protein sample at 4 °C. The suspension was stirred for 30 min at 4 °C and centrifuged at 6000 rpm for 15 min. The pellet was resuspended in 120 ml of 25 mM sodium phosphate, 1mM DTT, pH 7.6 and dialysed against 3 x 2 litres of the same buffer over a period of 15 h at 4 °C. The dialysate was centrifuged (30 000 x g; 10 min; 4 °C), filtered to 0.5 μm, diluted with 80 ml of filtered resuspension

buffer (as above) and loaded on to the HiLoad Q column. No βKR activity was detected in the pass so the enzyme was deemed to have bound to the matrix. A 250 ml gradient, to 100% start buffer (25 mM sodium phosphate, 1 mM DTT, 1 mM EDTA, pH 7.6) containing 1 M NaCl, was run and the eluted fractions (6 ml) were collected. Qualitative assays of the eluted fractions showed fractions 14 - 21 to contain βKR activity. This corresponded to the first 280 nm absorbance peak on the eluent trace, shown in figure 4.7. Aliquots (20 μl) from fractions surrounding and including this protein peak (9-24) were boiled with Laemmli loading buffer for 3 min and each loaded into a lane on the SDS-PAGE gels shown in figure 4.8.

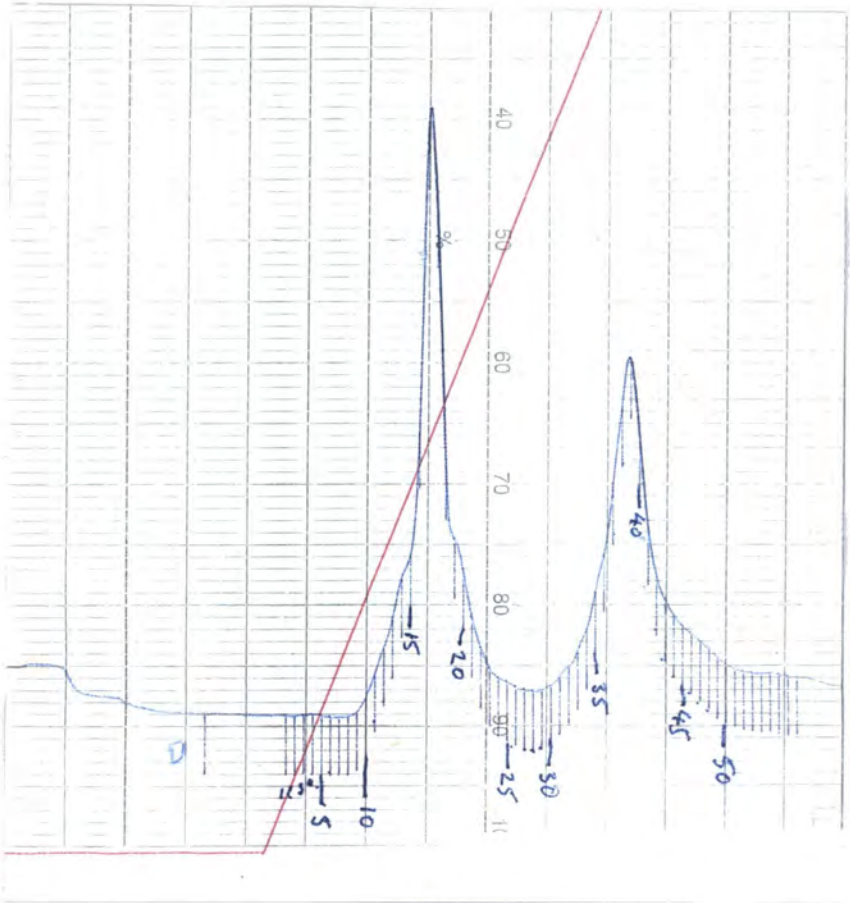

Figure 4.7 Absorbance trace (280 nm) of eluted protein from a HiLoad Q column at pH 7.6

Qualitative assays of the eluted fractions showed fractions 14 - 21, corresponding to the first absorbance peak at approximately 30% of the 0-1 M NaCl gradient, to contain βKR activity. No βKR activity was detected in the second peak (35-45) or in the pass from the column.

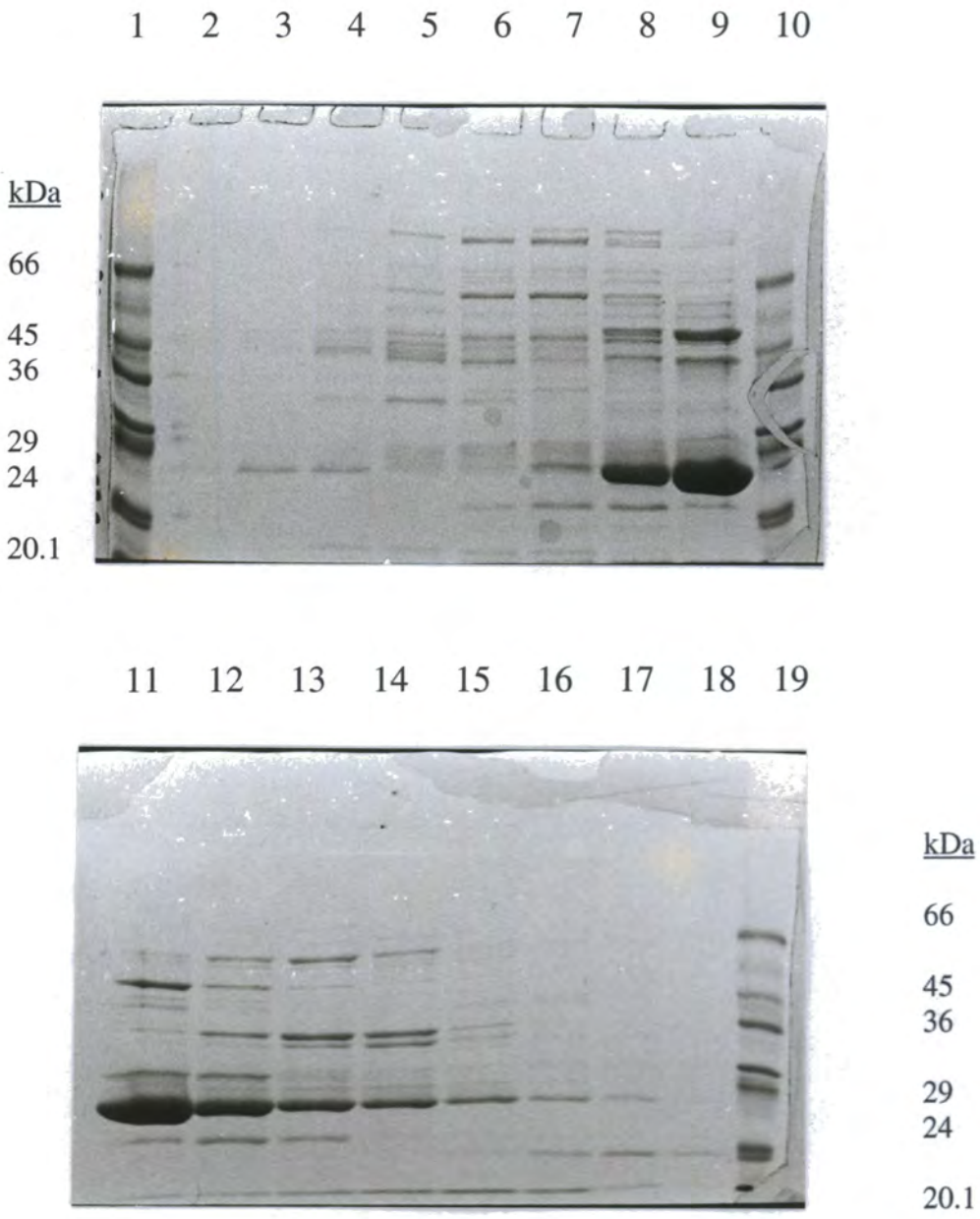

Figure 4.8 SDS-PAGE gel (5% acrylamide stacking/10% acrylamide resolving) showing βKR active fractions eluted from a HiLoad Q column at pH 7.6

Lane 1, SDS-VII Mw markers; lanes 2-9, fractions 9-16; lane 10, SDS-VII Mw markers; lanes 11-18, fractions 17-24; lane 19, SDS-VII Mw markers.

The combination of subtraction of proteins binding to the Q matrix at pH 7.0, and the pH 7.6 chromatography step, has considerably enriched the βKR protein (major species - lanes 8-9, 10-11) from the crude extract shown in figure 4.6.

4.4.3.3 *Step 2: Anionic exchange (Mono Q) pH 8.0*

It was decided to employ the high resolution of the FPLC system and an accompanying MonoQ column, for the second chromatographic step. The pooled active fractions (15-18; 24 ml) eluted from the HiLoad Q column at pH 7.6, were dialysed into 25 mM sodium phosphate, 1mM DTT, pH 8.0. The dialysate was centrifuged and filtered (0.2 μm filter) and loaded onto a 1 ml FPLC Mono Q column, equilibrated in 25 mM sodium phosphate, 1mM DTT, pH 8.0 buffer at 4 °C. The column was washed free of 280 nm absorbing material and a 25 ml gradient run from the equilibration buffer to buffer plus 1M NaCl. βKR activity eluted at the midpoint of the gradient as the major protein peak. Aliquots (20 μl) from fractions corresponding to this peak were loaded on the gel shown in figure 4.9. Though not 100% pure, the βKR preparation was deemed sufficiently homogenous to be used for crystallographic trials. The purest fractions from the column, fractions 14 and 15 - containing approximately 4 mg of βKR, were used for crystallographic trials - see §6.

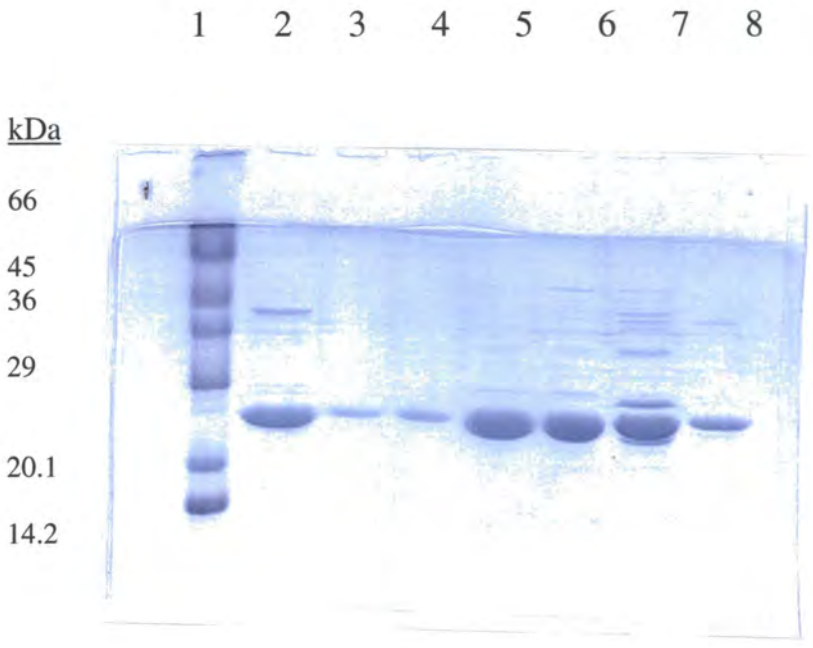

Figure 4.9 SDS-PAGE gel (5% acrylamide stacking/10% acrylamide resolving) showing βKR active fractions eluted from a Mono Q column at pH 8.0

Lane 1, Mw markers; lane 2, loaded sample (pooled fractions from HiLoad Q column at pH 7.6); lanes 3-8, fractions 11-16 (comprising the major protein peak).

The purity level of the βKR eluted in fractions 14 and 15 (lanes 5 and 6) was deemed sufficiently homogenous to be used for crystallographic trials. These fractions, containing approximately 4 mg of βKR in total, were dispatched to the University of Sheffield for such trials.

4.4.3.4 Method Improvements: Step 1 HiLoad Q matrix (pH 7.6) and Step 2: Mono Q matrix (pH 7.2)

Though βKR had been purified to a high level with the use of anionic Q matrices at pH 7.6 followed by pH 8.0 in the previous experiments, it was decided to attempt to attain homogeneity though adjustment of the buffer pH used. As further preparations of the protein were required for structural and other studies, it was decided to incorporate investigations of suitable buffer pH adjustments into these preparations.

As a large proportion of the pH induced charge shift of a protein generally occurs within a pH unit either side of a protein's isoelectric point (for *E. coli* βKR theoretical pI = 6.76), it was decided to perform the purification of the crude extract at pH 7.6 and the secondary purification of the resulting similarly charged protein species at pH 7.2. By using a chromatography buffer of pH 7.2, close to the pI of βKR (pH 7.2), it was hoped that contaminating proteins would have a significantly differing charge to that of βKR, perhaps to the extent of having passed through their respective isoelectric points and thus be incapable of binding to the anionic matrix.

Step 1 - HiLoadQ pH 7.6: A βKR crude extract was loaded on to a HiLoadQ column equilibrated with 25 mM sodium phosphate, 1 mM DTT, 1 M NaCl, pH 7.6, and the column washed free of 280 nm absorbing material. A gradient to buffer plus 1M NaCl, was run through the column and fractions collected. βKR activity was detected in the first major protein peak in the trace, at 30% through the gradient. Aliquots (20 µl) from fractions surrounding and including this protein peak (13-20) were boiled with Laemmli loading buffer for 3 min and each loaded into a lane on the SDS-PAGE gel shown in figure 4.10.

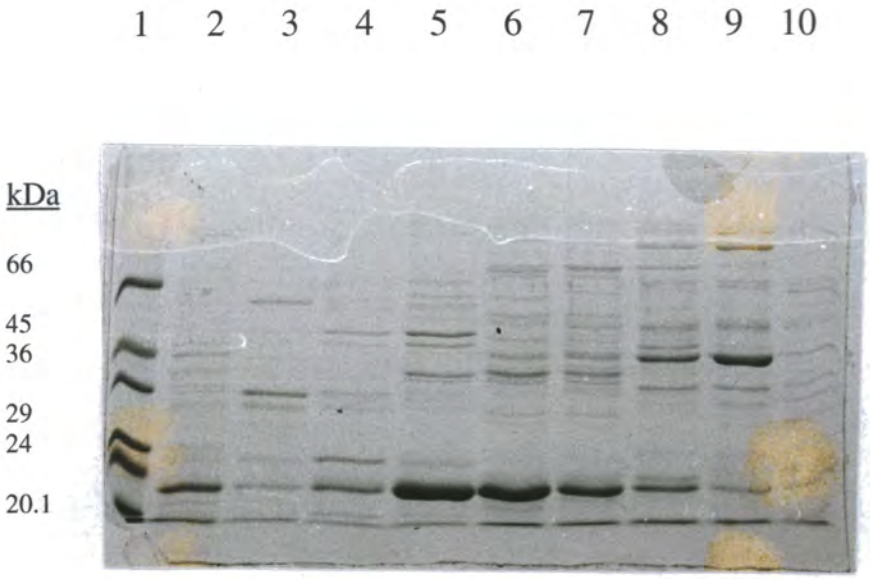

Figure 4.10 SDS-PAGE gel (5% acrylamide stacking/10% acrylamide resolving) showing βKR active fractions eluted from a HiLoad Q column at pH 7.6

Lane 1, SDS-VII Mw markers; lane 2, crude extract; lanes 3-10, fractions 13-20, corresponding to the protein absorbance peak containing βKR.

βKR is similarly purified as with the previous purification on a Q matrix at pH 7.6 (figure 4.8).

Step 2 - MonoQ pH 7.2: For the second step of purification, a MonoQ column was attached to the FPLC system and was equilibrated and charged with buffers reformulated to pH 7.2. The βKR sample was diluted with 5 ml of the reformulated equilibration buffer and carefully adjusted to pH 7.2 on a stirring plate via dropwise addition of 1M NaOH. The resulting 10 ml βKR sample was filtered through a 0.2 μm filter and used for two 5ml chromatography runs on the 1 ml Mono Q column. The majority of the protein loaded on each run bound to the column and was eluted during between 3-10 ml of the 25 ml gradient to 1M NaCl buffer and was found to be in a homogeneous state upon analysis via SDS-PAGE, figure 4.11 shows an SDS-PAGE gel from the first of the three runs. The unbound protein from the two runs was combined and reloaded on the column and similarly purified after binding completely to the column. Approximately (4 mg) of βKR was purified from the three chromatography run as estimated by from the SDS-PAGE gel.

Thus, a two-step purification procedure using an anionic-exchange matrix, with chromatography buffers at pH 7.6 followed by pH 7.2, was demonstrated to be capable of purifying over-expressed *E. coli* βKR.

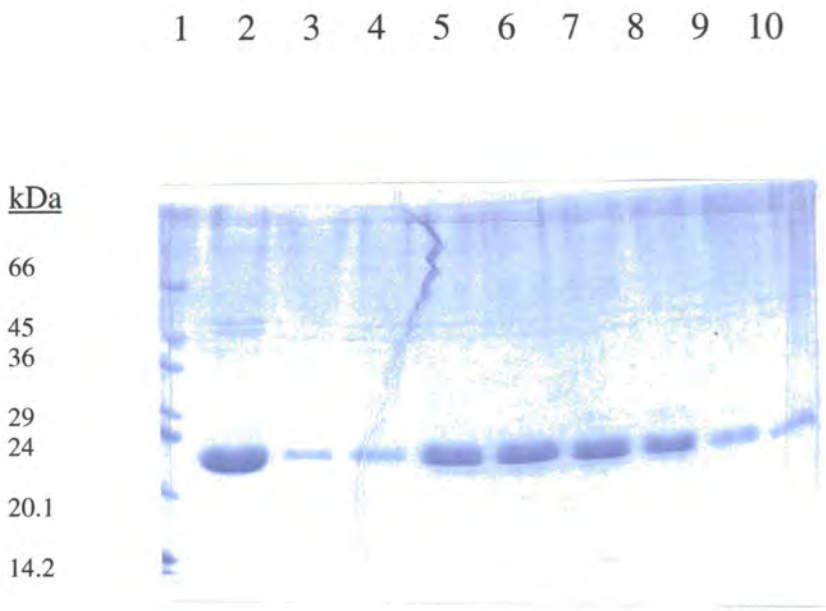

Figure 4.11 SDS-PAGE gel (5% acrylamide stacking/10% acrylamide resolving) showing βKR active fractions eluted from a Mono Q column at pH 7.2

Lane 1, SDS-VII Mw markers; lane 2, Loaded part-pure sample; lanes 3-10, fractions 3-10.

The majority of the part-pure βKR protein loaded on to the Mono Q column at pH7.2 bound. The eluted fractions of the major protein absorbance peak were found to contain βKR in a homogeneous state, as shown above (lanes 3-10).

4.4.4 Routine Purifications - HiLoad Q matrix (pH 7.6 and 7.2)

To eliminate the need for multiple loadings on a low capacity column, it was decided to use the 50 ml bed volume HiLoad Q column for both chromatographic steps. Though the resolution of this column, and the quality of the buffer gradient produced by the HiLoad chromatography system associated with it, was not as high as the resolution of the FPLC system, it was hoped that the level of purification obtained would be adequate for the sample usage required, i.e. structural studies. The protocol detailed below was used for routine preparations of the *E. coli* βKR when required.

For the first stage of purification, the *E. coli* βKR dialysate was loaded on to the HiLoad Q column equilibrated with buffer A (25 mM sodium phosphate, 1mM DTT, pH 7.6). The column was washed free of 280 nm absorbing material with 200 ml of buffer. Elution of βKR activity was carried out using a 360 ml linear gradient leading to 100% buffer B (buffer A including 1 M NaCl) at a flow rate of 5 ml min^{-1}. *E. coli* βKR activity was detected at approximately 300 mM NaCl in the gradient. βKR activity was generally detected in fractions 14 -21, coinciding with the first major protein peak. No activity was found in the second protein peak or in the pass from the column.

Further purification was achieved by pooling and dialysing the active fractions containing βKR into buffer A (reformulated to pH 7.2), centrifuging the sample at 30,000 g for 15 minutes, filtering through a 0.5 μm filter and reloading onto the Hi-Load Q column, previously equilibrated with buffer A (pH 7.2). βKR activity was eluted with a 360 ml gradient leading to 100% buffer B (buffer A including 1 M NaCl, pH 7.2). Aliquots (20 μl) from the active fractions were boiled with 5 μl of 5X Laemmli loading buffer for 3 min and analysed via SDS-PAGE gels - an example is shown in figure 4.12. It can be seen from these gels that the protein is essentially homogenous in the fractions containing the bulk of the eluted enzyme. Using the HiLoad (26/10) column for both steps, at pH 7.6 and subsequently at pH 7.2, provided a convenient method of milligram-scale purification of βKR from the over-expressing strain.

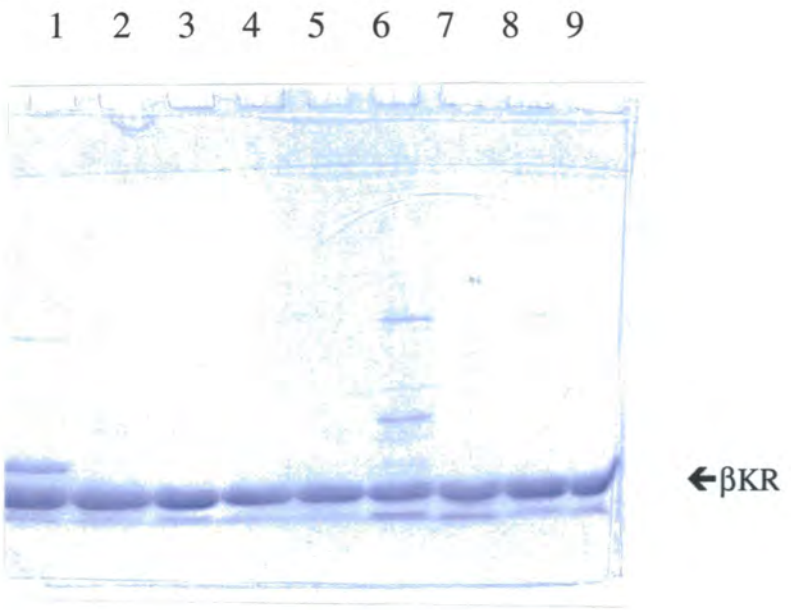

Figure 4.12 SDS-PAGE gels (5% acrylamide stacking/10% acrylamide resolving) showing βKR active fractions eluted from a HiLoad Q column at pH 7.2

Lanes 1-9 βKR active fractions.

The second stage routine purification on a HiLoad Q column at pH 7.2, was shown to be capable of purifying βKR to a near homogeneous state, as shown by the eluted fractions on the gel above.

4.4.5 Enzyme activity

The purification procedure developed for *E. coli* βKR was successful in its intended purpose of producing pure βKR for structural studies. Assays of enzyme activity were used in a qualitative fashion during purification. However, it was decided to obtain an idea of the amount of enzyme activity released from the over-expressing strain and the recoverability of this activity during purification by means of quantitative assay. For the first stage purification described in section 4.4.3.2. assays of the crude extract and active purified protein fractions were carried out. The specific activity of the freeze-thaw extract, approximately 80% pure by SDS-PAGE estimation, was found to be 35 U (μmol NADPH min-1) mg-1. Total protein concentration was measured by a Lowry assay – see §2.3.4. The purified protein had a specific activity of 41 μmol NADPH min^{-1} mg^{-1} and was estimated to be >95% pure (concentration of protein estimated on the basis of 1 mg ml^{-1} = 1.0 $AU_{280\ nm}$).

4.5 Amino acid sequencing of *E. coli* βKR

Amino acid sequencing was carried out on the over-produced protein. Approximately 300 pmole of purified *E. coli* βKR was loaded onto a Prospin column (Applied Biosystems) and treated according to the manufacturers instructions. The Problot filter from the spun column was loaded on to the sequencer disc of an ABI 477A Protein Sequencer and run for six cycles of Edman chemistry. Manual adjustment of the returned data by the operator, John Gilroy of the Department, gave the sequence MNFEGK as predicted by the Genbank DNA sequence [Rawlings and Cronan, 1992]. This confirmed the identity of the purified protein and established that the N-terminus was correctly formed in *E. coli*.

4.6 Summary

It was found from crystallographic analysis of *B. napus* βKR that it would be helpful to perform similar over-expression and purification experiments to allow crystallisation of the *E. coli* βKR to provide structural clues for plant enzyme.

Using the published sequence for *E. coli* βKR, primers were designed to amplify the gene sequence from chromosomal DNA and flank it with restriction sites suitable for its insertion into an over-expression vector. After restriction and ligation of the PCR

product and vector, the resulting plasmid, pETNEβ1, was tested for over-expression of the bacterial βKR enzyme. Once over-expression had been confirmed, litre scale culture of *E. coli* strain BL21(DE3) was carried out.

A freeze-thaw lysis method was used to release the over-produced protein from the cultures, giving preparations which were estimated to be 80% pure. A purification strategy was sought based around the two step ion-exchange method conceived and developed for use with the *B. napus* βKR protein. After testing various permutations of buffer pH and cationic and anionic matrices, a routine purification method suitable for purification of the enzyme from bulk cultures was devised. This method employed a anionic Q matrix in a 50 ml pre-packed Pharmacia HiLoadQ (26/10), equilibrated at pH 7.6 for the first stage of purification, the active fractions from which were then loaded onto the column in a buffer at pH 7.2 for the final stage of purification. The milligram quantities of *E. coli* βKR produced by this method were sent for crystallisation - see §6.

Chapter 5: Immunological study of *B. napus* βKR in crude seed extracts

5.1 Introduction

Previous to this work antibodies had been raised to avocado βKR [Sheldon *et al.*, 1990]. In this study, these antibodies were incapable of detecting βKR in rapeseed extracts (see §3.4.4). The availability of milligram quantities of purified *B. napus* βKR from the over-expression experiments would facilitate the production of antibodies to the *B. napus* enzyme. It was hoped that such antibodies would be used for the immunodetection of βKR isoforms in *B. napus* seed extracts via one and two dimensional western blots. Attempts would also be made to calculate the amount of βKR in developing seed extracts via quantitative western blotting and a βKR protein standard.

5.2 Anti-βKR polyclonal antibody production in mice

Anti-βKR polyclonal antibodies were initially raised by immunisation of mice. It was decided to attempt immunisations using totals of 6 μg and 45 μg of purified over-produced *B. napus* βKR for groups of three and five mice respectively. The lower level immunisation of 6 μg was carried out to observe the immune response to a lower level of antigen than normally used for antibody preparation in our laboratory for such antibody preparations. Whilst βKR was the predominant protein species in the purified preparation, it was decided to concentrate and size separate the βKR protein preparations via SDS-PAGE to reduce the number of contaminating *E. coli* proteins present in the antigen preparation.

5.2.1 Antigen preparation

The immunisation schedule required a total of 243 μg of βKR. A blotting efficiency of 50% was assumed, therefore a total of 0.5 mg of βKR was required for immunisation. For the primary immunisation, 150 μg of βKR was run out on four SDS-PAGE gels (5% acrylamide stacking/10% acrylamide resolving). The gels were cast at twice the normal thickness (1.5 mm) and were cast without well combs to allow protein to be loaded across the whole of the gel. The protein, 150 μg in four aliquots of 470 μl

of Laemmli buffer, was loaded on to the four gels. Freshly prepared SDS-running buffer was used to bathe the gels.

Upon completion of the electrophoresis, the gels were arranged with nitrocellulose membrane (Hybond C extra, Amersham) and blotting paper in a semi-dry blotter. The gels, membrane and paper were previously soaked in buffer; 0.05% SDS, 25 mM Tris, 192 mM glycine and 20% methanol (annular grade, BDH). The gels were subjected to a current of 0.8 mA cm^{-2} for a period of 1.5 h, to transfer the protein to the nitrocellulose membrane. The blots were allowed to air dry and were stained with Ponceau S dye (0.1 % (w/v) Ponceau S in 1 % (v/v) glacial acetic acid in Milli Q grade water) for 1 min. After rinsing with Milli Q grade water, a 1.5 mm wide band of βKR protein containing approximately 25 μg was clearly visible - the stained blot is shown in figure 5.1. The blots were placed on to a sterile glass plate. Flamed tweezers and a sterile razor blade were used to remove the βKR containing band. The strips of nitrocellulose were placed in 1 ml centrifuge tubes and stored at -20 °C. The processes above were repeated to provide nitrocellulose strips containing a total of 0.5 mg of βKR.

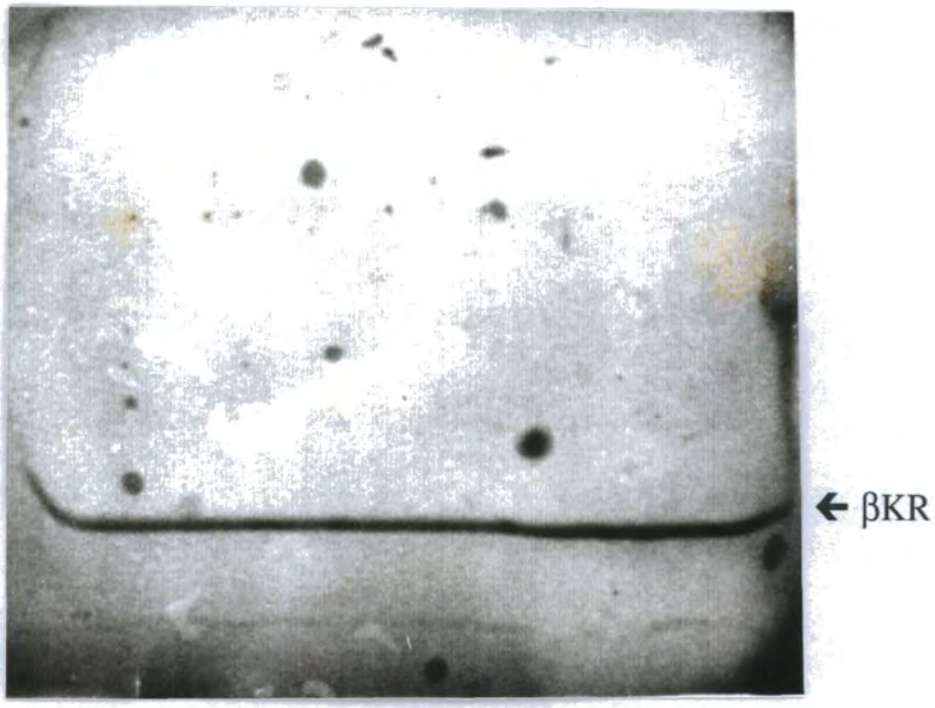

Figure 5.1 Ponceau S stained nitrocellulose blot showing gel purified band of βKR.

The band of βKR protein shown was excised from the nitrocellulose with a sterile razor blade and ground to a fine powder in a pestle and mortar to allow its injection for immunisation.

5.2.2 Immunisation procedure

For the first immunisation, the nitrocellulose strips containing βKR were ground to a fine powder in liquid nitrogen. Sterile saline (0.9% NaCl; 150 µl per immunisation) was added to the powder. An equal volume of Freund's complete adjuvant was added dropwise to the nitrocellulose-saline suspension on a vortex mixer so as to form an emulsion. Each of the mice was subcutaneously immunised with 300 µl of the respective antigen preparations. Five mice received 15 µg of βKR per mouse (group A), and three received 2 µg of βKR per mouse (group B) in the first immunisation. A second immunisation, containing the same amounts of antigen, was given without adjuvant three weeks after the primary injection and a third immunisation, without adjuvant was given 10 days later. The terminal bleeds were carried out 2 weeks after the final immunisation.

5.2.3 Serum characterisation

Blood was obtained from four of the five group A mice and all three of the group B mice. The blood samples were clotted at 37 °C for 30 min. The clot was separated from the side of the 1.5 ml microcentrifuge tube with a sterile Pasteur pipette. The ringed clots were placed at 4 °C overnight to contract. The serum and clots were centrifuged at 10,000 x g for 10 min at 4 °C. The serum was removed, spun again, and the supernatant was transferred to clean microcentrifuge tubes. The sera, approximately 0.3 ml from each mouse, were labelled A1-A4 and B1-B3. Sodium azide stock solution (2%) was added to each serum sample to give a final concentration of 0.02%, and the samples were stored at 4°C.

To characterise the cross reactivity of the sera two SDS-PAGE gels were run containing 14 alternating lanes of 100 ng βKR and 5 µl of a mixed-stage developing rape seed extract. (total protein 50 µg). This was the same extract as used to set up the βKR assay (§3.4.3), prepared from 5 g of seed extracted, via grinding homogenisation and centrifugation, in 10 ml of 100 mM KH_2PO_4/K_2HPO_4 1 mM DTT, 4 mM EDTA, pH 7.0. The gels were semi-dry blotted on to nitrocellulose membrane and stained with Ponceau S dye. The stained blots are shown in figure 5.2. Each of the pairs of antigen and extract lanes were cut from the blot to produce seven strips. To block the

nitrocellulose protein binding sites and prevent non-specific binding of the antibody, the strips were soaked in 1% haemoglobin-phosphate buffered saline (1%Hb-PBS) including 0.02% sodium azide overnight at 4 °C (PBS; 137 mM NaCl, 3 mM KCl, 8 mM $Na_2HPO_4 \cdot 2H_2O$, 2 mM KH_2PO_4, pH 7.4).

Each nitrocellulose strip was placed in a 50 ml Falcon centrifuge tube to which 3 ml of 1% Hb-PBS and 8 µl of one of the seven sera was added. The tube were placed on a roller for 2.5 h at room temperature. Five 5 ml washes with PBS-T (PBS + 0.1% Tween-20) were carried out over a period of 30 min on each of the seven strips. The strips, free of unbound primary antibodies from the sera, were transferred to a single hybridisation tube (Techne) to which 10 ml of 1%Hb-PBS and 10 µl of rabbit anti-mouse IgG antibodies (Pierce) were added. The strips were incubated for 1 h on a roller and then subjected to five 30 ml washes with PBS-T over a period of 30 min. The washed strips were then incubated for a further hour in 10 ml of 1%Hb-PBS containing 50 µCi of ^{125}I labelled donkey anti-rabbit IgG antibodies (Amersham). A final wash (5 x 30 ml; 30 min) was carried out, after which the strips were wrapped in Saran wrap (DuPont) and placed in cassettes with X-ray film (Fuji) at -80°C overnight.

The exposed and developed X-ray film is shown in figure 5.3. All sera gave a cross-reaction with the antigen containing lanes of the nitrocellulose strips. Sera A3, A4, B2 and B3 gave a strong cross reaction with a protein band at the same molecular weight as the βKR antigen in the rapeseed extract. Sera A1, A2 and B1 gave a weaker cross-reaction with the rapeseed extract at the same molecular weight as the βKR antigen. Serum A2 appeared to cross-react with a high-molecular weight species in the rapeseed extract, with a poor cross-reaction in the 27 kDa region. For this reason, A2 was excluded from the pooling of the other sera which constituted the anti-βKR polyclonal antibody preparation. An aliquot (15 µl) of each sera was retained from the pooling for possible future use. The pooled antibody preparation was aliquoted into 100 µl aliquots in sterile microcentrifuge tubes and stored at 4 °C

5.2.4 Testing of polyclonal anti-βKR antibodies for titre and specificity

To simultaneously check the specificity and titre of the polyclonal antibody

preparation, it was decided to repeat the previous SDS-PAGE gel preparation and expose the resulting blot to various dilutions of antisera. SDS-PAGE (5% acrylamide stacking/10% acrylamide resolving) gels were run containing twelve alternating lanes of 150 ng βKR and 50 μg of crude rapeseed protein. An extra lane, containing 50 μg of crude avocado mesocarp protein was also run on one of the gels. After electrophoresis, the proteins in the gels were transferred to two nitrocellulose membranes via a semi-dry blot as previously. The blots were stained with Ponceau S solution and cut into strips to provide five strips containing antigen and rapeseed extract, and one strip containing antigen, rapeseed extract and avocado extract. The nitrocellulose strips were blocked in 1%Hb-PBS overnight at 4 °C.

Each of the nitrocellulose strips were placed in a 15 ml Falcon tube with 2.5 ml of 1%Hb-PBS. A dilution series of the anti-βKR pooled sera was set up in the same solution. Aliquots of this dilution series were added to the strips such that the antisera were present in 2.5 ml of 1%Hb-PBS at dilutions of: 1:250, 1:500, 1:1000, 1:2500, 1:5000 and 1:10000. The nitrocellulose strip containing the sample of avocado protein was incubated with the 1:500 antisera dilution. The strips were incubated for 1 h 45 min on a roller, prior to washing with PBS-T (5 x 4 ml x 5 min). The secondary antibody, rabbit anti-mouse IgG (10 μl), was added to the collected strips in 10 ml of 1% Hb-PBS and was incubated for 1 h. The strips were washed with PBS-T and the tertiary ^{125}I labelled donkey anti-rabbit IgG antibody (5 μCi) in 10 ml of 1% Hb-PBS was added and incubated for 1h 15 min. After the final wash (5 x 50 ml x 5 min) the strips were reassembled and wrapped in Saran wrap and exposed to X-ray film at -80 °C overnight.

The developed film, shown in figure 5.4, showed that the combined anti-βKR antisera were capable of detecting the enzyme in its purified state at a dilution of 1:10000. The strips were further exposed for 2 hours to a fresh piece of X-ray film to examine more closely the cross-reaction with the avocado extract. The less exposed film (not shown) suggested that the antisera were cross reacting with two protein species in the avocado extract between 30 and 40 kDa. It was postulated at the time that these bands might represent the NADPH and NADH utilising forms of the enzyme reported by Caughey and Kekwick [1982].

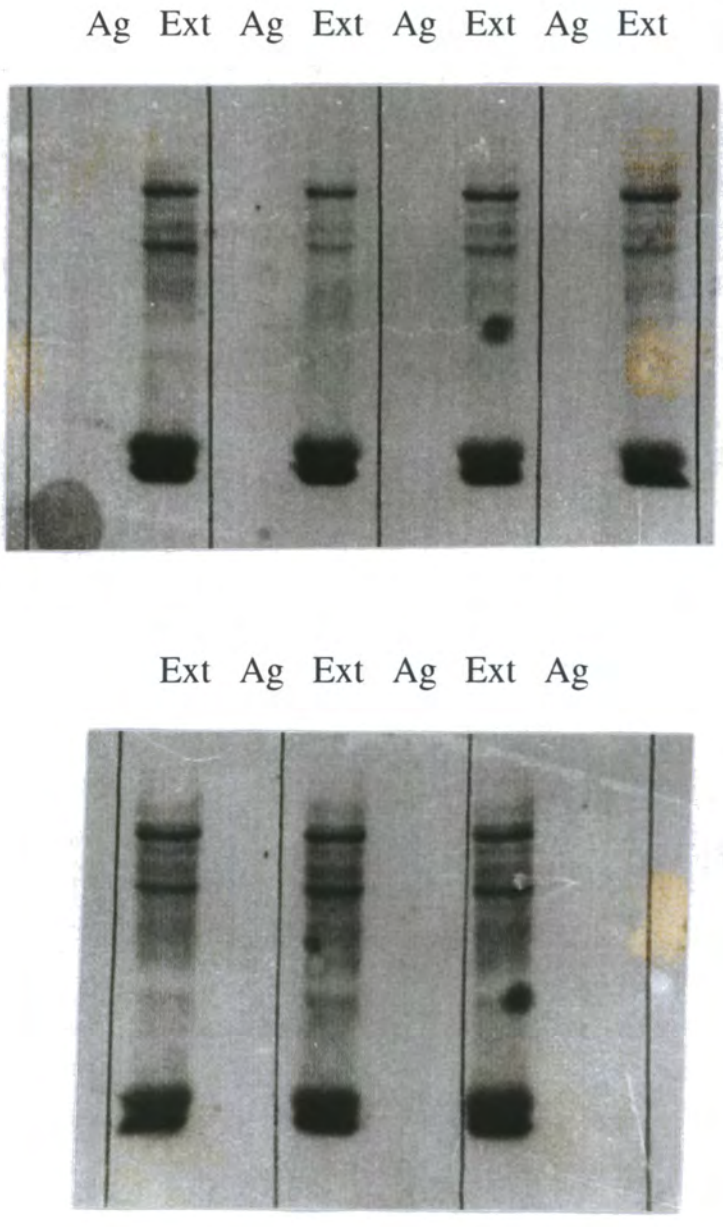

Figure 5.2 Nitrocellulose blots showing rapeseed extracts used for testing specificity of sera from βKR immunised mice.

The Ponceau S stained blot shown was transferred from two gels containing alternating lanes of 150 ng over-produced βKR antigen (marked 'Ag') and 50 μg of rapeseed total protein extract (marked 'Ext').

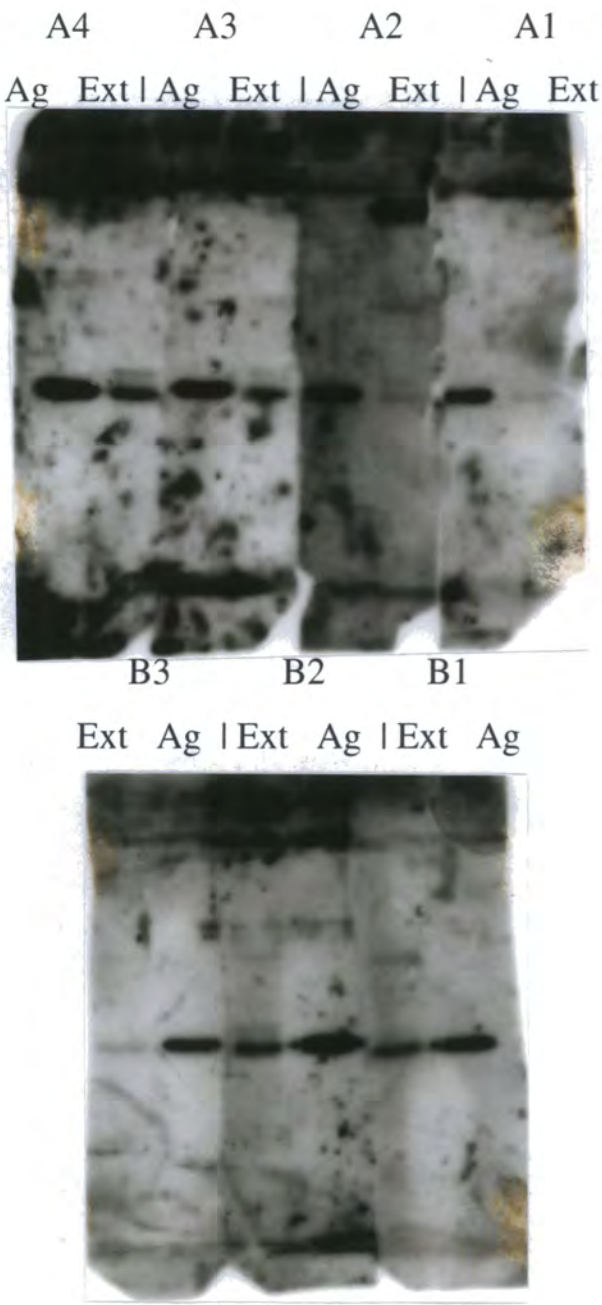

Figure 5.3 Autoradiograph showing the cross-reactivities of the antisera from the seven immunised mice.

'Ag' = 150 ng over-produced βKR antigen; 'Ext' = 50 μg of rapeseed total protein extract.

The autoradiograph shows the blot from the previous figure after immunodetection with anti-βKR mouse antisera. All sera gave a cross reaction with the antigen, whilst sera A3, A4, B2 and B3 gave a strong cross reaction in the extract and sera A1, A2 and B1 gave a weaker cross-reaction. Serum A2 appeared to cross react with a high molecular weight species in the rapeseed extract and was excluded from the pooling of the other sera.

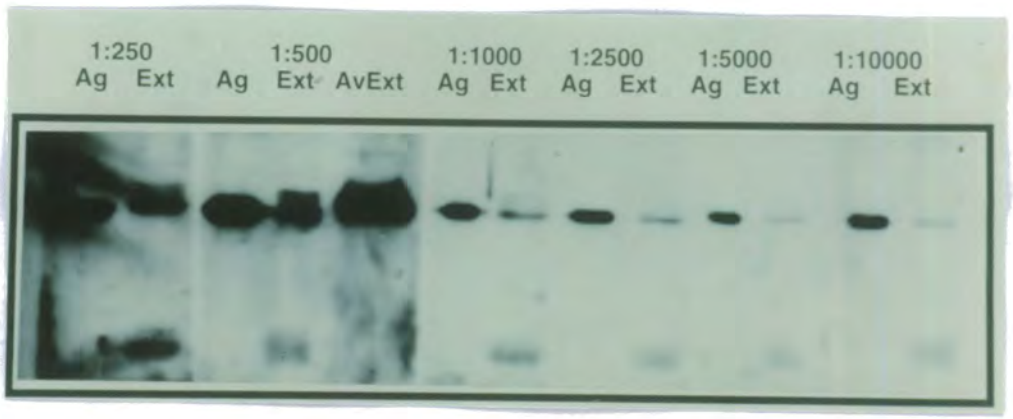

Figure 5.4 Autoradiograph showing the specificity and titre of the combined antisera from the βKR immunised mice.

'1:250' = dilution factor of antisera; 'Ag' = 150 ng βKR; 'Ext' = 50 μg crude seed protein extract; 'AvExt' = 50 μg avocado protein extract.

The above autoradiograph shows that the combined anti-sera were capable of detecting βKR in its purified state when used at a dilution of 1:10000.

5.3 Crude seed extract preparations

In the following experiments, various methods of extract preparation were used and developed, they are listed below.

5.3.1 Seed materials

Seeds of known developmental stages were obtained from glass house grown *Brassica napus* cv. Miranda (High Erucic Acid Rape) and bulk seed of estimated developmental stages from field grown cv. Falcon and cv. Spock. Developing seeds were also obtained from growth room grown *Brassica campestris* var. Oleifera. The seeds were stored in liquid nitrogen immediately after removal from the pods.

5.3.2 Boiling SDS-PAGE loading buffer method

In the initial experiments with mouse antibodies, batches of 30 seeds, of either mixed or known developmental stage, were ground to a fine powder in liquid nitrogen in a mortar and pestle. The frozen powder was added to 2 ml of Laemmli buffer [Laemmli, 1970] and boiled for 3 minutes. After cooling on ice, the samples were centrifuged for 10 min at top speed in a microcentrifuge and the supernatant was aliquoted (100 µl) and stored at -20 °C. Samples were thawed, boiled for 2 min, and briefly centrifuged prior to loading on SDS-PAGE gels.

5.3.3 Aqueous method

Due to the poor quality (in terms of weak βKR signal and high background in the gel lanes) of blots containing samples prepared in Laemmli buffer (above), a method that ensured removal of seed debris prior to boiling in Laemmli buffer was used. Thirty seeds, of mixed or known developmental stage, were ground to a fine powder in liquid nitrogen in a mortar and pestle. The frozen powder was added to 2 ml of buffer (50 mM Tris/HCl pH 7.5, 1 mM EDTA, 1 mM DTT, 0.1% Triton X-100) and centrifuged for 10 min at top speed in a microcentrifuge. The supernatant was removed from the pelleted debris and centrifuged again. The resulting supernatant was aliquoted (100 µl), flash frozen in liquid nitrogen and stored at -80 °C. Samples were thawed and concentrated Laemmli stock added, they were boiled for 3 min, and briefly centrifuged prior to loading on SDS-PAGE gels.

5.3.4 Ultracentrifugation-protease inhibitor method

To ensure that the minimum of degradation within the seed extract occurred during preparation, a method incorporating protease inhibitors was devised. This method also employed an ultracentrifugation step and a methanol/chloroform precipitation step which reduced the level of background in the gel lanes considerably. As with the previous two methods, 30 seeds (in this case stored in liquid nitrogen from harvest) were ground to a fine powder in a mortar and pestle cooled with liquid nitrogen. The powder was added to 2 ml of extraction buffer (50 mM Tris/HCl pH 7.5, 1 mM EDTA, 5 mM DTT, 1 mM PMSF, 5mM 6-amino-n-caproic acid, 2 μg ml^{-1} leupeptin, 0.2% (w/v) triton X-100, 100 μM pepstatin A), vortexed and homogenised with a Polytron for 30 s at 4°C. The suspension was centrifuged in 1 ml Eppendorf tubes at 10000 x g for 10 min at 4°C to remove cell debris. The supernatant, removed from below the fat pad, was then centrifuged at 70 000 rpm (200 000 x g) for 30 min at 4°C in a Beckman Optima TLX benchtop ultracentrifuge. The supernatant was aliquoted, flash frozen in liquid nitrogen and stored at -80°C prior to immediate use. Thawed aliquots (100 μl) were subjected to methanol/chloroform precipitation [Wessel, 1984 #1]. The resulting protein pellets were resuspended in the appropriate loading buffer (50 μl; therefore 10 μl approximately 0.3 seed). For one dimensional SDS-PAGE this was Laemmli loading buffer. Sigma "SDS-VII" (66, 45, 36, 29, 24, 14.2 kDa) and "High Molecular Weight" (205, 116, 97.4, 66, 45, 29 kDa) protein standard sets were used.

As the aqueous extraction method described in 5.3.3. had been used successfully in this laboratory with the same seed samples in the detection of enoyl reductase [Fawcett *et al.*, 1994] a precise study of the extraction conditions necessary to obtain the most specific and efficient detection of βKR from seed extracts was not carried out. However, the results with this βKR antibody preparation were not as specific as those obtained with use of the enoyl reductase antibody preparation. Hence the method described in 5.3.4. was devised in a effort to improve the specificity of the βKR immunodetection in later experiments.

5.4 1D western blotting of seed extracts with mouse antibodies

An aqueous seed extract (§5.3.3) from a 35 days after flowering (daf) stage of a

B. napus developing seed series (designated 'TC2') was loaded onto an SDS-PAGE gel (5% acrylamide stacking/10% acrylamide resolving) at loadings of 1, 5, and 10 µl; equivalent to 0.015, 0.075 and 0.15 of a seed respectively). Samples of βKR were loaded at the levels of 15, 30, 75 and 150 ng and samples of enoyl reductase (ER) were loaded at the levels of 10, 20, 50 and 100 ng. This was achieved by serial dilution of protein solutions of βKR and ER of known concentration. After electrophoresis was carried out the gel was blotted on to a nitrocellulose membrane. The membrane was blocked overnight in 1%Hb-PBS at 4 °C. The blocking solution was removed and the blot was incubated in 10 ml of 1%Hb-PBS containing a 1:1000 dilution of the anti-βKR antisera, and a rabbit anti-enoyl reductase antibody preparation held in the laboratory, for 1 h on a roller. After incubation washing was carried out with PBST (5 x 4 ml x 5 min). The secondary antibody, rabbit anti-mouse IgG (10 µl), was added to the blot in 10 ml of 1% Hb-PBS and was incubated for 1 h. Another wash took place before the tertiary ^{125}I labelled donkey anti-rabbit IgG antibody (5 µCi) in 10 ml of 1% Hb-PBS was added and incubated for 1h 15 min. After the final wash (5 x 50 ml x 5 min) the blot was wrapped in Saran wrap and exposed to X-ray film at -80 °C overnight.

The exposed autoradiograph is shown in figure 5.5. It is unsurprising that a higher signal is observed for the βKR standard loadings, as the tertiary antibody arrangement (mouse-rabbit-donkey IgG) used to detect it would have amplified the initial cross-reaction between βKR and the antibody. What is surprising is that although enoyl reductase can be seen in the extract lanes of the blot, a signal from βKR is practically absent. It was expected that the two enzymes, both being members of a multi-subunit fatty acid synthetase might be present in similar amounts at similar times in the developing seed. This initial result required further experimentation to check the specificity of the antibody preparation, check that the dual antibody detection system (βKR and ER) was not interfering with the βKR signal in the extract and more importantly to check the βKR levels in other stages of developing seed.

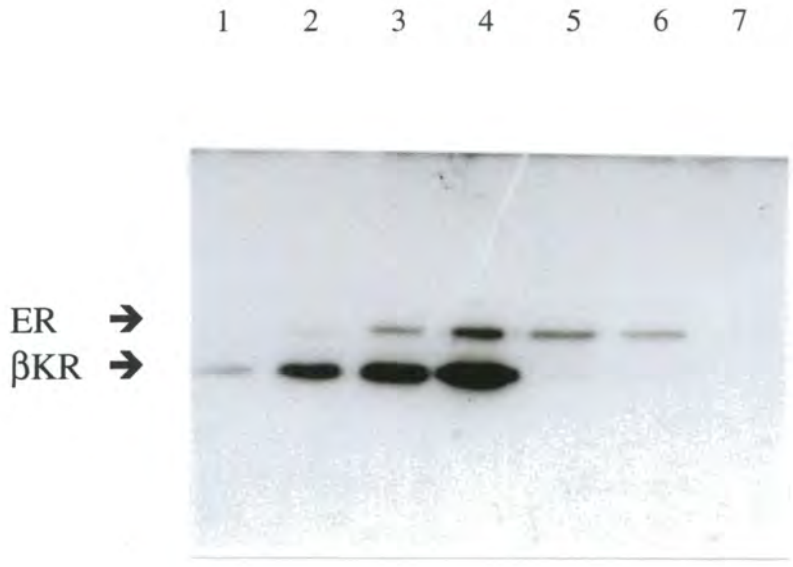

Figure 5.5 Autoradiograph showing detection of βKR and enoyl reductase antigens and detection of enoyl reductase in a developing seed extract

Lanes 1-4, dual loading of βKR (15, 30, 75 and 150 ng) and ER (10, 20, 50, 100 ng); lanes 5-7. rapeseed extract (35 days after flowering) 10, 5, 1μl (equivalent to 0.15, 0.075 and 0.015 of a seed).

Both βKR and ER standard samples are detected by their respective antibodies. ER can be seen in the extract lanes of the blot at a level of roughly 75 ng in the 10 μl seed extract. This corresponds to a level of 0.5 μg of ER per 35 daf seed. [Slabas *et al.*, 1990] estimated a 35 daf seed to contain 75 ng of ER by radio-immunoassay and quantitative western blotting. Surprisingly, βKR is practically absent by virtue of a lack of signal in the lanes corresponding to the seed extract.

The above experiment was repeated with an increased loading of the 35 daf extract on the gel, and the use of only the βKR polyclonal antibodies. The exposed autoradiograph of the blotted gel is shown in figure 5.6. On this occasion βKR is detected in the sample, though still at a low level. A sample from a Laemmli buffer protein extract of mixed stage seed from the high erucic acid rape variety Miranda, was also loaded on the gel at an equivalent seed per μl loading as the 10 μl loading of the 35 daf time course sample. βKR is clearly observed in the bulk mixed-seed extract, so it was decided to make fresh extracts from the staged time-course seeds.

A fresh set of aqueous seed extracts were made from the liquid N_2 stored staged seeds of TC 2 (time course 2; 22, 29, 35, 42, 49 days after flowering). Presuming that the previous 35 daf extract had degraded, 5 μl of each staged extract was loaded on to a gel with 7.5, 15, and 30 ng of βKR and 25, 50 and 100 ng of ER. A further sample of the HEAR Miranda extract (2.5 μl) was also included. The gel was blotted as before and the blot incubated with the two primary antibodies (mouse anti-βKR and rabbit anti-ER) and the secondary and tertiary antibodies (rabbit anti-mouse IgG and ^{125}I labelled donkey anti-rabbit IgG). The exposed blot is shown in figure 5.7. As with the previous extract, the new extracts showed a clear signal for ER in the extract and the protein standards, yet the signal for βKR is only visible in the lanes containing the βKR protein standard.

In order to reconfirm the capability of the antibody to detect βKR in a seed extract, aqueous extracts from bulk mixed stage seed from *B. napus* vars. Miranda and Jet Neuf were prepared by the Laemmli buffer extraction method (§5.3.2). Two SDS-PAGE gels (5%/12% acrylamide) were run, loaded with various levels of extract, 15 ng of βKR and molecular weight markers. The gels were blotted on to two nitrocellulose membranes which were subjected to immunodetection with the anti-βKR polyclonal antibody preparation. The exposed autoradiograph is shown in figure 5.8. The βKR signal is seen to increase in a linear fashion with the loading level in both samples. It is clearly observable in both extracts and the βKR standard. Also present in the HEAR Miranda extract is a higher molecular weight signal not previously observed as a distinct band but as a faint smear as seen in the Jet Neuf extract. This may have been indicative of the presence of βKR isoforms in the extract. Such a possibility was to be

further investigated once immunodetection results had been improved and made consistent.

5.5 2D western blotting of seed extracts with mouse antibodies

In addition to efforts to obtain a quantifiable βKR signal from developing seed series extracts using one dimensional electrophoresis, the detection of isoforms of βKR in two dimensional electrophoresis of seed extracts was also attempted. Both 1D and 2D forms of electrophoresis gave non-reproducible results plagued with high levels of background signal. An example of a 2D immunoblot showing possible detection of βKR in *B. napus* seed and leaf samples is given in figure 5.9.

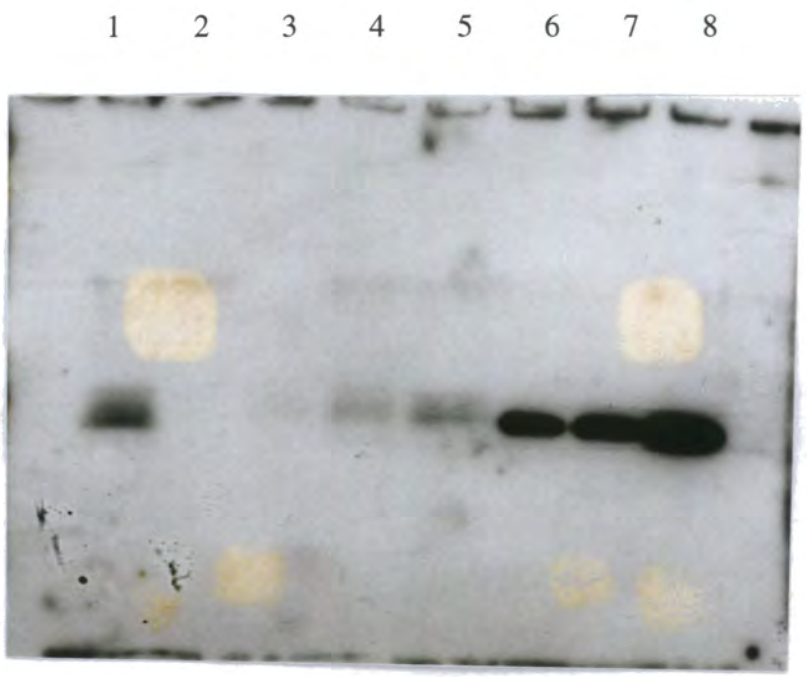

Figure 5.6 Autoradiograph showing detection of βKR antigen and partial detection of βKR in a developing seed extract

Lane 1, mixed stage seed extract (HEAR var. Miranda) 10 µl; lanes 2-5, rapeseed extract (35 days after flowering) 2, 5, 10, 20 µl; lanes 6-8, βKR (7.5, 15, 75 ng).

Whilst βKR is clearly detected in the extract from a mixed stage protein extract from the high erucic acid rape variety Miranda, βKR is detected at only a low level in the 35 days after flowering seed sample.

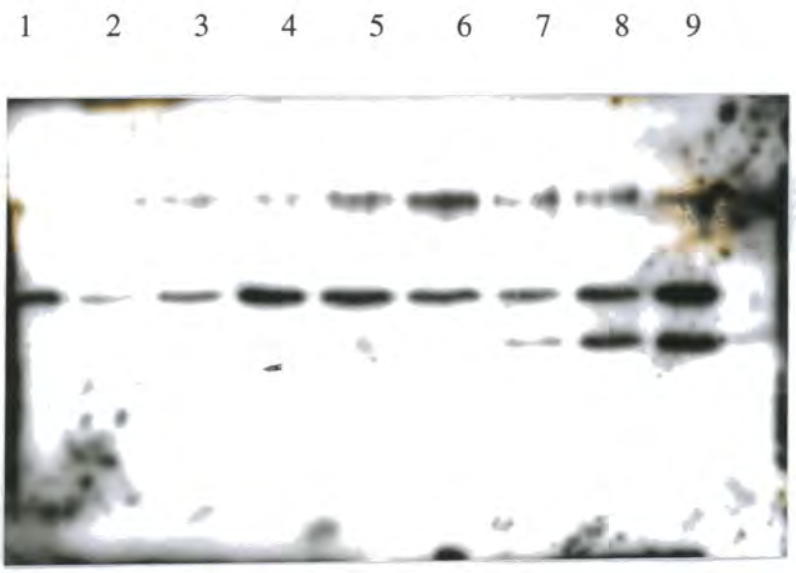

Figure 5.7 Autoradiograph showing detection of βKR and enoyl reductase antigens and detection of enoyl reductase in an extract from a developing seed series.

Lane 1, crude seed extract var. Miranda (2.5 µl); lanes 2-6, crude seed extracts (22, 29, 35, 42, 49 days after flowering) (5 µl); lanes 7-9, βKR (7.5, 15, 75 ng) and ER (25, 50, 100 ng).

It was observed that as with the previous extract, the new extracts showed a clear signal for ER in the extract and the protein standards, yet the signal for βKR is only visible in the lanes containing the protein standards. On this occasion the reduced loading of the Miranda extract fails to give a βKR signal whilst it does give an ER signal.

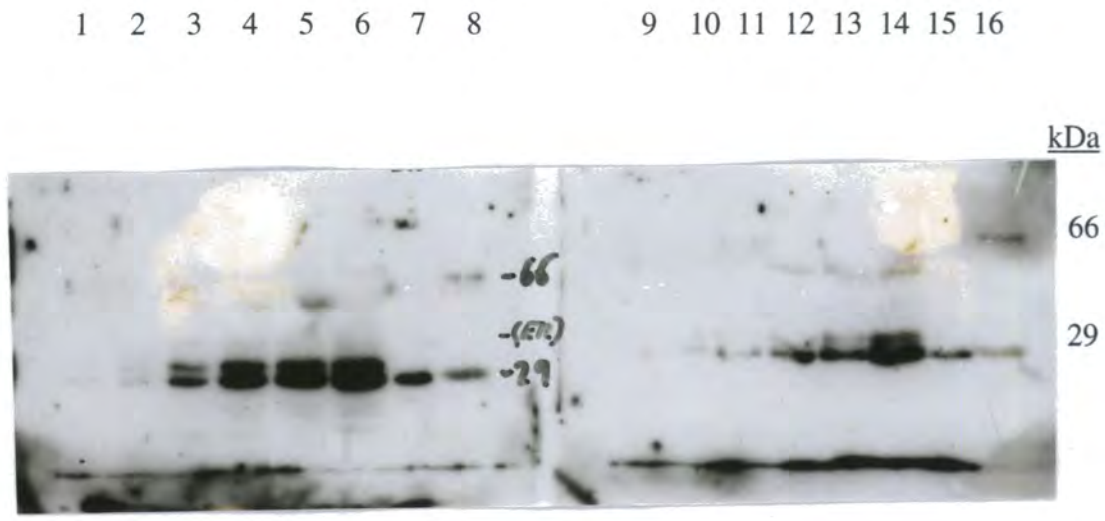

Figure 5.8 Autoradiograph showing detection of βKR in developing seed extracts from *B. napus* vars. Miranda and Jet Neuf.

Lanes 1-6, crude seed extract var. Miranda (1, 2.5, 5, 10, 15, 20 µl); lane 7, βKR (15 ng); lane 8, βKR (1.5 ng); lanes 9-14, crude seed extract var. Jet Neuf (1, 2.5, 5, 10, 15, 20 µl); lane 15, βKR (15 ng); lane 16, βKR (1.5 ng).

Unlike the immunodetection of βKR in the developing seed series, the signal is clearly seen in extracts from mixed stage bulk stored seed. Notably, a doublet is seen, more clearly in the Miranda extract, giving evidence for two or more βKR isoforms. This was unfortunately an isolated result. An identical protocol used on the stocks of staged developing seed held in the laboratory could not achieve this level of detection.

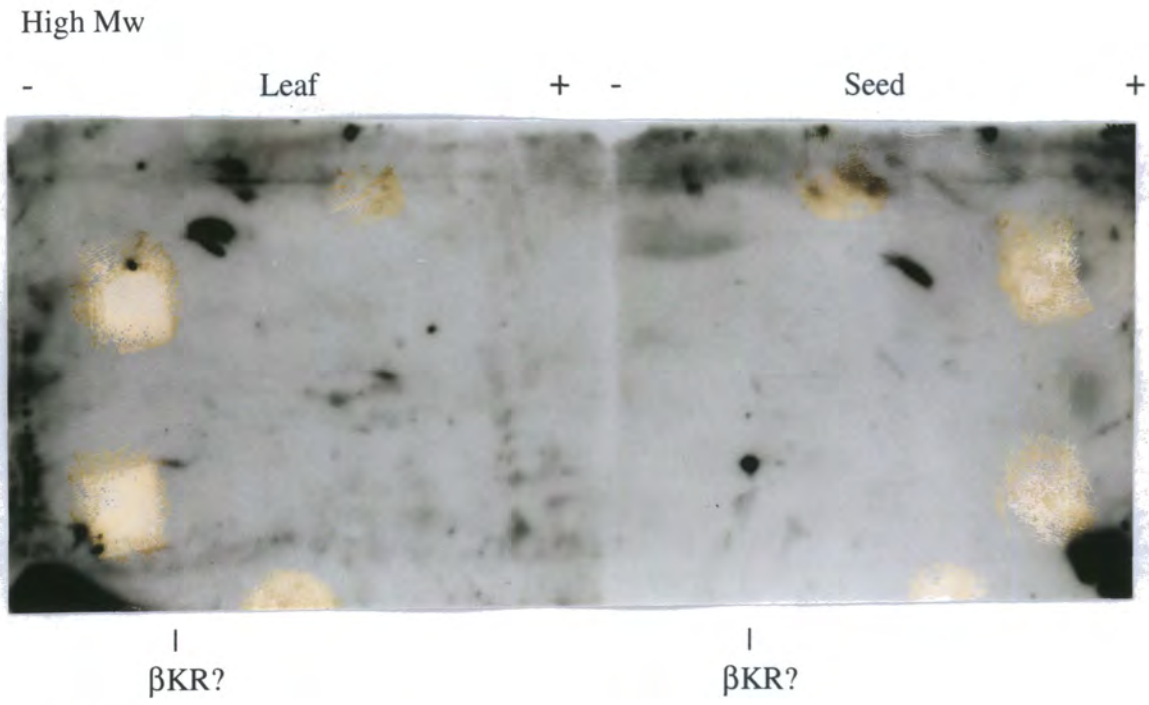

Figure 5.9 Two-dimensional gel electrophoresis autoradiograph showing possible detection of βKR in *B. napus* seed and leaf samples.

The above autoradiograph shows possible signals for βKR against a high background signal typical of the immunoblots carried out with the mouse antisera. The signals highlighted are in the correct region of the gel for a 29 kDa protein, but are inconclusive.

5.6 Testing of rabbit antibody preparations from Zeneca Pharmaceuticals

It was thought that the unexpected lack of a 1:1 ratio between levels of enoyl reductase (ER) and βKR and the poor signal obtained for βKR in extracts may have been due to poor cross reactivity of the mouse anti-βKR polyclonal antibodies. It was decided to raise further antibodies from preparations of pure over-produced ER and βKR

A sample of native over-produced *B. napus* βKR was sent to Zeneca Pharmaceuticals (Alderley Park, Macclesfield, Cheshire, U.K.) where it was subjected to non-denaturing electrophoresis and electro-elution and used to immunise two rabbits and a sheep. Samples of frozen sera containing polyclonal antibodies raised against βKR were sent as a gift and stored at -80 °C. A simultaneous preparation of antisera to enoyl reductase was also carried out.

Aqueous extracts from seeds of a developing seed series (TC2) of stages 22, 29, 35, 42 and 49 daf - corresponding to a third of a seed, were loaded on to two identically loaded SDS-PAGE gels together with known amounts of βKR (15, 75 or 150 ng) or ER (10, 50 and 100 ng). After electrophoresis, the gels were blotted on to nitrocellulose in a Bio-Rad wet blotter using 100 v for 1 h and a dry ice cooling pack. The gels were stained to check for protein transfer and were seen to be completely clear. The blots were stained with Ponceau S, which showed a good transfer of protein. The membranes were blocked overnight in 1%Hb-PBS-T at room temperature in a rolling incubator. The blocking solution was poured off and 10 ml of 1%Hb-PBS containing 10 µl of the appropriate antisera were added and incubated with the membranes for 1 h. The blots were then washed twice briefly with 50 ml of PBS-T and then a further three times for 10 min. The secondary antibody, ^{125}I labelled donkey anti-rabbit IgG (5 µCi) was added to the washed membranes and incubated for 1 h. A final wash, as previously, was carried out and the membranes were exposed to X-ray film at -80 °C overnight.

Figure 5.10 shows the autoradiograph of the two blots. The antisera cross-react with βKR and ER on the respective blots. As with the mouse antibody experiments, it appeared that there is a relatively higher level of ER than βKR during the period of development studied. A higher molecular weight species was detected by the βKR

antisera in all lanes (including the SDS-VII marker lane). This phenomenon also occurred during use of the mouse antibodies. It became apparent from this test of the antisera that the poor results obtained with the mouse antibodies were also likely to be obtained with the rabbit antibodies. Thus, several steps would have to be taken to improve the specificity and quality of detection both to ascertain the number of βKR isoforms present in seed extracts, and for detailed estimation of the amounts of βKR present throughout development. The first of these steps was to use the large amount of βKR protein available to purify the rabbit antibodies.

1 2 3 4 5 6 7 8 9 10 11 12 13 14 15 16 17 18 19 20

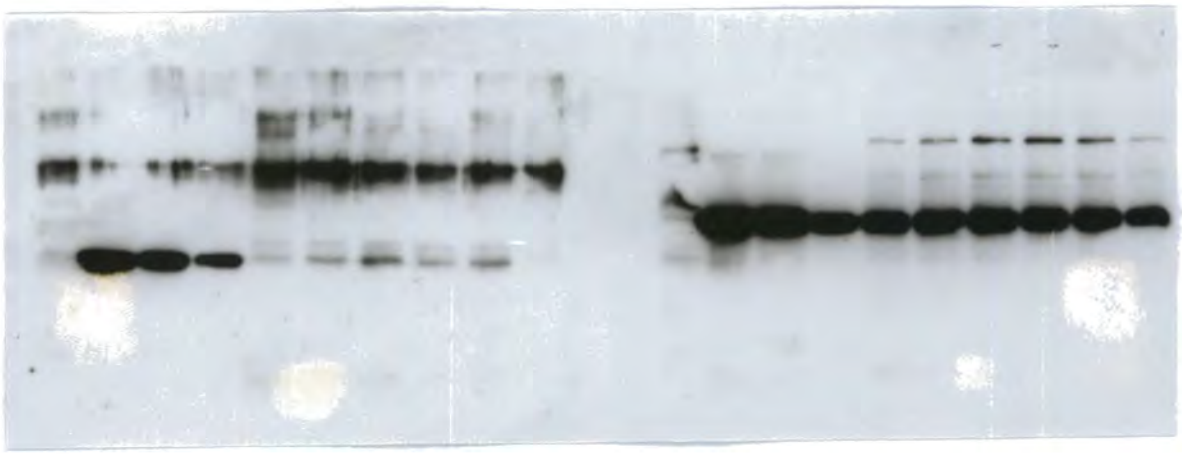

Figure 5.10 Autoradiographs showing the cross-reactivity of the Zeneca preparations of anti-βKR and anti-ER antisera.

Lanes 1-10: blot treated with anti-βKR sera; lanes 11-20, blot treated with anti-ER sera. Lane 1, SDS VII Mw markers; lane 2-4, βKR antigen (150, 75 and 15 ng), lanes 5-10, crude seed extracts (49, 42, 35, 31, 29, and 22 daf); lane 11, SDS VII Mw markers; lane 12-14, ER antigen (100, 50 and 10 ng), lanes 15-20, crude seed extracts (49, 42, 35, 31, 29, and 22 daf).

As with immunodetection of βKR in extracts using the mouse antibody preparation, there is a higher level of ER detected in the extract in comparison to βKR. In addition, the anti-βKR sera also detect a cross-reacting species at the same position as BSA (66 kDa), which itself was detected (though it was present in microgram as opposed to nanogram amounts).

5.7 Purification of rabbit anti-βKR antibodies

5.7.1 Affigel 10 - βKR matrix production for antibody purification

15 ml of purified *B. napus* βKR solution (1.5 mg ml^{-1}) was dialysed against 2 x 1 litre of 50 mM MES buffer pH 6.5 overnight at 4°C. Affigel-10 cross-linking matrix (Bio-Rad) (2 ml) was rinsed with cold Milli Q grade water in a sintered glass funnel. The dialysed protein solution was added to the moist cake of Affigel-10 and was agitated gently for 4 h at 4°C. The matrix was then transferred to a 5 ml luer-lock column (Sigma Techware) and the excess liquid drained under gravity. The matrix was washed with 4 ml of 50 mM MES pH 6.5. Absorbance readings (280 nm) were taken for the wash and the initial eluent. Comparison with a retained sample of the βKR solution showed that 85% of the protein was cross-linked to the Affigel-10 matrix. The matrix was treated with 0.2 ml ethanolamine to block any remaining cross-linking sites, and washed with storage buffer (50 mM Tris/HCl pH 7.0, 0.02% NaN_3) The matrix was stored in the column at 4°C prior to use.

5.7.2 Antibody purification

An aliquot of serum from a βKR-immunised rabbit (40 ml), previously stored at -80°C, was thawed, brought to 0.02% NaN_3 and stored at 4°C. Serum (10 ml) was pumped at 1 ml min^{-1} through the Affigel-10-βKR matrix, which was previously equilibrated with 50 mM Tris/HCl pH 7.0. The eluted serum was reapplied to the column four times before the matrix was washed with 200 ml of 50 mM Tris/HCl pH 7.0, after which the 280 nm absorbance of the eluent was found to be zero. To elute the bound antibodies, 50 ml of 4 M $MgCl_2$, 20 mM Tris/HCl pH 6.75 was pumped through the column at 0.5 ml min^{-1}. The eluent was collected with a Gilson 201 fraction collector in 2.5 ml fractions and 280 nm absorbance readings taken, the elution profile is shown in figure 5.11. Fractions of useful antibody concentration (ca. 200 μg ml^{-1}) were pooled and dialysed against 2 x 2 l of tris buffered saline (TBS) overnight at 4°C (TBS; 137 mM NaCl, 3 mM KCl, 25 mM Tris/HCl, pH 7.4) . The dialysed antibody solution (15 ml) was brought to 0.02% NaN_3 and stored at 4°C.

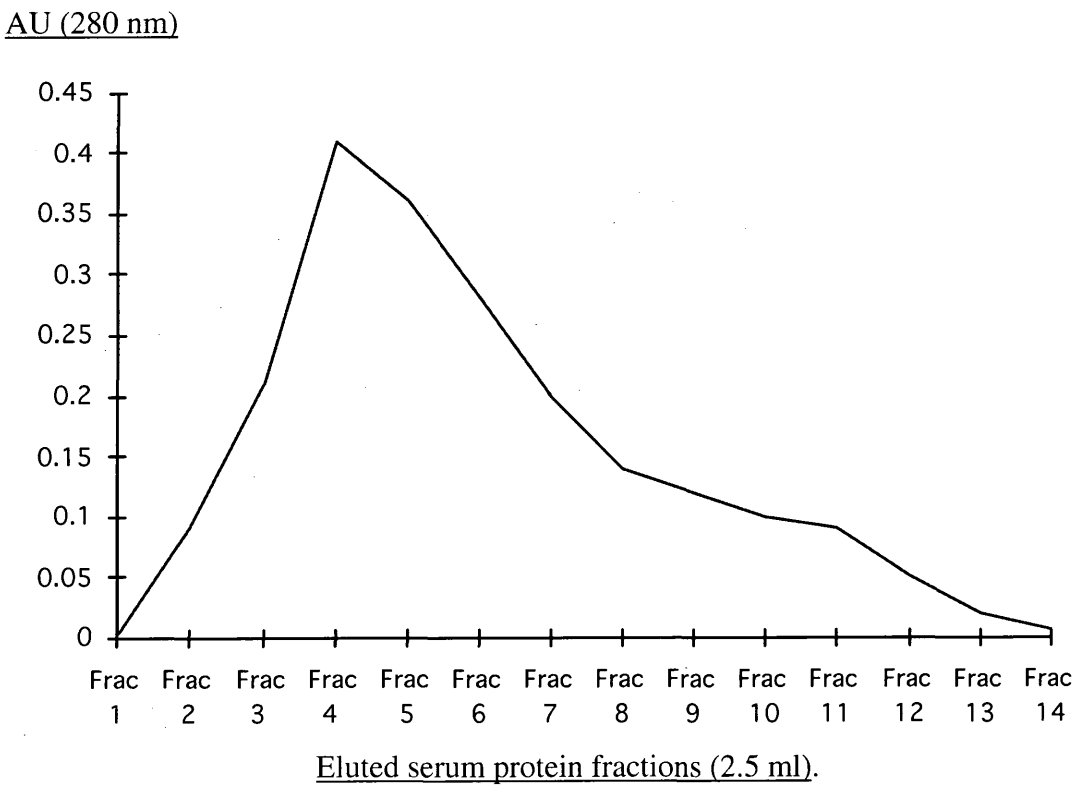

Figure 5.11 Elution profile of antibody containing fractions from an Affigel-10-βKR immobilised column.

The graph shows the absorbance (AU) at 280 nm of the 2.5 ml fractions eluted from the immobilised-βKR column loaded with anti βKR rabbit serum.

5.8 Immunodetection of βKR using rabbit antibodies

In addition to the purification of the anti-βKR serum, an additional measure was taken to improve the quality of the βKR signal obtained from immunoblots containing seed extracts. As outlined in §5.3.4., aqueous seed extracts were subjected to ultracentrifugation at 200 000 x g and methanol/chloroform extraction prior to the addition of 1D or 2D electrophoresis sample buffer.

5.8.1 1D western blotting of seed extracts with rabbit antibodies

One dimensional SDS-PAGE was carried out on such extracts from seeds of several varieties of *B. napus* namely, cv. Miranda, cv. Falcon and cv. Spock. The extracts, between 0.1-0.3 of a seed per lane, were run on a 5% acrylamide stacking/10% acrylamide resolving SDS-PAGE gel and blotted using a semi-dry procedure as outlined in §2.3.9., the blot from which was blocked with 1% (w/v) Hb-PBS, 0.02% (w/v) NaN_3 for four hours at room temperature. The blot was incubated for one hour with the purified antibody preparation at a dilution of 1:100 and after washing with PBS-T (5 x 50 ml x 5 min) was incubated with 50 μCi of ^{125}I-labelled donkey anti-rabbit IgG for one hour. After further washing, the blot was exposed to x-ray film.

At least two isoforms of βKR are clearly shown by immunodetection with the affinity purified anti-βKR antibodies figure 5.12. The predominant isoform, at 28 kDa, runs at the same molecular weight as the over-produced βKR. The other isoform has a molecular weight of between 30-32 kDa.. It is thought that this isoform is not encoded by the gene that gave rise to the 'JRS10.1' cDNA used for the over-expression of the enzyme. It does not necessarily follow however that the over-produced enzyme is the dominant βKR isoform in *B. napus* seeds. It may simply be subject to increased detection by virtue of its use as the immunising antigen in the production of the antibodies used.

Quantification of βKR in a developing seed extract was also attempted with the purified antibodies and the improved ultracentrifugation extraction and precipitation method (§5.3.4). Though the background signal was greatly reduced, the diffuse and variable nature of the βKR signal returned could not be consistently or accurately

quantified, even with use of a BioRad Phosphoimager and accompanying imaging software on many samples. Figure 5.13 shows a typical example of the best βKR signal obtained. This lack of consistency was possibly due to variation introduced at any one of the protocol steps; inaccurately staged seed series, extraction from the seeds (e.g. proteolysis), precipitation with methanol/chloroform (e.g. losses), electro-blotting (e.g. uneven transfer).

The method of quantitative western blotting of seed protein has been successfully performed for enoyl reductase in *B. napus* [Slabas *et al.*, 1990]. Despite much repeated experimentation using a similar method, no reliable data regarding the precise βKR content of a developing seed series can be presented here.

5.8.2 2D western blotting of seed extracts with rabbit antibodies

The ultracentrifugation / methanol chloroform precipitation crude extract preparation method (§5.3.4) and the use of purified antisera finally allowed clear immunodetection of βKR in two dimensionally electrophoresed seed extracts. Such detection gave further evidence for βKR isoforms of higher molecular weight, as seen with one-dimensional immunoblots.

The methanol/chloroform precipitates from 100 µl mixed stage *B. napus* cv. Spock seed extract aliquots were resuspended in 50 µl of 2D loading buffer (8 M urea, 268 mM β-mercaptoethanol, 2 % (v/v) Pharmalyte 3-10 ampholines (Pharmacia) and 0.5 % (v/v) Triton X-100) and allowed to incubate at RT °C for 1 hour. Each 50 µl sample was used to load one Immobiline DryStrip (pI 3-10.5). Following the methods in the accompanying instruction manual, the first dimension separation was run and the equilibrated strips placed on ExcelGel SDS gradient 8-18 gels for second dimension electrophoresis using ExcelGel SDS buffer strips in a MultiPhor II electrophoresis unit with a MultiDrive XL power supply (all Pharmacia) SDS-VII protein molecular weight standards were also loaded on to the second dimension gel to used. The gel was blotted, using semi-dry blotting as previously, on to nitrocellulose, which was taken through the same immunodetection procedure as for the one-dimensional gels.

At least four major isoforms were detected by the purified antibodies (figure

5.14). βKR I and II was found to be located in the anodic region of the strip at 30-32 kDa on the gel, whilst βKR III and IV was located in the cathodic region at 27-29 kDa. When these results are compared to the 1D results from §5.8.1., it can be postulated that the higher molecular weight component observed in one-dimensional immunodetection possibly comprised βKRs I and II. The βKR isoform that has been over-produced was either βKR III or IV, based on observed molecular weight, the strength of the immunodetection signal and the theoretical isoelectric point of the protein, pI 8.3 (the behaviour of the over-produced enzyme on ion-exchange matrices supports this), making the protein likely to focus in the cathodic region of the gel. However it should be noted that the pI scale was not calibrated, for example through use of carbamylated creatine kinase pI markers. Thus, the precise localisation of these isoforms can only be estimated from their position on the gel relative to placement of the pI 3-10.5 first dimension focussing strips. The signals for βKR III and IV are not focussed. This may be due to the fact that they are more abundant as proteins in the sample and/or have a greater affinity for the antibody preparation than βKRII and I. Alternatively there may be more than two βKR isoforms present in the cathodic region of the gel. The use of pI markers would have indicated whether the first dimension separation and focussing steps were functioning properly.

5.8.3 Investigation of βKR isoforms in *B. napus* and *B. campestris*

An equivalent sample of seed extract from *B. campestris* was run in parallel with the *B. napus* sample through the above two-dimensional electrophoresis procedure. The predominant isoform seen in *Brassica campestris* (see figure 5.12) samples was in the mid-basic (approximate pH 7-9) region of the focusing strip at a estimated denatured molecular weight of around 27-29 kDa, thus corresponding to βKR IV in *Brassica napus*. see figure 5.12. It can therefore be postulated that the predominant isoforms of βKR in *B. napus* seed are encoded by genes provided by the *B. campestris* parent.

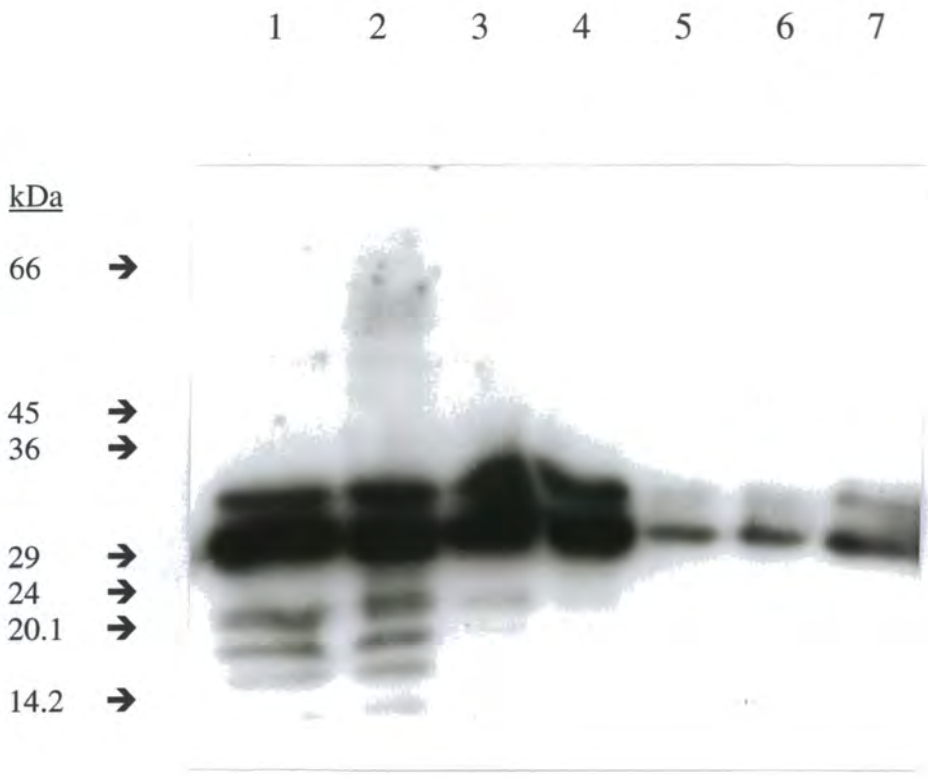

Figure 5.12 1D immunoblot of *B. napus* seed extracts, showing detection of two isoforms of βKR by purified rabbit antisera.

Lanes 1 & 2 Miranda; 3 & 4, Falcon; 5 & 6, Spock; 7, Spock embryo extract. (Lanes 1-4, 10 µl (0.3 seed) each, lanes 5-7 = 0.1 seed).

The above gel shows detection of at least two isoforms of βKR by the affinity purified anti-βKR anti body preparation. The predominant isoform, (28 kDa), runs at the same molecular weight as the over-produced βKR. The other isoform has a molecular weight of between 30-32 kDa.

Figure 5.13 Example of an anti-βKR immunoblot of a developing *B. napus* seed series.

Lanes 1-4, βKR antigen (7.5, 15, 75 and 112.5 ng); lanes 5-11 crude seed extracts (28, 32, 34, 38, 41, 45, and 47 daf).

Through use of the purified antisera and an improved extraction method, employing protease inhibitors, ultracentrifugation and methanol/chloroform precipitation, the background level was vastly reduced on anti-βKR immunoblots. However, owing to the diffuse and variable nature of the βKR signal detected on many repeated blots, the level of the enzyme in the samples could not be reliably quantified.

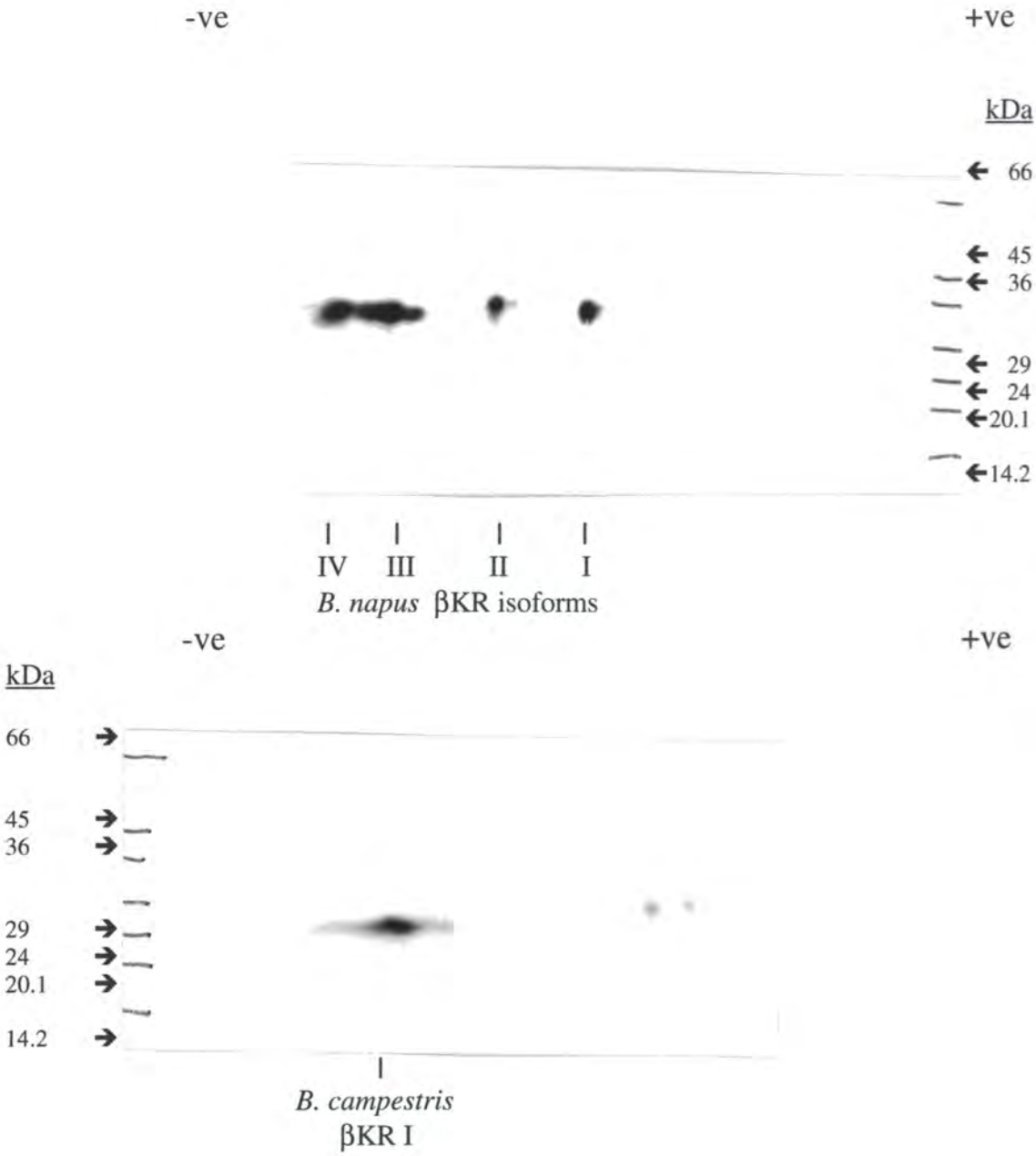

Figure 5.14 Immunodetection of βKR isoforms in crude extracts of *Brassica napus* cv Miranda and *Brassica campestris* separated by two dimensional electrophoresis.

Shown uppermost are four major βKR isoforms detected by the purified antibodies in a *B. napus* seed extract. βKR I and II are shown in the anodic region of the strip at 30-32 kDa on the gel, whilst βKR III and IV are shown in the cathodic region at 27-29 kDa. Below that is shown the detection of a major βKR isoform at 27-29 kDa in *B. campestris*, which appears to correspond to *B. napus* isoform IV. The original positions and orientations of the first dimension gels are marked relative to the second dimension gels which are positioned by reference to Mw marker points.

5.9 Summary

These experiments were aimed at elucidating the nature, number and relative amounts of βKR isoforms in *B. napus* seed, with a view to characterising the temporal presence of βKR in a developing seed series and its comparison with enoyl reductase (ER). Polyclonal antibodies were successfully raised in mice and though they were capable of detecting the antigen, they proved to be poor indicators of the βKR present in developing seed extracts. A great deal of experimentation was carried out in order to remedy this situation, with many single variable changes made to the protocols used. However, as experiments using both βKR and ER antibodies and proteins seemed to be giving adequate signal for ER, as antigen and in extracts, the quality of the antibodies was finally brought into question.

Production of βKR antibodies in rabbit ensued. The large amount of serum produced allowed antibody purification to be carried out using an immobilised βKR matrix. The use of these purified antibodies, together with an improved seed extraction method employing anti-proteolytic measures, ultracentrifugation and methanol/chloroform extraction, allowed analysis of the isoforms of βKR via one and two dimensional electrophoresis.

For the one dimensional analysis, use of purified antibodies raised against a translated predominant mRNA for βKR from *B. napus* seed for immunodetection of βKR in crude extracts suggested that the predominant βKR isoform in seed has a molecular weight of 27 kDa.

Two dimensional immuno-analysis showed there to be at least four major isoforms of βKR in seed extracts from *B. napus*, two appearing to correspond to each of the molecular weight variants seen in the single dimension analysis. Study of the βKR isoforms of a parent species of *B. napus*, namely *B. campestris*, suggested that two of the four isoforms present in the descendant plant were detectable in the parent.

The intended aim of this work, to obtain a developmental profile for βKR in the seed remains unobtained.

Chapter 6 Kinetic and structural investigation of βKR

6.1 Introduction

The abundance of over-produced and purified *B. napus* βKR was to be used to carry out studies on the kinetic mechanism and structure of the enzyme.

The objectives for the kinetic experiments were to obtain Km and V max values for AcAcCoA and the reductant NADPH, using pseudo (single substrate) Michaelis-Menten kinetics and to elucidate the kinetic mechanism of the enzyme in terms of a two-substrate two-product model. To give a prediction of the kinetics of the two-substrate, two-product reaction, velocity data were to be obtained from assays that anchor the substrate at one non-saturating concentration whilst varying the reductant and vice versa. Primary plots of such data should predict the sequence of events in the βKR reaction, whether ping-pong bi-bi or compulsory-order / ternary-complex mechanisms. The further elucidation of the mechanism was envisaged to necessitate inhibitor studies involving β-hydroxybutyryl-CoA and $NADP^+$ and looking for patterns of competitive and mixed inhibition to predict a kinetic mechanism using Cleland's rules.

The following points were noted: close attention to detail would have to be employed in the formulation of all solutions used, to maintain uniformity. This is especially important for the mechanistic work where subtle changes need to be recorded to allow sensible predictions to be made. The enzyme preparation should be aliquoted for storage, and each fresh aliquot assayed at the beginning and end of each period of work. The work should be carried out on the same spectrophotometer using the same cuvettes each time. The assays should be variations on the standard assay used to assess the purification of the enzyme. A workable amount of enzyme should be found using the standard assay. The amount of enzyme should be varied to determine the boundaries of linearity

Regarding structural studies, a major aim of the over-expression of the plant and bacterial enzymes was to provide milligram quantities of the proteins for possible crystallisation and subsequent diffraction analysis in the laboratory of Professor David

Rice at the Krebs' Institute for Biomolecular Research at the University of Sheffield. In addition to these experiments, it was envisaged that studies on structure such as circular-dichroism analysis and gel filtration could be carried out on *B. napus* and *E. coli* βKR, whilst awaiting the elucidation of any crystal structure.

6.2 Kinetic investigation of *B. napus* βKR

6.2.1 Assay of βKR

The assay used for the stability and kinetic experiments on βKR was essentially the same optical assay used to purify the enzyme (§2.3.5); the decrease in absorbance at 340 nm was recorded to monitor substrate dependent oxidation of NADPH.

6.2.2 Temperature and dilution effects on activity

The rape βKR enzyme was shown by Sheldon [1988] to be cold sensitive. Sheldon also showed that the avocado βKR enzyme was reversibly inactivated by storage at 4°C. Sheldon also mentions in other papers [Sheldon *et al.*, 1990; Sheldon *et al.*, 1992] that both enzymes, and *E. coli* βKR [Schulz *et al.*, 1971] are inactivated by dilution. Sheldon showed that NADPH (500 μM) could partially protect the plant enzymes from cold and dilution effects. In this study, on the basis of this information, the enzyme was maintained at room temperature when not in storage. The opinion was held that if the enzyme was dissociating upon dilution, a temperature of 4°C might increase this.

After purification βKR was stored as frozen pellets at -80°C in the buffer in which it eluted from the column: 25 mM sodium phosphate pH 7.0, 1 mM DTT, 1 mM EDTA, and approximately 150 mM NaCl, plus 0.02% sodium azide. The enzyme is relatively stable at room temperature in this solution when undiluted (enzyme concentration approximately 0.3 mg ml^{-1}). To dilute the enzyme to a working concentration for kinetic studies a suitable dilution buffer was sought.

According to Scopes [1987] diluted enzyme should be accompanied by at least 0.1 mg ml^{-1} of a suitable protein in an assay, as proteins can often be present in assays at concentrations as low as 1 μg ml^{-1}. In this case, βKR is present in the assay at 0.04 μg ml^{-1}. Without BSA present, an activity loss of 87% over 6 hours was observed upon

dilution. This information gave rise to a dilution buffer formulation, based on the purification buffer, of 25mM sodium phosphate pH 7.0, 1 mg/ml BSA, 1mM DTT (added fresh). In this solution, the activity of the enzyme decreased (varying between 40-50%) over a period of 1-2 hours after dilution (1:250 - 1:1000 dilutions tested - see figures 6.1 and 6.2). After this initial loss, the enzyme activity stabilised for periods of at least 72 hours with minimal activity loss. The decay did not follow a predictable pattern in the first 1-2 hours, but the dilution was suitably stable for the simple kinetic experiments outlined below. As a result of this phenomenon, βKR solutions were allowed to equilibrate for 2 hours post-dilution. This stability was monitored by measuring the activity of the equilibrated-diluted enzyme under standard assay conditions (100 μM NADPH; 800 μM AcAcCoA) before and after each set of data was collected. Datasets that were accompanied by an activity variation larger than 2% were discarded.

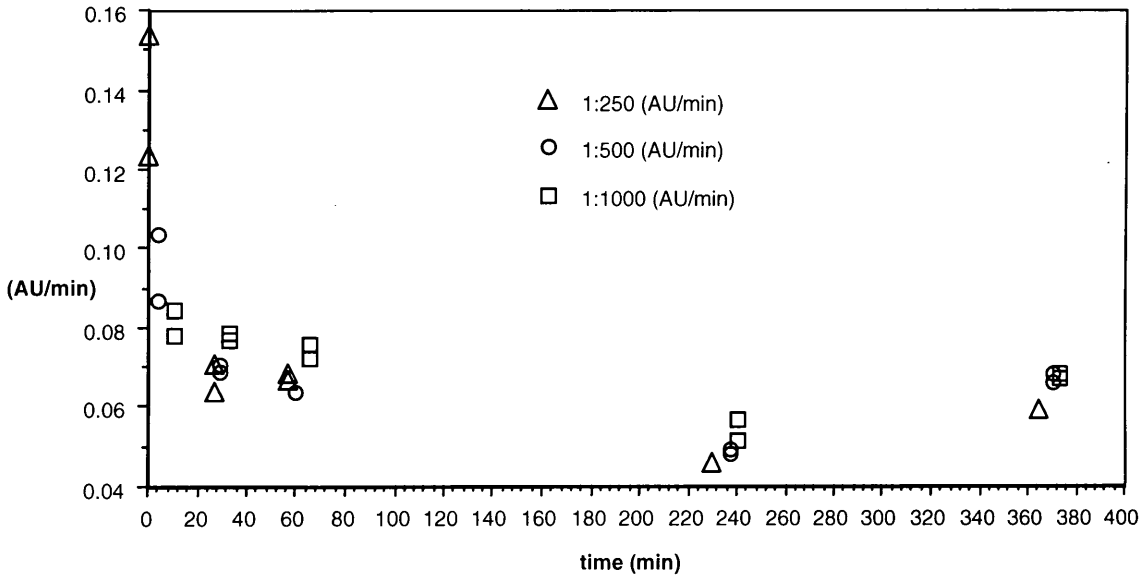

Figure 6.1 Graph showing activity of βKR after various dilutions

The plot shows that the initial loss of activity is rapid and that the total loss is unrelated to the extent of dilution over the range measured. The results shown are for volumes of βKR dilutions giving equivalent amounts of βKR in each assay. Dilution time course experiments, repeated as above, did not establish a predictable pattern of decay that might have been used to calculate a correction factor, as the decay pattern was irregular.

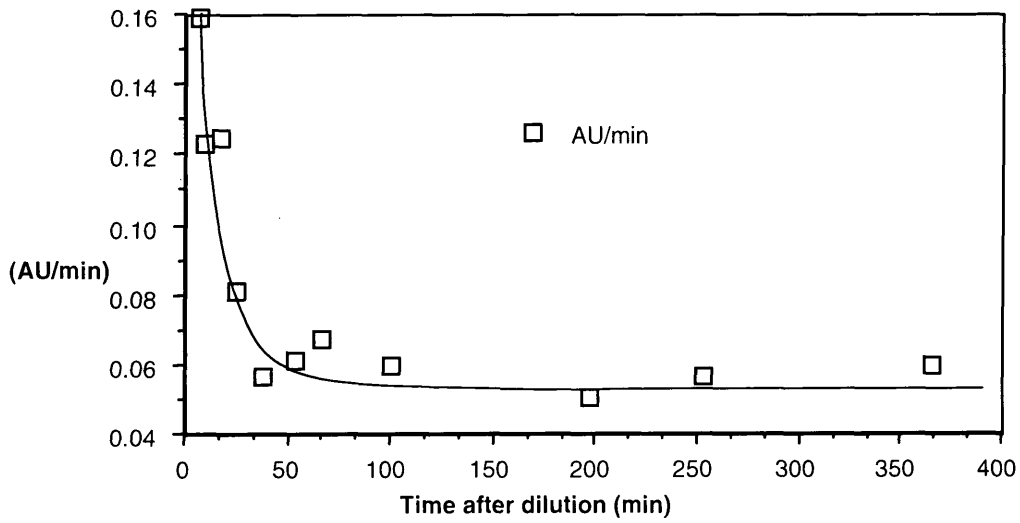

Figure 6.2 Graph showing activity decrease of a 1:250 dilution of βKR over 6.5 hours

An initial rapid loss is observed, after which (100 min) enzyme activity stabilises to within a workable range for limited kinetic experiments. This was the general pattern of activity loss. Hence, stock βKR dilutions were allowed to equilibrate for 2 hours after dilution before use in experiments.

6.2.3 Derivation of pseudo Michaelis-Menten constants

A working solution of enzyme, giving a linear response in terms of volume used and initial velocity, was required for these experiments. To provide this, βKR was diluted, at a 1:500 dilution of 0.658 mg/ml as measured by use of the calculated extinction coefficient – see §2.4.6, into 25 mM sodium phosphate pH 7.0, 1 mM DTT, 1 mg ml^{-1} BSA. Bearing in mind the above activity decay phenomena, assays were carried out in triplicate from a four-assay master cocktail which had equilibrated for at least two hours after dilution. Each assay contained 100 mM potassium phosphate buffer pH 7.0, βKR (5 μl) [6.58 ng in assay], 100 μM NADPH and Milli Q grade water to a final assay volume of 100 μl.. The assays were initiated by the addition of the appropriate amount of a substrate analogue, acetoacetyl-CoA (AcAcCoA), to give final concentrations ranging between 75 and 800 μM. The assay components and the thioester substrate were pre-incubated separately for 2 min at 20°C, prior to each assay.

Initial velocity measurements were determined for a the range of AcAcCoA concentrations and the data were used to create velocity vs [substrate], Lineweaver-Burk and Eadie-Hofstee plots both manually and using the Apple Macintosh Hypercard Stack "Enzyme Kinetics" [Gilbert, 1989] to calculate Km and V max via direct linear and maximum likelihood estimations.

Initial velocity, Lineweaver-Burk and Eadie-Hofstee plots of the data are shown in figure 6.3. The value obtained for Km, 492 μM, compares with a value of 261 μM obtained for the enzyme purified from *B. napus* seed [Sheldon *et al.*, 1992]. The Vmax value obtained for this model substrate is 57562 (μmol NADPH min^{-1} μmol $βKR^{-1}$). The tabulated data are shown in table 6.1.

Pseudo Michaelis-Menten constants for NADPH were not obtained with the substrate analogue acetoacetyl-CoA. Using the assay protocol developed here, more meaningful data from a natural substrate homologue such as acetoacetyl-acyl carrier protein (AcAcACP) could be obtained in the future.

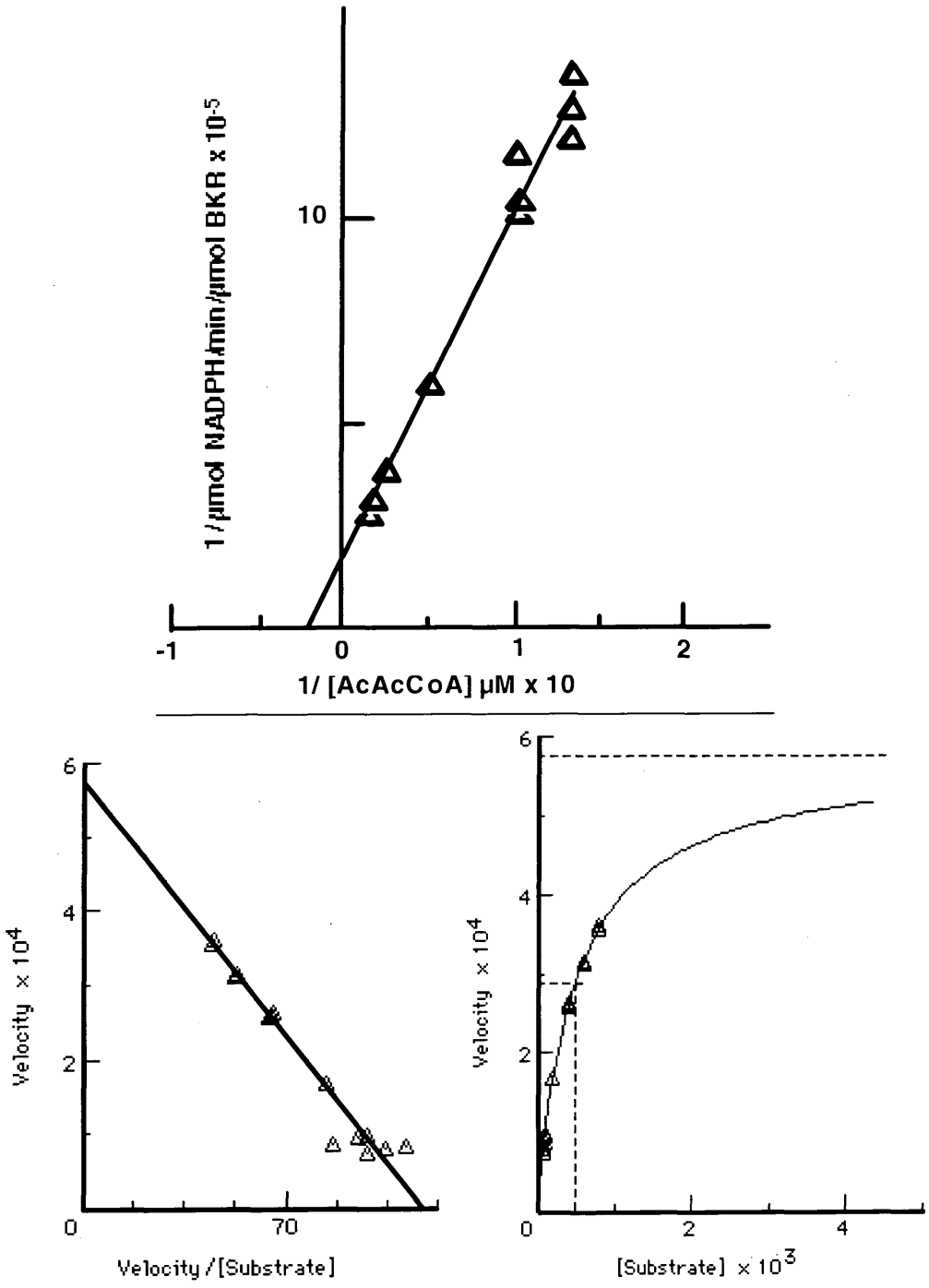

Figure 6.3 Graphs of data used to determine pseudo Michaelis-Menten constants for AcAcCoA.

Double-reciprocal $\frac{1}{V}$ vs $\frac{1}{[S]}$ (Lineweaver-Burk) plot, V vs $\frac{V}{[S]}$ (Eadie-Hofstee) plot and V vs [S] plot of data used to obtain pseudo Michaelis-Menten constants of *B. napus* βKR .

The lower two graphs are the graphical output of the 'Enzyme Kinetics' software package used to calculate the constants (marked by dotted lines on the V vs. [S] graph). (Velocity = µmol NADPH/min/µmol βKR; Substrate = [AcAcCoA] µM)

AcAcCoA	Km (μM)	Vmax (units/μmol βKR)
Estimate	492	57562
St. Error	17	990
Low Confidence Interval	457	55462
High Confidence Interval	529	59661

Table 6.1 Pseudo Michaelis-Menten Constants for Acetoacetyl-CoA

The Km value obtained for the over-produced βKR enzyme, 492 μM, compares with a value of 261 μM obtained for the enzyme purified from *B. napus* seed [Sheldon, 1988].

6.2.4 Bireactant initial velocity studies

An investigation of the possible kinetic mechanisms of βKR catalysis was carried out via a bireactant initial velocity study [Cleland, 1970]. Three sets of assays were set up employing non-saturating NADPH concentrations, i.e. 10, 20 and 40 μM as opposed to a fixed 100 μM near-saturating concentration. Assays were carried out in triplicate from a four-assay master cocktail. Each assay contained 100 mM potassium phosphate buffer pH 7.0, βKR at a 1:500 dilution of 0.628 mg/ml (5 μl) [6.28 ng in assay], the required concentration of NADPH and Milli Q grade water to a final assay volume of 100 μl. The required amount of serially diluted stock solution containing 8, 4 and 1 mM AcAcCoA, was added to provide a final AcAcCoA concentration of 75-800 μM and to initiate the assay. The initial velocity data obtained from the three datasets (10, 20 and 40 μM NADPH) were plotted as reciprocals versus the reciprocals of the AcAcCoA concentrations and the relationship between the gradients of the lines of best fit observed.

Figure 6.4. shows the plot from the bireactant initial velocity study. A convergence pattern characteristic of a fixed or random order ternary complex mechanism is seen. A bireactant ping-pong mechanism would produce parallel lines on such a plot, so the data suggested that such a mechanism can be ruled out for *B. napus* βKR.

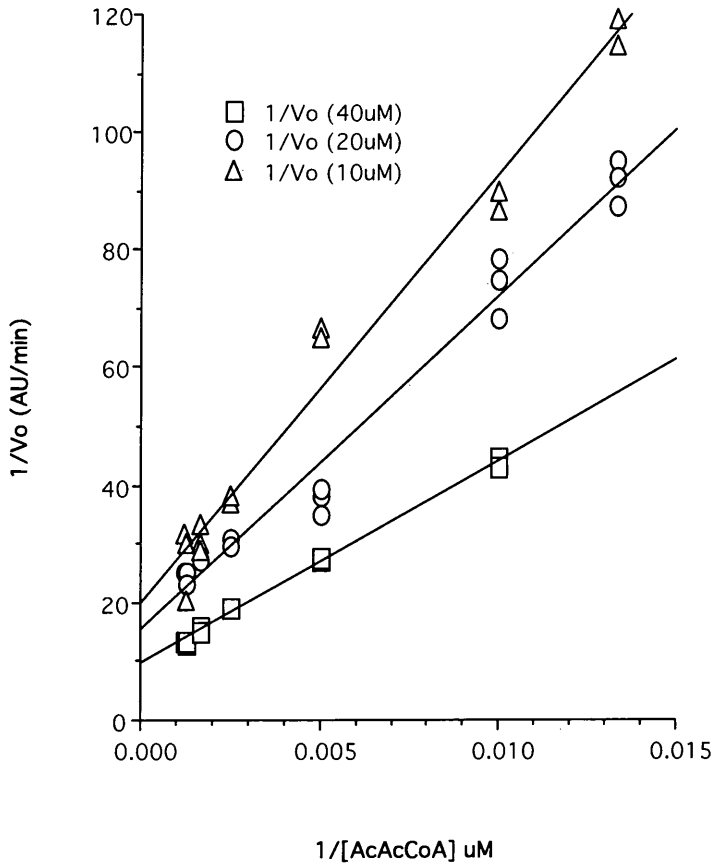

Figure 6.4 Double-reciprocal plot from the bireactant initial velocity study.

A convergence pattern characteristic of a fixed or random order ternary complex mechanism (non-parallel) is seen.

6.2.5 Product inhibition studies

The order of addition of the substrates to the postulated ternary complex enzyme was to be investigated in the conventional manner using product inhibition studies. However, the level of instability of βKR upon dilution to a working concentration was too high and unpredictable for such experiments; which required the comparison of data points over periods of several days.

A trial set of assays using $NADP^+$ as inhibitor were carried out. The necessary accuracy needed to obtain meaningful plots, and thus indications of inhibition characteristics for each substrate an d product combination, was found to be unobtainable despite a range of stabilising measures taken, see §6.2.2, including the addition of 20% glycerol to the dilution buffer and replacement of BSA with lysozyme. It was therefore necessary to find an alternative approach to observe substrate-enzyme complex formation.

6.2.6 Ultrafiltration binding assays

In the absence of product inhibition kinetic data, and to eliminate the need for dilution of the enzyme, it was decided that a method of equilibrium dialysis should be used to investigate the order of substrate binding. This was reasoned on the basis that the order of addition of substrates to the enzyme might be worked out if the substrates are tested for enzyme-binding in the absence of each other. The idea of using spun microconcentrator columns with a molecular weight cut-off of 10 kDa to retain the enzyme in an enzyme-substrate binding assay was conceived. This would allow measurement of substrate concentration changes in the eluent when the column is spun and the protein was retained above the ultrafiltration membrane.

A semi-quantitative binding assay was devised using Ultrafree-MC centrifugal micro-concentrators (Millipore, UK) to retain the enzyme and potentially bound substrate molecules above a 10 kDa cut-off ultrafiltration filter. Assays were carried out to assess the binding of each of the two substrates to the enzyme in the absence of the other. Assays were arranged so that the substrates would be mixed with the pure protein above the filter in a molar ratio of approximately 1 βKR (tetramer) : 10 NADPH and 1 βKR (tetramer) : 5 AcAcCoA in a final volume of 100μl (Mw of βKR (tetramer) = 108216).

The substrate to be tested (either NADPH or AcAcCoA) was pre-absorbed onto the ultrafiltration membrane by means of saturation with a 2 mM stock solution. After washing with Milli Q grade water, a solution of known substrate concentration was passed through the filter and the concentration checked to ensure the absence of binding or bleeding effects.

The enzyme-substrate mixture was allowed to equilibrate for 5 min prior to ultrafiltration, which was carried out in a centrifuge at 5000 g for 10 min at 20 °C. The time period was sufficient for 95% of the binding assay volume to pass though the filter. The retentate (5 μl) was diluted back to the original volume (100 μl) to allow approximations of substrate concentration to be carried out on both the retentate and ultrafiltrate. The buffer used throughout these studies including the optical assays was 100 mM imidazole-HCl, 1 mM DTT, pH 7.0.

NADPH binding was assayed directly via absorbance readings (340 nm) of the ultrafiltrate. βKR solutions at the concentrations used had negligible absorbance at 340 nm. A downward shift in absorbance value between the binding assay solution and the ultrafiltrate could therefore be attributed directly to depletion of NADPH.

Acetoacetyl-CoA binding was assessed via the βKR optical assay used previously. The amount of AcAcCoA in a known volume of ultrafiltrate was measured by bringing the solution to 50μM NADPH and observing the total absorbance decrease at 340 nm upon the addition of βKR. Samples were referenced against a solution of 25 μM AcAcCoA.

The results of the ultrafiltration binding studies are shown in tables 6.2 and 6.3 The data in table 6.2 show that NADPH will pass through the ultrafiltration membrane in the absence of βKR. However, when βKR is present in the pre-filtrate, NADPH is proportionally retained by the enzyme above the filter.

Thus an interaction between NADPH and the enzyme in the absence of the other substrate was observed. As this method can provides only semi-quantitative data the ratio of substrate to enzyme (NADPH/βKR) in table 6.2 cannot be used to predict true binding ratios. The ratio is included to demonstrate continuity in the data between experiments.

The data in table 6.3 show the passage of AcAcCoA through the filter to be unaffected by the presence of βKR in the pre-filtrate. Thus AcAcCoA was not seen to interact with the enzyme in the absence of NADPH, and therefore is unlikely to be the first substrate to bind to the enzyme during catalysis. Ultrafiltrates from βKR solutions were found to have no absorbance at 280 nm or appreciable βKR activity, confirming the retention of the enzyme by the ultrafiltration membrane. In both sets of experiments, the βKR activity of the retentate was unaffected. With hindsight, a more complete experiment would have tested the binding of $NADP^+$ in the absence of AcAcCoA or β-hydroxybutyryl-CoA, however this was not carried out at the time as the principal interest was in the formation of the ternary complex in the forward reaction.

βKR (μM) (tetramer)(Prefiltrate)	0	12.3	13.4	7.6	6.6
NADPH (μM) Total (Prefiltrate)	100	100	100	100	100
NADPH (μM) Free (Ultrafiltrate)	93.9	37.6	34.8	58.9	61.6
NADPH (μM) Bound (Estimate)	6.1	62.4	65.2	41.1	38.4
NADPH/βKR	N/A	5.1	4.9	5.4	5.8

[βKR] measured using Abs @ 280nm and the formula Abs 280 [1 mg/ml} = (5690nW + 1280nY + 120nC) / Mr

NADPH Total estimated from dilution of stock solution of known [NADPH] (Abs 340nm)

Table 6.2 Ultrafiltration binding studies using NADPH and βKR

The data show passage of NADPH through the filter in the absence of βKR. When βKR is present, NADPH is proportionally retained by the enzyme above the filter. Thus NADPH is seen to interact with βKR in the absence of the second substrate Acetoacetyl-CoA.

βKR (μM) (tetramer) (Prefiltrate)	0	7.9	7.7	4.0	3.9
[AcAcCoA] (μM) (Prefiltrate)	25	25	25	25	25
Δ[NADPH] (μM) (βKR Optical Assay)	-23	-24	-25	-23	-24
AcAcCoA/βKR	N/A	•0	•0	•0	•0

[AcAcCoA] in test assay derived from amount of AcAcCoA added to the prefiltrate

Table 6.3 Ultrafiltration binding studies using Acetoacetyl-CoA and βKR

Quantification of Acetoacetyl-CoA was carried out via an NADPH optical assay. The data show the change in [NADPH] in the test assay (and hence [AcAcCoA] present in the ultrafiltrate) to be unaffected by the presence of βKR above the filter. Thus βKR does not appear to interact with AcAcCoA in the absence of NADPH.

6.2.7 Kinetic Mechanism and the stabilising role of NADPH

The data from the bireactant initial velocity study and ultrafiltration binding studies gave evidence that the catalysis carried out by βKR employs a fixed order ternary complex mechanism with NADPH being the first substrate to interact with the enzyme. A graphical depiction of the possible mechanisms investigated is shown in figure 6.5. Previous studies on *B. napus* and other βKRs [Sheldon *et al.*, 1992], have shown the enzyme to be partially protected from dilution by the inclusion of NADPH in the dilution buffer, suggesting that some interaction does take place between the enzyme and NADPH in the absence of the β-keto substrate.

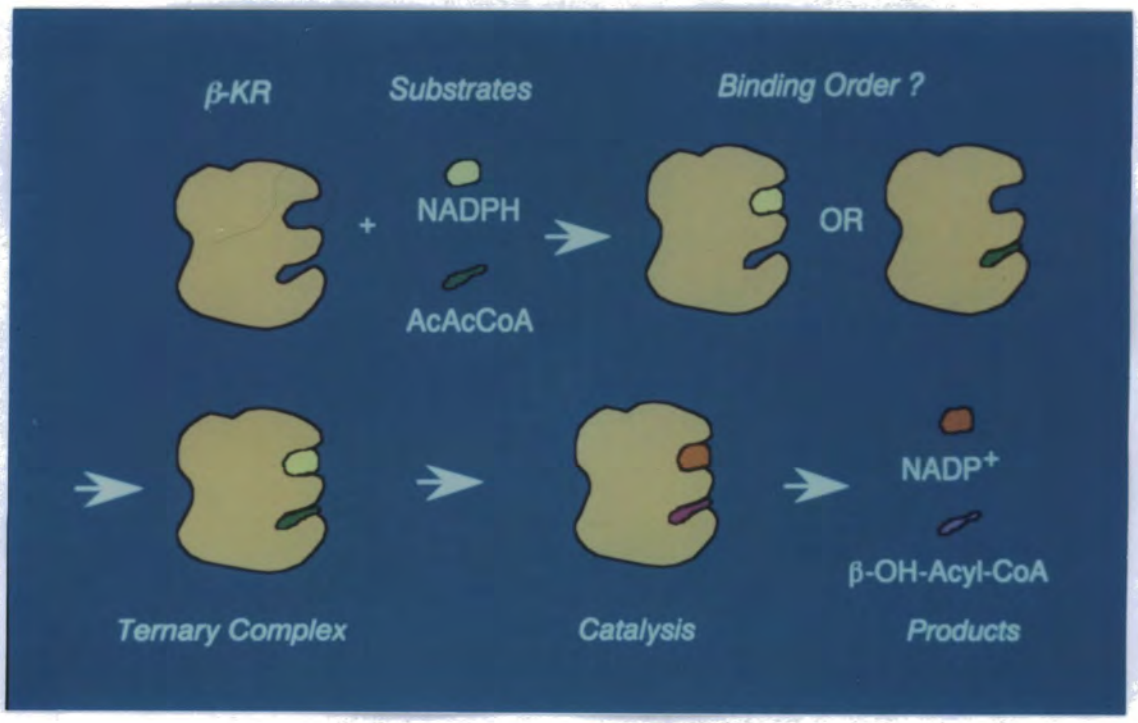

Figure 6.5 Proposed mechanism for βKR catalysis

Data from the above experiments support the hypothesis that the catalysis carried out by βKR employs a fixed order ternary complex mechanism. Of the two binding order outcomes depicted, βKR is postulated to employ the first one, where NADPH binds first.

6.3 Structural studies on *B. napus* and *E. coli* βKR

6.3.1 Circular Dichroism studies - *B. napus*

Professor N.C. Price of the University of Stirling kindly allowed these experiments to be carried out in his laboratory. In order to determine the relative amount of alpha-helix and beta-sheet secondary structure in the purified *B. napus* molecule, circular dichroism (CD) studies were carried out. To do this, spectra of pure βKR solutions were recorded using a Jasco J600 spectropolarimeter at 20°C and quartz cells (Hellma) with a path length of 0.02 cm. Mean residue weight was calculated from the predicted amino acid sequence of the expressed *B. napus* βKR cDNA. Analysis of the secondary structure content was undertaken by using the CONTIN procedure [Provencher and Glöckner, 1981].

Samples of the pure plant protein at two different concentrations (986 and 274 μg ml^{-1}) were subjected to CD analysis to obtain data for structural prediction. A dilution effect on the protein structure is shown by the differences in the mean residue ellipticity spectra shown in figure 6.6. The decrease in protein concentration causes an attenuation of the α-helix-associated absorption bands, indicating an unfolding transition possibly accompanied by the loss of multimeric structure. A similar concentration dependent transition was observed in a binding domain peptide of the yeast transcription factor GCN4, the α-helical folding of which is stabilised upon binding to its DNA substrate [Weiss *et al.*, 1990].

The CONTIN program output reflects the structural change upon dilution. The shift in secondary structure of the protein upon dilution was predicted to be: α-helix: 26% to 18%, β-sheet; 49% to 58%, and remainder: 25% to 24% (see figure 6.7). The α-helical folding affected by the dilution transition is perhaps essential for catalysis or inter-subunit interactions, thus possibly explaining the loss of catalytic activity observed when βKR was diluted to workable concentrations (ca. 0.0628 μg ml^{-1}) for kinetic analysis.

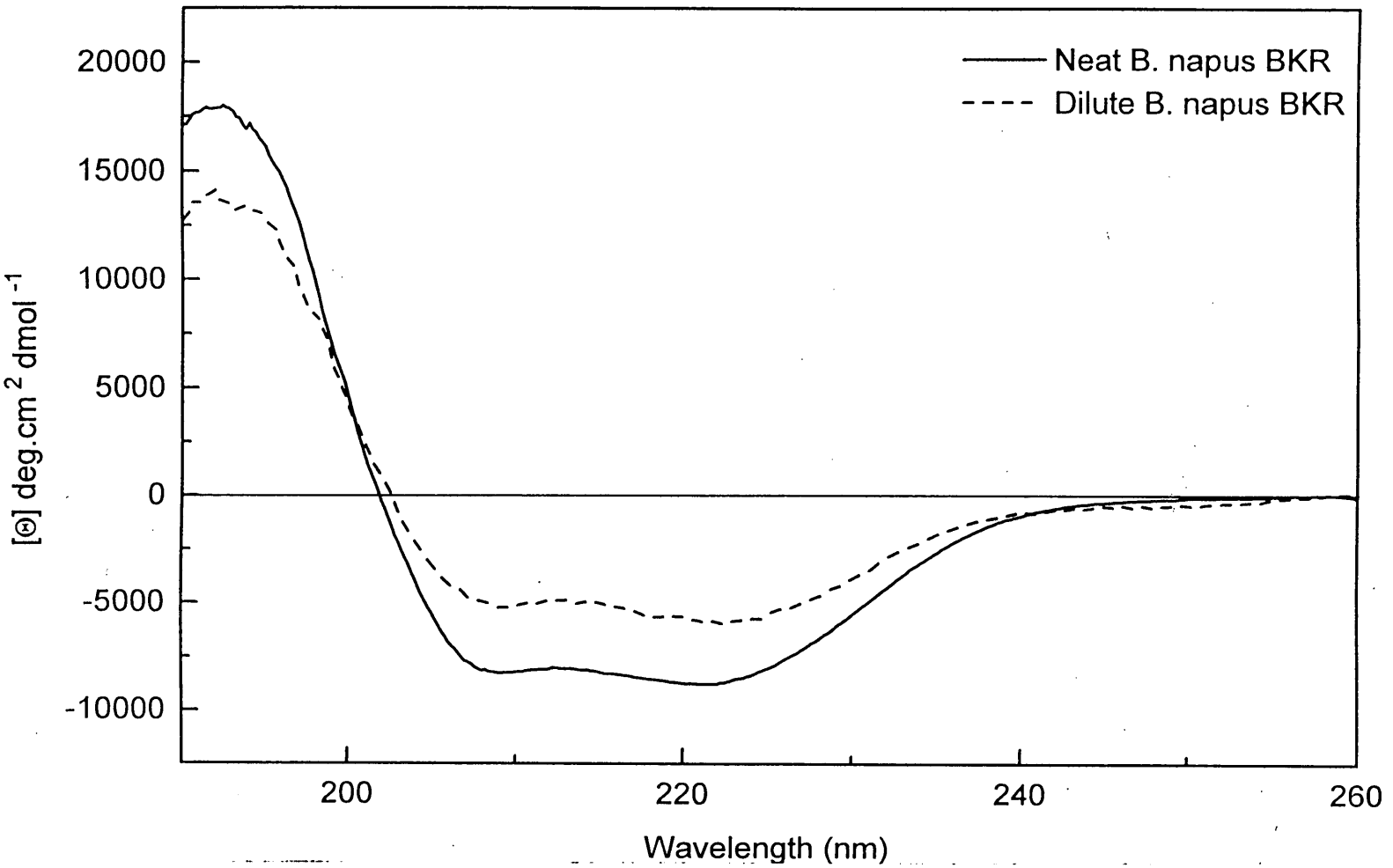

Figure 6.6 Mean residue ellipticity spectra βKR and a 1:5 βKR dilution

A dilution effect on the protein structure is shown by the differences in the mean residue ellipticity spectra shown above.

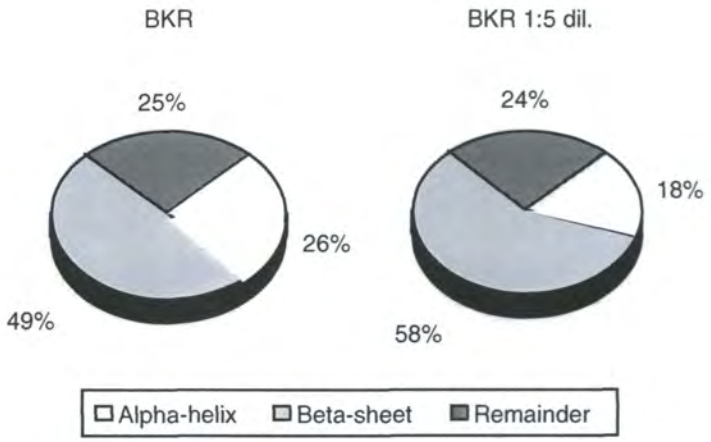

Figure 6.7 Pie charts showing the shift of βKR secondary structure content upon dilution (1:5) as measured by circular dichroism.

The CONTIN program predicts a shift in secondary structure upon dilution. The changes in α-helical folding resulting from dilution may explain the activity loss observed for βKR during dilution for kinetic analysis..

6.3.2 Circular Dichroism studies - *E. coli*

For the *E. coli* βKR enzyme, spectra were again recorded using a Jasco J600 spectropolarimeter at 20°C using quartz cells (Hellma) with a path length of 0.02 cm. Mean residue weight was calculated from the predicted amino acid sequence of the expressed *E. coli* βKR cDNA. Analysis of the secondary structure content was undertaken by using the CONTIN procedure [Provencher and Glöckner, 1981].

The *E. coli* protein was subjected to CD analysis at a concentration of 714 μg ml^{-1}. A comparison between the corrected spectra of the plant and bacterial enzymes is shown in figure 6.8

CONTIN procedure output. The CONTIN program output for the *E. coli* enzyme predicts a secondary structure of α-helix: 21%, β-sheet: 57%, and remainder: 21%. This compares to values of α-helix: 26%, β-sheet: 49%, and remainder: 25% obtained for the plant enzyme.

These secondary structure predictions will be validated once the three dimensional structures of the plant and bacterial over-expressed proteins is determined.

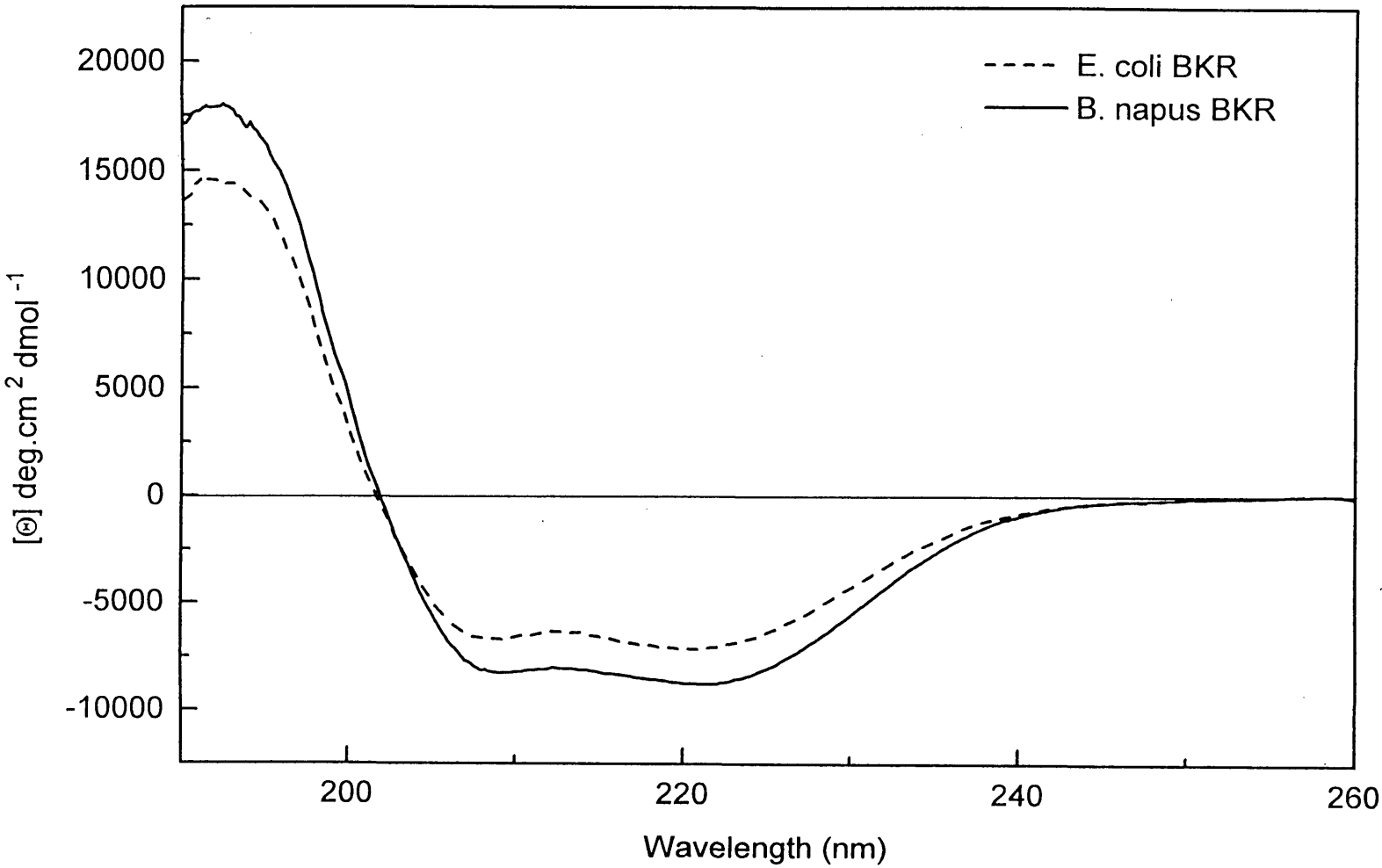

Figure 6.8 Corrected spectra of *E. coli* and *B. napus* βKR proteins

6.3.3 Size determination via gel filtration - *B. napus* βKR

Previous gel filtration studies of the plant βKR enzyme indicated that it has a tetrameric structure [Sheldon, 1988]. In order to predict the quaternary structure of the over-expressed βKR protein, an analytical scale gel filtration experiment was carried out. A 45 μg sample of the pure *B. napus* protein was analysed using a SMART chromatography workstation fitted with a Superose 12 PC column (Pharmacia). The protein standards listed in table 6.4 were each separately applied to the column in 50 mM sodium phosphate buffer pH 7.0 plus 100 mM NaCl. The precise nature of the liquid handling and computerised absorption monitoring systems employed in the SMART workstation, and the precise stable packing of the Superose 12 PC column allowed an accurate comparison of the protein standards to be made. The combined elution profiles of the protein standards are shown in figure 6.9. The retention volumes of the protein standards are also shown in table 6.4. These data were used to produce the graph in figure 6.10. The gel filtration standards data gave the equation for the line of best fit to be:

$$\text{kDa} = \frac{\text{retention vol. (ml)} - 1.32}{-6.67 \times 10^{-4}}$$

Purified plant BKR was applied to the column, 20 μl (30μg) of Mono S FPLC fraction 22 (see figure 3.20), and the automated program run. The eluent was monitored for absorbance at 280 nm. The principal absorption peak eluted at a retention volume of 1.24 ml (see figure 6.11). When inserted into the above equation, this retention volume gives a molecular weight of 120 kDa. This value suggests a tetrameric structure for the over-produced protein, as previously observed for βKR previously purified from *B. napus* [Sheldon *et al.*, 1992].

Protein Standard	kDa	Retention volume (ml)
Bovine serum albumin	66	1.28
Alcohol dehydrogenase	150	1.23
β-amylase	220	1.17
Apoferritin	443	1.04
Thyroglobulin	669	0.87

Table 6.4 Retention volumes of protein standards used to determine native size of over-produced βKR.

The above proteins were each separately loaded on to a gel filtration column and eluted. The retention volume of each was noted for the purposes of calibrating the column.

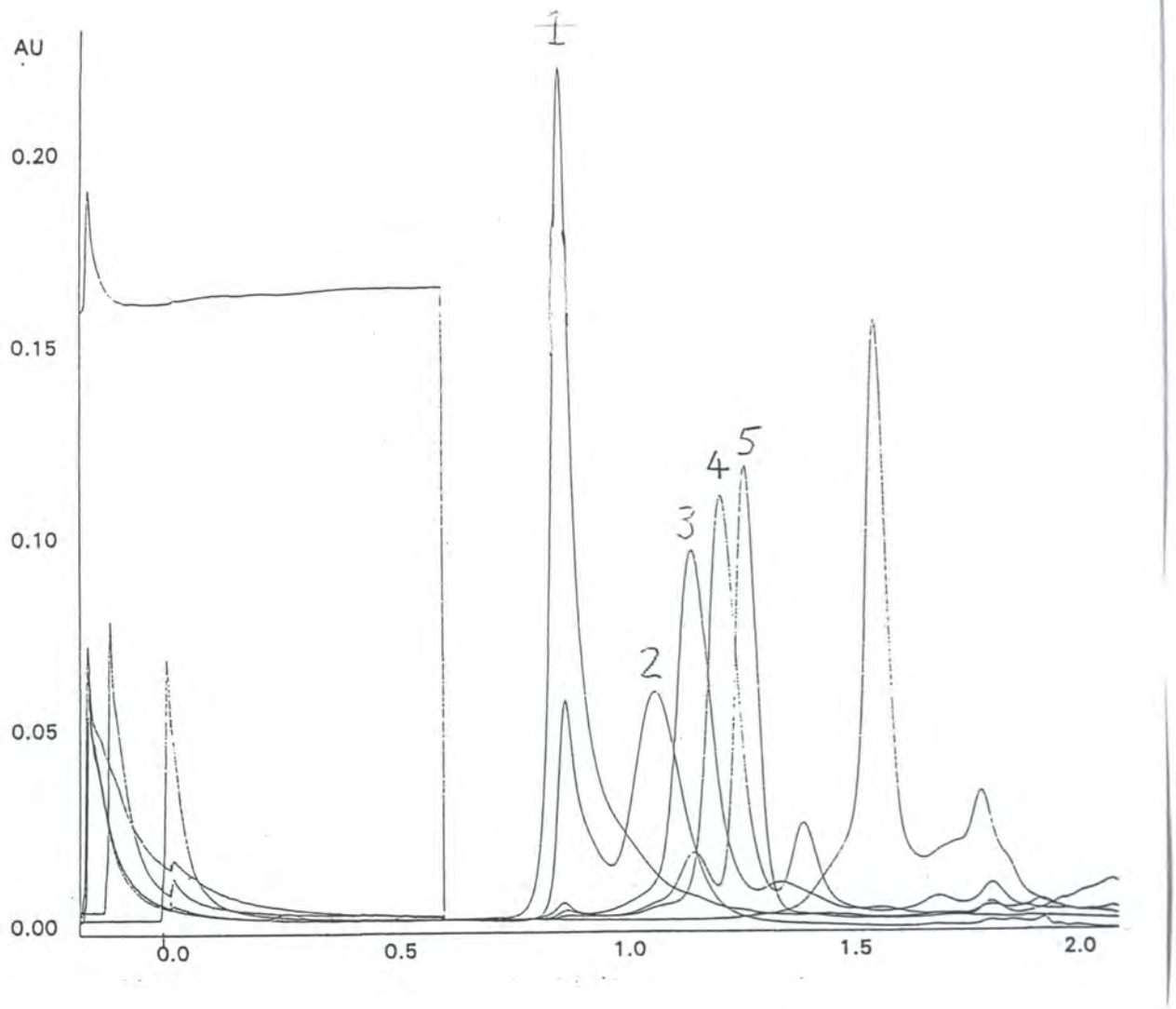

Figure 6.9 Elution profiles of protein standards on Superose 12 PC gel filtration column

Peaks (left to right from 0.9 ml) peak 1, Thyroglobulin, 669 kDa; peak 2, Apoferritin, 443 kDa; peak 3, β-amylase, 220 kDa; peak4, Alcohol dehydrogenase, 150 kDa; peak5, Bovine serum albumin, 66 kDa.

The absorbance at 280nm of six separate protein standards eluting from a gel filtration column was used to produce retention volume data. This data was plotted against the molecular weight of the standards to calibrate the column.

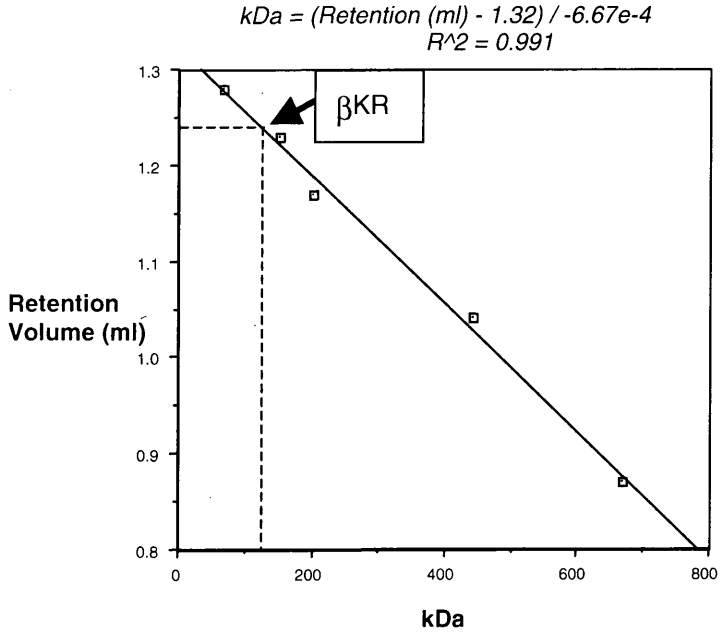

Figure 6.10 Graph showing retention volumes of protein standards used to estimate native size of *B. napus* βKR.

The above plot gave the equation for the line of best fit to be:

$$\text{kDa} = \frac{\text{retention vol. (ml)} - 1.32}{-6.67 \times 10^{-4}}$$

The position of βKR (retention volume = 1.24 ml) on the line of best fit is marked.

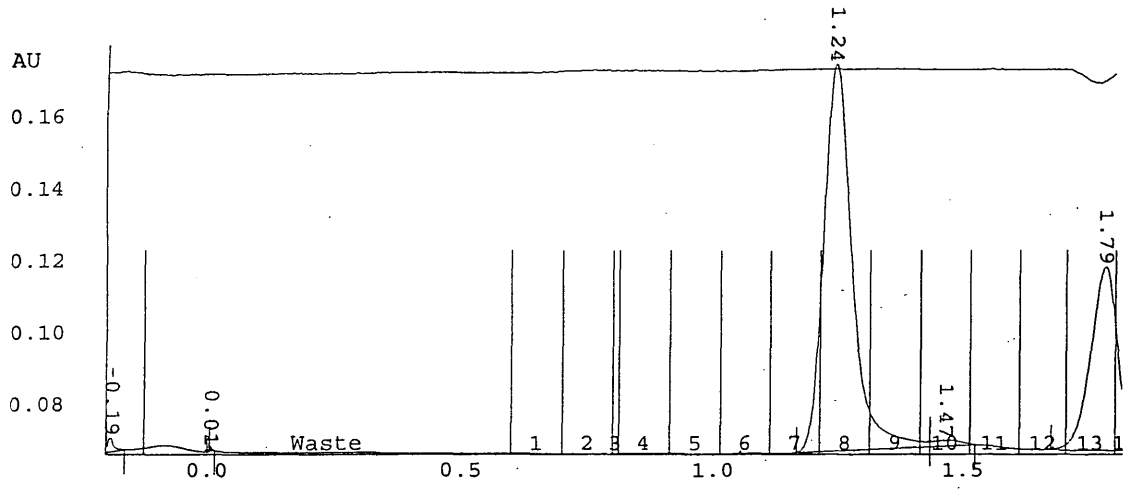

Figure 6.11 Elution profile of purified plant BKR from a Superose 12 PC column.

The eluent was monitored for absorbance at 280 nm. The principal absorption peak eluted at a retention volume of 1.24 ml, this retention volume gave a molecular weight of 120 kDa for over-produced *B. napus* βKR.

6.3.4 Glutaraldehyde fixation of *B. napus* and *E. coli* βKR: SDS-PAGE analysis

To visualise the multimeric structure of the purified βKR proteins via denaturing SDS-PAGE, a glutaraldehyde fixation method was used [White *et al.*, 1993]. Purified protein (50 μg) was diluted into a 1 ml Eppendorf tube containing 1 ml of 50 mM sodium phosphate pH 7.0. Glutaraldehyde, 40 μl of 25% (w/v) Sigma grade 1, was added, thoroughly mixed and the solution was incubated at room temperature for 2 min. 50 μl of 2M $NaBH_4$ was added and the solution was further incubated for 20 min. Sodium deoxycholate (3 μl of 10%) and 35 μl of 100% trichloroacetic acid were added and the solution placed on ice for 5 min. The suspension was centrifuged at 13000 rpm for 15 min. The supernatant was discarded and the pellet dispersed in 600 μl of ice-cold acetone, and centrifuged again to pellet the protein. This wash-step was repeated a second time. The pellet was drained, allowed to air-dry, and resuspended in 50 μl SDS-PAGE loading buffer.

Glutaraldehyde cross-linking of the purified *B. napus* βKR, at the protein concentration and time frame used, allowed the visualisation of the tetrameric over-expression product (figure 6.12). This is further evidence that the protein is assembled similarly in *E. coli* as *in planta*.

Likewise, the simultaneous experiment using purified over-produced *E. coli* βKR also shown in figure 6.12, the bacterial protein appears to be present in both dimeric and tetrameric form, possibly in a dimer/tetramer equilibrium. Whilst X-ray structure cannot be used to provide definitive data on the quaternary structure of a protein in solution, the crystal packing of E. coli βKR is tetrameric - see §6.4.6.2. Therefore it is likely that *E. coli* βKR could exist as a tetramer in solution, or as a dimer-tetramer equilibrium at very low concentrations [David Rice - personal communication].

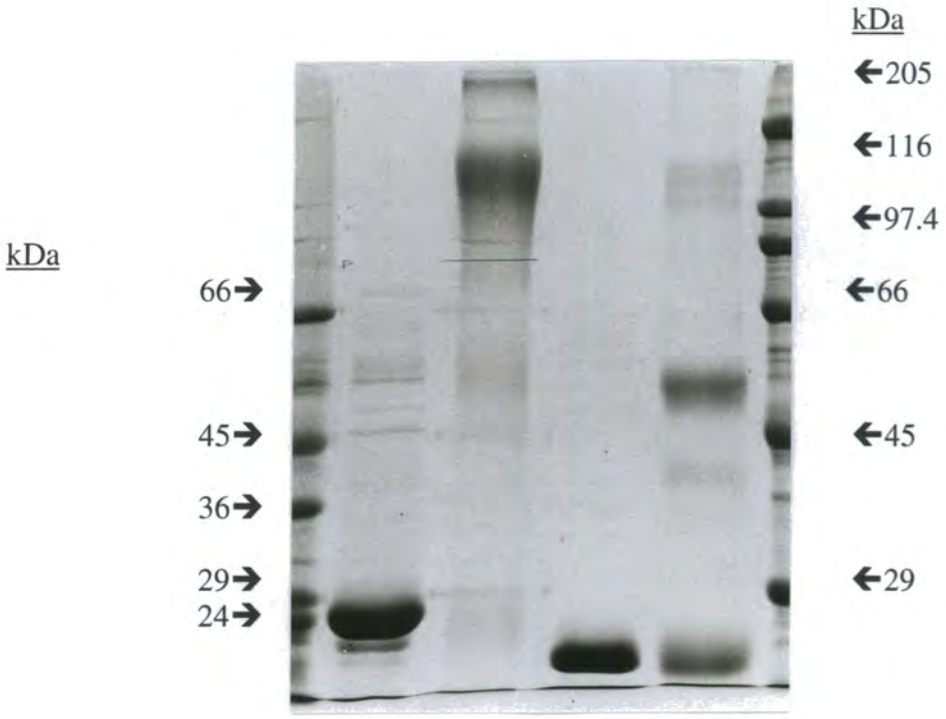

Figure 6.12 Glutaraldehyde cross-linking of over-produced B. napus and E. coli βKR to observe quaternary structure via a conventional SDS-PAGE (5% acrylamide stacking/10% acrylamide resolving) gel.

Lane 1, *B. napus* βKR (minus glutaraldehyde); lane 2, *B. napus* βKR (plus glutaraldehyde); lane 3, *E. coli* βKR (minus glutaraldehyde); *E. coli* βKR (plus glutaraldehyde).

The use of glutaraldehyde cross-linking on each of the purified *B. napus* and *E. coli* βKRs allowed the visualisation of a tetrameric structure in the case of *B. napus* βKR and a dimer/tetramer equilibrium in the case of *E. coli* βKR, on the above denaturing SDS-PAGE gel.

6.4 Crystallisation and X-ray diffraction studies of βKR

6.4.1 Preparation of samples for crystallography

Samples of purified βKR protein were precipitated with ammonium sulphate to aid stability, and sent as a suspension to the crystallographers in the group of Professor David Rice at the University of Sheffield. Routinely, the buffer solution in which the protein was purified was brought from 25 mM sodium phosphate to 50 mM sodium phosphate to counteract the slight acidification that occurs on the addition of ammonium sulphate. The protein solution was chilled in a water-ice slurry and placed on a stir plate. Finely ground ammonium sulphate was slowly added over a period of 5 minutes to give 70 % saturation. The protein suspension was stirred for a further hour at 4 °C. The protein suspension was stored at this temperature until ready for dispatch. Figure 6.13 shows the relative levels of βKR in a 70% ammonium sulphate pellet, and the accompanying supernatant, on an SDS-PAGE gel. This level of ammonium saturation used was sufficient to precipitate all of the βKR in a 1 mg ml^{-1} solution. Both the *E. coli* and *B. napus* proteins behaved similarly upon precipitation.

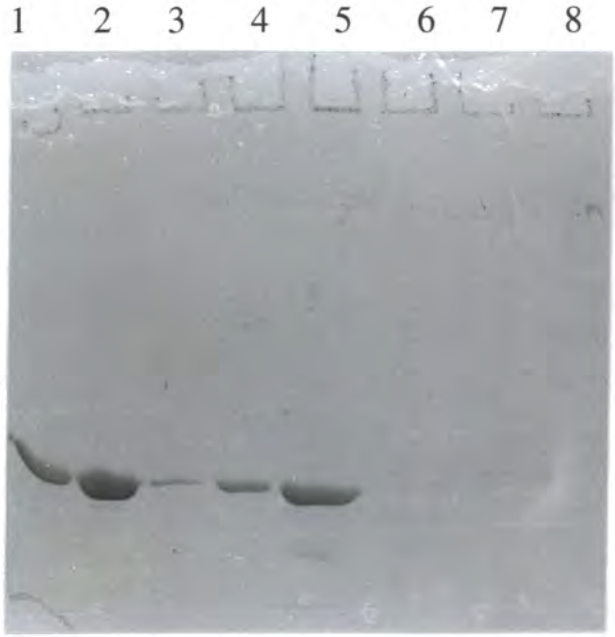

Figure 6.13 Ammonium sulphate precipitation of purified *E. coli* βKR

Lane 1, purified βKR (5 μg); lane 2, purified βKR (25 μg), lane 3, pellet resuspension 1 μl; lane 4, pellet resuspension 5 μl; lane 5, pellet resuspension 25 μl; lane 6, supernatant 1 μl; lane 7, supernatant 5 μl; lane 8, supernatant 25 μl.

The SDS-PAGE (5% acrylamide stacking/10% acrylamide resolving) gel above shows the relative levels of βKR in a 70% ammonium sulphate pellet, and the accompanying supernatant. A 20 ml solution of 1 mg ml^{-1} βKR was subjected to ammonium sulphate precipitation. An aliquot (100 μl) of the resulting suspension was spun briefly in a microcentrifuge. The pellet was resuspended in 100 μl of the original buffer (25 mM sodium phosphate pH 7.0) and together with the supernatant, was subjected to methanol/chloroform precipitation. Both samples were re-suspended in 100 μl of 1X SDS loading buffer.

6.4.2 Crystallisation and diffraction analysis of *B. napus* βKR

Various crystallisation solutions were tested by the crystallographers in order to produce crystals of βKR from *B. napus*. These were tested by dialysing away the ammonium sulphate used for storage and transit into a phosphate buffer containing EDTA and DTT. The protein solution was adjusted to 10 mg ml^{-1} using Amicon microconcentrators and added to an equal volume of precipitant solution. Hanging drops of protein solution were allowed to equilibrate with reservoirs of precipitant solution via vapour diffusion at 17 °C. Crystals of *B. napus* βKR so obtained were found to have a unit dimension of 80x80x300 Å and diffracted to 3 Å. Figure 6.14 shows crystals of βKR plus NADP grown from a polyethyleneglycol 400, citrate buffer at pH 4.5.

6.4.3 Crystallisation of *E. coli* βKR

The plant βKR crystals had a very small unit cell dimension and as a result the structure of the enzyme remained unresolved. In order to obtain some structural cues, the *E. coli* βKR protein, was similarly over-expressed, purified (§4) and subjected to crystallisation trials by Rafferty *et al.* [1998] in the group of Professor Rice at Sheffield. βKR protein samples stored as precipitate in 85% saturated ammonium sulphate, 25 mM sodium phosphate, pH 7.0, 1 mM DTT were dialysed against 10 mM sodium phosphate, pH 7.0, 1 mM EDTA, 1 mM DTT. The concentration of the protein was adjusted to 10 mg ml^{-1} using an Amicon Centricon 10 micro-concentrator by centrifugation at 3000 x g. Samples of the protein (10 µl) were mixed with an equal volume of a precipitant solution of polyethylene glycol of average molecular weight 1450 in the range 15-25%(w/v) in 100 mM sodium citrate buffer, pH 4.5, and allowed to equilibrate by vapour diffusion with reservoirs of precipitant solution at 290 K. Crystals with a hexagonal-plate morphology and maximum dimensions 0.5 x 0.5 x 0.2 mm were obtained after approximately 1 week. Figure 6.15 shows crystals of apo βKR grown from a polyethylene glycol 1450, sodium phosphate buffer at pH 7.0.

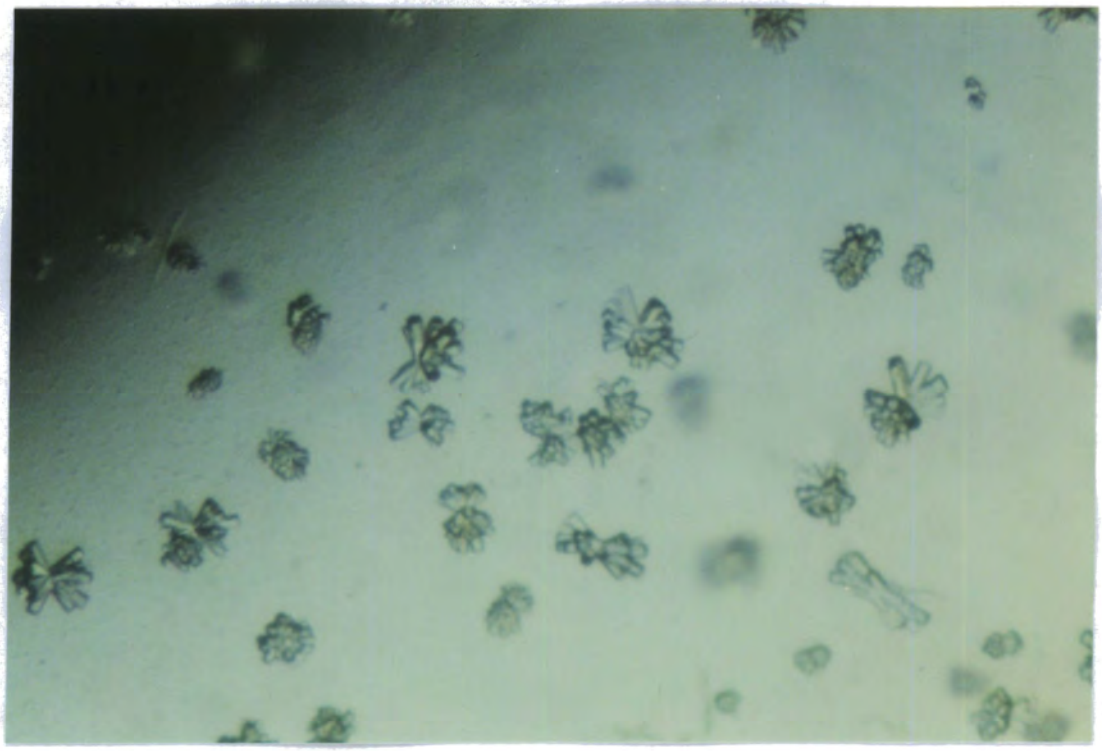

Figure 6.14 Crystals of *B. napus* βKR plus NADP grown from a polyethyleneglycol 400, citrate buffer solution at pH 4.5.

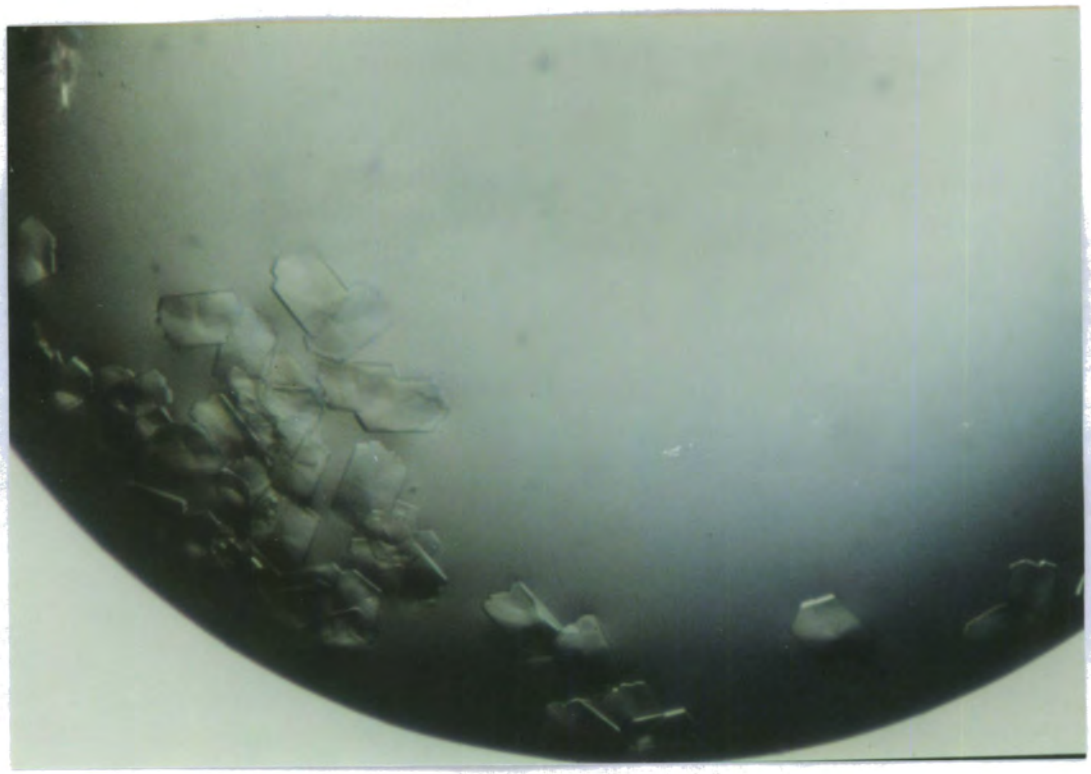

Figure 6.15 Crystals of *E. coli* apo βKR grown from a polyethylene glycol 1450, sodium phosphate buffer solution at pH 7.0.

6.4.4 Diffraction analysis of E. coli βKR

Crystals of βKR were grown by the hanging-drop vapour-diffusion method from buffered PEG solutions by Rafferty *et al.* as described above. The enzyme was found to crystallise in the space group $P6_122$ with cell dimensions a=b=68.1Å c=359.2Å. It has one dimer in the asymmetric unit and a solvent content of 63%. 3.5Å resolution native X-ray diffraction data were collected at room temperature on a MAR image plate on station 9.5 at the CLRC Daresbury Laboratory - see figure 6.16. The images were processed and the resulting data were merged and scaled via the use of dedicated software. The native data set, obtained from one crystal, was 97% complete to 3.5Å. This medium resolution native data set was replaced in the latter stages of refinement by a 2.5Å resolution set. This was collected at room temperature on a MAR image plate detector on station 9.6 at the CLRC Daresbury Laboratory. This data was processed, merged and scaled to give a data set obtained from one crystal which was 98% complete to 2.5Å. A native crystal was also soaked in a stabilising solution containing 10 mM NADPH and this binary complex data set was also collected on a MAR image plate on station 9.6 at the CLRC Daresbury Laboratory from one crystal and was 99% complete to 2.5Å.

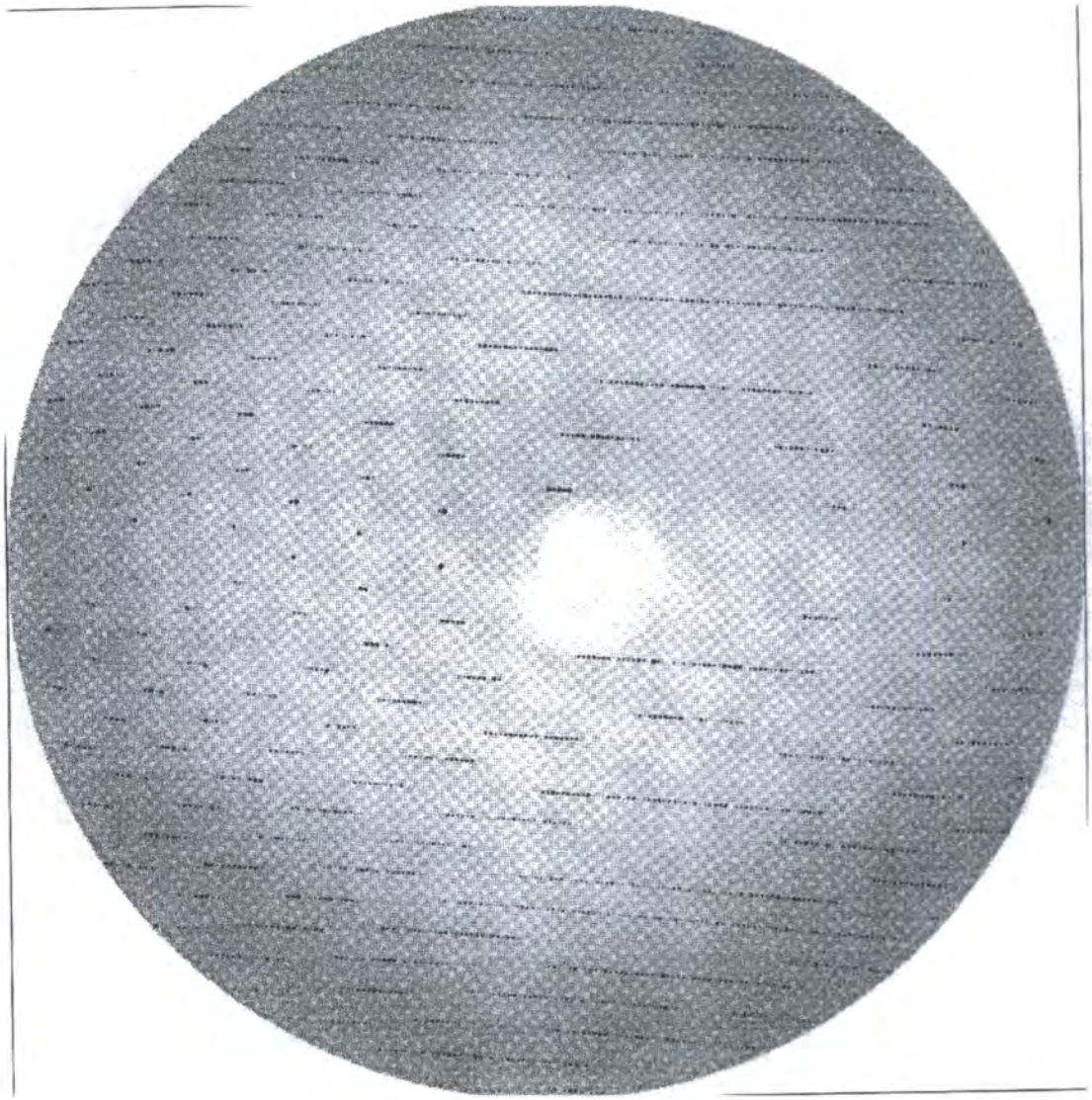

Figure 6.16 X-ray diffraction pattern for E. coli βKR crystals

An X-ray diffraction image taken at CLRC Daresbury Laboratory on station 9.5, recorded on a large MAR image plate. The diffraction limit to the edge of the image is 3.5Å and a rotation angle of 3° was used.

This figure was kindly provided by Professor David Rice, University of Sheffield. It originally appeared in a paper by Rafferty *et al.* [1998].

6.4.5 Production of *E. coli* βKR in an methionine auxotrophic strain

To aid the structural determination of *B. napus* and *E. coli* βKR via X-ray crystallography, a methionine auxotrophic strain of *E. coli* transformed with the βKR expression constructs was required. This would allow the production of βKR proteins containing the heavy atom amino acid derivative seleno-methionine as a diffraction reference marker. This derivatised protein was required to elucidate the correct phases from the Fourier transformation obtained from the X-ray diffraction data of the native protein crystals.

An *E. coli* strain deficient in methionine synthesis was provided by Dr Toon Stuitje of the Free University of Amsterdam. The strain contained a Tn 10 transposon carrying tetracycline resistance, inserted in the metC gene of the methionine synthetase operon. To create the strain, *E. coli* BL21(DE3) cells were transfected with P1 phage containing the Tn10 transposon. Methionine auxotrophs were selected for by subtractive plating out on minimal and methionine supplemented media. Cells containing this transposon were made transformation competent using $CaCl_2$ and transformed separately with pETNEβ1 (encoding *E. coli* βKR) and pETJRS10.1 (encoding *B. napus* βKR) by the author. Both the transposon and the plasmids were selected for using tetracycline and ampicillin respectively. Transformants were checked for over-expression via a trial culture and SDS-PAGE analysis (see figure 6.17), then sent for growth at Zeneca Pharmaceuticals (Cheshire, UK), in controlled minimal media in which the endogenous supply of methionine had been replaced by selenomethionine. The crude extract from these cells was purified and provided for crystallography using the same methods as for the unmodified *E. coli* and *B. napus* over-expressed proteins.

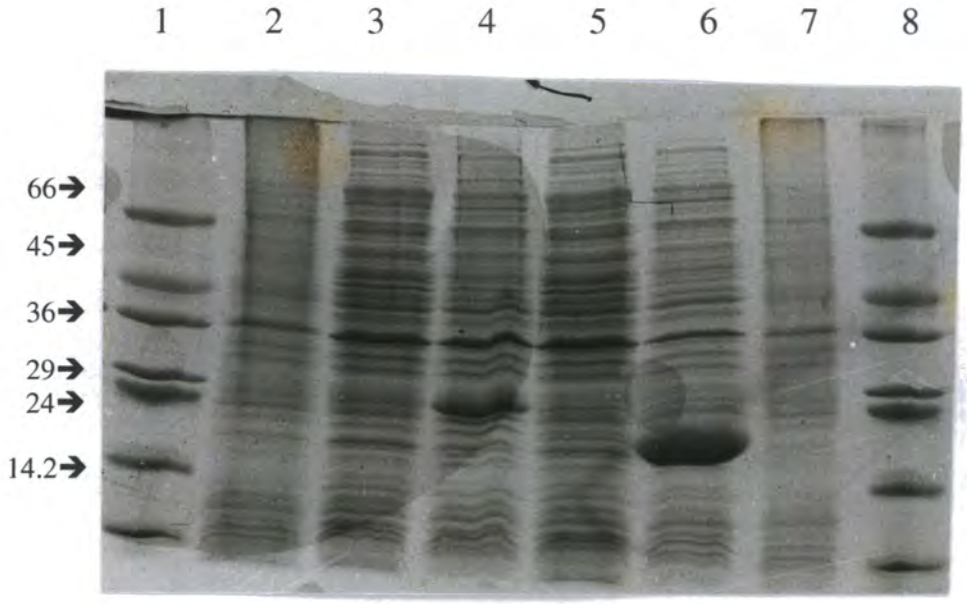

Figure 6.17 SDS-PAGE (5% acrylamide stacking/10% acrylamide resolving) gel showing over-expression of a *B. napus* and *E. coli* βKR in strains BL21(DE3) MetC, pETJRS10.1 and pETNEβ1 respectively

Lane 1, SDS-VII Mw markers; lane 2, protein extract from cells containing pET-11d (empty over-expression vector); lane 3, MetC mutant BL21(DE3) pETJRS10.1 transformant (uninduced); lane 4, MetC mutant BL21(DE3) pETJRS10.1 transformant (IPTG induced); lane 5, MetC mutant BL21(DE3) pETNEβ1 transformant (uninduced); lane 6, MetC mutant BL21(DE3) pETNEβ1 transformant (IPTG induced); lane 7, protein extract from cells containing pET-11d; lane 8, SDS-VII Mw markers

The over-expression of βKR protein is clearly observable at 27 kDa for the *B. napus* over-expression plasmid pETJRS10.1 and at 20 kDa for the *E. coli* βKR over-expression plasmid pETNEβ1.

6.4.6 Determination of the crystal structure of *E. coli* βKR at a resolution of 2.5Å

The structure of *E. coli* βKR at a resolution of 2.5 Å has been determined via a collaboration with workers in the group of David Rice at the University of Sheffield. The description below draws from papers kindly provided to the author by Professor David Rice and Dr John Rafferty to allow inclusion of the data here [Rafferty *et al.*, 1998; Fisher *et al.*, *in press*]. This work used the βKR protein samples described in §6.4.1., together with further samples of βKR provided by other workers in the Durham laboratory.

6.4.6.1 Structural determination

The structure of βKR was determined in the absence of substrate and cofactor by a combination of molecular replacement and multiple isomorphous replacement (MIR) techniques using a map calculated at a spacing of 2.5Å. A mercury and a selenomethionine derivative - see §6.4.4., were used to determine the phases. The initial map was improved by solvent flattening and two-fold non crystallographic symmetry averaging and permitted identification of a number of α-helices and some β-strands. Automated trace linking of the regions of highest density was carried out and used in combination with a model derived from 3α, 20β-hydroxysteroid dehydrogenase (HSD) [Ghosh *et al.*, 1994] to guide the positioning of the polypeptide chain.

A new map was calculated by combining the phase information from this partial structure with that from the MIR solution. A number of iterations were then performed until the positions had been determined for approximately 70% of the side chains. The resulting structure was refined via least squares analysis using computer software. This was followed by further cycles of phase combination, model building and refinement. In the latter stage of this process, the initial low resolution 3.5Å native data was replaced by a higher resolution 2.5Å data set collected in a separate X-ray diffraction session.

The crystal structure reveals a homotetramer where each subunit forms a single domain comprising a seven stranded parallel β-sheet flanked by seven α-helices. For guidance, the amino acid sequence for *E. coli* βKR with numbering corresponding to that used in the text for *E. coli* βKR is shown in figure 6.18, as part of a sequence

alignment which is further discussed below. The derived structure reveals a dimer in an asymmetric unit and a final model comprising 217 residues in an 'A chain' and 216 residues in a 'B chain' out of the total of 244 residues per chain. No interpretable density was observed for three loop regions spanning residues Ile89-Lys99, Ser138-Ala149 and Arg190-Ser193 in the A subunit and Ile89-Glu102, Ser138-Ala149 and Arg190-Ala191 in the B subunit. All side chains were fitted except those for residues Asp 100, Glu101, Gln203, Tyr242, Met243 and Val244 in the A subunit and Trp103, Phe115, Lys119, Lys128, Tyr242, Met243 and Val244 in the B subunit.

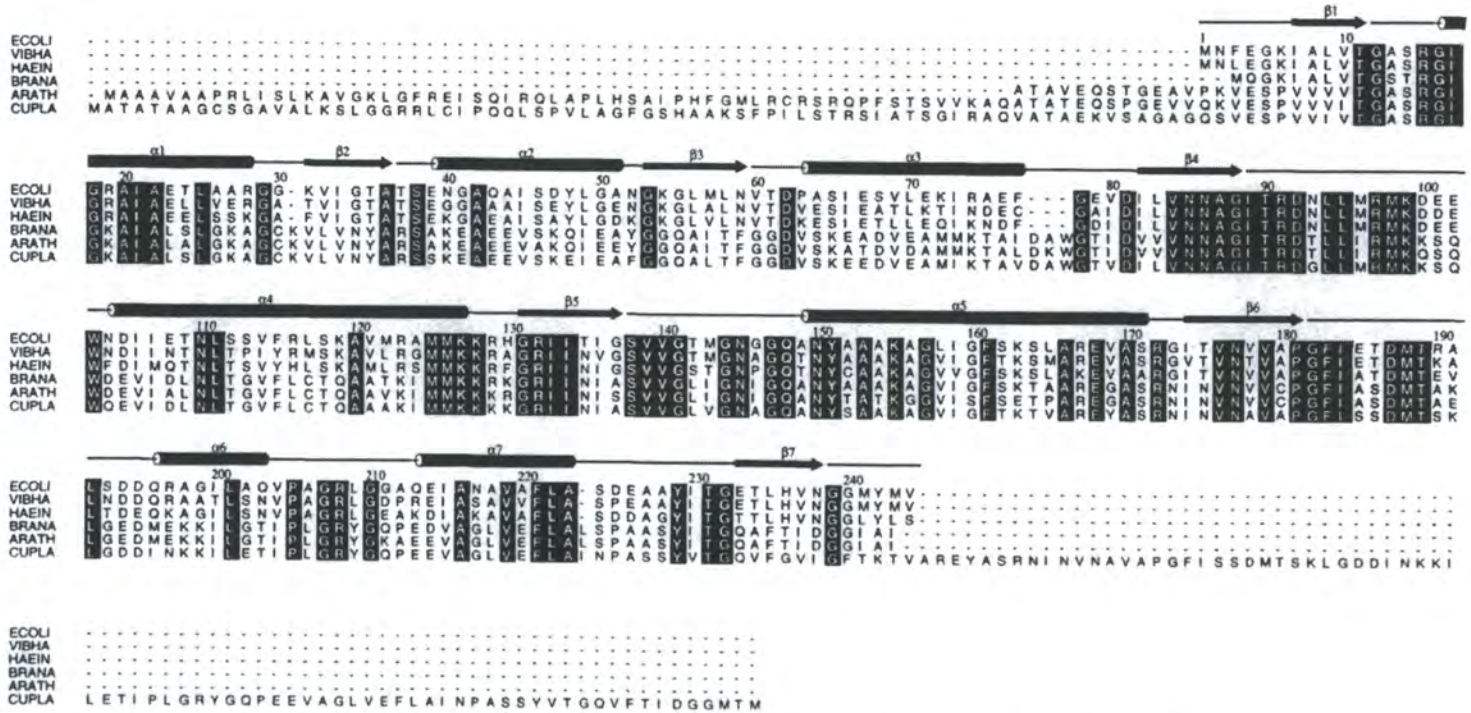

Figure 6.18 Multiple sequence alignment of various βKR amino acid sequences and *E. coli* βKR.

A multiple sequence alignment of the βKRs from *E. coli* (ECOLI), *Vibrio harveyi* (VIBHA), *Haemophilus infiuenzae* (HAEIN), *Brassica napus* (BRANA), *Arabidopsis thaliana* (ARATH) and *Cuphea lanceolata* (CUPLA). The sequence numbering and secondary structure relating to *E. coli* βKR is given above the sequences. The α helices are shown as tubes and the β strands as arrows. Residues conserved in all six sequences appear in blocked typeface. (Produced using the program ALSCRIPT [Barton, 1993]). Taken from Fisher *et al.* (in press)

6.4.6.2 Overall structure

The βKR subunit was found to comprise a single domain of dimensions 40x40x50Å and is formed from seven β-strands (β1-β7) creating a parallel β-sheet, and seven α-helices (αA-αG) plus a number of loops of varying length which modify the functional characteristics of the enzyme. The parallel β-sheet is flanked on one side by helices αA, αB & αG and on the other by helices αC, αD & αE, with helix αF sitting along the "top edge" of the β-sheet above the COOH-terminal ends of strands β1 & β7 - see figure 6.19. This fold is highly reminiscent of the Rossmann fold commonly found in dinucleotide binding enzymes.

Starting from Met1 a segment of extended chain precedes strand β1 (Gly5 to Val 10) followed by a short loop of five residues to helix αA (G1y16 to Arg28) which leads immediately into strand β2 (Gly30 to Ala36). This strand is followed by helix αB (Asn40 to Leu49) and a turn before strand β3 (Gly53 to Asn59). There is another long loop (Val60 to Ile66) which is followed by helix αC (Glu67 to Ala75) and another short loop (Glu76 to Asp81) before strand β4 (Ile82 to Gly88), where the next eleven residues in subunit A and fourteen in subunit B (Ile89 to Lys99A/Glu102B) lack interpretable density. The start of the next interpretable density region begins with a short linker before the long helix αD (Asn104 to Lys127) which is followed by strand β5 (His130 to Gly137). This is then followed by a second region of uninterpretable density (Ser138 to Ala149) after which helix αE (Tyr151 to Ala170) begins the next interpretable region of density. This helix leads straight into strand β6 (Thr175 to Phe183) followed by a long loop region (Ile184 to Arg197), which incorporates the third missing region (Arg190-Ser193A/Ala191B), before the short helix αF (Ala198 to Gln203). A long turn then leads into helix αG (Gln213 to Ala223) before the final strand β7 (Gly232 to Asn238) and a small turn (Gly239 to Met241) with the final three residues of the COOH-terminus lacking interpretable density in both subunits.

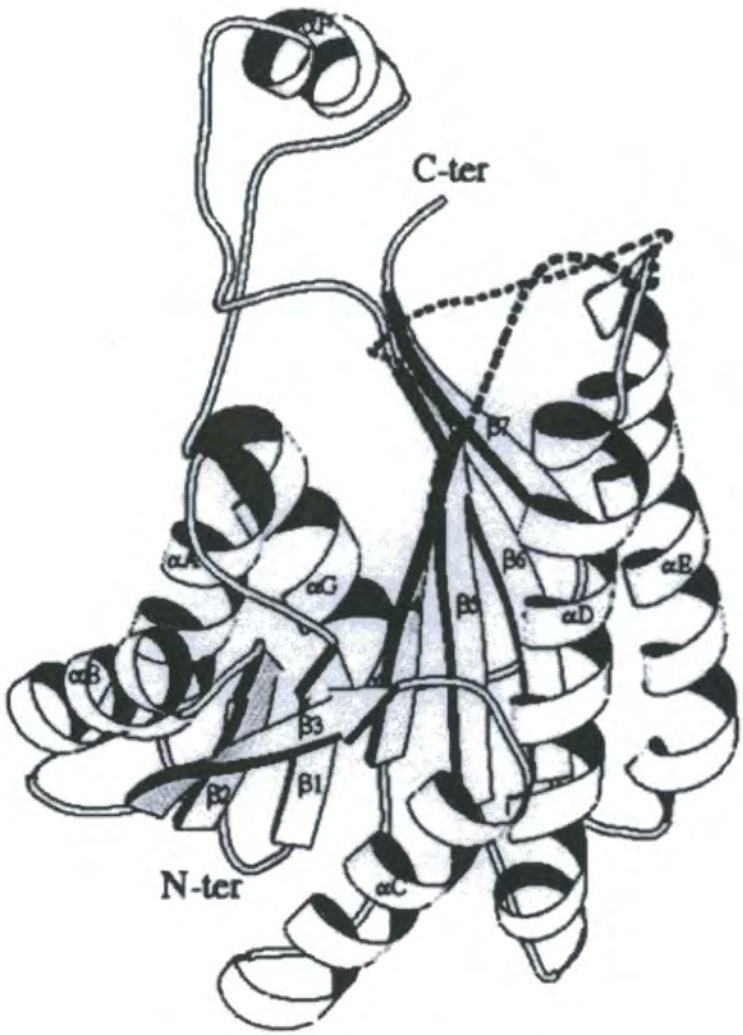

Figure 6.19 E. coli βKR subunit structure

Shown is a representation of one subunit of the NADPH bound βKR tetramer (NADPH molecule has been omitted for clarity) with (α helices and β strands are shown as coiled ribbons and flattened arrows, respectively, and numbered as in the text. The missing (uninterpretable) loop regions are denoted by the dotted lines. (Produced using the program MOLSCRIPT [Kraulis, 1991].) Taken from Fisher *et al.* (in press).

6.4.6.3 *Subunit interfaces*

An obvious tetramer is observed in the packing in the crystal, with approximate dimensions 80x80x70Å - see figure 6.20. Each monomer in the tetramer makes contact with all three symmetry related partners. The solvent accessible surface areas of an isolated monomer and a tetramer were calculated and are approximately 11000Å^2 and 36000Å^2, respectively. On formation of the tetramer, approximately 2000Å^2 (18%) of the solvent accessible surface is buried per monomer.

6.4.6.4 *Nucleotide binding site*

The initial structure determination of βKR was made using crystals grown in the absence of the nucleotide cofactor. Thus the exact location of the nucleotide binding site was determined by difference Fourier experiments using data to 2.5Å from crystals soaked in stabilising solutions containing 10 mM NADPH. The resulting maps have interpretable density for the adenine ring, the associated ribose, the phosphate group attached to its C2'-hydroxyl and the pyrophosphate - see figure 6.21. The nicotinamide ring and its associated ribose cannot be located in the electron density map. Analysis of the βKR /NADPH binary complex shows that the NADPH cofactor is bound in an extended conformation and the adenine ribose sugar ring is found as the C2'-endo conformer.

The binding pocket for the adenine ring on βKR is formed by the side chains of Thr37, Asn59 and Thr109. The C2'-hydroxyl group of the adenine ribose to which the phosphate group is attached in the NADP(H) co-factor, sits in a region flanked by Ser14, Arg15 and Thr37. The presence of the basic residue Arg 15 stabilises the negative charge on the adenine ribose phosphate group and its location corresponds with those of equivalent stabilising residues in other structurally related enzymes which bind NADP(H), for example, mouse lung carbonyl reductase [Tanaka *et al.*, 1996a]. The pyrophosphate moiety of the nucleotide lies close to the COOH-terminal end of the β-sheet where it interacts with residues, which form the loop between strand β1 and helix αA, and residues from the first turn of helix αA. There are no positively charged side chains close to the pyrophosphate moiety and thus its stabilisation on the enzyme is via a series of hydrogen bonds and the helix dipole of αA.

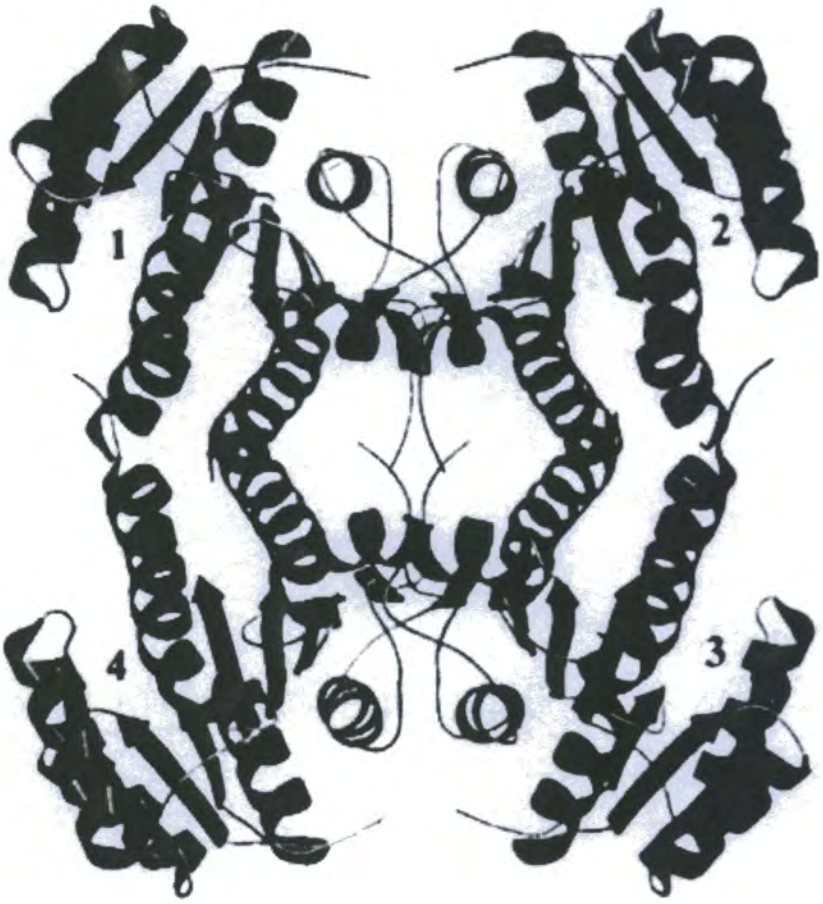

Figure 6.20 E. coli βKR tetrameric crystal packing

Shown is the βKR tetramer viewed along one of the three molecular twofold axes. Subunits are numbered 1,2,3 and 4. (Produced using the programs MOLSCRIPT [Kraulis, 1991] and RASTER 3D [Merrit and Murphy, 1994].) Taken from Fisher *et al.* (in press).

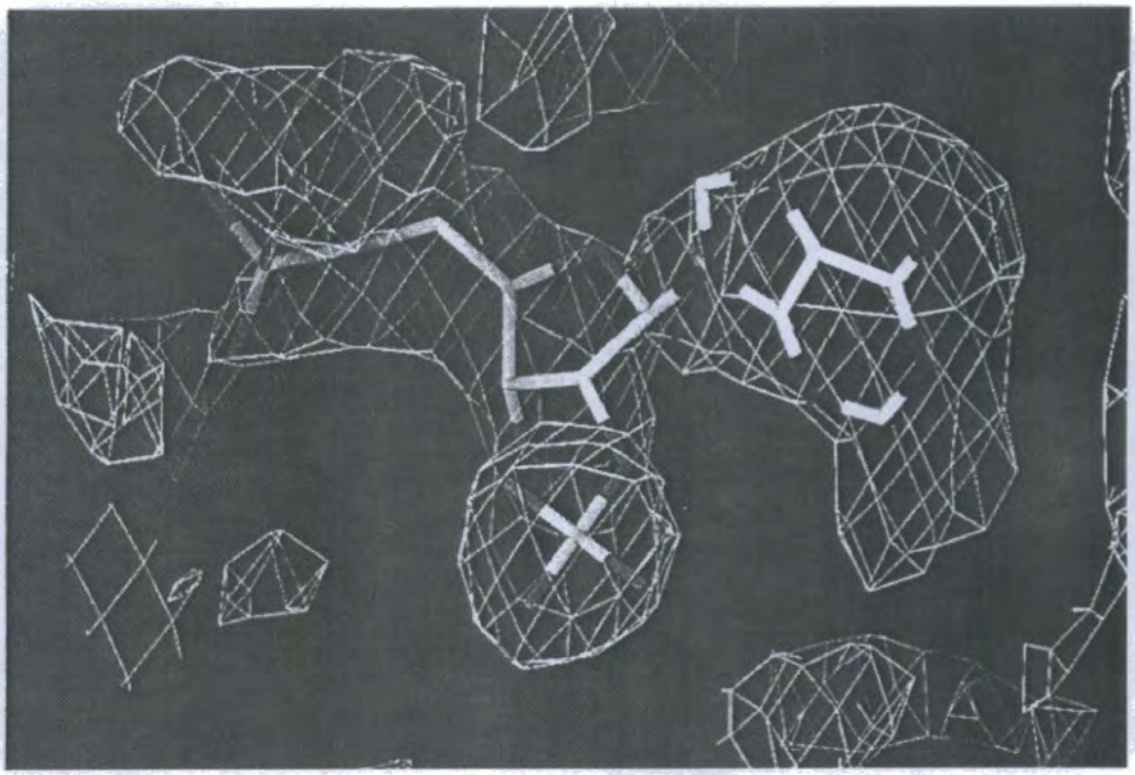

Figure 6.21 NADPH cofactor

The bound NADPH cofactor is shown modelled using clear, interpretable electron density data at 2.5Å for the nicotinamide ring, the associated ribose, the phosphate group attached to the C2'-hydroxyl and the pyrophosphate moieties. Taken from Fisher *et al.* (in press).

There is a general similarity between the folding pattern of βKR and the Rossmann fold and if a comparison is made between the mode of nucleotide binding in βKR with that in glyceraldehyde 3-phosphate dehydrogenase (GAPDH) [Skarzynski *et al.*, 1987], which possesses a typical Rossmann fold, the general location on the enzyme of the adenine ring, its associated ribose and the pyrophosphate moiety of the cofactors are similar. However, in the case of βKR the extra phosphate group attached to the C2' oxygen of the adenine ribose has added interactions with the protein which play an important role in locating the NADP(H) cofactor. Nucleotide binding enzymes often show structural conservation of a helix whose role is to stabilise the binding of the pyrophosphate moiety of the cofactor.

Least squares superimposition of the central β-strands and flanking helices of βKR and those of GAPDH (Brookhaven Protein Data Bank (PDB) entry 1GD1) shows that strands β1 to β4 and helices αA and αG in βKR have close equivalents in GAPDH. A particularly good overlap is observed between helix αA in βKR and the nucleotide binding helix in GAPDH - see figure 6.22. The turn linking the first β strand and the first helix in nucleotide binding enzymes is usually rich in glycine residues and often contains a sequence fingerprint GxGxxG/A where x is any residue [Wierenga *et al.*, 1985]. The superimposition shows that residues Gly12 and Gly18 in βKR have close structural correspondence to the glycines at the first and last positions of the fingerprint, despite the loop linking strand β1 and helix αA possessing an additional inserted residue. The positively charged residue Arg15 in the loop interacts with the phosphate attached to the C2' oxygen of the adenine ribose. A common method for recognising the adenine ribose hydroxyl groups in nucleotide binding enzymes, employs hydrogen bonds from the side chain of an acidic residue on an adjacent β strand which is linked in turn to the loop between strand β1 and helix αA. In GAPDH this residue is Asp32 [Skarzynski *et al.*, 1987] but in βKR, where a negatively charged acidic residue might interfere with NADP(H) binding, the equivalent residue is Ala36.

Figure 6.22 βKR/GAPDH and cofactor

Depicted is a stereoview of a superposition of the βKR Cα backbone trace and cofactor and the GAPDH Cα backbone trace and cofactor viewed down the nucleotide-binding helix. The extra residue in the loop linking β1 and the nucleotide-binding helix αA in βKR is shown and the positions of residues Glyl2 and Gly18 in βKR are indicated. Taken from Fisher *et al.* (in press).

6.4.6.5 *Location of the active site and substrate binding pocket*

A multiple sequence alignment of βKR from *E. coli* [Rawlings and Cronan, 1992], *Vibrio harveyi* [Shen and Byers, 1996], *Haemophilus infiuenzae* [Fleischman et al., 1995], *Brassica napus* (sequence derived from clone pJRS10.1 - see §3), *Cuphea lanceolata* [Klein *et al.*, 1992] and *Arabidopsis thaliana* [Slabas *et al.*, 1992a] illustrated in figure 6.18 reveals that there are 85 completely conserved residues. There are a further 24 'strongly conserved' residues which occur in *E. coli* and at least four out of the five other sequences. Mapping of the completely conserved residues onto the three dimensional structure of the *E. coli* enzyme, shows them lying mainly within the core of the subunit formed by the central three strands (β4-6) of the β-sheet and around the binding site for the nucleotide cofactor. The conservation of sequence diminishes upon moving away from the core region. Two of the loop regions in the structure for which there is no interpretable density (residues 89 to 99 and 138 to 149) do in fact show a high degree of sequence conservation (73% completely conserved), which strongly suggests that they might be critical for enzyme function.

6.4.6.6 *Structural and mechanistic similarities between βKR and other oxidoreductases*

The three-dimensional co-ordinates of βKR were compared with those of all other proteins in the January 1998 release of the Brookhaven PDB. To do this, βKR and the proteins in the PDB are represented in a simplified manner as linear helices and strands in three-dimensional space. These secondary structure elements (SSES) and their interrelationships are represented as a mathematical graph which is then searched using an algorithm. Similarities were found to numerous dehydrogenases. However, a very strong similarity was shown between βKR and 3α,20β-hydroxysteroid dehydrogenase (HSD) from *Streptomyces hydrogenans* [Ghosh *et al.*,1994], mouse lung carbonyl reductase (MLCR) [Tanaka et al., 1996a] and 1,3,8-trihydroxynaphthalene reductase (THNR) from *Magnaporthe grisea* [Andersson *et al.*, 1996]. The strongest similarity with βKR was observed for mouse lung carbonyl reductase (PDB entry '2cyd') where 14 SSEs were denoted as equivalent in the two structures. As previously discussed, βKR belongs to a large family of oxidoreductases, the short chain

dehydrogenases and epimerases (the SDR family)- see §1.6. This family, which includes HSD, MLCR and THNR, was identified as carrying a signature motif YxxxK, where x is any residue. The tyrosine and lysine residues are believed to be involved in the proposed catalytic mechanisms of the enzymes [Jörnvall *et al.*,1995]. There is a good superposition of helices αA, αC, αD, αE and αG, and the central β-sheet from βKR with αA, αC, αD, αE and αG and the central β-sheet from HSD, MICR and THNR.

When all atoms of the adenine ring, ribose and pyrophosphate moieties of the respective nucleotide co-factors of βKR, HSD, MLCR and THNR were superimposed, good overlap was observed between the side chains of the equivalent catalytic tyrosine and lysine residues (βKR Tyr151, Lys155; HSD Tyr152, Lys156; MLCR Tyr149, Lys153; THNR Tyr178, Lys182). The tyrosine side chains superimpose slightly less well than those of the lysine residues, with a distance of 0.5-1.0Å between the positions of their respective phenolic oxygen atoms. These phenolic oxygen atoms are believed to donate a proton to their respective reaction intermediates in the SDR catalytic mechanisms - see figure 6.23. A neighbouring highly conserved serine residue - see figure (see figure 1.7) has also been identified as a likely participant in the mechanisms of many of these enzymes and thus forms a possible catalytic triad with the Tyr and Lys residues [Tanaka *et al.*, 1996b; Thoden *et al.*, 1996]. The position of this proposed catalytic serine residue superimposes well in the structures of HSD, MLCR and THNR, however, the equivalent residue in βKR, Ser138, is not observed in the electron density map.

The similarity of βKR to other members of the SDR family also extends to the mode of assembly of the subunits into tetramers. For example, βKR shows a similarly small value for the buried solvent accessible surface area about the R axis upon tetramerisation (200Å^2 (2%)), as observed similarly for MLCR by Tanaka *et al.* (1996a). The comparison also highlights the fact that regions in other family members equivalent to parts of the missing loops in βKR are involved in formation of the interface about the Q axis of the tetramer molecule.

In addition, in most of the NADP(H)-dependent enzymes of the SDR family there is a similarly small uncharged side chain at the position equivalent to Ala36 in

βKR mentioned above, which would allow binding of the phosphate group at the C2' oxygen of the adenine ribose of the NADPH.

The fatty acid elongation cycle contains two reductive steps and the aligned sequences of the two *E. coli* enzymes which catalyse them, βKR and ENR, share an overall 22% identity over the 244 residues of βKR - see figure 6.24. ENR is composed of subunits which have a very similar dinucleotide binding fold to that seen in βKR and which also form into a similar tetramer [Rafferty *et al.*, 1995].

When the residues conserved between βKR and ENR are plotted onto the structure of βKR, there is some limited clustering of residues within the hydrophobic core of the enzyme formed by the packing of helices αA and αG against strands β1, β4, β6 and β7 of the β-sheet, but otherwise the conserved residues appear distributed throughout the secondary structure elements. There is apparently little conservation of sequence near the active site, with the notable exception of the putative catalytic residue Lys155 in βKR, which corresponds to Lys163 in ENR. The phenolic hydroxyl groups of Tyr151 in βKR and the proposed catalytic residue Tyr156 in ENR, although not picked out by the sequence alignment, are also located in similar, but not identical, positions in the three dimensional structures.

There is a difference of approximately 2.3Å in the positions of the phenolic oxygen atoms relative to the catalytic lysine side chains. It is clear that a common underlying structure, comprising a single domain formed from the classical dinucleotide binding fold, has been utilised to carry out the two reductive steps. It is therefore postulated that this represents a divergence of the two enzymes from a common reductase ancestor in the FAS elongation cycle, given the additional similarity in sequence. The comparison with ENR also suggests a likely region in βKR for the formation of a substrate-binding cleft which would be bounded on one side by residues Gly88 to Lys99 and Thr135 to Lys155 and on the other side by residues Arg15 to Ile17, Asn175 to Asn177 and Ile184 to Arg197. Many of these residues are not observed in the electron density map of βKR and might perhaps only become ordered upon substrate binding. This has been observed for a disordered segment of approximately 10 residues in an *E. coli* ENR-NAD+ binary complex, which becomes ordered and observable in

electron density maps upon the binding of a diazaborine-NAD bi-substrate analogue [Baldock *et al.*, 1996].

By analogy with the proposed mechanisms for HSD [Ghosh *et al.*, 1994] and ENR [Rafferty *et al.*, 1995], a plausible mechanism for the reduction by βKR of its 3-oxoacyl substrate can be envisaged in which there is an attack of a hydride ion from NADPH upon the carbon of the keto group at position C-3 followed by the formation of an alkoxide ion intermediate (see figure 6.23). In a subsequent step, a proton could then be donated to the oxygen of the alkoxide ion to give the reduced secondary alcohol product. Examination of the region in βKR close to the modelled position for the C4 of a nicotinamide ring of the NADPH confirms that the conserved Tyr151 and Lys155 are located such that Tyr151 might act as the base which donates the proton to the alkoxide ion in the catalytic mechanism whilst Lys155 might act to stabilise a transition state and/or effect the pKa of the Tyr151 hydroxyl group.

The small difference in the positions of the phenolic oxygen atoms of the putative catalytic tyrosine residues in βKR and ENR mentioned above, might reflect the difference in the substrates of the two enzymes. There is an additional two bonds separating the site of hydride transfer and that of proton donation in the double-bond containing substrate of ENR, compared with the keto substrate of βKR. Although Ser138 of the catalytic triad proposed for other members of the SDR family is disordered in βKR, the preceding residue, Gly137, is observed and thus a position for Ser138 can be estimated which places it near the active site where it might be capable of interacting with the substrate or transition states during catalysis.

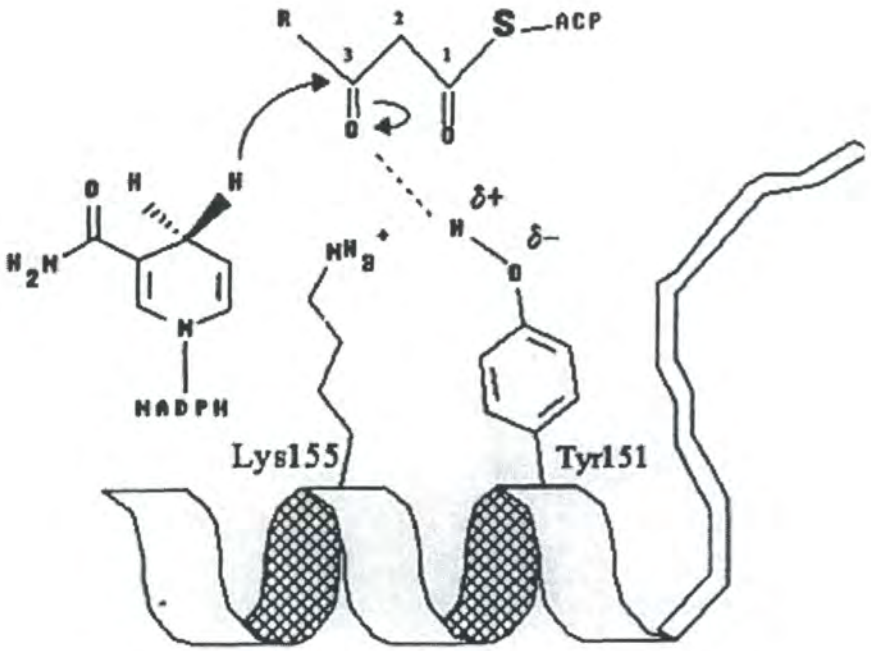

Figure 6.23 Proposed βKR catalytic mechanism

This figure shows the proposed catalytic mechanism for the reduction by βKR of the keto group in a β-ketoacyl ACP substrate. An attack of a hydride ion from NADPH upon the keto group at position C-3 takes place. This forms an alkoxide ion intermediate to which a proton from the ionised tyrosine residue could then be donated to give the reduced secondary alcohol product. The tyrosine group may be stabilised by the side chain of the lysine residue. Taken from Fisher *et al.* (in press).

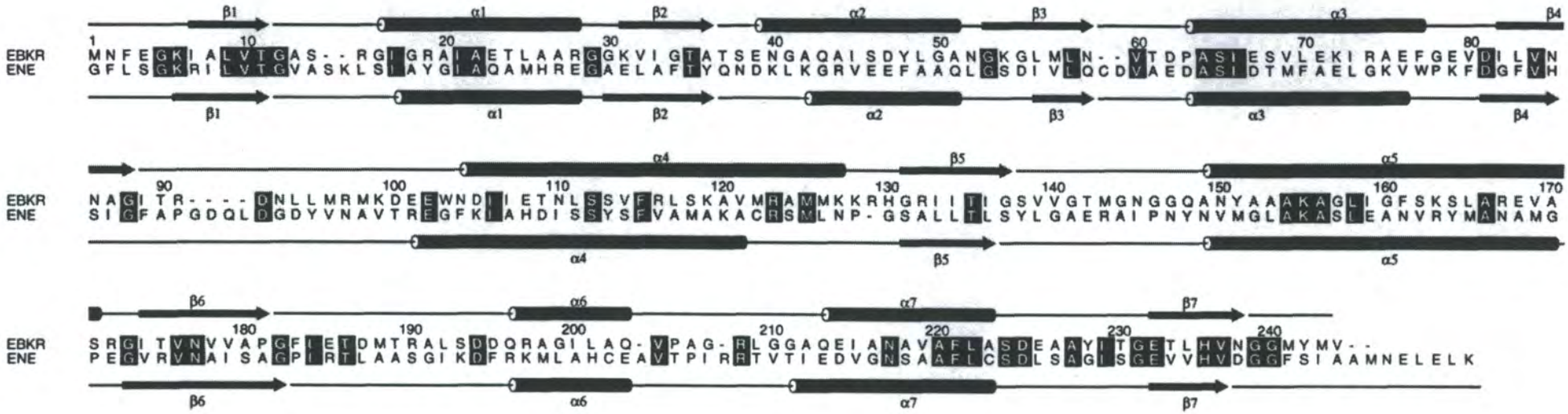

Figure 6.24 Sequence alignment of βKR and ENR amino acid sequences from *E. coli*.

A sequence alignment of βKR (EBKR) and ENR (ENE) from *E. coli* is shown. The sequence numbering and secondary structure for βKR is shown above the sequences whilst the secondary structure for ENR is shown below the sequences. The α helices are shown as tubes and the β strands as arrows. Residues conserved in both sequences appear in blocked typeface (Produced using the program ALSCRIPT [Barton, 1993]

6.5 Summary

Pseudo Michaelis-Menten constants were obtained for the substrate analogue AcAcCoA, the values of Km 492 μM compares with a value of 261 μM for the enzyme previously purified from *B. napus* seed. The V max value obtained for the over-produced enzyme was 57562 μmol NADPH min^{-1} μmolβKR^{-1}. A bireactant initial velocity study showed, by the convergence pattern observed on a reciprocal plot of the data obtained, that βKR employs a fixed or random order ternary complex mechanism as opposed to a bireactant ping-pong mechanism.

Whilst enzyme preparations for the above kinetic studies were suitably stable to allow faith in the data obtained, the delicate nature of the enzyme proved problematic during attempts to carry out product inhibition studies. Such studies, using NADP and β-hydroxybutyryl-CoA as product inhibitors, would have produced inhibition pattern data that could have been used to determine that nature of the ternary complex. Unfortunately the level of variability of enzyme activity when diluted to a working concentration rendered such studies virtually impossible, as data from several hours of experiments would need to be compared. Despite consultation with the literature and an authority on kinetics, Professor Paul Engel of University College Dublin, no way of reliably standardising the data could be found.

To circumvent this problem, an ultrafiltration variation on the conventional technique of equilibrium dialysis was devised. The data from these ultrafiltration experiments suggested that βKR employs a fixed order ternary complex mechanism with NADPH binding first. Secondary evidence for this was obtained from crystallographic studies (see below) and the observation that βKR required addition of NADPH prior to AcAcCoA in assays if non-chaotic data were to be obtained.

In addition to the preparation of many protein samples for crystallographic study, structural studies undertaken by the author included circular dichroism, gel filtration and glutaraldehyde cross-linking of native structure. Circular dichroism studies revealed a secondary structure change upon dilution of the *B. napus* βKR enzyme, perhaps responsible for the enzyme's inactivation under such conditions. Gel filtration,

predicted a tetrameric structure for *B. napus* βKR, whilst glutaraldehyde cross-linking visually confirmed this on an SDS-PAGE gel. The *E. coli* enzyme was observed in a possible dimer tetramer equilibrium by the same cross-linking technique.

Crystallographic studies of the two βKR enzymes are progressing at the University of Sheffield with the aid of methionine auxotrophic strains produced using a transposon construct and the original over-expression plasmids. The crystal structure of *E. coli* βKR has been determined to medium resolution. The structural fold of the enzyme is reminiscent of the Rossmann fold seen in many dinucleotide-binding proteins but with additional features which facilitate substrate binding and catalysis within the same domain as observed for other members of the short chain alcohol dehydrogenase (SDR) family.

This structure of *E. coli* βKR provides insight into substrate binding in lipid biosynthesis and reveals an evolutionary link with the other oxidoreductase of the fatty acid elongation cycle, enoyl ACP reductase (ENR). From the location of a bound NADPH cofactor molecule and multiple sequence comparisons with other reductases from the SDR super family, Tyr151, Lys155 and Ser138 are proposed as important active site residues in βKR.

A structural comparison of βKR with the three-dimensional co-ordinates of all proteins in the Brookhaven Protein Data Bank shows a high degree of similarity between the structure of βKR and that of ENR, 3α,20β-hydroxysteroid dehydrogenase, mouse lung carbonyl reductase and 1,3,8-trihydroxynaphthalene reductase. By superimposition of the five structures, the catalytic lysine residue in βKR is confirmed to be structurally equivalent to the lysine in the other enzymes. The side chain phenolic oxygen of the catalytic tyrosine residue in βKR, which acts as a proton donor in a proposed reaction mechanism, is also seen to be approximately structurally equivalent.

to the side chain phenolic oxygen of the other enzymes.

Chapter 7: Discussion

7.1 Over-expression of βKR enzymes

The 'pET vector' based expression system used in this study has been successful in producing ample amounts of βKR protein from both *B. napus* and *E. coli*. Problems often associated with protein over-expression experiments, such as lack of expression (perhaps through disadvantageous codon usage in a eukaryotic gene, instability of the encoded mRNA or protein, or toxicity of the gene product) or vigorous expression and translation (resulting in the formation of inclusion bodies), were thankfully not encountered here.

However, it should be noted that both expression constructs used in this study, encoding *E. coli* βKR and *B. napus* βKR, were produced by means of a PCR amplification and were not sequenced other than to check that they were in frame with the start codon of the expression plasmid. Taq polymerase from *Thermus aquaticus*, which was used in the construction of the *B. napus* βKR construct has been found to have an error rate of approximately 1.1×10^{-4} errors/bp [Barnes, 1992] - 'errors/bp' indicating total errors e.g. base substitutions, frameshifts, etc. The average error rate determined for this enzyme in this and other studies is 1×10^{-4} errors/bp. $Vent_R$ polymerase from *Thermococcus litoralis* (New England Biolabs), which was used in this study to amplify the βKR coding sequence from *E. coli* chromosomal DNA, has an error rate of 57×10^{-6} errors/bp [Mattila *et al.*,1991], thus the likelihood of there being errors in the *E. coli* βKR construct is reduced. Without checking the nucleotide sequence of the constructs it is impossible to know how many PCR errors were incorporated into the coding sequence of the enzymes, or of what nature (e.g. substitution or frameshift) the errors might be. For a PCR error to have consequences in the final protein structure, it must cause a frameshift, possibly leading to a truncated

protein product, or a codon change which alters the amino acid incorporation in the translated protein. The redundancy of the genetic code means that some base changes will not be effective to alter the amino acid sequence. Despite the oversight of not sequencing the expression constructs, this study produced catalytically active proteins of the expected molecular weight, as discernible by SDS-PAGE. The *E. coli* βKR product of one of the constructs has been studied structurally and no truncation or amino acid changes from the predicted sequence were apparent - though it is possible that the modelling and refinement processes of the structural prediction might mask a conservative amino acid change, especially if it was positioned in the uninterpretable regions of the structural model.

The recombinant *B. napus* βKR enzyme appeared to have 71% of the reported activity of the plant enzyme. The difference observed, if not due to errors in or differences between the corresponding assays performed, is postulated to be due to the recombinant nature of the enzyme, perhaps because of a PCR error.

A formal study of the activity of the recombinant enzymes versus native enzymes was not carried out. Such a study would have been able to indicate if the recombinant enzymes were fully active due to, for instance, correct folding within *E. coli* or possessing the correct amino acid sequence despite possible PCR introduced errors. For this latter reason, comparisons of the recombinant enzymes with the native enzymes in this study must be treated with caution.

The level of recombinant protein expression, coupled with the modified double-freeze-thaw lysis method (§4.4.2) and convenient two-step, one-matrix purification methods devised in this study, provide a rapid and efficient method for the production of milligram quantities of active βKR proteins. This should also hold true for mutated versions of the protein that were produced to explore active site residues (see §7.3).

The purification of βKR from *B. napus* seed by Sheldon delivered 0.22 mg of

the enzyme from 100 grams of developing seed, whereas up to 50 mg could be purified from a one litre culture of βKR over-expressing *E. coli* strain. The over-expressed βKR proteins were the predominant protein species in crude extracts, particularly so in the part-lysed freeze-thaw extracts. This excess of protein simplified purification procedures; lessening the need for the precise monitoring of recovery and yield that is essential during the purification of native enzymes.

The *in vitro* reconstitution of the type-II *E. coli* fatty acid synthetase complex has been reported [Heath and Rock, 1995]. This work involved the over-expression of *fabG* (βKR) as a 'His-tag' fusion protein. This study demonstrates the over-expression and purification of the unmodified coding sequence.

7.2 Expression and isoforms of βKR in *B. napus*

The *B. napus* seed βKR cDNA clone used in this study for over-expression, namely JRS10.1 was previously cloned in this laboratory by José Martinez-Rivas. Northern blot analysis of mRNA isolated from *B. napus* leaves and seeds has shown the expression of this clone to be 20 times higher in seed than in leaf [Martinez-Rivas *et al.*, 1993]. This is unsurprising in a tissue synthesising large quantities of storage triacylglycerol. It is important however to note that like enoyl-ACP reductase there is a continual demand for more enzyme throughout the entire lipid deposition stage in maturing rape seeds. Thus the rate of deposition of lipid appears not controlled by an initial threshold catalytic level of the enzyme as would have perhaps been anticipated.

Analysis of 'JRS10.1' mRNA abundance via the method of reverse transcriptase – polymerase chain reaction (RT-PCR) has suggested that it is the predominant βKR transcript in *B. napus* seeds, from four expressed βKR genes [Dr. A. White - personal communication]. These two pieces of evidence cannot necessarily be extrapolated from the mRNA level to the protein level, i.e. a predominant transcript does not necessarily give rise to a predominant protein isoform. For instance, an abundant transcript may be

susceptible to high levels of mRNA degradation or may encode a protein with a high degradation turnover.

The two dimensional western blot evidence for four major βKR isoforms, presented in chapter 5, has since been obtained separately by Dr A. White in this laboratory. His work on the genes encoding βKR in *B. napus* has shown that there are five genes in the plant, four of which are expressed - a comparison between the sequence of one of these genes and the cDNA sequence encoded by clone pJRS10.1 is shown in figure 7.1. Correspondingly, four isoforms are observable via 2D western blotting. They are present in near equal amounts [Dr. A. White- personal communication]. The observation of four isoforms present in equal quantities in *B. napus* seed, echoes the findings of Fawcett *et al.* [1994] for enoyl reductase (§1.2.9). Evidence would therefore suggest that the two or more apparent isoforms observed in this study in addition to the four major isoforms - see figure 5.14 may not correspond to separate isoforms, but may have been the result of poor focussing of the existing isoforms in the relevant region of the first dimension gel.

It would seem from immunodetection studies that the enzyme over-expressed in this study is a major isoform in *B. napus* seed, provided that it does not have unusually high antigenicity in comparison to the other isoforms - the antibodies used to detect the 10.1 gene product as a predominant isoform, here and in the work of Dr White, were raised against the 10.1 gene product.

In addition to the detection and identification of isoforms, quantification of the amount of βKR in *B. napus* developing seeds was one of the aims of this work. The quantitative western blotting method previously used to quantify enoyl reductase from the same source [Slabas *et al.*, 1990], failed to provide reliable data for βKR in the hands of the author, despite much experimentation using the same protocol and adaptations of it. An enzyme linked immunoabsorbent assay (ELISA) for βKR has since

been developed in the laboratory for the comparative quantification of βKR between leaf samples. No assays of seed material have produced reliable data as yet [Dr Andrew White – personal communication].

The differences observed in immunodetection levels between enoyl reductase and βKR in seed samples (§5.4, particularly figure 5.7), if real, are surprising. It might be expected that these two FAS complex enzymes would be present in similar amounts in the developing seed. The discovery that KAS enzymes of *Cuphea lanceolata* are susceptible to feedback inhibition by accumulation of β-ketoacyl-ACPs [Winter *et al.*, 1997] might suggest βKR has some regulatory importance and that protein levels in the seed cannot match those of an enoyl reductase in a solely synthetic role.

Alternatively, the discrepancy between βKR and ER levels may have been caused by βKR being more readily degraded by proteolysis than enoyl reductase in the seed extracts examined. Further work, perhaps using ELISA detection, is required.

In previous work on βKR [Sheldon, 1988] the plant derived *B. napus* βKR enzyme bound to a Mono Q matrix at pH 5.9 and eluted at 0.2 M NaCl in the gradient. The fact that the plant protein bound to the anionic exchange column, presumably being acidic at pH 5.9 does not correlate with the over-expressed βKR being able to bind to a cationic matrix (Fast S) at pH 6.0 (§3.5.3.), presumably being basic at this pH. The over-expressed B. napus βKR, perhaps unsurprisingly, did not bind to the anionic column when tested at the same pH. A computer generated titration curve, generated from the deduced amino acid sequence (figure 7.2) shows the protein encoded by pETJRS10.1 to be basic at pH 5.9 - 6.0. This anomaly may suggest that the protein purified by Sheldon was a different isoform to the protein over-produced here in this work.

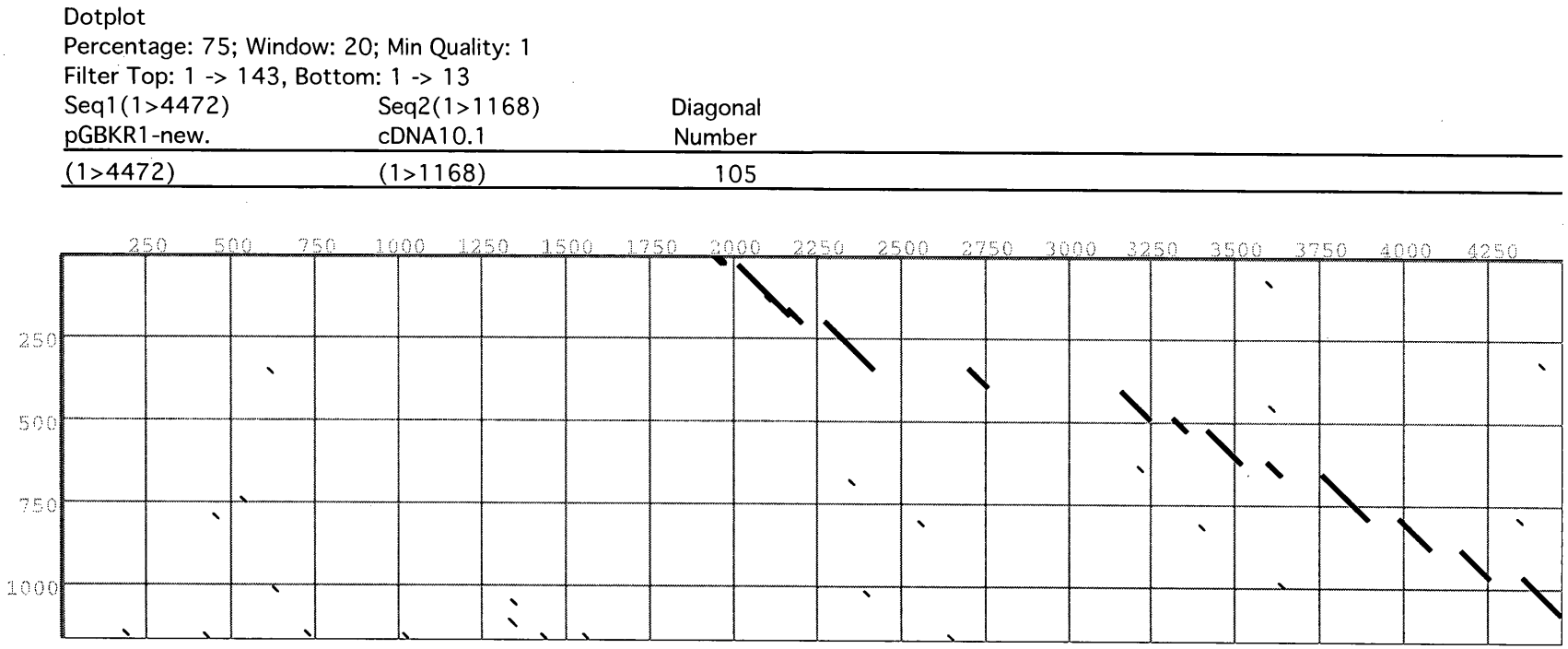

Figure 7.1 Dot plot of DNA sequence homology between *B. napus* βKR genomic clone pGBKR1 and the βKR encoding cDNA from pJRS10.1

The above dot plot shows good homology between the cDNA and a genomic clone encoding *B. napus* βKR, ranging between position ~1950bp and position ~4470 bp of the genomic clone. The eleven gaps may indicate intronic sequence in the genomic clone. *Figure provided by Dr Andrew White*

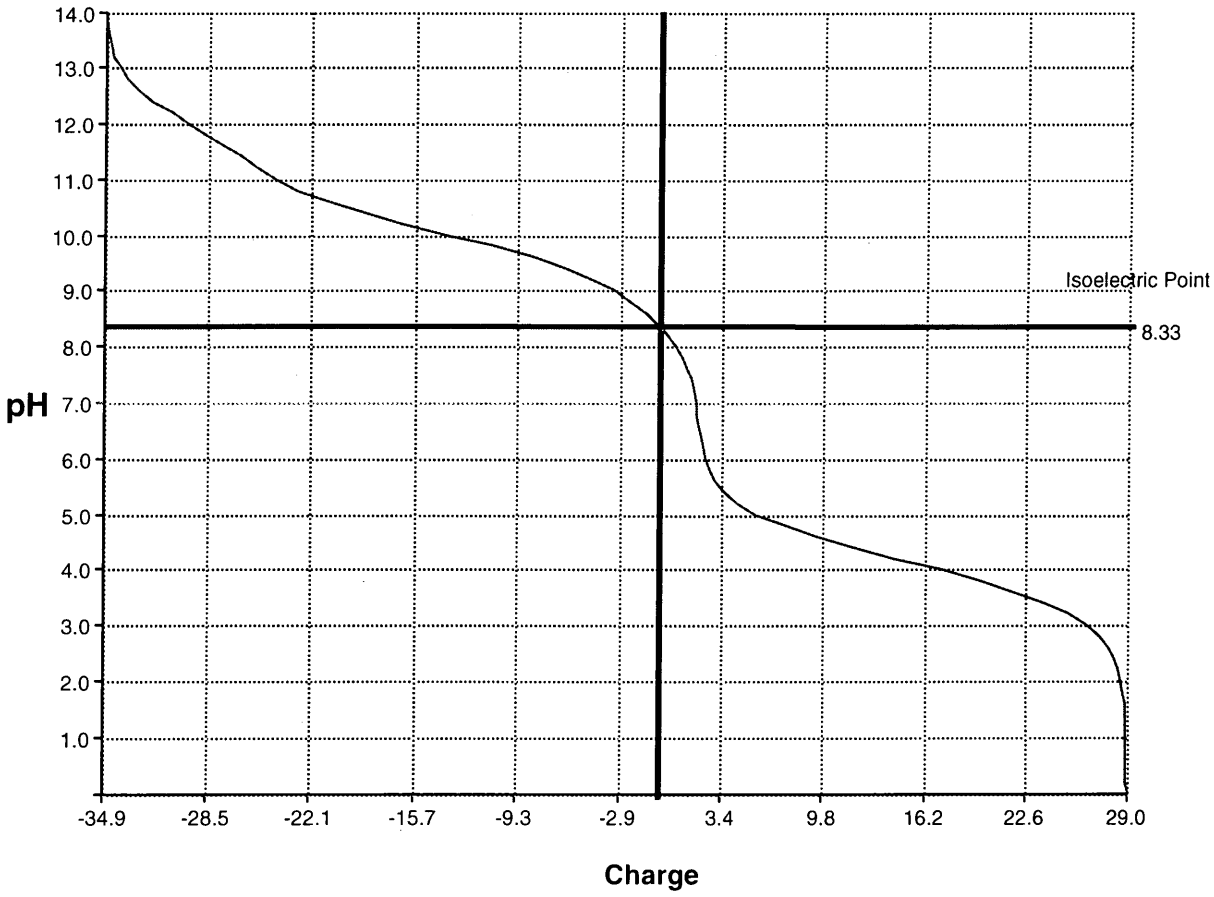

Figure 7.2 Computer generated titration curve for the deduced amino acid sequence of the *B. napus* βKR cDNA over-expressed in this study.

The above curve was generated by DNA-Star software from the deduced amino acid sequence of the βKR coding sequence present in the over-expression plasmid pETJRS10.1. The theoretical pI of the protein, 8.33, is marked at the inflection of the titration curve where the net charge of the protein is zero.

7.3 Kinetic Mechanism and Structure of βKR

The order of addition of substrates to βKR was investigated once it was established, through bireactant initial velocity studies, that a ternary complex formed during catalysis. The inactivation of βKR upon dilution encountered in this study hampered attempts to perform product inhibition assays on the plant enzyme. Attempts to obtain a prediction of the decay to allow normalisation of the inhibition data failed as the decay pattern was found to be non-reproducible. Advice from Professor Engel at University College Dublin led to the study of enzyme activity decay via time-course experiments (§6.2.2). It was suggested that there might have been a heterogeneous population of 'type A' and 'type B' enzyme molecules, with differing levels of inactivation, in the 1:500 enzyme dilution being used for the inhibition experiments, and that this might explain the irreproducibility. The three enzyme dilutions tested (1:250, 1:500, 1:1000) showed relatively little difference in their final βKR activities, suggesting that dilutions between 1:250 and 1:1000 (the useful range for the required inhibition assays) converted all of the enzyme molecules to the more inactive form - if such a form should exist.

Previous studies on *B. napus* and other βKRs [Sheldon *et al.*, 1992] have shown the enzyme to be partially protected from dilution inactivation by the inclusion of NADPH in the dilution buffer. Also, in this study, it was found that NADPH must be pre-incubated with the enzyme in the assay volume, prior to addition of the thioester substrate, in order to obtain meaningful initial velocity data. Initiation of the assay with the enzyme as the final component gave rise to spurious initial velocities differing by up to 70% (data not shown). The dilution of the enzyme into the assay volume might have caused this phenomenon. NADPH may prevent dilution induced unfolding of α-helical regions, a phenomenon observed in the obtained CD spectra of diluted (1:5) βKR (§6.3.1).

To circumvent the problem of dilution inactivation of βKR and its debilitating effect on the collection of reliable time- course data, an ultrafiltration binding assay was devised. Results obtained with this method demonstrated that the enzyme employs a fixed order ternary complex mechanism with NADPH binding first. The above phenomena of NADPH interaction with βKR, namely protection of βKR from dilution, and its possible stabilising action in assays, are concordant with the hypothesis formed from the limited kinetic experiments and the ultrafiltration study, that NADPH is capable of binding to the enzyme in the absence of the other substrate and thus is the first to bind in a fixed order ternary complex mechanism.

A more complete mechanistic investigation would have included ultrafiltration studies using NADP+ and the product homologue β-hydroxybutyryl-CoA. This however was not carried out in the time allowed for these experiments.

The structure of *E. coli* βKR at a resolution of 2.5 Å has been determined by workers in the group of David Rice at the University of Sheffield. This work has provided a description of the overall fold and nucleotide binding site of the enzyme and the relationship of the structure of enzyme to other short chain alcohol dehydrogenases. The structural determination also provides information on a likely substrate binding site and the catalytic mechanism of the enzyme. In addition, the structure suggests an evolutionary link between βKR and the structurally related fatty acid biosynthetic enzyme enoyl ACP reductase.

The crystal structure reveals a homotetramer where each subunit forms a single domain comprising a seven stranded parallel β-sheet flanked by seven α-helices. The subunit has a topology highly reminiscent of a Rossmann dinucleotide binding fold [Birktoft and Banaszak, 1984]. Comparison with the structure of enoyl-ACP reductase (ENR) [Rafferty *et al.*, 1995] and difference Fourier analysis of data from a crystal soaked in a stabilising solution containing NADPH, was used to locate the active site.

The research shows that βKR has a conserved triad of tyrosine, lysine and serine residues located at its active site, characteristic of a member of the short chain alcohol dehydrogenase protein superfamily - see §1.6. The tyrosine and lysine residues are found to superimpose well with the equivalent residues in other members of the family. The structure of βKR, which catalyses a carbon-oxygen double bond reduction, is very similar to that of ENR, the carbon-carbon double bond oxidoreductase in FAS, and confirms an evolutionary link in the generation of a biosynthetic pathway. The phenolic oxygen of the tyrosine in βKR, postulated to be the base required by the catalytic mechanism, is shifted in slightly in position relative to that of the corresponding tyrosine in ENR. This is thought to agree with the differences in the reduction chemistry catalysed by the two enzymes.

The crystal structure determination provides a comparison to some of the results in this thesis obtained in the limited structural and kinetic experiments performed by the author. Circular dichroism experiments predicted a secondary structure for *E. coli* βKR of α-helix: 21%, β-sheet: 57%, and remainder (random coil): 21%. In comparison the crystal structure model for *E. coli* βKR predicts a secondary structure of α-helix: 38%, β-sheet: 21%, and remainder (uninterpretable regions and random coil): 41%. This data does not agree well. This may be due to a conformational change having taken place in the *E. coli* βKR sample used for the CD analysis, causing it to differ in structure in solution from the structure observed in the crystalline form. It might also be due to some interfering substance having been present in the CD analysis.

Another difference between the results obtained by the author and those working on the crystal structure of the enzyme was in the arrangement of subunits in *E. coli.* βKR. The glutaraldehyde-fixation experiment results suggested that *E. coli* βKR exists as a dimer/tetramer mixture in solution. Whilst the structural model for *E. coli* βKR

cannot be used to provide definitive data on the quaternary structure of βKR in solution the crystal packing of the enzyme shows a homotetramer, similar to the structure observed for enoyl reductase by the same workers. The issue of whether *E. coli* βKR is tetrameric in solution might have been answered had the gel filtration experiment showing that the recombinant *B. napus* βKR enzyme was tetrameric been repeated with the recombinant *E. coli* βKR enzyme when it became available.

Further information on plant βKR amino acid sequences was provided by the avocado βKR partial sequence cloned in this study (§3.2). An alignment of the published plant βKR sequences (*B. napus*, *Arabidopsis* and *Cuphea lanceolata*) and the deduced avocado partial βKR sequence is shown in figure 7.3. Note that the partial sequence of the avocado sequence does not encompass either of the proposed active sites for the SDR enzymes, but that the SDR active site residues conserved between *E. coli* and *B. napus* βKR are conserved between the three plant species.

Amino acid sequence data for the purified avocado βKR protein was previously obtained by Philip Sheldon [Sheldon, 1988]. Three of the tryptic peptides sequenced by Sheldon, peptides 9, 14 and 26, aligned with the translated partial avocado βKR cDNA sequence. The alignments are shown in figure 7.4. Peptide 9 has complete identity with the deduced sequence. Peptide 26 has a single non-conservative substitution of threonine in the deduced sequence to glutamine in the peptide sequence. The codon change needed for this substitution would require two base errors in the cDNA sequence. Thus, if the original sequencing of the peptide and the present DNA sequencing of the two clones are correct, this sequence heterogeneity may be evidence for isoforms of βKR in avocado. Further heterogeneity is seen in the alignment with peptide 14. Four substitutions and one omission are present in the peptide; glycine to threonine, glycine to isoleucine, threonine to serine, glycine to proline and the omission

of a serine. Three of the above changes also would require two base changes per codon.

Comparison with the deduced sequences of βKR cDNAs from *Arabidopsis*, rapeseed, and *Cuphea* shows that the above mentioned substitutions are peculiar to the avocado peptide sequences, as the supposed anomalies are echoed in the other plant species. If the amino acid sequences of the avocado tryptic peptides were correctly sequenced, then the deduced amino acid sequence similarities between species provide evidence that the βKR protein purified by Sheldon is not coded for by the sequences obtained in this work.

An NADH-linked form of βKR from avocado been reported previously [Caughey and Kekwick, 1982] for which no sequence data exist. As the SDR motif sequences are missing from the partial avocado βKR sequence obtained in this study, no prediction can be made as to its substrate specificity. The future isolation of the complete sequence for this gene, with the aid of the sequence already obtained, might reveal whether or not this sequence encodes an NADH utilising βKR. It is perhaps more likely, however, that if the avocado peptide and deduced sequences derive from different βKR isoforms, they are probably both NADPH-linked isoforms.

```
Avocado       GPP------- --------GC RE-------- ---------F G---------
Arabidopsis   AAAVAAPRLI SLKAVGKLGF REISQIRQLA PLHSAI-PHF G-MLRCRSRQ
Rapeseed      ATTVAATKLT SLKAVKKLGF REIRQVRQWT PLQSSM-PHF G-SRQSFA--
Cuphea        ATATAAGCSG AV-ALKSLGG RRLCIPQQLS PVLAGFGSHA AKSFPILSTR
Consensus     A...AA.... ...A...LG. RE.....Q.. P.....-.HF G-........

Avocado       ---------- ---------- ---------- ------TR-- --------GK
Arabidopsis   PFSTSVVKAQ -ATATEQSPG EVVQKVESPV VVITGASRGI GKAIALALGK
Rapeseed      --TSTVVKAQ -ATAVEQSTG EAVPKVESPV VVVTGASRGI GKAIALSLGK
Cuphea        SIATSGIRAQ VATAEKVSAG AG-QSVESPV VIVTGASRGI GKAIALSLGK
Consensus     ........AQ -ATA...S.G .....VESPV V..TGASRGI GKAIAL.LGK

Avocado       AGCKVLVNYA RSSKEAEEVS KEIEASGGQA LTFGGDVSKE ADVEAMIKTA
Arabidopsis   AGCKVLVNYA RSAKEAEEVA KQIEEVGGQA ITFGGDVSKA TDVDAMMKTA
Rapeseed      AGCKVLVNYA RSAKEAEEVS KQIEAVGGQA ITFGGDVSKE ADVEAMMKTA
Cuphea        AGCKVLVNYA RSSKEAEEVS KEIEAFGGQA LTFGGDVSKE EDVEAMIKTA
Consensus     AGCKVLVNYA RS.KEAEEVS K.IEA.GGQA .TFGGDVSKE .DVEAM.KTA

Avocado       VDAWGTVDVL INNAGITRDT LLMRMKKSQW QEVIDLNLTG VFLCTQAATK
Arabidopsis   LDKWGTIDVV VNNAGITRDT LLIRMKQSQW DEVIALNLTG VFLCTQAAVK
Rapeseed      IDAWGTIDVV VNNAGITRDT LLIRMKKSQW DEVIDLNLTG VFLCTQAATK
Cuphea        VDAWGTVDIL VNNAGITRDG LLMRMKKSQW QEVIDLNLTG VFLCTQAAAK
Consensus     .DAWGT.DV. VNNAGITRDT LL.RMKKSQW .EVIDLNLTG VFLCTQAA.K

Avocado       IMM------- ---------- ---------- ---------- ----------
Arabidopsis   IMMKKKRGRI INISSVVGLI GNIGQANYTA TKGGVISFSE TPAREGASRN
Rapeseed      IMMKKRKGRI INIASVVGLI GNIGQANYAA AKAGVIGFSK TAAREGASRN
Cuphea        IMMKKKKGRI INIASVVGLV GNAGQANYSA AKAGVIGFTK TVAREVASRN
Consensus     IMMKK..GRI INI.SVVGL. GN.GQANY.A .K.GVI.F.. T.ARE.ASRN

Avocado       ---------- ---------- ---------- ---------- ----------
Arabidopsis   INVNVVCPGF IASDMTAELG EDMEKKILGT IPLGRYGKAE EVAGLVEFLA
Rapeseed      INVNVVCPGF IASDMTAKLG EDMEKKILGT IPLGRYGQPE DVAGLVEFLA
Cuphea        INVNAVAPGF ISSDMTSKLG DDINKKILET IPLGRYGQPE EVAGLVEFLA
Consensus     INVN.V.PGF I.SDMT..LG .D..KKIL.T IPLGRYG..E .VAGLVEFLA

Avocado       ---------- ---------- ---------
Arabidopsis   LSPAASYITG QAFTIDGGIA I--------
Rapeseed      LSPAASYITG QAFTIDGGIA I--------
Cuphea        INPASSYVTG QVFTIDGGMT M--------
Consensus     ..PA.SY.TG Q.FTIDGG.. .--------
```

Figure 7.3 Comparison of deduced amino acid sequences of βKR cDNAs from avocado, *Arabidopsis*, rapeseed and *Cuphea*

'Avocado' = Partial deduced sequence from clones 2B and 2C; 'Arabidopsis' = Genbank/x64464 [Slabas et al., 1992a]; 'Rapeseed' = Genbank/x64463 [Slabas et al., 1992a]; 'Cuphea' = Genbank/x64566 [Klein et al., 1992].

The above alignment confirms the reliability of the deduced avocado βKR sequence. The partial avocado βKR deduced sequence does not include either of the SDR family motifs. No additional information is therefore provided by the deduced sequence as regards the nature of these motifs in plant βKR enzymes. The alignment suggests that the peptides in the following figure, if correctly sequenced, may derive from a different βKR isoform than that encoded by the partial sequence.

```
Avocado         GPPGCREFGT RGKAGCKVLV NYARSSKEAE EVSKEIEASG GQALTFGGDV
AV pep9         ---------- ---------- ---------- ---------- ----------

Consensus       .......... .......... .......... .......... ..........

Avocado         SKEADVEAMI KTAVDAWGTV DVLINNAGIT RDTLLMRMKK SQWQEVIDLN
AV pep9         ---ADVEAMI K--------- ---------- ---------- ----------

Consensus       ...ADVEAMI K......... .......... .......... ..........

Avocado         LTGVFLCTQA ATKIMM
AV pep9         ---------- ------

Consensus       .......... ......
```

Alignment of avocado peptide 9 with the deduced amino acid sequence of the cloned βKR cDNA fro.. avocado.

```
Avocado         GPPGCREFGT RGKAGCKVLV NYARSSKEAE EVSKEIEASG GQALTFGGDV
AV pep14        ---------- ---------- ---------- ----EIEAST IQALSFGPDV

Consensus       .......... .......... .......... ....EIEAS. .QAL.FG.DV

Avocado         SKEADVEAMI KTAVDAWGTV DVLINNAGIT RDTLLMRMKK SQWQEVIDLN
AV pep14        -K

Consensus       .......... .......... .......... .......... ..........

Avocado         LTGVFLCTQA ATKIMM---- ---------- ---------- ----------

Consensus       .......... ......---- ---------- ---------- ----------
```

Alignment of avocado peptide 14 with the deduced amino acid sequence of the cloned βKR *cDNA from avocado.*

```
Avocado         GPPGCREFGT RGKAGCKVLV NYARSSKEAE EVSKEIEASG GQALTFGGDV
AV pep 26       ---------- ---------- ---------- ---------- ----------

Consensus       .......... .......... .......... .......... ..........

Avocado         SKEADVEAMI KTAVDAWGTV DVLINNAGIT RDTLLMRMKK SQWQEVIDLN
AV pep 26       ---------- -TAVDAWGQV DVLINNAGIT R--------- ----------

Consensus       .......... .TAVDAWG.V DVLINNAGIT R......... ..........

Avocado         LTGVFLCTQA ATKIMM
AV pep 26       ---------- ------

Consensus       .......... ......
```

Alignment of avocado peptide 26 with the deduced amino acid sequence of the cloned βKR cDNA from avocado

Figure 7.4 Alignments of avocado βKR peptides with the deduced amino acid sequence of the cloned βKR cDNA from avocado

'Avocado' = Partial deduced sequence from clones 2B and 2C

The sequence anomalies observed with the tryptic peptides [Sheldon, 1988] shown above are peculiar to the peptides. This may suggest that the purified protein and the deduced protein could be different isoforms of avocado βKR or that the amino acid/DNA sequencing is incorrect.

References.

Andersson A, Jordan D, Schneider G, and Lindqvist Y (1996) Crystal structure of the ternary complex of 1,3,8-trihydroxynapthalene reductase from *Magnaporthe grisea* with NADPH and an active-site inhibitor. *Structure* **4**:1161-1170.

Andrews J and Ohlrogge J (1991) Fatty acid and lipid biosynthesis and degradation. In: *Plant Molecular Biology, Physiology and Biochemistry.* Eds: DT Dennis and D. Turpin. Longman Scientific and Technical, Harlow, Essex.

Ashton AR, Jenkins CLD and Whitfeld PR (1994) Molecular-cloning of 2 different cDNAs for Maize Acetyl CoA Carboxylase. *Plant Molecular Biology* **24**:35-49.

Baldock C, Rafferty JB, Sedelnikova SE, Bithell S, Stuitje AR, Slabas AR and Rice DW (1996) Crystallization of *Escherichia coli* enoyl reductase and its complex with diazaborine. *Acta Cryst.* **52**:1181-1184.

Barton GJ (1993) ALSCRIPT - a tool to format multiple sequence alignments. *Protein Engineering* **6**:37-40.

Birktoft JJ and Banaszak LJ (1984) Structure-function relationships among nicotinamide-adenine dinucleotide dependent oxidoreductases. In: Hearn MTW (ed) "*Peptide and Protein Reviews*"vol. **4** pp 1-46, Dekker, New York .

Bruck FM, Schuch R and Spener F (1994) Malonyl-CoA-acyl carrier protein transacylase from developing seeds of *Cuphea-lanceolata* J. Plant Physiol. 143 550-555.

Caughey I and Kekwick RGO (1982) The characteristics of some components of the fatty acid synthetase system in the plastids from the mesocarp of avocado (*Persea americana*) fruit. *Eur. J. Biochem.* **123**: 553-561.

Chen J and PostBeittenmiller D (1996) Molecular cloning of a cDNA encoding 3-ketoacyl-acyl carrier protein synthase III from leek. *Gene* **182**:45-52.

Chuman L and Brody S. (1989) Acyl carrier protein is present in the mitochondria of plants and in eukaryotic micro-organisms. *Eur. J. Biochem.* **184**:643-649.

Cleland WW (1970). Steady state kinetics. In: '*The Enzymes.*' New York, Academic Press. 3, ed. pp7-10.

Clough RC, Matthis AL, Barnum SR and Jaworski JG (1992) Purification and characterization of 3-ketoacyl-acyl carrier protein synthase-III from spinach - a condensing enzyme utilizing acetyl-Coenzyme-A to initiate fatty-acid synthesis. *J. Biol.Chem* **267**:20992-20998.

Cooper CL, Hsu L, Jackowski S and Rock CO (1989) 2-acylglycerol phosphoethanolamine acyltransferase acyl-acyl carrier protein synthetase is a membrane-associated acyl carrier protein-binding protein. *J. Biol. Chem.* **264**:7384-7389.

Cottingham IR, Austin A, Sidebottom C and Slabas AR (1988) Purified enoyl (ACP) reductase from rape seed (*Brassica napus*) contains two closely related polypeptides which differ by a six amino acid N-terminal extension. *Biochim. Biophys. Acta.* **954**: 201-207.

Cottingham IR, Austin AJ and Slabas AR (1989) Inhibition and covalent modification of rape seed (*Brassica napus*) enoyl-ACP reductase by phenyglyoxal. *Biochim. Biophys. Acta.* **995**:273-278.

Coves J, Joyard J and Douce R (1988) Lipid requirement and kinetic-studies of solubilized UDP-galactose - diacylglycerol galactosyltransferase activity from spinach chloroplast envelope membranes *Proc. Nat. Acad. Sci USA* **85**:4966-4970.

Cronan JE and Rock CO (1994) The presence of linoleic-acid in Escherichia coli cannot be confirmed. *J. Bacteriol.* **176**:3069-3071.

Dai DH, Pape ME, Lopez-Casillas F, Luo XC, Dixon JE and Kim KH (1986) Molecular cloning of cDNA for acetyl-coenzyme A carboxylase. *J. Biol. Chem.* **261**:12395-12399.

de Boer HA, Comstock LJ, and Vasser M (1983) The *tac* promoter: a functional hybrid derived from the *trp* and *lac* promoters. *Proc. Natl. Acad. Sci. USA* **80**:21-25.

Dehesh K, Jones A, Knutzon DS and Voelker TA (1996) Production of high-levels of 8/0 and 10/0 fatty-acids in transgenic canola by overexpression of *Ch FatB2*, a thioesterase cDNA from *Cuphea hookeriana* *Plant Journal* **9**:167-172.

DeSilva J, Robinson SJ and Safford R (1992) The isolation and functional characterisation of a *B. napus* acyl carrier protein 5' flanking region involved in the regulation of seed storage lipid synthesis. *Plant Mol. Biol.* **18**:1163-72.

Egin-Buhler B and Ebel J (1983) Improved purification and further characterisation of acetyl CoA carboxylase from cultured cells of parsley (*Petroselinium hortease*). *Eur. J. Biochem.* **133**:335-339.

Elborough K M, Simon J W, Swinhoe R, Ashton AR and Slabas AR (1994a) Studies on wheat Acetyl Coa Carboxylase and the cloning of a partial cDNA. *Plant Molecular Biology* **24**:21-34.

Elborough KM, Swinhoe R, Winz R, Kroon JTM, Farnsworth L, Fawcett T, Martinez-Rivas JM and Slabas AR (1994b) Isolation of cDNAs from *Brassica napus* encoding the biotin-binding and transcarboxylase domains of acetyl-CoA carboxylase - assignment of the domain-structure in a full-length *Arabidopsis thaliana* genomic clone *Biochem. J.* **301**:599-605.

Elborough KM, Winz R, Deka RK, Markham JE, White AJ, Rawsthorne S and Slabas AR (1996) Biotin carboxyl carrier protein and carboxyltransferase subunits of the multisubunit form of Acetyl-CoA carboxylase from *Brassica napus* - cloning and analysis of expression during oilseed rape embryogenesis. *Biochem. J.* **315** 103-112.

Fawcett T, Simon WJ, Swinhoe R, Shanklin J, Nishida I, Christie WW and Slabas AR (1994) Expression of mRNA and steady-state levels of protein isoforms of enoyl-ACP reductase from *Brassica napus*. *Plant Mol. Biol.* **26**:155-163.

Fernandez M and Lamppa G. (1990) Acyl carrier protein import into chloroplasts does not require the phosphopantetheine: evidence for a chloroplast holoACP synthase. *Plant Cell* **2**:195-206.

Fleischmann RD *et al.* (1995) Whole-genome random sequencing and assembly of *Haemophilus influenzae* Rd. *Science* **269**:496-512.

Frommer WB and Ninnemann O (1995) Heterologous expression of genes in bacterial, fungal, animal and plant cells. *Ann. Rev. Plant Physiol. & Plant Mol. Biol.* **46**:419-444.

Fuhrmann J, Johnen T and Heise KP (1994) Compartmentation of fatty-acid metabolism in zygotic rape embryos. *Journal Of Plant Physiology* **143**:565-569.

Ghosh D, Wawrzak Z, Weeks CM, Duax WL and Erman M (1994) The refined 3-dimensional structure of 3-alpha,20-beta-hydroxysteroid dehydrogenase and possible roles of the residues conserved in short-chain dehydrogenases. *Structure* **2**:629-640.

Gilbert DG (1989). *Enzyme Kinetics* - Hypercard Stack. 1.0 for Apple Macintosh DogStar Software / Biology Dept. Indiana University, Bloomington, Indiana.

Gill SC and von Hippel P (1989) Calculation of protein extinction coefficients from amino-acid sequence data. *Anal. Biochem.* **182**:319-326.

Green PR and Bell RM (1984) Asymmetric reconstitution of homogenous *Escherichia coli sn*-glycerol-3-phosphate acyl-transferase into phospholipid vesicles. *J. Biol. Chem.* **259**:14688-14694.

Gourse RL de Boer HA and Nomura M (1986) DNA determinants of RNA synthesis in *E. coli*: growth rate dependent regulation, feedback inhibition, upstream activation, anti-termination. *Cell* **44**:197-205.

Grodberg J and Dunn JJ (1988) OmpT encodes the *Escherichia coli* outer-membrane protease that cleaves T7- RNA polymerase during purification. *J. Bacteriol.* **170**:1245.

Guerra DJ and Ohlrogge JB. (1986) Partial purification and characterisation of two forms of malonyl coenzyme A:acyl carrier protein transacylase from soybean leaf tissue. *Arch. Biochem. Biophys.* **246**:274-285.

Gulliver BS and Slabas AR (1994) Acetoacyl-acyl carrier protein synthase from avocado - its purification, characterization and clear resolution from acetyl CoA-ACP transacylase. *Plant Mol. Biol.* **25**:179-191.

Harwood JL, Walsh MC and Walker KA (1990) Enzymes of fatty acid synthesis. *Methods in Plant Biochemistry* **3**:193-217.

Heath RJ and Rock CO (1995). Enoyl-acyl carrier protein reductase (*fabI*) plays a determinant role in completing cycles of fatty acid elongation in *Escherichia coli*. *J. Biol. Chem.* **270**:26538-26542.

Heath RJ and Rock CO (1996a) Roles of the fabA and fabZ beta-hydroxyacyl-acyl carrier protein dehydratases in *Escherichia coli* fatty-acid biosynthesis. *J. Biol. Chem.* **271**: 27795-27801.

Heath RJ and Rock CO (1996b) Regulation of fatty-acid elongation and initiation by acyl-acyl carrier protein in *Escherichia-coli*. *J. Biol. Chem.* **271**:1833-1836.

Hellyer A and Slabas AR (1990) Acyl-(acyl carrier protein) thioesterase from oil seed rape - purification and characterisation. In: Quinn BJ and Harwood JL (eds) "*Plant Lipid Biochemistry, Structure and Utilisation*" Portland Press, London.

Hendren RW and Bloch K (1980) Fatty acid synthetases from *Euglena gracilis*. *J. Biol. Chem.* **255**:1504-1508.

Hilt KL. (1984) The isolation and characterization of malonyl-CoA:ACP transacylase from the mesocarp of *Persea americana*. Ph.D. Thesis, University of California, Davis CA.

Hoj PB and Mikkelsen JD (1982) Partial separation of individual enzyme activities of an ACP-dependent fatty acid synthetase from barley chloroplasts. *Carlsberg Res. Commun.* **48:**285-305.

Ikemura T (1981) Correlation between the abundance of *Escherichia coli* transfer RNAs and the occurrence of the respective codons in its protein genes. A proposal for a synonymous codon choice that is optimal for the *E. coli* translational system. *J. Mol. Biol.* **151**:389-409.

Itakura K, Hirose T, Crea R, Riggs AD, Heyneker HL, Bolivar F and Boyer HW (1977) Expression in *Escherichia coli* of a chemically synthesised gene for the hormone somatostatin. *Science* **198**:1056-63.

Jackowski S and Rock CO (1987) Acetoacetyl-acyl carrier protein synthase, a potential regulator of fatty acid biosynthesis in bacteria. *J. Biol. Chem.* **262**:7927-7931.

Jaworski JG, Clough RC, and Barnum SR (1989). A cerulenin insensitive short chain 3-ketoacyl ACP synthase in *Spinacia oleracea*. leaves *Plant Physiol.* **90** 41-44.

Jörnvall H, Persson B, Krook M, Atrian S, Gonzalez-Duarte R, Jeffery J and Ghosh D (1995) Short-chain dehydrogenases reductases (SDR). *Biochemistry* **34**:6003-6013.

Johnson BH and Hecht MH (1994). Recombinant proteins can be isolated from *Escherichia-coli*-cells by repeated cycles of freezing and thawing. *Bio-Technology* **12**(13): 1357-1360.

Kang F, Ridout CJ, Morgan CL and Rawsthorne S (1994) The activity of acetyl-CoA carboxylase is not correlated with the rate of lipid-synthesis during development of oilseed rape (*Brassica napus* L) embryos. *Planta* **193**:320-325.

Kang F and Rawsthorne S (1996) Metabolism of glucose-6-phosphate and utilization of multiple metabolites for fatty-acid synthesis by plastids from developing oilseed rape embryos. *Planta* **199**:321-327.

Kater MM, Koningstein GM, Nijkamp JJ and Stuitje AR (1991) cDNA cloning and expression of *Brassica napus* enoyl-acyl carrier protein reductase in *Escherichia coli*. *Plant Mol. Biol.* **17**:895-909.

Kater MM, Koningstein GM, Nijkamp HJJ and Stuitje AR (1994) The use of a hybrid genetic system to study the functional relationship between prokaryotic and plant multienzyme fatty acid synthetase complexes. *Plant Mol. Biol.* **25**:771-790.

Kauppinen S, Siggaard-Anderson M and von Wettstein-Knowles P (1988) β-ketoacyl ACP synthase of *E.coli* : nucleotide sequence of the *fabb* gene and identification of the cerulenin binding site.*Carlsberg Res. Commun.* **53**: 357-370.

Kim Y, Ohlrogge JB and Presegard JH. (1990) Motional effects on NMR structural data-comparison of spinach and *Escherichia coli* acyl carrier proteins. *Biochem. Pharmacol.* **40**:7-13.

Klein B, Pawlowski K, Horicke-Grandpierre C, Schell J and Topfer R (1992) Isolation and characterization of a cDNA from *Cuphea lanceolata* encoding a β-ketoacyl-ACP reductase *Mol. Gen. Genet.* **233**:122-128.

Knudsen J and Grunnet I (1982) Transacylation as a chain-termination mechanism in fatty acid synthesis by mammalian fatty acid synthetase. *Biochem J.* **202**:139-143.

Knutzon DS, Thompson GA, Radke SE, Johnson WB, Knauf VC and Kridl JC (1992) Modification of *Brassica* seed oil by antisense expression of a stearoyl-acyl carrier protein desaturase gene. *Proc. Natl. Acad. Sci. USA* **89**:2624-2628.

Konishi T and Sasaki Y. (1994) Compartmentalization of 2 forms of acetyl-CoA carboxylase in plants and the origin of their tolerance toward herbicides *Proc. Nat. Acad. Sci. USA* **91**:3598-3601.

Krook M, Marekov L and Jörnvall H (1990) Purification and structural characterization of placental NAD+-linked 15-hydroxyprostaglandin dehydrogenase - the primary structure reveals the enzyme to belong to the short-chain alcohol-dehydrogenase family. *Biochemistry* **29**:738-743.

Kraulis PJ (1991) MOLSCRIPT: a program to produce both detailed and schematic plots of protein structures. *J. Appl. Crystallogr.* **24**:946-950.

Kunst L, Taylor DC and Underhill EW (1992) Fatty acid elongation in developing seeds of *Arabidopsis thaliana*. *Plant Physiol. Biochem.* **30**:425-434.

Laemmli UK (1970). Cleavage of structural proteins during the assembly of bacteriophage T4. *Nature* **227**:680-685.

Lambalot RH and Walsh CT (1995) Cloning, overproduction, and characterization of the *Escherichia ooli* holo-acyl carrier protein synthase *J. Biol. Chem.* **270**:24658-24661.

Lamppa G and Jacks C (1991). Analysis of two linked genes coding for the acyl carrier protein (ACP) from *Arabidopsis thaliana (columbia). Plant Mol. Biol.* **16:**469-474.

Lessire R and Stumpf PK. (1983) Nature of the fatty acid synthetase systems in the parenchymal and epidermal cells of *Allium porrum* L. leaves. *Plant Physiol.* **73** 614-618.

Lichtenthaler HK and Golz A. (1995) Chemical regulation of acetyl-CoA formation and *de novo* fatty acid biosynthesis in plants. In: Kader J and Mazliak P (eds) *"Plant Lipid Metabolism"* Kluwer Academic Publishers, Amsterdam, Netherlands.

Loader NM, Woolner EM, Hellyer A, Slabas AR and Safford R. (1993) Isolation and characterization of 2 *Brassica napus* embryo acyl-ACP thioesterase cDNA clones. *Plant Mol. Biol.* **23**:769-778.

MacKintosh RW, Hardie DG and Slabas AR (1989). A new assay procedure to study the induction of β-keto ACP synthase I and II, and the complete purification of β-ketoacyl ACP synthase I from developing oil seed rape. *Biochem. Biophys. Acta.* **1002**:114-124.

Magnuson K, Carey MR and Cronan JE (1995) The putative *fabJ* gene of *Escherichia coli* fatty-acid synthesisis the *fabF* gene. *J. Bacteriol.* **177**:3593-3595.

Mandel M and Higa A (1970) Calcium-dependent bacteriophage DNA infection. *J. Mol. Biol.* **53**:159-162.

Martinez-Rivas JM, Thomas NC, Chase D, Fawcett T and Slabas AR (1993). cDNA cloning and over-expression of 3-oxoacyl-ACP reductase from *Brassica napus* seed. *Grasas y Aceites* **44**:119-122.

Masterson C, Wood C and Thomas DR (1990) L-acetylcarnitine, a substrate for chloroplast fatty-acid synthesis. *Plant Cell. Environ.* **13**:755-765.

McKinley-McKee JS, Winberg J-O and Pettersson G (1991) Mechanism of action of *Drosophila melanogaster* alcohol-dehydrogenase. *Biochem Int.* **25**:879-885.

Merrit EA and Murphy MEP (1994) Raster3D version 2.0 - A program for photorealistic molecular graphics. *Acta. Cryst.* **D50**:869-873.

Moffatt BA and Studier FW (1987) T7 lysozyme inhibits transcription by T7 RNA-polymerase. *Cell* **49**:221.

Morbidoni HR, De Mendoza D and Cronan JE Jr. (1996) *Bacillus subtilis* acyl carrier protein is encoded in a cluster of lipid biosynthesis genes. *J. Bacteriol.* **178**:4794-4800.

O'Farrell PH (1975) High resolution two-dimensional electrophoresis of proteins. *J. Biol. Chem.* **250**: 4007-4021.

Olsen JG, Kadziola A, Siggaard-Andersen M, Chuck JA, Larsen S and von Wettstein-Knowles P (1995) Preliminary x-ray diffraction analysis of beta-ketoacyl-[acyl carrier protein] synthase-I from *Escherichia-coli. Prot. Peptide Lett.* **1**:246-251.

Oswood MC, Kim Y, Ohlrogge JB and Prestegard JH. (1997) Structural homology of spinach acyl carrier protein and *Escherichia coli* acyl carrier protein based on NMR data. *Proteins-Structure Function And Genetics* **27**:131-143.

Parker WB, Marshall LC, Burton JD, Somers DA, Wyse DL, Gronwald JW and Gengenbach BG (1990) Dominant mutations causing alterations in acetyl-Coenzyme-A carboxylase confer tolerance to cyclohexanedione and aryloxyphenoxypropionate herbicides in maize. *Proc. Nat. Acad. Sci.* USA **87**:7174-7179.

Peterson GL (1983). Determination of total protein. *Meth. Enzymol.* **91**: 95-121. *Plant Mol. Biol.* **23**:769-778.

Pollard MR and Stumpf PK (1980) Biosynthesis of C20 and C22 fatty acids by developing seeds of *Limnanthes alba. Plant Physiol.* **66**:649-653.

Post-Beittenmiller D (1996) Biochemistry and molecular-biology of wax production in plants. *Annual Review Of Plant Physiology And Plant Molecular Biology* **47**:405-430.

Provencher SW and Glöckner J (1981). Estimation of globular protein secondary structure from circular-dichroism. *Biochemistry* **20**:33-37.

Rafferty JB, Simon JW, Baldock C, Artymiuk PJ, Baker PJ, Stuitje AR, Slabas AR and Rice DW (1995) Common themes in redox chemistry emerge from the X-ray structure of oilseed rape (*Brassica napus*) enoyl acyl carrier protein reductase. *Structure* **3**:927-938. .

Rafferty JB, Simon JW, Stuitje AR, Slabas AR, Fawcett T and Rice D (1994) Crystallisation of the NADH-specific enoyl acyl carrier protein reductase from *Brassica napus. J. Mol. Biol.* **237**:240-242.

Rafferty JB, Fisher M, Landridge SJ, Martindale W, Thomas NC, Simon JW, Bithell S, Slabas AR and Rice DW (1998) The crystallization of the NADP-dependent β-keto acyl carrier protein reductase from *Escherichia coli. Acta Crystallographica* **D54**:427-429.

Rawlings M and Cronan JE (1992). The gene encoding *Escherichia coli* acyl carrier protein lies within a cluster of fatty acid biosynthetic genes. *J. Biol. Chem.* **267**:5751-5754.

Roesler KR, Savage LJ, Shintani DK, Shorrosh BS and Ohlrogge JB. (1996) Copurification, co-immunoprecipitation, and coordinate expression of acetyl-coenzyme-a carboxylase activity, biotin carboxylase, and biotin carboxyl carrier protein of higher-plants. *Planta* **198**:517-525.

Roughan G, Postbeittenmiller D, Ohlrogge J and Browse J. (1993) Acetylcarnitine A substrate for fatty-acid synthesis in plants. *Plant Physiology* **101**:1157-1162.

Roughan G. (1987) On the control of fatty acid compositions of plant glycerolipid. In: Stumpf PK, Mudd JB, Nea WD (eds) "*The Metabolism, Structure and Function of Plant Lipids*" pp 247-254, Plenum, New York.

Saito K, Hamajima A, Ohkuma M, Murakoshi I, Ohmori S, Kawaguchi A, Teeri TH and Cronan JE (1995) Expression of the *Escherichia coli* fabA gene encoding beta-hydroxydecanoyl thioester dehydrase and transport to chloroplasts in transgenic tobacco. *Transgenic Research* .**4**:60-69.

Sambrook J, Fritsch EF and Maniatis T (1989). *Molecular Cloning: A Laboratory Manual.* New York, Cold Spring Harbor Laboratory, Cold Spring Harbor.

Sawers G and Jarsch M (1996) Alternative regulation principles for the production of recombinant proteins in *Escherichia coli. Appl. Microbiol & Biotech* 46,1-9

Schulz H and Wakil SJ (1971) Studies on the mechanism of fatty acid synthesis. On the mechanism of β-ketoacyl-[ACP] reductase from *Escherichia coli. J. Biol. Chem.* **246**:1895-1901.

Scopes, RK (1987) Protein Purification: Principles and Practice, ed 2., Springer New York N.Y.

Serre L, Verbree EC, Dauter Z, Stuitje AR and Derewenda ZS (1995) The *Escherichia coli* malonyl-CoA-acyl carrier protein transacylase at 1.5-angstrom resolution - crystal-structure of a fatty-acid synthase component. *J. Biol. Chem.* **270**:12961-12964.

Shearman CA, Rossen L, Johnston AWB and Downie JA (1986) The *Rhizobium leguminosarum* nodulation gene nodF encodes a polypeptide similar to acyl-carrier protein and is regulated by nodD plus a factor in pea root exudate. *EMBO J.* **5**:647-652.

Sheldon PS (1988). *A study of plant plastid NADPH dependent β-Ketoacyl-[Acyl Carrier Protein] Reductase.* [Ph.D.] University of Birmingham.

Sheldon PS, Keckwick RGO, Sidebottom C, Smith CG and Slabas AR (1990). 3-oxoacyl-(acyl-carrier protein) reductase from avocado (*Persea americana*) fruit mesocarp. *Biochem. J.* **271**: 713-720.

Sheldon PS, Kekwick RGO, Smith CG, Sidebottom C and Slabas AR (1992). 3-Oxoacyl-[ACP] reductase from oilseed rape (*Brassica napus*). *Biochim. Biophys. Acta.* **1130**: 151-159.

Shen Z and Byers D (1996) Isolation of *Vibrio harveyi* acyl carrier protein and the *fabG, acpP*, and *fabF* genes involved in fatty acid biosynthesis. *J. Bacteriol.* **178**:571-573.

Shewry PR, Williamson MS and Kreis M (1987) 'Effects of mutant genes on the synthesis of storage components in developing barley endosperms' in developmental mutants. In: Thomas H and Grierson D (eds) *"Higher Plants"* (SEB Semin. Ser.) vol 32 pp 95-118. Cambridge University Press, Cambridge.

Shimakata T and Stumpf PK (1982). The procaryotic nature of the fatty acid synthetase of developing *Carthamus tinctorius L.* (Safflower) seeds. *Arch. Biochem. Biophys.* **217**:144-154.

Shimakata T and Stumpf PK (1982a) Isolation and function of spinach leaf β-ketoacyl-ACP synthases. *Proc. Natl. Acad. Sci.* **79**:5808-5812.

Shimakata T and Stumpf PK (1982b) Purification and characterisations of β-ketoacyl-[ACP] reductase, β-hydroxyacyl-[ACP] dehydrase and enoyl-[ACP] reductase from *Spinacia oleracea* leaves. *Arch. Biochem. Biophys.* **218**: 77-91.

Shorrosh BS, Dixon RA and Ohlrogge JB. (1994) Molecular-cloning, characterization, and elicitation of Acetyl- CoA carboxylase from Alfalfa. *Proc. Nat. Acad. Sci. USA* **91**:4323-4327.

Siggaard-Andersen M, Wissenbach M, Chuck JA, Svendsen I, Olsen JG and von Wettstein -Knowles P (1994) The fabJ encoded beta-ketoacyl-[acyl carrier protein] synthase-IV from *Escherichia coli* is sensitive to cerulenin and specific for short-chain substrates. *Proc. Nat. Acad. Sci* **91**:11027-11031.

Siggaard-Andersen M (1988) Role of *Escherichia coli* β-ketoacyl-ACP synthase-I in unsaturated fatty-acid synthesis. *Carlsberg Res. Commun.* **53**:371-379.

Siggaard-Andersen M, Kauppinen S, and von Wettstein-Knowles P. (1991) Primary structure of a cerulenin binding β-ketoacyl [acyl carrier protein] synthase from barley chloroplasts. *Proc. Nat. Acad. Sci. USA* **88** 4114-4118.

Skarzynski T, Moody PCE and Wonacott AJ (1987) Structure of holo-glyceraldehyde-3-phosphate dehydrogenase from *Bacillus stearothermophilus* at 1.8Å resolution. *J. Mol. Biol.* **193**:171-187.

Slabas AR Chase D Nishida I Murata N Sidebottom C Safford R Sheldon PS Keckwick RGO Hardie G and Mackintosh RW (1992a) Molecular cloning of higher-plant 3-oxoacyl-(acyl carrier protein) reductase. *Biochem. J.* **283**:321-326.

Slabas AR, Cottingham I, Austin A, Fawcett T and Sidebottom CM (1991) Amino acid sequence analysis of rape seed (*Brassica napus*) NADH-enoyl-ACP reductase. *Plant Mol. Biol.* **17**:911-914.

Slabas AR, Cottingham IR, Austin A, Hellyer A, Safford R and Smith CG (1990) Immunological detection of NADH-specific enoyl-ACP reductase from rape seed (*Brassica napus*) - induction, relationship of and polypeptides, mRNA translation and interaction with ACP. *Biochim. Biophys. Acta* **1039**:181-188.

Slabas AR and Fawcett T (1992) The biochemistry and molecular biology of plant lipid biosynthesis. *Plant Mol. Biol.* **19**:169-191.

Slabas AR and Hellyer A (1985) Rapid purification of a high molecular weight subunit polypeptide form of rape seed acetyl CoA carboxylase. Plant Sci. Lett. 39:177-182.

Slabas AR, Sidebottom CM, Hellyer A, Kessell RMJ and Tombs MP (1986) Induction, purification and characterisation of NADH-specific enoyl acyl carrier protein reductase from developing seeds of oil seed rape (*Brassica napus*). *Biochim. Biophys. Acta* **877**:271-280.

Soll J and Alefsen H (1993). The protein import apparatus of chloroplasts. *Physiol. Plant.* **87**:433-440.

Stapelton SR and Jaworski JG. (1984) Characterisation and purification of malonyl coenzyme A:[acyl carrier protein] transacylase from spinach and *Anabaenna variablis.Biochem. Biophys. Acta* **794** 240-248.

Studier FW, Rosenberg AH, Dunn JJ and Dubendorff JW (1990) Use of T7 RNA-polymerase to direct expression of cloned genes *Meth. Enzymol.* **185:**60-89.

Studier FW and Moffatt BA (1986) Use of bacteriophage-T7 RNA-polymerase to direct selective high-level expression of cloned genes. *J. Mol. Biol.* **189**:113-130.

Stumpf PK and Barber G (1957) Fat metabolism in higher plants. IX. Enzymatic synthesis of long chain fatty acids by avocado particles. *J. Biol. Chem.* **227**:407-417.

Tabor S and Richardson CC (1985) A bacteriophage-T7 RNA-polymerase promoter system for controlled exclusive expression of specific genes. *Proc. Natl. Acad. Sci.USA.* **82**:1074-1078.

Tanaka N, Nonaka T, Nakanishi M, Deyashiki Y, Hara A and Mitsui Y (1996a) Crystal-structure of the ternary complex of mouse lung carbonyl reductase at 1.8-Å resolution - the structural origin of coenzyme specificity in the short-chain dehydrogenase reductase family. *Structure* **4**:33-45.

Tanaka N, Nonaka T, Tanabe T, Yoshimoto T, Tsuru D and Mitsui Y (1996b) Crystal-structures of the binary and ternary complexes of 7-alpha-hydroxysteroid dehydrogenase from *Escherichia coli. Biochemistry* **35**:7715-7730.

Theg SM and Scott SV (1993). Protein import into chloroplasts. *Trends Cell Biol.* **3**:186-190.

Thoden JB, Frey PA, Holden HM (1996) High-resolution X-ray structure of UDP-galactose 4-epimerase complexed with UDP-phenol. *Protein Sci.* **5**:2149-2161.

Tobias JW, Shrader TE, Rocap G and Varchavsky A (1991) The N-end rule in bacteria. *Science* **254**:1374-1377.

Toomey RE and Wakil SJ (1966) Studies on the mechanism of fatty acid synthesis. XV. Preparation and general properties of β-ketoacyl-[acyl carrier protein] reductase from *Escherichia coli. Biochim. Biophys. Acta.* **116**:189-197.

Topfer R, Martini N and Schell J (1995) Modification of plant lipid-synthesis. *Science* **268**:681-686.

Truchet G, Roche P, Leronge P, Vasse J, Camet S, de Billy F, Prome J-C and Denarie J (1991) Sulphated lipo-oligosaccharide signals of Rhizobium meliloti elicit root nodule organogenesis in alfalfa. *Nature* **351**:670-673.

Turnham E and Northcote DH (1983) Changes in the activity of acetyl-CoA carboxylase during rapeseed formation. *Biochem. J.* **212**:223.

Vagelos PR, Alberts AW and Majerus PW (1969) β-Ketoacyl Acyl Carrier Protein Reductase. In: Lowenstein JM (ed) *"Methods in Enzymology"* vol **XIV** pp. 60-63, Academic Press, New York .

Verwoert IIGS, Vanderlinden KH, Nijkamp HJJ and Stuitje AR (1994) Developmental specific expression and organelle targeting of the *Escherichia coli fabD* gene, encoding malonyl Coenzyme A-acyl carrier protein transacylase in transgenic rape and tobacco seeds. *Plant Mol. Biol.* **26**:189-202.

Vieira J and Messing J (1982). The PUC plasmids, an M13MP7-derived system for insertion mutagenesis and sequencing with synthetic universal primers. *Gene* **19**:259-268.

Voelker TA, Worrell AC, Anderson L, Bleibaum J, Fan C, Hawkins DJ, Radke SE and Davies HM. (1992) Fatty acid biosynthesis redirected to medium chains in transgenic oilseed plants. *Science* **257**:72-74.

von Heijne G, Steppuhn J and Herrmann RG (1989) Domain-structure of mitochondrial and chloroplast targeting peptides. *Eur. J. Biochem.* **180**: 535-545.

Wada H, Gombos Z, and Murata N (1990) Enhancement of chilling tolerance of a cyanobacterium by genetic manipulation of fatty acid desaturation. *Nature* **347**, 200-203.

Wada H, Shintani D and Ohlrogge J. (1997) Why do mitochondria synthesize fatty acids? Evidence for involvement in lipoic acid production. *Proc. Nat. Acad. Sci. USA* **94** 1591-1596.

Wagner UG, Bergler H, Fuchsbichler S, Turnowsky F, Hogenauer G and Kratky C (1994) Crystallization and preliminary X-ray diffraction studies of the enoyl-ACP reductase from *Escherichia coli J. Mol. Biol.* **243**:126-127.

Waldrop GL, Rayment I and Holden HM (1994) 3-dimensional structure of the biotin carboxylase subunit of acetyl-CoA carboxylase. *Biochemistry* **33**:10249-10256.

Weaire PJ and Kekwick RGO (1975) The synthesis of fatty acids in avocado mesocarp and cauliflower bud tissue. *Biochem. J.* **146**: 425-437.

Weiss MA, Ellenberger T, Wobbe CR, Lee JP, Harrison SC and Struhl K (1990). Folding transition in the DNA-binding domain of GCN4 on specific binding to DNA. *Nature* **347**:575-578.

Wessel D and Flugge UI (1984). A method for the quantitiative recovery of protein in dilute solutions in the presence of detergents and lipids. *Anal. Biochem.* **138**:141-143.

White MF, Fothergill-Gilmore LA, Kelly SA and Price NC (1993). Substitution of His-181 by alanine in yeast phosphoglycerate mutase leads to cofactor-induced dissociation of the tetrameric structure. *Biochem. J.* **291**:479-483.

Wierenga RK, Maeyer MCH and Hol WGJ (1985) Interaction of pyrophosphate moieties with alpha-helixes in dinucleotide binding-proteins. *Biochemistry* **24**:1346-1357.

Winter E, Brummel M, Schuch R and Spener F (1997) Decarboxylation of malonyl-(acyl carrier protein) by 3-oxoacyl-(acyl carrier protein) synthases in plant fatty acid biosynthesis. *Biochem. J.* **321**:313-318.

Yamada M, Tsuboi S, Osafune T, Suga T and Takishima K (1990) Multifractional properties of non-specific lipid transfer protein from higher plants.: In: Quinn PJ Harwood JC (eds) *"Plant Lipid Biochemistry, Structure and Utilization"*, pp 278-280, Portland Press, London .

Yang LM, Fernandez MD and Lamppa GK. (1994) Acyl carrier protein (ACP) import into chloroplasts - covalent modification by a stromal holoACP synthase is stimulated by exogenously added CoA and inhibited by adenosine 3',5'-bisphosphate. *Eur. J. Biochem* **224** 743-750.